Modeling Simulation and Performance Evaluation of Parabolic Dish Solar Power Plant

By

Aklilu Tesfaye

A thesis submitted in partial fulfillment of the requirements for the degree of

MASTER OF SCIENCE IN SCHOOL OF MECHANICAL ENGINEERING

(Thermal Engineering Stream)

Advisor

Dr.-Ing. Abebayehu Assefa

Addis Ababa University

January 2011

ADDIS ABABA UNIVERSITY

SCHOOL OF GRADUATE STUDIES

Modeling, Simulation and Performance Evaluation of Parabolic Dish Solar Power Plant

By

Aklilu Tesfaye

Faculty of Technology

Approved by Board of Examiners

1. *Dr.-Ing. Edessa Dribssa* _____

   Chairman Dep.'s Graduate Committee *Signature*

2. *Dr.-Ing. Abebayehu Assefa* _____

   Advisor *Signature*

3. *Dr. Tesfaye Dama* _____

   Internal Examiner *Signature*

4. *Dr.-Ing. Edessa Dribssa* _____

   External Examiner *Signature*

Abstract

A solar parabolic dish electric power generation system is one option for a high temperature solar concentrator that is capable to achieve a high system performance. This results from the fact that it combines an excellent concentrator, a very efficient cavity receiver and a high performance heat engine.

The Stirling dish system produces electricity using concentrated solar thermal energy to drive a Stirling engine. The system utilizes a parabolic mirror equipped with dual-axis tracking to concentrate solar radiation onto a thermal receiver integrated in the Stirling engine. The receiver consists of a heat exchanger designed to transfer the absorbed solar energy to the working fluid, typically, hydrogen. The Stirling engine then converts the absorbed thermal energy to mechanical power by expanding the gas in a piston-cylinder in a manner similar to a gas or diesel engine. The linear motion is converted to a rotary motion to turn a generator to produce electricity.

The electrical output of the system is proportional to the size of the reflector, its optical losses and the efficiencies of the Stirling engine and the generator.

This thesis outlines the theory and models for the collector, receiver, and Stirling engine, the parasitic power. An energy prediction model was created for solar Stirling dish systems to predict the location dependent long term performance of these systems. The model analyzes the performance of the parabolic mirror, receiver, Stirling engine, and the parasitic power consumption to predict the net power produced.

The power plant analyzed in this paper has a capacity of generating 10MW electric power. The performance prediction models were implemented in EES and TRNSYS and include location dependent properties that affect the performance based on the direct normal insolation, ambient temperature, density of air (altitude), sun elevation angle, and the wind speed.

The cost and financial analysis is made for the Dish System. Solar Advisor Model is used to make this analysis under Kombolcha weather condition. This analysis is used to determine the different costs associated with the power plant. The cash flow for the 30 years of operation of the power plant is also shown.

Acknowledgement

I am heartily thankful to my advisor, Dr.-Ing. Abebayehu Assefa, whose encouragement, guidance and support from the initial to the final level enabled me to develop an understanding and ability to prepare this thesis.

I owe my deepest gratitude to Habtamu Tkubet, Mekuanint Mesfin and friends who are always beside me and played part a great role in the completion of my work.

I also want to appreciate all of my instructors / colleague in the Department of Mechanical Engineering, Addis Ababa University for their continuous encouragement.

Finally, I would like to thank my family for the everlasting confidence, constant support and endless love.

Aklilu Tesfaye

TABLE OF CONTENT

LIST OF FIGURES

LIST OF TABLES

Nomenclature

A	Area
A_a	Cavity aperture area
A_i	Inner surface area of the cavity
Beale	Beale number
C	Thermal capacitance
DNI	Direct normal insolation
d	Diameter of the collector
e	Regeneration effectiveness
f	Engine operating frequency
f_f	Friction factor
g	Gravitational constant
h	Convection coefficient
I_b	Beam radiation incident on the receiver surface
$I_{bm,\ corr}$	Corrected beam radiation
k	Thermal conductivity
K	Term for minor pumping losses
L	Length
m	Mass of working fluid
M	Molar mass
n	Number of standard deviations for the receiver model
n_r	Engine speed
N	Pump or fan speed
Nu	Nusselt number
P	Pressure
P_{gross}	Gross engine power
P_{net}	Net engine power
P_{head}	Pump pressure head
Pr	Prandtl number
p	Distance from the concentrator surface to the focal point of the aperture

P_{mean}	Mean engine pressure
Q,q	Heat transfer
R	Resistance
R	Ideal gas constant
R_a	Rayleigh number
R_e	Reynold's number
S	Stroke of the engine piston
Sc	Schmidt number
T	Temperature
v	Velocity
V	Volume
V_{max}	Maximum swept volume
V_{min}	Minimum swept volume (V_{max} subtracted by the displacement volume)
V_{sw}	Swept volume
V_{swc}	Swept volume of the compression space
V_{swe}	Swept volumes of the expansion spaces
W_n	Beam spread projected onto the focal plane of the receiver
W	Work
West	West number

Greek Letters

α	Receiver absorptance
α_{eff}	Effective absorptance
α_i	Inner surface absorptance of the cavity
β	Thermal expansion coefficient
Γ	Flux capture fraction which equals the intercept factor
Δ Q	Power intercepted for a specific ring
Δr	Total beam spread in the plane perpendicular to the centerline of the reflected light
E_s	Emissivity of a surface
ε	Angular size of the sun
ε_v	Volumetric ratio

η	Efficiency
η_{Carnot}	Carnot efficiency
η_{SE}	Stirling engine efficiency
θ	Receiver aperture angle (0 is horizontal, 90 is vertically down)
$\Theta_{T,cw}$	Normalized cooling water inlet temperature
μ	Dynamic viscosity
υ	Kinematic viscosity
ρ	Mirror specular reflectance
σ_{slope}	Spread of the collector beam due to error in the mirror slope
Σ_{senso}	Spread of the collector beam due to sensor error
σ_{drive}	Spread of the collector beam due to the tracking drive error
σ_{align}	Spread of the collector beam due to mirror alignment
$\sigma_{reflect}$	Spread of the collector beam caused by mirror reflection discrepencies
σ_{sun}	Spread of the collector beam caused by the width of the sun
σ	Stefan Boltzmann's constant
τ_c	Transmittance of the hybrid receiver cover
τ_d	Transmittance of the hybrid receiver cover for isotropic diffuse radiation
$d\Phi/d\psi$	Change in the radiant flux with respect to the change in the angle in the collector
ΦR	Normalized mirror reflectance
Ψ	Angle between the line between the collector vertex and focus, and the line for the location on the collector where light is reflecting from
ψ_{rim}	Collector rim angle
Subscripts	Subscripts
Amb	Ambient
Ap	Receiver aperture
C, c	Compression space
Cav	Receiver cavity
Cond	Conduction
Conv	Convection
Cw	Cooling water

E, e	Expansion space
Eff	Effective
forced	Forced convection
g	Working fluid (gas)
h	Heater
k	Cooler
m	Mean
min	Minimum
max	Maximum
natural	Natural convection
r	Regenerator
SE	Stirling engine
SW	Swept (volume)
w	Wall of cavity
wall	Wall of cavity

Acronyms

EES	Engineering Equation Solver
NREL	National Renewable Energy Laboratory
SAIC	Science Applications International Corp
SBP	Schlaich–Bergermann und Partner
SES	Stirling Energy Systems
WGA	Wilkinson, Goldberg, and Associates, Inc

CHAPTER ONE

1.1 Introduction

Most of today's electrical energy is generated by plant with a low cost of production and high reliability. However, concerns about the longer term sustainability of fossil fuel-based generation, particularly related to climate change, non-renewability of the resources and largely unaccounted future environmental costs, becomes the major problem to a continuing development of the energy industry. To avoid such problem the industries are searching a sustainable, low carbon emitting, renewable energy sources.

Solar energy is an unlimited energy resource, set to become increasingly important in the longer term, for providing electricity and heat energy on a large scale. It is an energy resource that could be used in large, centralized power generation plants; smaller distributed heat and power plants; or scaled down, at the individual consumer level. Carbon emissions and greenhouse gas impacts are very low.

As interest for clean renewable electric power technologies, a number of solar concentrator power plants are being considered for deployment around the globe. It is essential that plant designs be optimized for each specific application. The optimum design must consider the capital cost.

Among all the renewable technologies available for large-scale power production today and for the next few decades, CSP is one with potential to make major contributions of clean energy because of its relatively conventional technology and ease of scale-up.

Ethiopia has a huge potential in solar energy particularly in the Southwest where the deserts have some of the best solar resource levels in the world

Benefit of developing sustainable energy

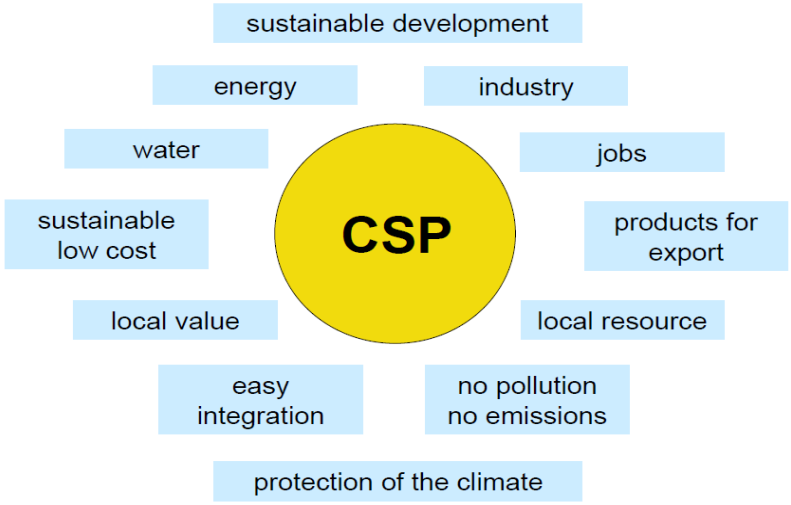

Figure 1.1 Benefit of Developing Sustainable Energy

Solar energy can be converted to electricity in two ways:

- Photovoltaic (PV devices) or "solar cells" – change sunlight directly into electricity. PV systems are often used in remote locations that are not connected to the electric grid. They are also used to power watches, calculators, and lighting road signs.
- Solar Power Plants - indirectly generate electricity when the heat from solar thermal collectors is used to heat a fluid which produces steam that is used to power generator.

1.2 Solar Collectors

The solar collector is the key element in a solar energy system. It is also the novel technology area that requires new understandings in order to make captured solar energy a viable energy source for the future.

Solar collectors can be either non concentrating or concentrating.

- Non concentrating collectors – have a collector area (i.e. the area that intercepts the solar radiation) that is the same as the absorber area (i.e., the area absorbing the radiation). Flat-plate collectors are the most common and are used when temperatures below about 80^0C are sufficient, such as for space heating.
- Concentrating collectors – where the area intercepting the solar radiation is greater, sometimes hundreds of times greater, than the absorber area. The function of a solar

collector is simple; it intercepts incoming insolation and changes it into a useable form of energy that can be applied to meet a specific demand.

1.2.1 Concentrating Solar Collectors

When higher temperatures are required, concentrating solar collectors are used. Solar energy falling on a large reflective surface is reflected onto a smaller area before it is converted into heat. This is done so that the surface absorbing the concentrated energy is smaller than the surface capturing the energy and therefore can attain higher temperatures before heat loss due to radiation and convection wastes the energy that has been collected. Most concentrating collectors can only concentrate the parallel insolation coming directly from the sun's disk (beam normal insolation), and must follow (track) the sun's path across the sky. Three types of solar concentrators are in common use;

parabolic troughs, parabolic dishes and central receivers. Figure 1.2 shows these concepts schematically.

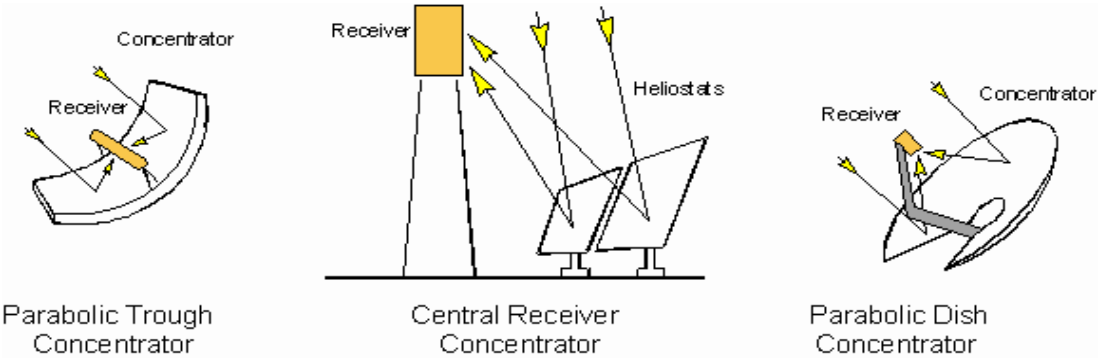

Figure

Figure 1.2 Three Commonly Used Reflecting Schemes for Concentrating Solar Energy to Attain High Temperatures. (DOE, 2006)

1.2.1.1 Parabolic Trough

A parabolic trough collector has a linear parabolic-shaped reflector that focuses the sun's radiation on a linear receiver located at the focus of the parabola. The collector tracks the sun along one axis from east to west during the day to ensure that the sun ray is continuously focused on the receiver.

Figure 1.3 Parabolic Trough trough assembly (Patnode, 2006)

Because of its parabolic shape, a trough can focus the sun at 30 to 100 times its normal intensity (concentration ratio) on a receiver pipe located along the focal line of the trough, achieving operating temperatures over 400 degrees Celsius. A collector field consists of a large field of single-axis tracking parabolic trough collectors. The solar field is modular in nature and is composed of many parallel rows of solar collectors aligned on a north-south horizontal axis.

A working fluid is heated as it circulates through the receivers and returns to a series of heat exchangers at a central location where the fluid is used to generate high-pressure superheated steam. The steam is then fed to a conventional steam turbine/generator to produce electricity or mechanical power. After the working fluid passes through the heat exchangers, the cooled fluid is recirculated through the solar field.

The plant is usually designed to operate at full rated power using solar energy alone, given sufficient solar energy. However, all plants are hybrid solar/fossil plants that have a fossil-fired capability that can be used to supplement the solar output during periods of low solar energy.

1.2.1.2 Solar Power Tower

A solar power tower or central receiver generates electricity from sunlight by focusing concentrated solar energy on a tower-mounted heat exchanger (receiver). This system uses

hundreds to thousands of flat sun-tracking mirrors called heliostats to reflect and concentrate the sun's energy onto a central receiver tower. The energy can be concentrated as much as 1,500 times that of the energy coming in from the sun.

Energy losses from thermal-energy transport are minimized as solar energy is being directly transferred by reflection from the heliostats to a single receiver, rather than being moved through a transfer medium to one central location, as with parabolic troughs. Power towers must be large to be economical.

This is a promising technology for large-scale grid-connected power plants. Though power towers are in the early stages of development compared with parabolic trough technology, a number of test facilities have been constructed around the world.

Figure 1.4 Central Receiver Systems (DOE, 2006)

1.2.1.3 Solar Dish

A dish-Stirling system is a type of concentrating solar power (CSP) system that consists of a parabolic dish-shaped collector, receiver and Stirling engine. The collector focuses direct normal solar radiation on the receiver, which transfers heat to the engine's working fluid. The engine in turn drives an electric generator. A dish-Stirling power plant can consist of a single dish or a field of dishes.

Parabolic dish-engine plants arrange mirrors in a configuration similar to a satellite dish and concentrate solar energy on a power conversion unit. In this unit, solar energy heats a working fluid, which is usually hydrogen gas, and powers an engine with an electricity generator. High efficiency Stirling engines are typically used in these plants and the units are modular with capacities ranging from 10 to 25 kW.

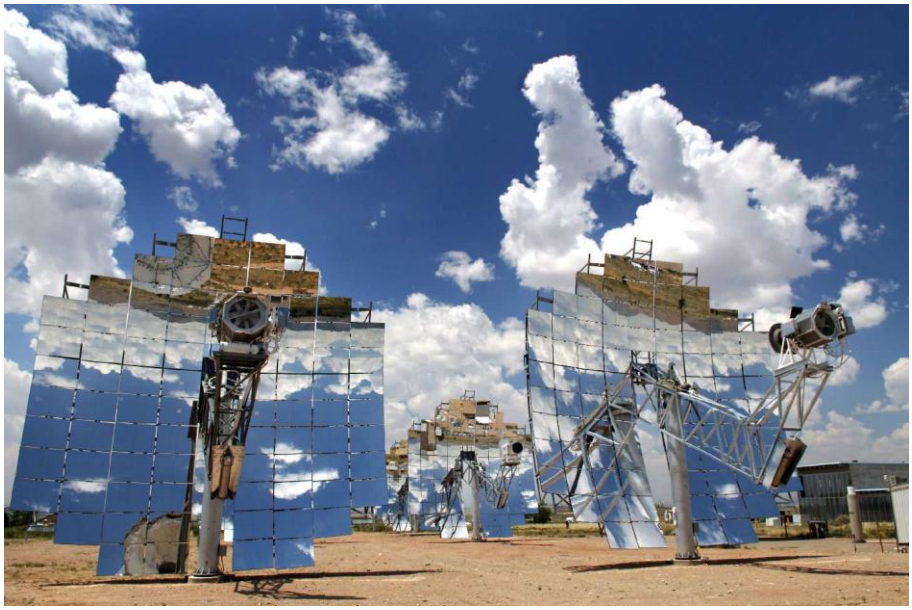

Figure 1.5 Dish Systems at Sandia National Labs (SES website, 2006)

A solar dish/engine system utilizes concentrating solar collectors that track the sun on two axes, concentrating the energy at the focal point of the dish because it is always pointed at the sun. The solar dish's concentration ratio is much higher than the solar trough, typically over 2,000, with a working fluid temperature over 650^{o}C. The power-generating equipment used with a solar dish can be mounted at the focal point of the dish, making it well suited for remote operations or, as with the solar trough, the energy may be collected from a number of installations and converted to electricity at a central point.

The engine in a solar dish/engine system converts heat to mechanical power by compressing the working fluid when it is cold, heating the compressed working fluid, and then expanding the fluid through a turbine or with a piston to produce work. The engine is coupled to a pump for water pumping purpose and an electric generator to convert the mechanical power to electric power.

This technology also has the capability of combining the thermal output of several dishes to supply a central multi-megawatt power plant. In the market-introduction phase, pilot demonstrations of several tens of dish-Stirling units will compete in generation cost with photovoltaic systems of similar size. The lower cost will be achieved through: improvements in mirrors and support structures, improvements in hybrid heat-pipe and volumetric receivers coupled to sterling and Brayton engines, and development of control systems for fully automatic operation; and improvements in system integration by reduction of parasitic loads, optimization of startup procedures, better control strategies, and hybrid operation of the Stirling and Brayton engines.

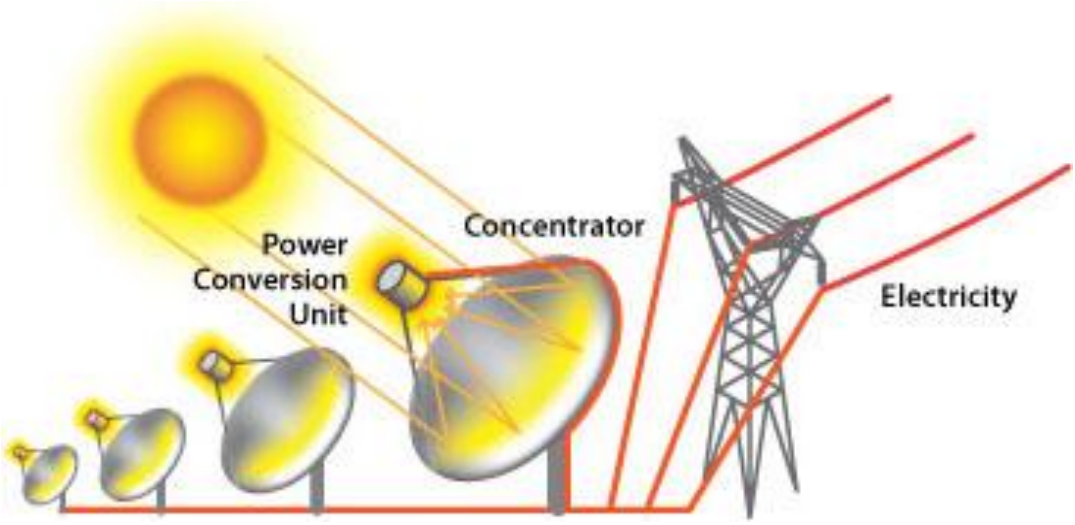

Figure 1.6 Stirling Dish Power Plants with Grid Connection (http://en.wikipedia.org)

1.3 Concentrating Solar Power

Systematic development of three CSP technologies troughs, towers, and dishes has led to the ever-increasing ability of these technologies to concentrate and harness solar energy for electricity production and other uses with efficiency, reliability, and cost effectiveness.

Commercial applications from a few kilowatts (kW) to hundreds of megawatts (MW) are now feasible. Today world has pursued a focused program on research and development in the field of concentrating solar power.

1.4 Status of CSP

Parabolic dish-engine technologies actually date back to the 1800's but modern technology development started in the late 1970's and early 1980's. Since that time, several prototype units have been tested and most recently a six dish test system was installed at the Sandia National Laboratory in 2005 (Solar PACES, 1997; Stoddard et al., 2006). The first large plant utilizing Stirling dish technology, rated at 1.5 MW, came online in January 2010 in Peoria, AZ, and plants rated for several hundred MW are in the planning stages. Stirling Energy Systems has also developed a power purchase agreement with Southern California Edison for the next 20 years. Stirling Energy Systems will deploy 20,000-34,000 solar dish Stirling systems at the Solar One site in the Mojave Desert, and will sell off the generated electricity to SCE.46 At their Solar Two site, they will construct between 12,000-36,000 solar dish Stirling systems and sell the electricity to San Diego Gas & Electric as a result of another 20-year power purchase agreement (D. Howard , 2010).

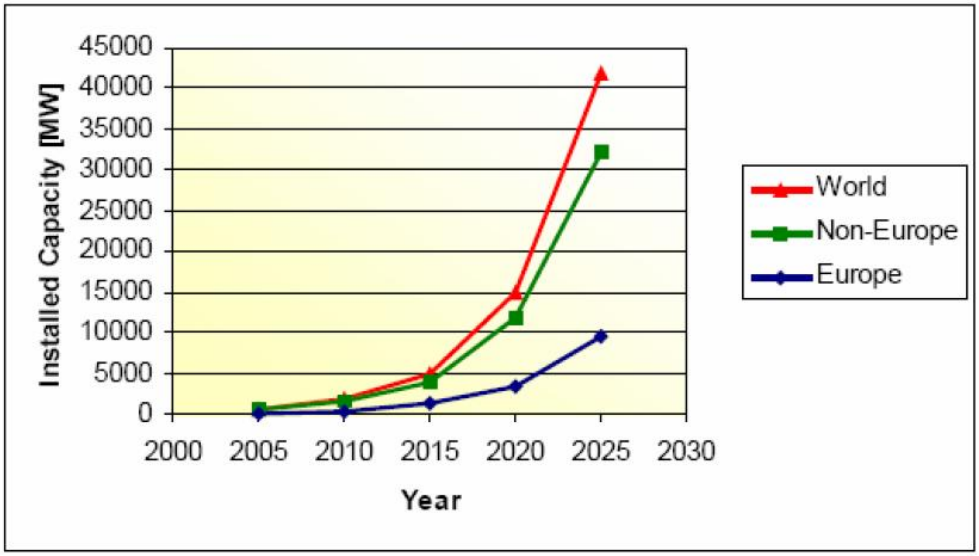

Figure 1.7 Atheene Scenario on the Development of Concentrated Solar Power Systems (www.dlr.de/sokrates)

1.5 Background of the Study

The Dish Stirling Systems have decades of recorded operating history. Dish Stirling Systems are flexible in terms of size and scale of deployment. Owing to their modular design, they are

capable of both small-scale distributed power output and, suitable for large, utility scale projects with thousands of dishes arranged in a solar park. This technology uses no water in the power conversion process (either for steam generation or cooling) and the only water needed is for the washing of the mirrors.

Table 1.1 Water Use by Power Plant (http://www.seia.org/cs/state_fact_sheets)

Power Plant Type	Water Use (Gallons/MWh)
Nuclear	620
Coal	670
Combined Cycle Natural Gas	250-300
Parabolic Tough (Wet Cooled)20	1,000
Parabolic Trough (Dry Cooled)21	80
Dish/Stirling	4.4
Photovoltaic (PV)	4.4

Dish Stirling technologies are furthermore attractive due to their high efficiency and modular design, which gives the systems several key advantages, including a higher degree of slope tolerance and site flexibility, meaning it does not require flat land, significantly reducing grading costs and environmental impact; high overall availability due to the fact that there is no singular point of failure and scheduled maintenance on the dishes can occur on individual units while the others continue to generate power; and a low-cost of manufacture and deployment as a result of high-throughput automotive style production and assembly (Concentrating Solar Power Projects).

Table 1.2 Characteristics of Concentrating Solar Power System

(http://www.nrel.gov/csp/solarpaces)

System	Peak Efficiency	Annual Efficiency	Annual Capacity Factor
Trough	21%	10 to 12%(d) 14 to 18%(p)	24%(d) 25 to 70%(p)
Power Tower	23%	14 to 19%(p)	25 to 70%(p)
Dish/Engine	29%	18 to 23%(p)	25%(p)
(d)=demonstrated	(p)=Projected based on pilot scaling		

The typical parabolic dish system's electrical peak output is only 25kW. They are compact, requiring only four acres per installed MW, and can be erected in a matter of days. Stirling-powered parabolic dish systems are the most efficient solar generating technology, and can ramp up to grid synchronization within a minute. Since sun light is free, they have no fuel cost. Their environmental impact is small due to the lack of a need for cooling water, since the Sterling engine is air-cooled. However, parabolic dish systems have the highest initial capital costs out of all the other solar thermal technologies at $2,650/kW (Concentrating Solar Power Projects). Because a single parabolic dish systems can be operated as a standalone generating unit, power plant operators benefit from being able to assess performance prior to investing hundreds of millions of dollars to build out a solar thermal plant based on parabolic trough or power tower technologies.

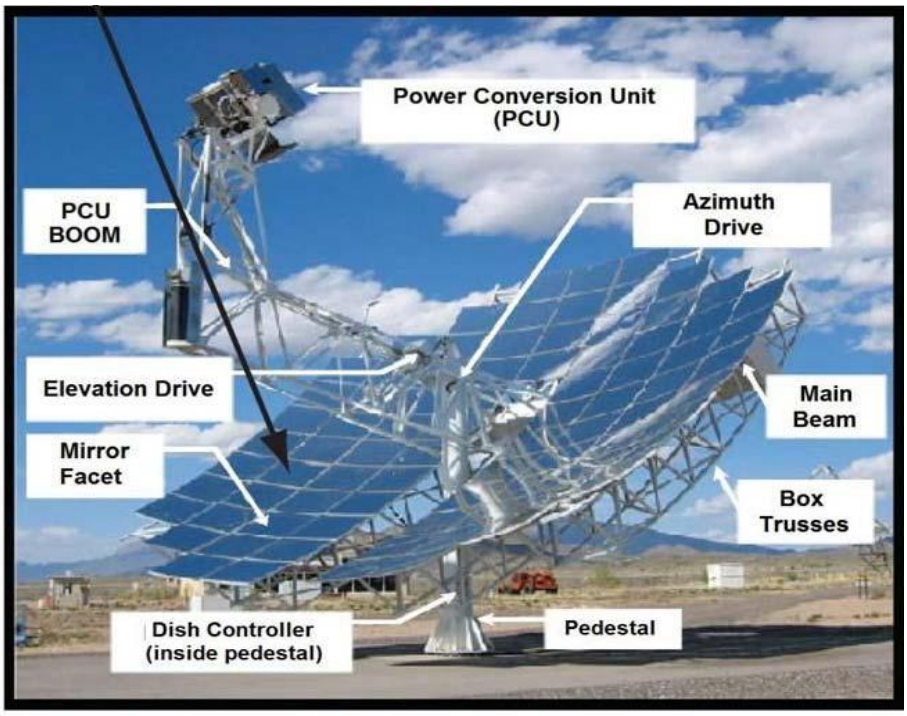

Figure 1.8 Sandia Photo of Their STC Dish (www.StirlingEnergy.com)

The Dish Stirling System consists of a solar concentrator in a dish structure that supports an array of curved glass mirrors. The parabolic dish tracks the sun throughout the day and concentrates the radiation onto the heat absorption unit of a Stirling engine. The focused solar thermal energy is then converted to grid-quality electricity. The conversion process involves a closed cycle, high-efficiency solar Stirling engine using an internal working fluid (usually hydrogen or helium) that is recycled through the engine. The working fluid is heated and pressurized by the solar receiver, which in turn powers the Stirling engine.

Sometimes the dish solar concentrator cannot completely meet the desired input to the Stirling engine due to hourly variation of temperature below the required amount for the power plant, so proper modeling and simulation must be performed prior to the development of the dish solar concentrator. The result would integrate the capital cost, performance and financial constraints into a single model. This allows detailed design of project optimization to be carried out where all interactions between cost and performance can be accounted.

An efficient engine provides more output for a given size concentrator, leading to lower cost power. The high efficiency Stirling engine is the leading candidate for concentrating parabolic

dish solar collectors. Because Stirling engine efficiency increases with hot end temperature, it is necessary to operate the engine at as high a temperature as possible. Temperatures beyond the operating capabilities of existing engines are easily obtained by solar concentration. Stirling engines, therefore, operate at thermal limits of materials used for their construction. Typical temperatures range from 650^0C to 800^0C resulting in engine conversion efficiencies of around 30% to 40%.

Because of their high heat transfer capabilities, hydrogen and helium have been used as a working gas for dish Stirling engines. Hydrogen, thermo dynamically a better choice, generally results in more efficient engines than does helium (Sandia, Stirling Energy Systems). Helium, on the other hand, has fewer material compatibility problems and is safer to work with.

Dish-Stirling engine systems require long life design. To make systems economical a system life time of at least 10 years with minimum maintenance is generally required. Desired engine life times for electric/mechanical power production are 40,000 to 60,000 hours approximately 10 times longer than that of a typical automotive internal combustion engine. Major overhaul of engines, including replacement of sealing and bearings, may be necessary within the 40,000 to 60,000 hour life time, which adds to the operating cost. A major challenge, therefore, in the design of dish/Stirling engines is to reduce the potential for wear in critical components or create novel ways for them to perform their tasks.

1.6 Objective of the Thesis

This thesis has the following main objectives.

- To properly design and model a parabolic dish power plant, taking into consideration the different losses associated with collection of the solar irradiance and other thermal losses;
- To simulate the model using the proper simulation software (e.g. TRNSYS, EES) and make performance evaluation;
- To make cost and financial analysis of the power plant using the appropriate software (Solar Advisor Model (SAM)).

1.7 Methodology

First literature review of relevant materials on parabolic dish collectors and power production from Stirling engine is conducted. The literatures available are from electronic media, journals, and books. Secondary data are referred from previous and related research studies, existing statistical data, etc.

Necessary weather data are collected from available sources. Next the power plant is modeled using EES and TRNSYS. TRNSYS software is used to simulate the power plant at weather conditions. This software is selected than similar software's for its simplicity and flexibility. Cost and financial analysis is also made using Solar Advisor Model (SAM). Finally conclusion and recommendation are made.

1.8 Outline of the Thesis

This thesis has six chapters. The first chapter deals with the introduction part. The second chapter deals with the solar dish field model. In this chapter different solar associated terms and the different heat losses from the parabolic dish are discussed briefly. The third chapter is used to model the Stirling dish power plant. This chapter includes modeling of the different components in the power plant. The fourth chapter is used to simulate the power plant at weather conditions off reference values. In this chapter TRNSYS software is used. The results of the simulation are also given in this chapter. Cost and financial analysis of the power plant is made using solar advisor model (SAM) in the fifth chapter. The different costs associated with parabolic dish solar electric generation systems and the different financial terms are briefly discussed. The final chapter is used to present the different conclusions and recommendations derived from the thesis work.

CHAPTER TWO

Stirling Dish System Component Modeling

2.1 Introduction

The Stirling dish system shown in Figure 2.1 produces electricity using concentrated solar thermal energy to drive a Stirling engine. The system utilizes a parabolic mirror equipped with dual-axis tracking to concentrate solar radiation onto a thermal receiver integrated in the Stirling engine. The receiver consists of a heat exchanger designed to transfer the absorbed solar energy to the working fluid, typically, hydrogen. The Stirling engine then converts the absorbed thermal energy to mechanical power by expanding the gas in a piston-cylinder in a manner similar to a gas or diesel engine. The linear motion is converted to a rotary motion to turn a generator to produce electricity. The Stirling dish systems can produce electricity from the sun with efficiencies up to 29 % (Teagan, 2001).

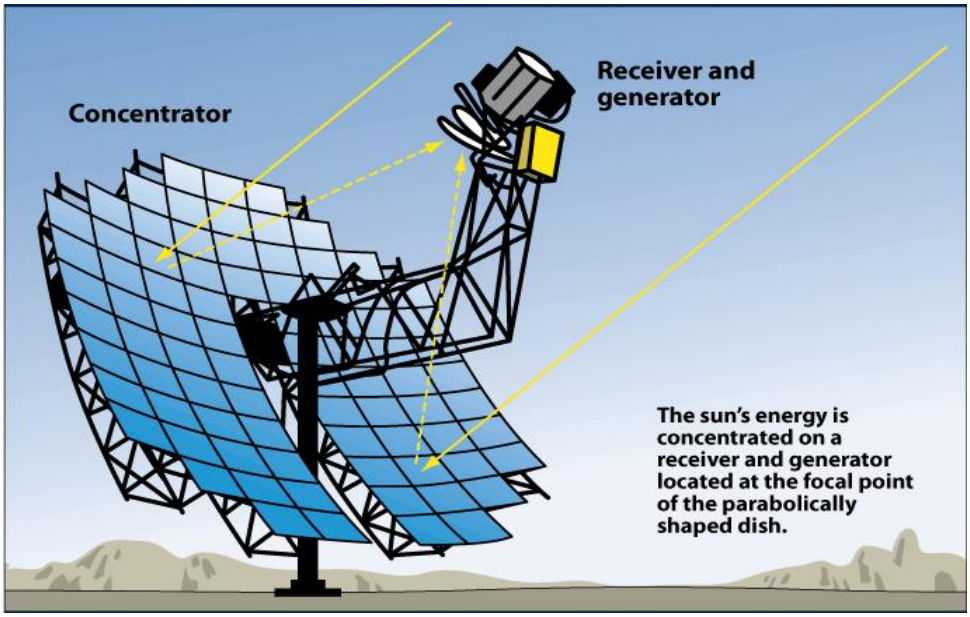

Figure 2.1 Solar dish/Engine System (source: Florida State university)

2.2 Sizing and Structural Design of Parabolic Solar Dish

2.2.1 Concentrators

Solar concentrators used for engine applications are generally point-focus parabolic dish concentrators. A reflective surface, metalized glass reflects incident sunlight to a small region called the focus. Because they concentrate solar energy in two dimensions, these collectors track the sun's path along two axes. Here the size of the solar collector for dish/Stirling system is determined by the minimum monthly average beam radiation, 283.2Wh/m^2, thermal loss, and reflectivity of the reflector. With current technologies, a 5-kW_e dish/Stirling system requires a dish of approximately 5.5 meters in diameter, and a 25-kW_e system requires a dish approximately 10 meters in diameter.

Concentrators use reflective surfaces of aluminum or silver, deposited either on the front or back surface of glass. Thin glass mirrors with a silvered back surface have been used in the past. Some current designs use thin polymer films with aluminum or silver deposited on either the front or back surface of the film.

The ideal shape for reflecting surface of a solar concentrator is paraboloid .This shape is ideal because a reflecting paraboloid concentrates all solar radiation coming directly from the sun to a very small region at the concentrator's focal point. Some concentrators for dish/Stirling systems used multiple spherically shaped mirrors faces supported by a truss structure in Figure 2.2, with each facet individually aimed so as to approximate a paraboloid. This approach to concentrator design makes very high focusing accuracy possible.

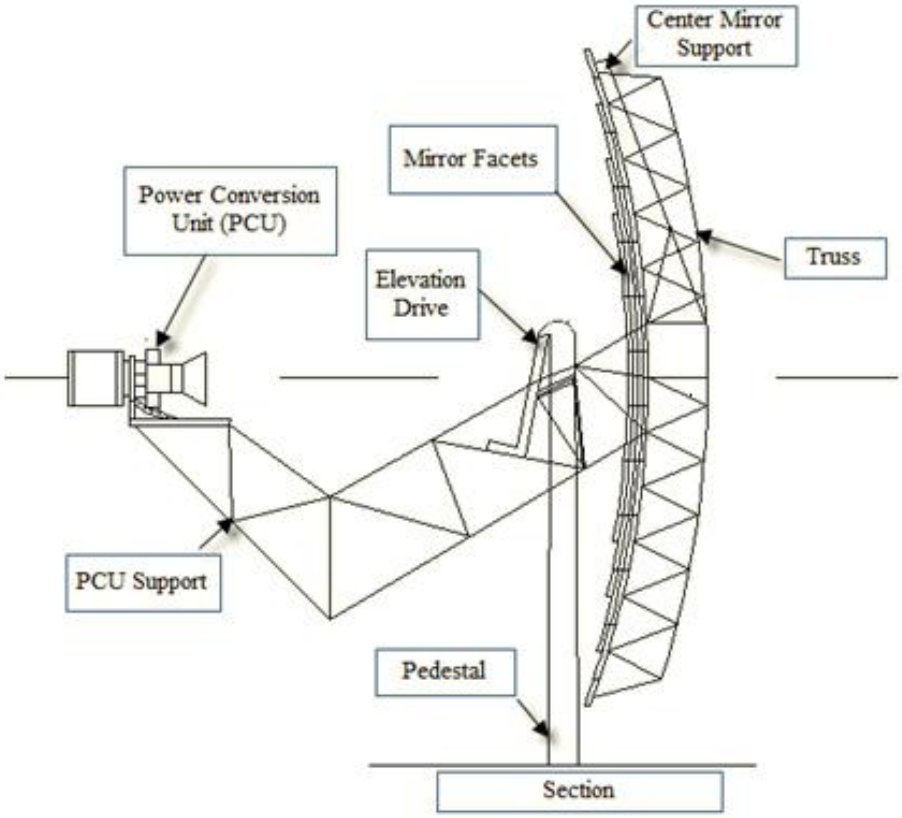

Figure 2.2 Faceted Parabolic Dish Concentrator with Truss Support

A recent innovation in solar concentrator design is the use of stretched membranes. Here a thin reflective membrane is stretched across a rim (or hoop), with a second membrane closing off the space behind. A partial vacuum is drawn in this space, bringing the reflective membrane into an approximately spherical shape.

If many facets are used, there focal regime will be a number of facet diameters away, and the spherical shape of the facets provides adequate solar concentration for the dish/Stirling applications.

If only one new or a few stretched membranes are used the surface shape should approximate a paraboloid. This approximation can be achieved by initially forming the membrane in to a near paraboloid, and using the pressure difference between front and back to support the surface and maintain its shape.

In addition to having adequate reflective materials and shape, effective dish Stirling concentrators focus the maximum available light by tracking the sun's path. In order to track the sun, concentrators must be capable of moving about two axes.

Generally there are two ways of implementing this, both having advantages:

- The first is azimuth elevation tracking, in which the dish rotates in a plane parallel to the earth (azimuth) and in another plane perpendicular to it (elevation).This gives the collector up/down and left/right rotations. Rotational rates about both axes vary throughout the day but are predictable. The faceted concentrator in Figure 2.3 uses an azimuth-elevation tracking mechanism.
- In the polar tracking method, the collector rotates about an axis parallel to the earth's axis of rotation. The collector rotates at a constant rate of 15 degrees per hour, the same rotation rate as the earth. The other axis of rotation, the declination axis, is perpendicular to the polar axis. Movement about this axis occurs slowly and varies by ± 23.5 degrees over a year (a maximum rate of 0.016 hours per hour).

2.2.2 Parabolic Concentrator Property

The paraboloid has the unique property that an-axis parallel beam of radiation will be reflected by the surface and concentrated at its focus (or conversely, a point source located at the focus will produce a parallel beam on reflection). This feature is illustrated in the diagram below - parallel rays enter from the left and are brought to a focus at a single point.

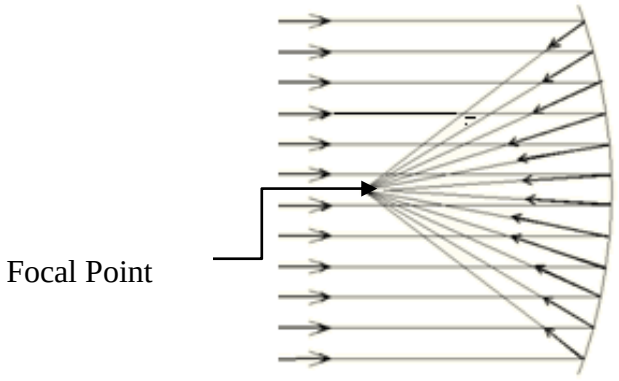

Figure 2.3 The Focusing Action of a Parabola

If it were required to generate electricity, the parabolic concentrator must be sized to deliver about four times more thermal energy than the rated electrical output due to an average net system efficiency of around 25 % to 30 %.

2.2.3 Collector Design Criteria

The parabolic concentrator reflects direct normal solar radiation into the aperture of the receiver where it is concentrated on the absorber. The aperture must be designed to be large enough to enable a significant fraction of reflected radiation from the concentrator to be transmitted onto the absorber, although there is a drawback with designing it too large. Increasing the aperture size will increase the amount of solar radiation intercepted by the receiver, but also increase the losses due to convection and radiation out of the aperture. Convection and radiation losses decrease the effective radiative energy absorbed in the receiver. Analysis is necessary to determine the impact of receiver loss mechanisms resulting from errors in the collector system, aperture diameter and the temperature of the absorber.

2.2.3.1 Intercept Factor

The intercept factor is the fraction of solar radiation reflected from the parabolic collector that enters the aperture. It is influenced by the size of the aperture, errors in the collector system, the collector rim angle and nonparallel sunlight. Increasing the intercept factor will increase the fraction of the energy entering the receiver, although this may not always be beneficial. If there is an increase in the intercept factor as a result of reducing errors in the parabolic reflecting collector surface, then an increase in the intercept factor will improve the system performance. If the increase in the intercept factor is accomplished by increasing the size of the aperture, there are competing effects; an analysis is required to determine if the increase in energy intercepted by the receiver will be greater than the energy lost due to thermal losses.

2.2.3.2 Beam Spread

The beam spread is the distance light spreads perpendicular to its direction of propagation after it has reflected off of the collector surface. Reducing the spread of the beam between the point where it reflects off of the collector and to where it enters the focal plane of the receiver will allow for the aperture to be designed smaller, leading to an increase in system performance. Ray tracing can be used to determine how far the beam of sunlight will spread, and the parameters to

solve for the beam spread include the collector rim angle, nonparallel rays, collector errors, and focal length.

2.2.4 Analysis of Solar Dish Data

The design of the dish for trapping solar radiation requires precise knowledge regarding the ability of beam radiation at the location of interest. Since solar radiation reaching on the earth's surface depends up on climatic conditions of the place, a study of solar radiation under local climatic conditions is essential.

In developing countries such as Ethiopia, due to the absence or malfunctioning of measuring instruments, reliable solar radiation data is not available. In the absence and scarcity of trustworthy solar radiation data, the use of empirical model to predict and estimate solar radiation seems inevitable. However, for this paper, the data used for the Kombolcha is found from the design SEWERA website. The weather data of year 2001 G.C for Kombolcha weather condition is used for this paper.

2.2.4.1 Direct Normal Radiation from SEWERA Data

The hourly direct normal radiation is calculated for every month and the minimum average is taken for the solar dish design.

Table 2.1 Summary Showing Results of Average Direct Normal Radiation for Each Month of the Year 2001

Monthly Average Direct Normal Radiation of Kombolcha [W/m^2]												
	Jan	**Feb**	**March**	**April**	**May**	**June**	**July**	**Aug**	**Sep**	**Oct**	**Nov**	**Dec**
6:01- 7:00	31	17	38	53	76	68	27	14	35	86	122	69
7:01- 8:00	337	274	274	278	270	289	174	162	221	355	485	440
8:01- 9:00	545	479	463	422	417	440	325	292	364	517	670	646
9:01-10:00	652	559	546	478	476	480	365	355	442	587	728	701
10:01-11:00	697	634	542	527	532	500	418	399	462	580	757	774
11:01-12:00	708	678	584	527	519	499	428	385	477	587	703	771
12:01-13:00	765	649	594	495	496	504	427	440	471	524	726	721
13:01-14:00	743	658	580	507	456	438	341	463	459	505	713	713
14:01-15:00	702	594	533	449	440	411	348	358	403	487	658	634
15:01-16:00	701	529	465	365	379	395	324	368	359	402	563	578
16:01-17:00	541	434	339	299	326	273	322	264	319	286	434	473
17:01-18:00	370	270	209	140	182	172	176	155	118	113	144	192
18:01-19:00	37	33	32	16	19	22	19	12	4	0	0	1
Average	525.3	446.8	399.9	350.5	352.9	345.5	284.2	282	318	386.8	515.6	516.4

After determination of minimum average direct normal radiation, sizing of the dish is performed with the minimum value.

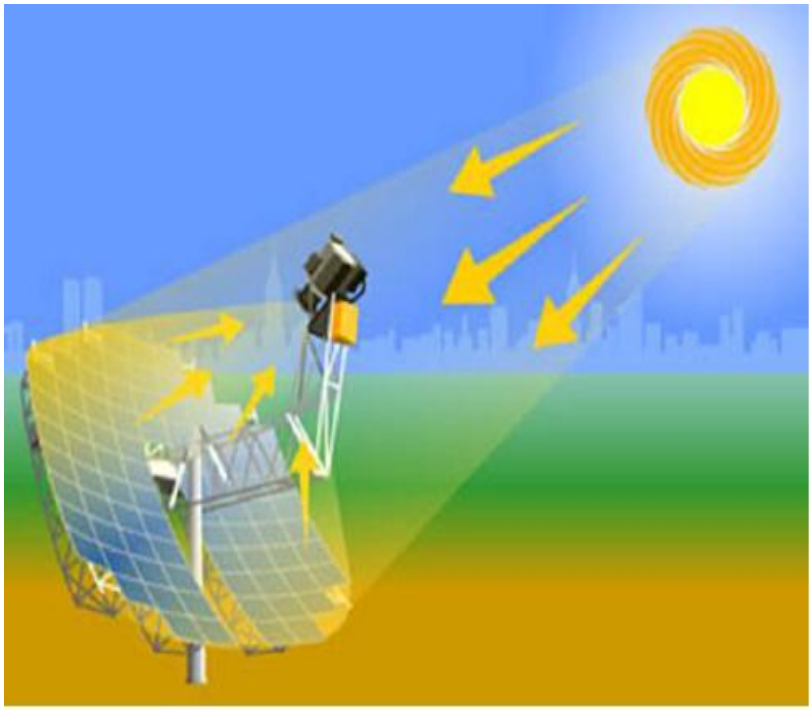

Figure 2.4 Parabolic Dish (www.StirlingEnergy.com)

2.2.4.2 Sizing of the Collector

Sizing of the diameter of the dish is done based on the solar radiation intensity falling on one meter square area of the selected site.Thus as can be seen in Table 2.1, above, the minimum monthly average solar radiation intensity falling on $1m^2$ area from the listed months is August. The minimum average direct normal radiation is $282W/m^2$ for the selected site. This beam radation is used for the analysis of the dish sizing.

The peak hours that the dish traps solar radiation is 13 hours per day, from 6 AM in the morning to 19 PM in the evening as shown in Table 2.1. The solar dish is sized assuming the reflectivity of the dish surface (aluminum) to be 0.94.

There is $282W/m^2$ of energy for the concentrator dish at the minimum radiation month (August) and to collect 25 kW energy area of πr^2 is required. From this relation, the radius of the concentrator dish is calculated as:

$$r^2 = \frac{25000W \times 1m^2}{282\pi} = 28.24m^2 \quad \text{..... (2.1)}$$

$$r = 5.33 \pm 0.05 \ \ m = 5.38m$$

A 0.05m tolerance is added to the radius for the shading effect of the power conversion unit and its support. From the above calculation, 5.38 m radius dish is used to supply enough solar power for the required power by the Stirling engine. The aperture diameter is then:

$$D_A = 10.76m$$

The area of the dish can also be calculated as:

$$\boldsymbol{A = \frac{\pi D^2}{4} = \frac{115.86\pi}{4}} \quad \text{..... (2.2)}$$

$$\boldsymbol{A = 91m^2}$$

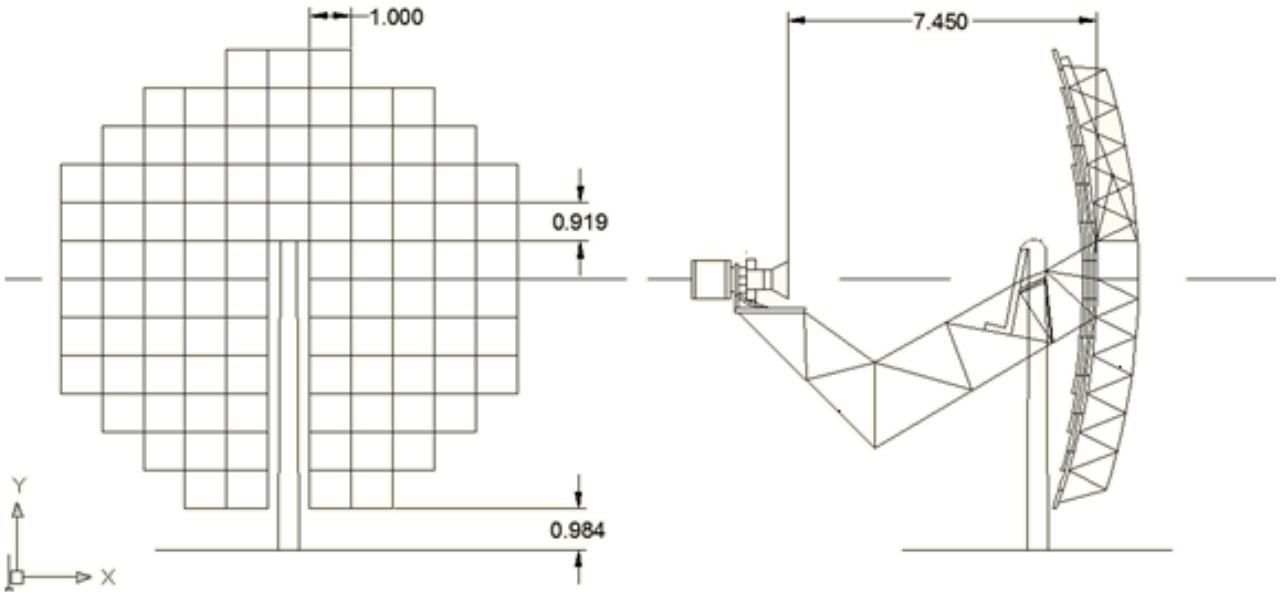

Figure 2.5 Parabolic Reflector Structure for 25kW Stirling Dish System

2.2.4.3 Focal Point Depth

A parabola is a one dimensional curve and is a section through a paraboloid - a paraboloid is formed by rotating a parabola about its axis. The equation of a parabola is:

$$y = ax^2 \quad \text{..... (2.3)}$$

where: a is a constant.

For a parabola with a focal length of f:

$$a = \frac{1}{4f} \quad \text{..... (2.4)}$$

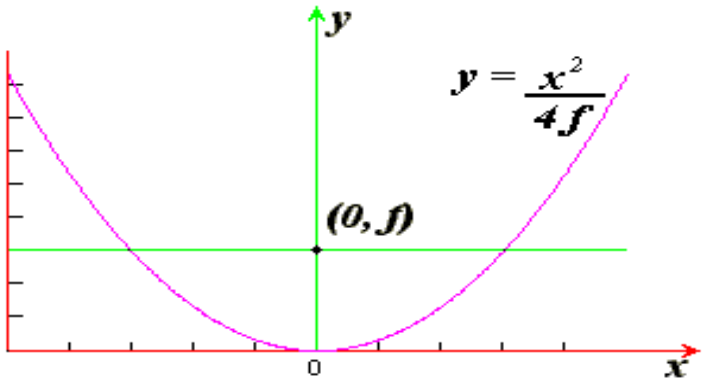

Figure 2.6 Parabola Equation

Parabola - focal length = f

The axis of the parabola is coincident with the y-axis and the focus is located at (0, f). Assuming the depth of the dish 1m and from the radius, it is possible to take two points on the parabola one at the origin and the other at the surface (aperture).Take coordinates (0, 0) and (5.38, 0.984) and substituting in Equation (2.3):

$$y = ax^2$$
$$a = 0.034$$

And from Equation (2.2)**,** f can be calculated as:

$$\boldsymbol{a = \frac{1}{4f} \quad \Rightarrow \quad f = 7.45\ m}$$

Thus the engine is positioned at 7.45m away from the origin of the parabolic dish.

The number of rectangles the dish is broken up into is:

$N_{rect} = 99$

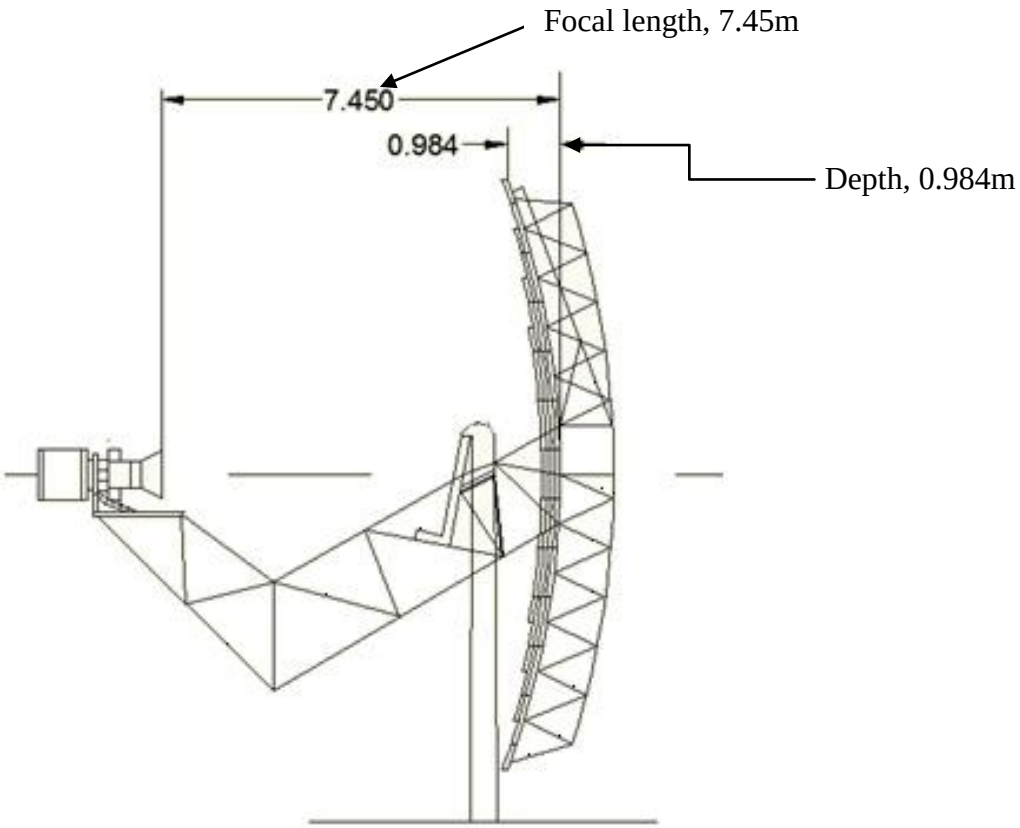

Figure 2.7 Focal Length of Parabolic Dish

In designing a parabolic reflector, it is often convenient to use its depth *d* instead of its focal length. The formula for obtaining the depth is:

$$d = \frac{D^2}{16f} = \frac{10.76^{\ 2}}{16 * 7.45} \qquad \Rightarrow d = 0.984m \quad \text{..... (2.5)}$$

2.2.4.4 Length of a Parabolic Segment

The formula for calculating the length *L* of a parabolic segment from the vertex to the edge is:

$$L = \frac{\ln\left(\sqrt{(4a^2D^2)+1}\right) + aD}{4a} + \frac{D\sqrt{(4a^2D^2)+1}}{4} \quad \text{..... (2.6)}$$

This formula is useful for calculating the length of a support rib on the outside of the parabolic reflector.

2.2.4.5 Surface Area of a Parabolic Reflector

The surface area of a parabolic reflector is calculated with this formula:

$$S = \pi \frac{\left(2D^2 + 1\right)^{\frac{3}{2}} - 1}{6a^2} \quad \text{..... (2.7)}$$

Where a, is defined in Equation (2.4). This formula is useful for estimating the amount of reflective materials needed for the parabolic reflector.

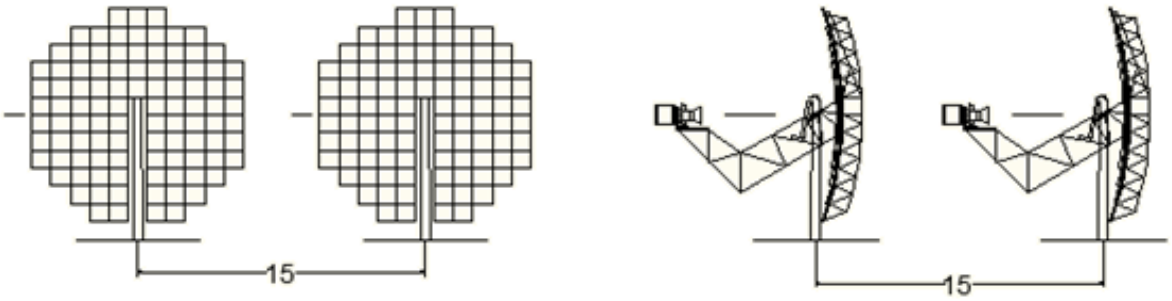

Figure 2.8 Distance Between Two 25 kW Stirling Dishes

2.2.4.6 Concentration Ratio

It is beneficial to obtain a high concentration ratio in the concentrator system since the aperture can then be designed smaller resulting in reduced thermal losses, and the intercept factor will be larger for a specified aperture diameter.

The extent to which the aperture area of the receiver is reduced relative to that of the concentrator is called the geometric concentration ratio, which can be expressed as:

$$\boldsymbol{CR_g = \frac{A_{app}}{A_{rec}} = \frac{91m^2}{0.0266m^2} = 3421} \quad \text{..... (2.8)}$$

where: $D_{receiver}$ = 184 mm selected integrated with the engine

A fundamental trade-off exists, between increasing the geometric concentration ratio and reducing the cost of the collector because collectors with high concentration ratios must be manufactured precisely. Generally, a direct correlation exists between the accuracy of the concentrator and its cost.

2.2.5 Power at Focal Point (Receiver) and Efficiency of the Collector

The concentrator of a dish/Stirling system intercepts radiation from the sun over a large area and concentrates into a small area. The receiver absorbs this energy and transfers most of it to the Stirling engine. The amount of heat going to the engine may be called (Q_{Input}), useful heat. A simple energy balance equation, called the fundamental solar collection equation, describes the theory underlying many aspects of the concentrator and receiver design. Equation (2.9) governs the performance of all solar energy collection systems and gives the design of dish/Stirling systems. The fundamental solar collection equation is:

$$\dot{Q}_{Input} = I_{bn} A_{pp} E \left(\cos\theta_i\right) \rho \phi \tau \alpha - \dot{Q}_{Loss,cav} \quad \text{..... (2.9)}$$

where:

Q_{Input} = Instantaneous rate of thermal energy coming from the receiver.

$$\dot{Q}_{Loss,Cav} = h_{cav} A_{cav} \left(T_{Cav} - T_a\right) + \sigma_B \varepsilon_{cav} F_{cav,a} \left(T^4_{Cav} - T^4_S\right) \quad \text{..... (2.10)}$$

I_{bn} = Beam normal solar radiation (insolation), hourly value is used.

A_D = Area of the concentrator dish

A_{rec} = Area of the receiver aperture

E = Fraction of concentrator aperture area not shaded by receiver struts and so on.

A = Receiver absorbance

τ = Transmittance of anything b/n the reflector and the absorber (such as window covering the receiver)

θ_i = The angle of incidence (angle b/n the suns ray and the line perpendicular to the aperture; for parabolic dish concentrators, this angle is 0 degrees.)

ρ = Concentrator surface reflectance

σ = Stefan-Boltzmann radiation transfer constant

ϕ = Capture fraction or intercept (fraction of energy leaving the reflector that enters the receiver).

Equation (2.9) shows that the amount of solar radiation reaching the receiver depends up on the amount available (determined by I_{bn} and θ_i). The effective size of the concentrator is determined by A_D and E and the concentrator surface reflectance (ρ).

Receiver thermal performance depends on receiver design, determined by τ and α and convection, conduction, and radiation losses.

The heat transfer rate that is delivered to the receiver, focal point of the collector; due to the collector is given by:

$$\dot{Q}_{FOCALPOINT} = I_{bn} A_D E \cos\theta_i \rho \phi \tau \alpha \quad \text{..... (2.10)}$$

where:

I_{bn}= 282 W/m^2 is the minimum insolation chosen (design value)

A_D= 91 m^2

E = 0.96 (Unshaded aperture area fraction, E is typically more than 0.95 in most designs.)

α = 1 and τ= 1

ρ = 0.94 (the surface of the concentrator is aluminum and the surface reflectance of aluminum is 0.94).

Assume ϕ = 0.85

$$\dot{Q}_{FOCALPOINT} = 282 * 91 * 0.96 * 1 * 0.85 * 0.94 * 1$$

$$\dot{Q}_{FOCALPOINT} = 19.68\,kW$$

The above values are for a unit dish only; to get for the entire field this value must be multiplied by number of dish in the field (400).

2.2.6 Concentrator Performance

The primary measure of concentrator performance is how much of the insolation arriving at the collector aperture passes through an aperture of a specified size located at the focus of the concentrator. This measure is called concentrator or optical efficiency and is defined as:

$$\eta_{Collector} = E(\cos\theta_i)\rho\phi \quad \text{..... (2.11)}$$

$$\eta_{Collector} = 0.96 * 1 * 0.94 * 0.85 = 0.77$$

2.2.7 Supporting Structure

Solar dish system construction can be abridged as follows: in concrete fundament, strong metal pedestal is fixed, carrying rotating truss structure of mirrors support and converter supporting arm, which stretches out to the focus of the mirrors system. At the end of the arm (in the focus) thermo electrical converter is located.

Sun tracking part of the system should be supported in its center of gravity. The aim is to achieve necessary strength and stiffness of the construction using material as less as possible. The mirrors carrying structure can in the same time be used as a part of the cooling system. The instrumentation, inverter, etc. is located nearby or on the pedestal. The solar dish is supposed to carry the total engine package together with the legs of the package supporting legs.

2.2.8 Tracking Mechanism

To get maximum thermal heat input to the receiver, the solar dish should track the sun, and the analysis is done assuming Ptolemaic view. Ptolemaic view says “the earth is fixed and the sun’s apparent motion is described in a coordinate system fixed to the earth with the origin being at the site of interest”.

The solar dish traces the sun using a sun tracer from 6 AM in the morning to 19 PM in the afternoon.

Parabolic dish concentrators must track about two independent axes so the rays of the sun remain parallel to the axes of the concentrator. There are two common implementations of two axes tracking; azimuth-elevation and polar (equatorial) tracking. Azimuth elevation tracking allows the concentrator to move about one tracking axis perpendicular to the surface of the earth (the

azimuth axis) and another axis parallel to it (the elevation axis). Polar tracking uses one tracking axis aligned with the axis of rotation of the earth (the polar axis) and another axis perpendicular to it (the declination axis).

The solar dish should trace the sun continuously in solar altitude axis and azimuth axis to increase the efficiency of power generation. In this paper tracking of the sun in azimuth axis can be done seasonally by manual rotation. However hourly tracking of the sun is indispensable, to this idea a solar tracker is used for solar altitude axis tracking. Solar tracker tracks the motion of the sun across the sky to maximize power output. A good solar tracker can typically lead to an increase in power generation capacity of 30-50%.

2.3 Receiver Integrated in the Stirling Engine

The receiver is the interface between the concentrator and the engine. It absorbs concentrated solar flux and converts it to thermal energy that heats the working gas on the Stirling engine. The absorbing surface is usually placed behind the focal point of a concentrator so that the flux density on the absorbing surface is reduced. An aperture is placed at the focus to reduce radiation and convection heat loss from the receiver. The cavity walls behind the receiver aperture and absorber surface are refractory surfaces. The size of the absorber and cavity walls is typically kept to a minimum to reduce heat loss and receiver cost.

The receiver has two functions:

- To absorb as much, on the solar radiation reflected by the concentrator, as possible.
- To transfer this energy as heat to the engine's working gas.

Although a perfect reflecting parabolic reflects parallel rays to a point, the sun's rays aren't quite parallel because the sun isn't a point source. Also any real concentrator isn't perfectly shaped. Therefore concentrated radiation at the focus is distributed over a small region with the highest concentration of flux in the center, decreasing exponentially towards the edge.

Receivers for dish/Stirling engines system are cavity receivers with a small opening (aperture) through which concentrated sun light enters. The absorber is placed behind the aperture to reduce the intensity of concentrated solar flux. The insulated cavity between the aperture and the absorber reduces the amount of heat lost. The receiver aperture is optimized to be just large enough to admit most of the concentrated sunlight but small enough to limit radiation and

convection losses. In the receiver, two methods are used to transfer absorbed solar radiation to the working gas of the Stirling engine. In the first type of receiver, the directly illuminated tube receiver, small tubes though which the engines working gas flows are placed directly in the concentrated solar flux region of the receiver, (Figure 2.9) and (Figure 2.10).

The other type of receiver uses liquid metal intermediate heat transfer fluid (Figure 2.11).The liquid metal is vaporized on the absorber surface and condenses on tubes carrying the engine's working gas. This second type of receiver is called a reflux receiver because the vapor condenses and flows back to be heated again.

2.3.1 Types of Receivers Used in Dish/Stirling System

In general, two types of receivers could be used with parabolic dish concentrators:

- External (Omni directional)
- Cavity receivers

External receivers have absorbing surfaces in direct view of the concentrator and depend on direct radiation absorption. Cavity receivers have an aperture (opening) through which reflected solar radiation passes. The cavity ensures that most of the entering radiation is absorbed on the internal absorbing surface.

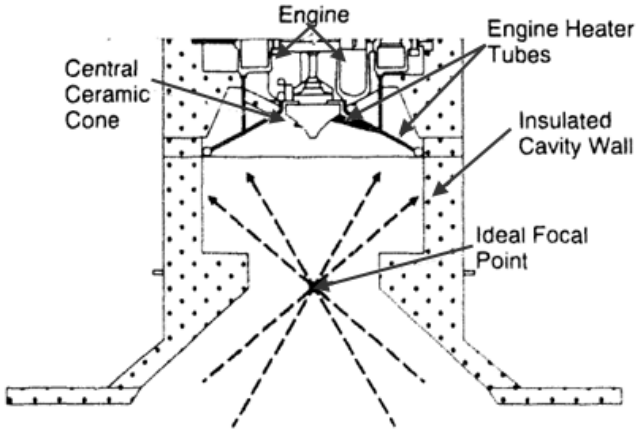

Figure 2.9 Directly Illuminate Tube Receiver (www.nrel.gov)

Because they generally have lower heat loss rates at high operating temperatures, only cavity receivers (instead of external receivers) have been used in dish/Stirling systems to date. External receivers however have been used in lower temperature parabolic dish applications.

A major advantage of cavity receivers is that the size of the absorber may be different from the size of the aperture. With a cavity receiver, the concentrator's focus is usually placed at the cavity aperture and the highly concentrated flux spreads inside the cavity before encountering the larger absorber surface area. This spreading reduces the flux rate of energy deposited per unit surface area incident on the absorber surface. When incident flux on the absorbing surface is high, it is difficult to transfer heat through the surface without thermally over stressing materials.

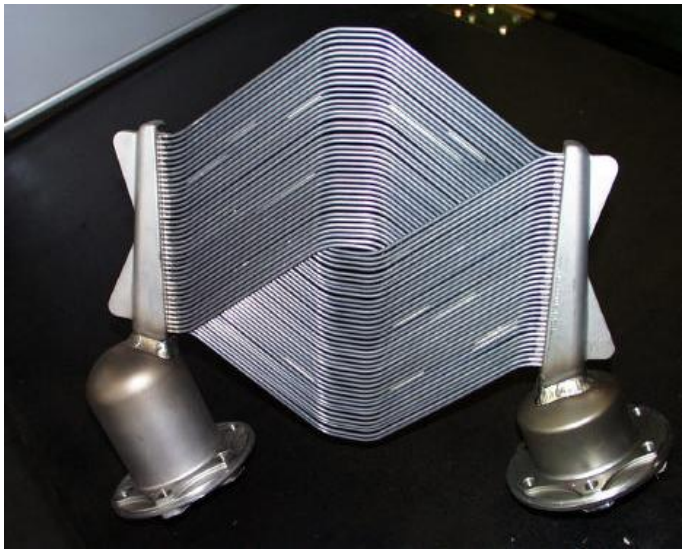

Figure 2.10 Stirling DIR Cavity Receiver (Ministerio De Educación Y Ciencia, 2006)

A second advantage of cavity receivers is reduced convection heat loss. the cavity enclosure not only provides protection from wind but also, depending on its design and angle, can reduce natural convection cavity receivers have generally lower overall heat loss and preferable to external receiver for high temperature applications such as dish/Stirling system.

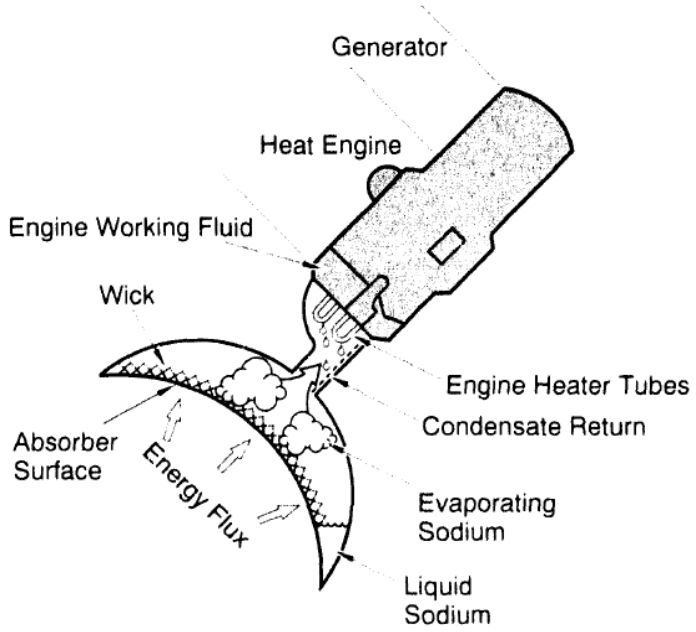

Figure 2.11 Heat pipe absorber for a Stirling dish receiver (Teagan, 2001)

Figure 2.12 shows a cavity receiver. The light enters through the cavity aperture (just in front of the inner shield for this receiver) to be absorbed on the cavity walls (coiled tubes in this case as solar-only receiver). A tube receiver was developed which is directly connected to the cylinder heads of the Stirling engine. The receiver consists of very thin tubes, approximately 3mm in diameter, which resists very high temperatures about 850^0C. Coiled tubes form an almost closed area which is the absorber surface shown in Figure 2.12. The concentrated solar radiation heats the working gas to approximately 650^0C.

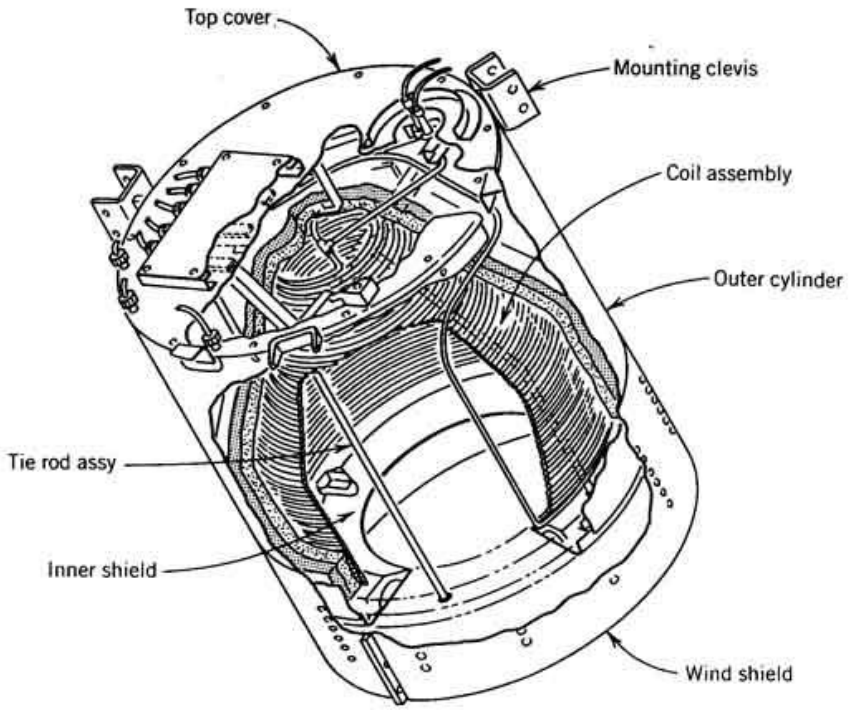

Figure 2.12 Cavity (Focal Plane) Receivers, (Courtesy of Sandia National Laboratories)

Typically, the plane of the cavity aperture is placed near the focus of the parabola and normal to the axis of the parabola. Thus, such a receiver is sometimes called a focal plane receiver.

In this thesis a cavity receiver is selected with the respective Stirling engine from standard catalog, it is integrated in the Stirling engine. Cavity receiver is selected for it is recommended in solar dish/Stirling systems and the advantages discussed in this section.

2.3.2 Cavity Receivers Heat Loss

The receiver of a Stirling dish system is responsible for the major thermal losses that occur before the energy is converted into electricity in the Stirling engine.

Mechanisms that contribute to the total receiver thermal loss include conduction through the receiver housing, convection from the cavity, and radiation through the aperture opening to the ambient environment. A receiver energy balance with the loss mechanisms can be viewed in Figure 2.13.

Conduction losses through the receiver housing represent a small fraction of the total receiver loss, natural convection losses represent about 40 % of the receiver losses, and radiation is the primary receiver loss mechanism. Radiation represents the largest fraction of receiver losses during mid-day periods when the receiver orientation reduces the convection losses, but convection can represent the majority of losses during the morning and evening when the aperture is oriented horizontally (Paul R. Fraser, 2008.).

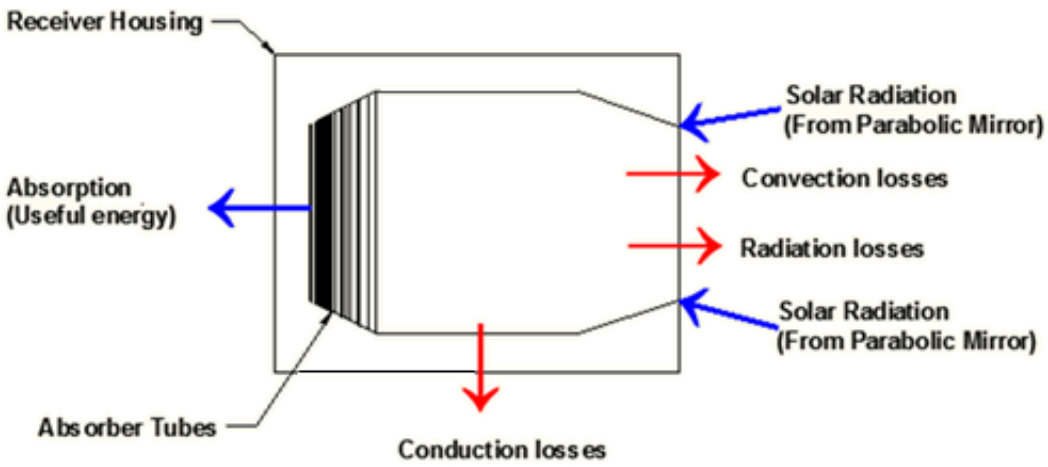

Figure 2.13 Receiver Energy Balance for a Dish/Stirling System

Heat loss from a cavity receiver of the type shown in Figure 2.12 can be computed similar to Omni directional receivers. The general idea of a cavity receiver is to uniformly distribute the high flux incident on its aperture over the large internal surface area of the cavity in order to reduce the peak flux absorbed at any point. Ideally, in a well-insulated cavity, the cavity temperature is reasonably uniform and heat loss occurs primarily by convection and radiation from the cavity aperture.

$$\dot{Q}_{Loss,Cav} = h_{cav} A_{cav} (T_{Cav} - T_a) + \sigma_B \varepsilon_{cav} F_{cav,a} (T^4_{Cav} - T^4_S) \quad \text{..... (2.11)}$$

where:

h_{cav} = Convective heat-transfer coefficient at outside surface of cavity receiver ($W/m^2 K$)

A_{cav} = Area of cavity receiver (m^2)

T_{cav} = Temperature of cavity receiver (K)

T_a = Ambient temperature (K)

σ_B = Stefan-Boltzmann constant ($5.67 \times 10^{-8} W/m^2 K^4$)

$\varepsilon_{cav,g}$ = Emittance of the glass

$F_{cav\ a}$ = Radiation shape factor

T_s = Sky temperature in K (typically assumed to be 6 K lower than ambient temperature)

Where the subscript "cav" refers to the cavity since the opening of a cavity can be quite small compared to the surface area of an Omni directional receiver, the heat loss is greatly reduced. In a typical calculation, the cavity temperature T_{cav} is assumed uniform and heat loss is computed as a function of this cavity temperature.

Conduction heat loss through the insulation and through the receiver support structure is computed in TRNSYS modeling part as shown in Appendix A.

2.3.3 Heat Input to Stirling Engine

As discussed above, the concentrator of a dish/Stirling system intercepts radiation from the sun over a large area and concentrates it into a small area. The receiver absorbs this energy and transfers most of it to the Stirling engine. The amount of heat going to the engine (heat received per unit time) called useful heat $\dot{Q}_{Inputt}$ is expressed as:.

$$\dot{Q}_{Input} = I_{bn} A_{pp} E \ \cos\theta_i \ \rho\phi\tau\alpha - \dot{Q}_{Loss,Rec} \quad \text{..... (2.12)}$$

Equation (2.12) is used to determine the useful heat delivered by the engine. In this equation, the first term is the heat transferred to the focal point of the solar dish, engine receiver; and the second term is the heat loss from the receiver. The net will be the useful heat to the Stirling engine (heat received by the engine per unit time).

As shown in Table 2.1 all other months have a greater monthly average beam radiation than that of August and since the dish is designed with minimum monthly average beam radiation, the solar dish can deliver greater power for the other the months.

Table 2.2 Summary Showing Results for Different Field Layouts

Summary Results for Different Field Layouts		
	Option 1	***Option 2***
Gross energy collected by the dish (kW)	10	25
Radius of the concentrator dish (m)	3.4	5.38
Area of the collector (m^2)	36.32	91
Focal Length (m)	5.45	7.45
Depth of the parabolic reflector	0.53	0.984
Number of dish required to collect 10 MW gross energy	1000	400
Diameter of the receiver selected integrated with the engine (mm)	140	184
Collector separation North-South and East-West (m)	12	15
Total solar field area (m^2)	144000	90000

The other requirement from the Stirling engine is, as seen in the literature part of Stirling engine, there are of two types: free piston and kinematic type. For this paper, kinematic type of Stirling engine is chosen.

2.4 Stirling Engine and Working Principle

Stirling engines are external combustion engines that use air or other gases as working fluid. A Stirling engine is a type of closed-cycle regenerative heat engine with a gaseous working fluid. "Closed-cycle" means the working fluid is permanently contained within the engine's system, which also categorizes it as an external heat engine. "Regenerative" refers to the use of an internal heat exchanger called a regenerator which increases the engine's thermal efficiency. The Stirling engine can run on any heat source, including chemical, solar, geothermal and nuclear. They can also burn any solid or liquid fuels as their heat source. This makes them very attractive, particularly in situations where conventional fuels are expensive and hard to obtain. Because some types of Stirling engine are so simple to make and yet so effective, they are excellent choices for power generation in developing countries. There are many design varieties of the Stirling engines; most of which fall into the category of reciprocating piston engine.

In the conversion of heat into mechanical work, the Stirling engine has the potential to achieve the highest efficiency of any real heat engine. It can perform theoretically up to the full Carnot cycle, though in practice this is limited. The practical limitations are the non-ideal properties of the working gas, and the engine material properties such as friction, thermal conductivity, tensile strength, creep, rupture strength and melting point.

In theory, the Stirling engine is the most effective device for converting heat to mechanical work; however it requires high temperature. Because concentrating solar collectors can produce high temperatures necessary for efficient power production, the Stirling engine and the concentrating solar collector are a good match for the production of power from the sun.

To maximize power, engines typically operate at high pressure, in the range of 5 to 20 Mpa. Operation at these high gas pressures makes gas sealing difficult, and seals between the high pressure region of the engine and those parts at ambient pressure have been problematic in some engines. New designs to reduce or eliminate this problem are currently being developed.

2.4.1 Basic Theory of the Stirling Engine

The Stirling cycle is shown in the diagram in Figure 2.14. The basic idea is that when gas in a closed cylinder is moved into the hot part of the cylinder, it expands, its pressure increases, and it can do work. When the gas moves into the cold part of the cylinder, its pressure is reduced. Once the gas reaches the lower pressure, it is compressed back to its original volume. The gas performs more work during its expansion than is required during its compression. Thus, the entire cycle results in the net positive output of work.

As shown in Phase 1 of Figure 2.14, the piston is at bottom dead center, and the displacer is in as far as it can go. The gas is in contact with the cold space, and the gas pressure is low. Note that the gas is at the same pressure at any instant in every part of the engine, but that this pressure is changing with time. Because the pressure is low, the piston can be moved in easily to compress the gas at the low temperature. At the end of this compression process, the engine has reached Phase 2, as shown in Figure 2.14.

Now it is time to increase the gas pressure. This is not done by burning a fuel inside the gas as is done in an internal combustion engine. The gas is moved from the cold space through a heat exchanger, which cause it to enter the hot space at a high temperature. Note that the gas in the heater, cooler, regenerator, and hot and cold spaces, is always at the same pressure at any instant, since the gas flow passages are large and do not restrict the passage of the gas.

As shown in Phase 3 of Figure 2.14, the gas is compressed, hot, and at high pressure. At this point it is ready to expand and to work on the piston. As the piston moves out of the cylinder, the displacer moves with it, in order to keep as much of the gas as possible in the hot space so that the pressure is kept as high as possible to do the maximum amount of work on the piston. This expansion and outward movement of the piston results in the attainment of Phase 4, as shown in Figure 2.14.

The next step is to reduce the gas pressure by moving it from the hot space through the heat exchangers to the cold space. This is done by moving the displacer from its position, as shown in Phase 4, back to its inward position, as shown in Phase 1. The cycle is now complete. Note that the piston has expanded the gas by moving outward when the gas is hot and at high pressure, and has compressed the gas when it is cold and at low pressure. Thus, the original plan has been accomplished, and the cycle has produced network to the outside.

For this four-phase process to continue indefinitely, heat must be continually added to the hot end from some outside source like a fire or a solar collector, and the cold end must be continually cooled by a stream of water or air.

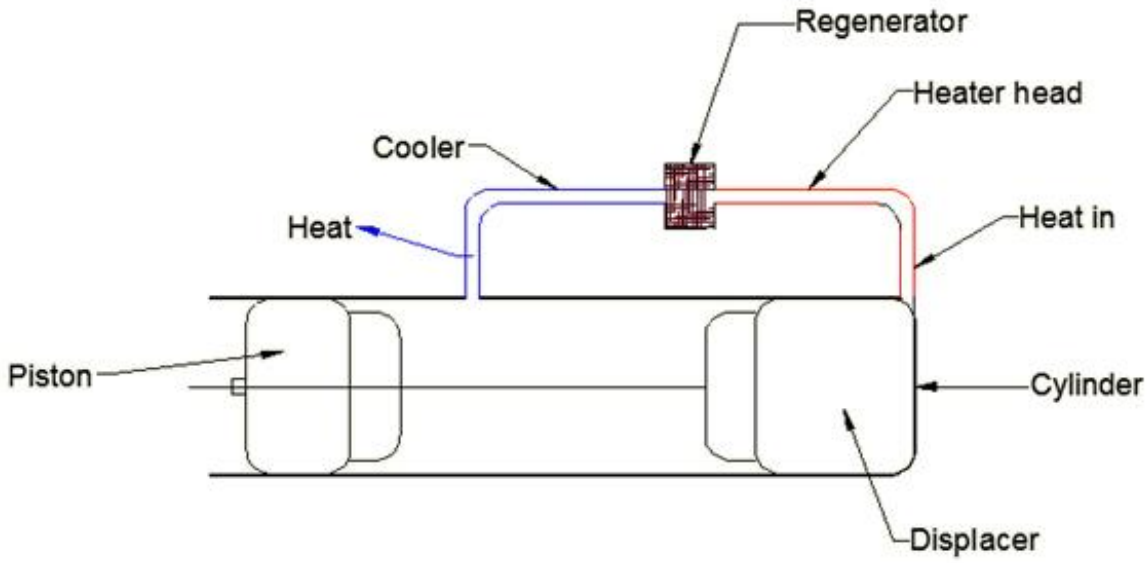

Phase 1: Piston at bottom dead center. Displacer at top dead center. All gas in cold space.

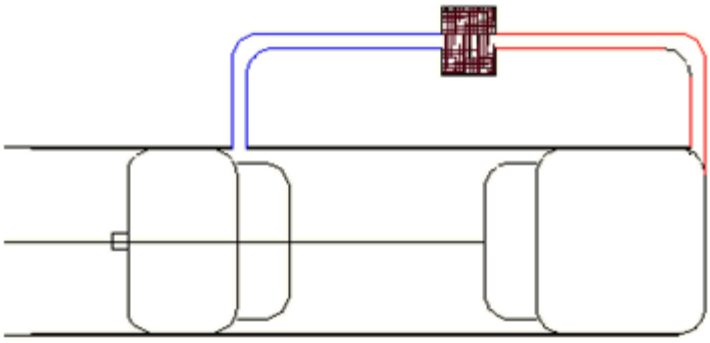

Phase 2: Displacer remaining at top dead center. Piston has compressed gas at lower temperature.

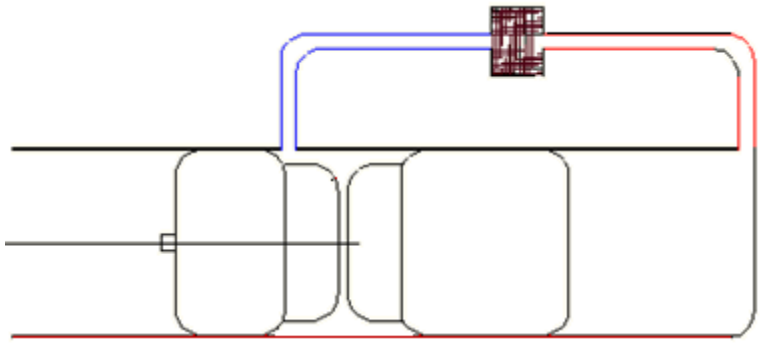

Phase 3: Piston remaining at top dead center. Displacer has shifted gas through cooler, regenerator, and heater into hot space

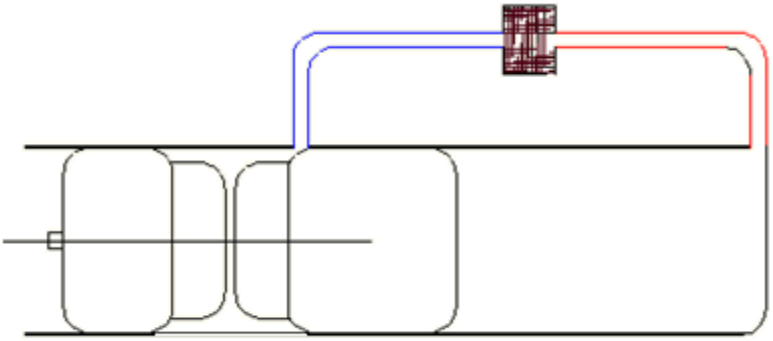

Phase 4: Hot gas expanded. Displacer and piston have reached bottom dead center together. With piston stationary, displacer now forces gas through heater, regenerator and cooler into cold space, thus Reattaining phase 1.

Figure 2.14 The Stirling Engine Cycle

The piston and the displacer clearly cannot move on their own. It should be known how the movements are accomplished. There are at least two ways to make the two components of the simple Stirling engine move:

The Stirling engine can be attached to cranks through connecting rods, as is commonly done in automobile engines or gas forces can be used in a carefully designed way so that they bounce on gas springs, with the displacer always ahead of the piston in its in-and-out oscillation. Of the two methods, the use of cranks called the crank-driven, or kinematic Stirling, is the more easily understood method. The second method, which uses oscillating motions of the piston and

displacer on springs, is called the free-piston Stirling. The crank-driven Stirling is easier to understand yet harder to make, while the free-piston Stirling is harder to understand yet easier to make in at least some of its forms.

2.4.2 Heat Engine versus Stirling Engine

A heat engine is a Stirling engine when:

- The working fluid is contained in one body at nearly a common pressure at each instant during the cycle.
- The working fluid is manipulated so that it is generally compressed in the colder portion of the engine and expanded generally in the hot portion of the engine.

Transfer of the compressed fluid from the cold to the hot portion of the engine is done by manipulating the fluid boundaries without valves or real pumps. Transfer of the expanded hot fluid back to the cold portion of the engine is done the same way. A reversing flow regenerator (regenerative heat exchanger) may be used to increase efficiency.

The Stirling cycle is potentially a better cycle than other cycles because it has the potential for higher efficiency, low noise and no pollution, that is, a hot and a cold gas space are connected by a gas heater and cooler and regenerator. As the process proceeds to produce power, the working fluid is compressed in the cold space, transferred as a compressed fluid into the hot space where it is expanded again, and then transferred back again to the cold space. Net work is generated during each cycle equal to the area of the enclosed curve in pressure volume diagram.

2.4.3 Power Control

For most Stirling engines, the engine power is controlled by varying the mean pressure within the expansion and compression space by varying the mass of the working fluid. This is accomplished by pumping gas in or out of the engine from an external tank (Walker, 1980). To increase the power from the Stirling engine, a system of valves is used to move high pressure gas from an external tank to the engine, and to decrease power, the working fluid is compressed back into the external tank (Stine, 1999).

Another method of controlling the Stirling engine power is to vary the volume within the piston cylinders with a variable stroke engine such as the SAIC (STM 4-120) Stirling engine (Walker,

1980). This method for power control can be accomplished by using a variable angle swash plate drive which enables the stroke to be controlled (Stine, 1999). This method effectively alters the displaced volume during each cycle and therefore changes the output power.

2.4.4 Regenerator

A regenerator consisting of many metal mesh disks is often used in Stirling engines to improve the efficiency of the engine (Stine, 1994). Thermal energy is absorbed by the regenerator when working fluid passes from the expansion space to the compression space, and therefore cools the working fluid before entering the compression space. Thermal energy is transferred from the regenerator to the working fluid and it is therefore pre-heated when the working fluid moves from the compression to the expansion space. The regenerator in a Stirling engine can obtain efficiencies of greater than 98 %, which indicates the working fluid will leave the regenerator close to the temperature of the space it occupies (Urieli and Berchowitz, 1984). A regenerator does not improve the output power of a specific engine design, but rather contributes to a minor reduction in output power due to the pressure losses across the regenerator. A large improvement in engine efficiency by using a regenerator far outweighs the minor reduction in specific power.

CHAPTER THREE

Component Model Using EES

3.1 Overview of Engineering Equation Solver (EES)

The basic function provided by EES is the solution of a set of algebraic equations. EES can also solve differential equations, equations with complex variables, do optimization, provide linear and non-linear regression, generate publication-quality plots, simplify uncertainty analyses and provide animations.

There are two major differences between EES and existing numerical equation-solving programs. First, EES automatically identifies and groups equations that must be solved simultaneously. This feature simplifies the process for the user and ensures that the solver will always operate at optimum efficiency. Second, EES provides many built-in mathematical and thermo physical property functions useful for engineering calculations.

The library of mathematical and thermo physical property functions in EES is extensive. EES allows the user to enter functional relationships in three ways. First, a facility for entering and interpolating tabular data is provided so that tabular data can be directly used in the solution of the equation set. Second, the EES language supports user-written Functions and Procedures similar to those in Pascal and FORTRAN. EES also provides support for user-written routines, which are self-contained EES programs that can be accessed by other EES programs. The Functions, Procedures, Subprograms and Modules can be saved as library files which are automatically read in when EES is started. Third, external functions and procedures, written in a high level language such as Pascal, C or FORTRAN, can be dynamically-linked into EES using the dynamic link library capability incorporated into the Windows operating system. These three methods of adding functional relationships provide very powerful means of extending the capabilities of EES.

3.2 Stirling Engine Modeling

The Stirling engine is an external heat (or combustion) engine that converts heat from the absorber to mechanical power in a manner similar to internal combustion engines. Unlike internal combustion engines, however, heat is applied externally to the piston heater head in a

Stirling engine. Because the Stirling engine relies on an external source for heat input, the cycle itself operates as a closed system since the working fluid is contained within the cylinders and not vented to atmosphere like exhaust gases from internal combustion engines. The addition of a regenerator into a Stirling engine improves the efficiency of the engine by pre-cooling the working fluid as it moves from the expansion space to the compression space, and pre-heating the working fluid as it moves from the compression space into the expansion space. The working fluid is often hydrogen which is heated to over 700°C with a maximum pressure around 20 MPa yielding a thermal-to-mechanical efficiency of approximately 40 %,[2].

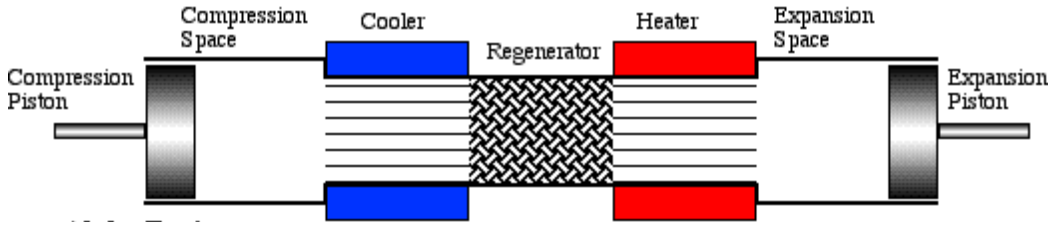

Figure 3.1 Stirling Engine Components (Urieli, 2007)

Advantages of Stirling Engines (Urieli and Berchowitz, 1984)

1. Maximum potential efficiency for a heat engine operating between the same temperatures
2. Flexible fuel usage such as biomass, solar, geothermal, waste heat, and fossil fuels
3. Lower nitrogen oxides compared to internal combustion engines
4. Quiet and minimal vibration
5. Free-piston Stirling engines have very high reliability
6. Stirling engines allow for operation as a refrigerator or a heat pump
7. Have the highest specific work output for any closed regenerative cycle

Disadvantages of Stirling Engines (Urieli and Berchowitz, 1984)

1. Stirling engines often have a slower response to an increase or decrease in load

2 Lower specific power output so added weight and volume would be less practical for automotive purposes

3. Hydrogen or helium seals can be problematic for kinematic Stirling engines

3.2.1 Stirling Engine Working Fluids

Working fluids commonly used in Stirling engines consist of air, helium, or hydrogen. The selection of a specific working fluid is based on the following fluid properties: thermal conductivity, specific heat, density, and viscosity. A working fluid with a higher thermal conductivity, density and higher specific heat will improve the heat transfer capabilities of the gas and improve the efficiency of the heat exchangers. A working fluid with a lower density and viscosity will reduce the pressure drop through the regenerator, working space, and dead space and consequently improve the engine efficiency. Two dimensionless numbers related to heat transfer are the Prandtl and Grashof numbers given by Equation (3.1) and (3.2) where g is the gravitational constant, β is the thermal expansion coefficient, T_s is the source temperature, T_∞ is the ambient temperature, L is the characteristic length, μ is the dynamic viscosity, k is the thermal conductivity, and υ is the kinematic viscosity. Increasing both of these numbers would improve the heat transfer capabilities of the heater and cooler and therefore improve the efficiency of the engine.

$$G_r = (g * \beta * (T_s - T_\infty) * L^3) / (v * \alpha) \quad \text{..... (3.1)}$$

$$P_r = (C_p * \mu) / k \quad \text{..... (3.2)}$$

Air can be used as a working fluid since it has a higher density than hydrogen or helium, and there will be less seal losses (Stine, 1999). The temperature of internal components is limited when using air in the engine since the materials will degrade due to the presence of oxygen, so the system efficiency can be negatively affected. Using air as a working fluid is not a good choice for high performance Stirling engines because air has a low thermal conductivity and therefore cannot maintain an increase in the engine efficiency at higher engine speeds. Estimates

for the performance of the three working fluids can be observed in Figure 3.2 at various operating speeds.

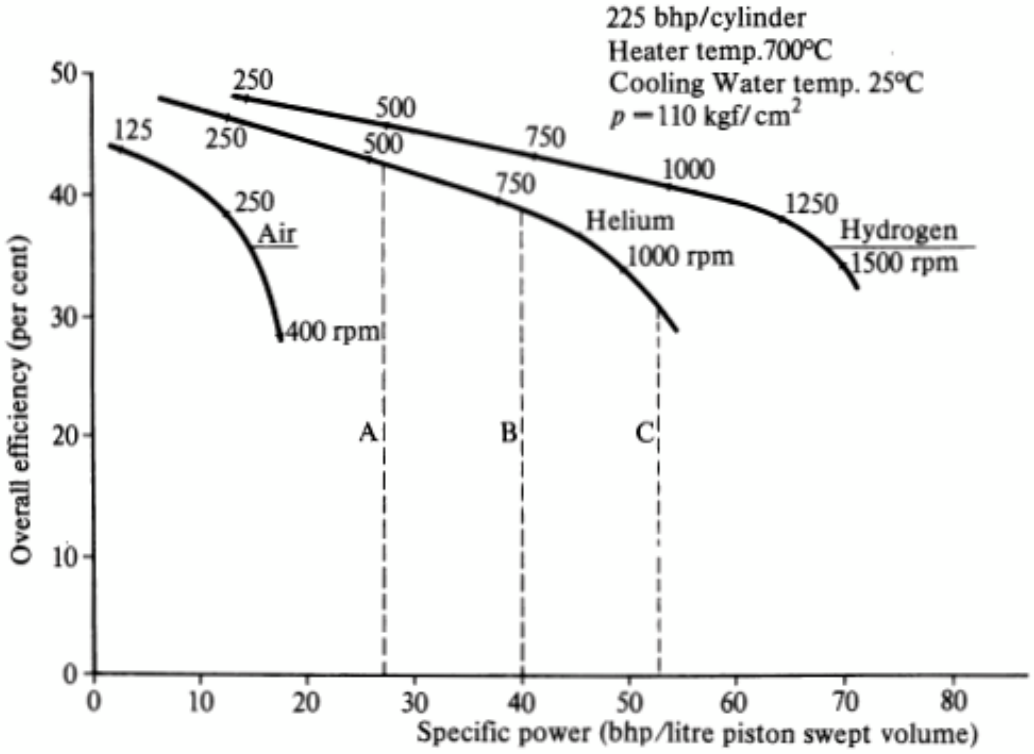

Figure 3.2 Calculated Performances for Stirling Engines with Several Working Fluids (Walker, 1980)

The working fluid for high performance Stirling engines is often hydrogen or helium since they have a larger thermal conductivity and thermal capacitance than air as shown in Figure 3.3 and Figure 3.4 respectively. Each of the four Stirling cycle processes last less than 10 ms in an engine, so the choice of the working fluid depends highly on the thermal conductivity of the gas (Stine and Harrigan, 1985). A higher specific heat for the working fluid also improves the effectiveness of transferring energy to the regenerator. The heat transfer capability of the working fluid has been shown to be related to the density and specific heat with the following correlation (Walker, 1980):

$$Q\alpha\sqrt{\rho^2 * C^3}\alpha\sqrt{M^2 * C^3} \quad \text{....} \qquad (3.3)$$

Hydrogen has the highest factor for the heat transfer in equation (3.3) with a value of 104

kJ1.5/(kg0.5-K1.5-kmol), then helium with 44, and finally air at 29. Hydrogen should be the most effective working fluid at transferring heat, which is supported with a performance comparison with helium.

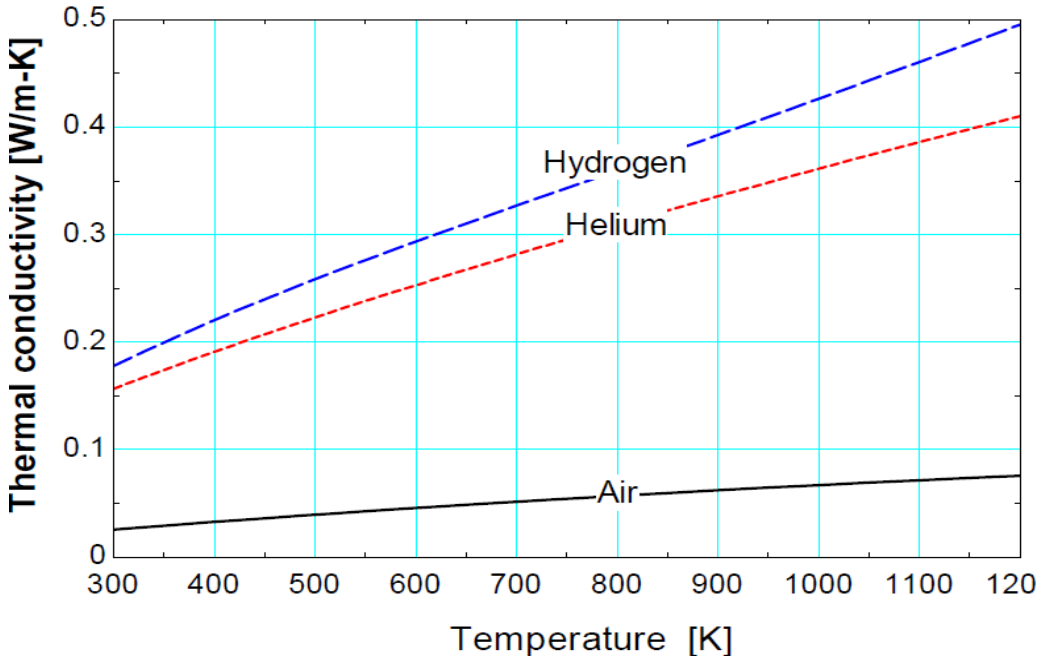

Figure 3.3 Thermal Conductivities of Working Fluids as a Function of Temperature (Klein, 2007)

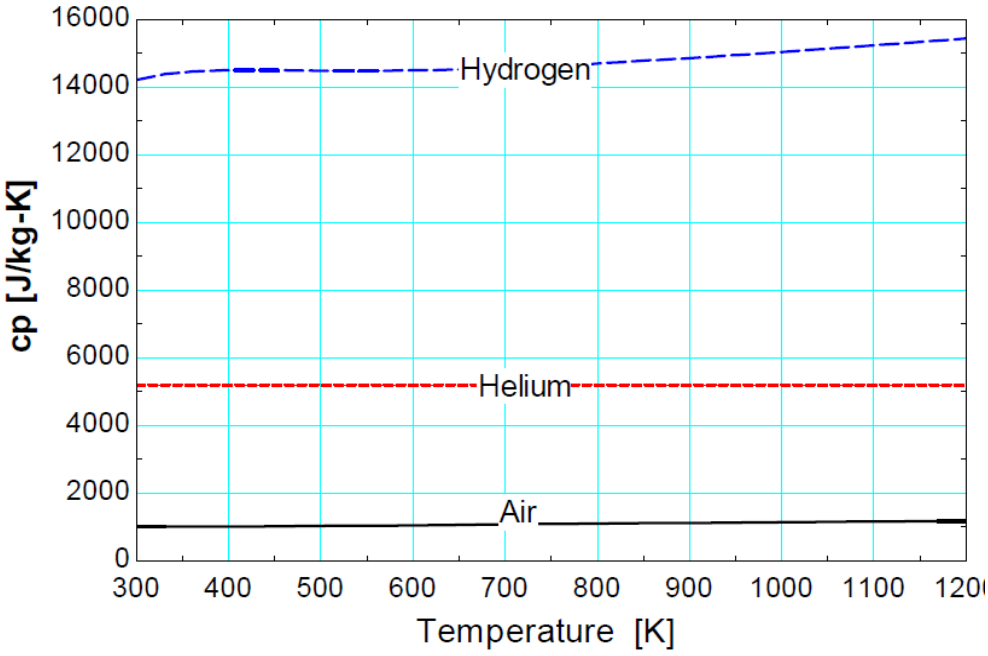

Figure 3.4 Specific Heats for Working Fluids as a Function of Temperature (Klein, 2007)

The pressure losses in the working spaces and the regenerator are dependent on the viscosity and density of the working fluid. A working fluid with a lower viscosity and density will result in lower pressure drops, which in principle improves thermal efficiency. A comparison of the viscosities and densities for the working fluids is given in Figure 3.5 and Figure 3.6 respectively.

Despite the many benefits of using hydrogen and helium for the working fluids, one disadvantage of helium and hydrogen is that the seal losses will be greater and more difficult to control. Two additional drawbacks of hydrogen are that it may absorb into various materials causing hydrogen embrittlement, and it is combustible when in contact with oxygen. Overall, hydrogen is the primary choice for the working fluid since it has the most effective transport properties to improve the Stirling engine performance.

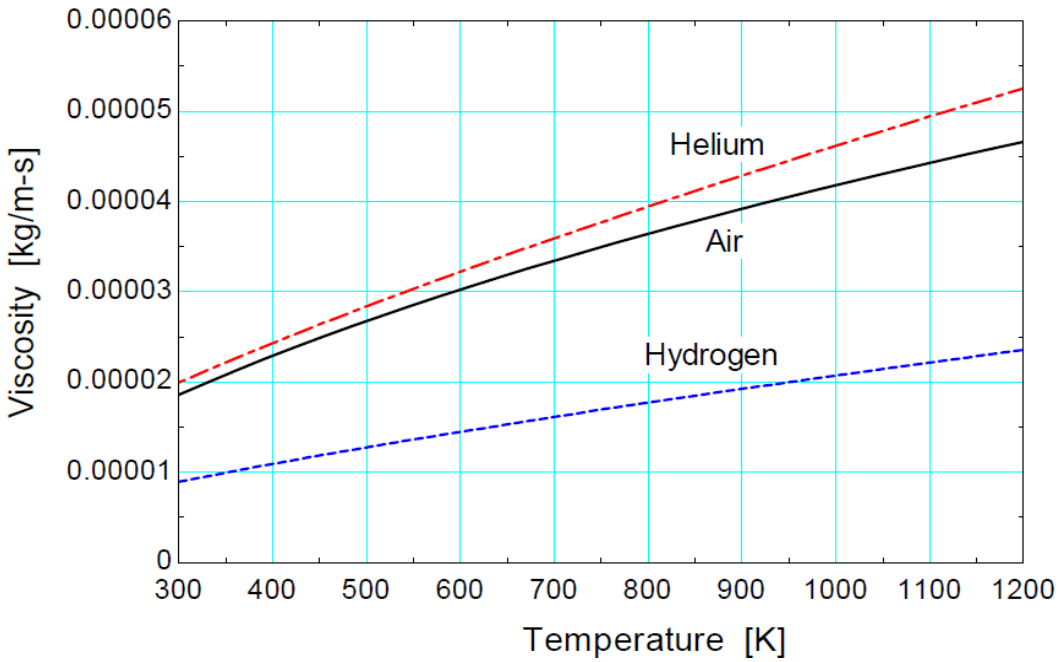

Figure 3.5 Viscosity for Working Fluids as a Function of Temperature (Klein, 2007)

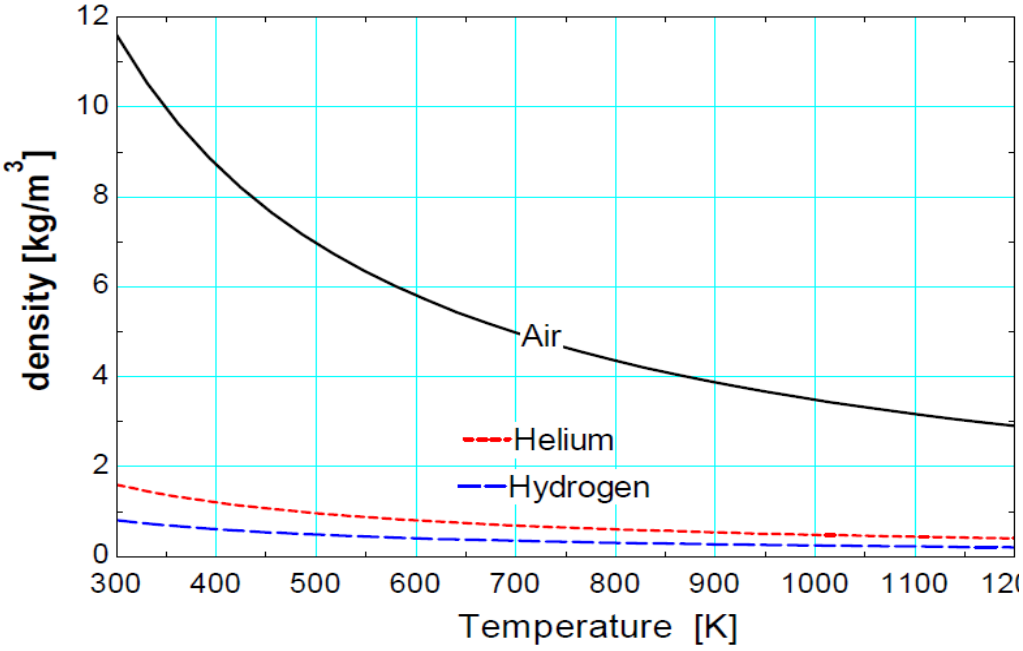

Figure 3.6 Working Fluid Densities as a Function of Temperature (Klein, 2007)

Table 3.1 Working Gas Properties

Working Gas: Hydrogen			
Gas Constant	R	4120	m^3 Pa/(K kg)
Specific Heat Capacity (Constant Pressure)	c_p	14570	J/(K kg)
Specific Heat Capacity (Constant Volume)	c_v	10450	J/(K kg)
Ratio of Specific Heats	γ	1.39	-

3.3 Stirling Engine Analysis Methods

The Stirling engine performance can be analyzed using many different existing methods. These methods range from the most ideal cases such as the Ideal and Adiabatic analyses, to a slightly more realistic model of a Stirling engine using the Quasi-Steady flow method, to the most practical Stirling engine performance prediction models that have been validated against data.

The following sections will summarize the theoretical and practical models that exist for predicting Stirling engine performance.

3.3.1 Ideal Stirling Engine Analysis

The ideal Stirling cycle consists of four internally reversible processes as depicted in Figure 3.7 (Moran and Shapiro, 2004).

Process 1-2: Isothermal compression at a temperature T_C while transferring heat from the working fluid to an external sink.

Process 2-3: Constant volume heating of working fluid by the regenerator

Process 3-4: Isothermal expansion at a temperature of T_H. External heat transfer to working fluid

Process 4-1: Constant volume cooling.

Heat transfer from working fluid to regenerator: A regenerator with a theoretical 100% effectiveness stores some of the energy rejected in process 4-1 and uses it in the heat input process 2-3. Heat at temperature T_H is supplied externally in process 3 and 4; energy rejection from the system at temperature T_C occurs in process 1 to 2.

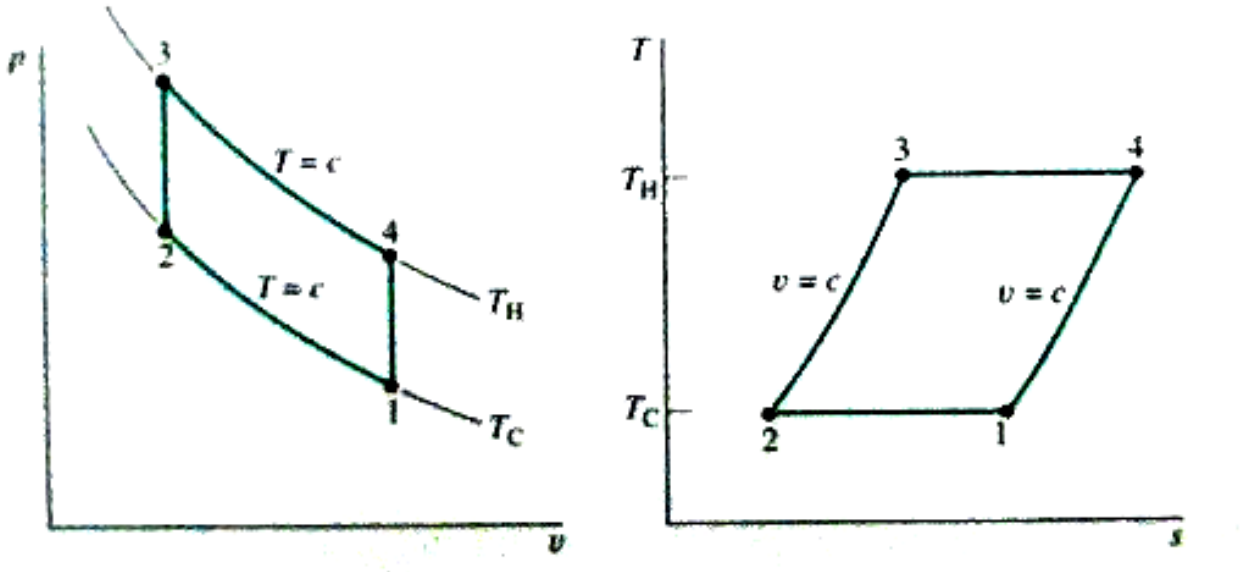

Figure 3.7 Ideal Stirling cycle P-V and T-S diagrams (Moran and Shapiro, 2004)

The Stirling cycle differs from the Carnot cycle in that the two isentropic processes are replaced with two constant volume processes, which significantly increase the area in the P-V diagram and thus the net work per cycle (Walker, 1980). This difference can be observed in Figure 3.8. The efficiency, or fraction of heat supplied to the amount of work, produced in each cycle is comparable between the Stirling and Carnot cycles.

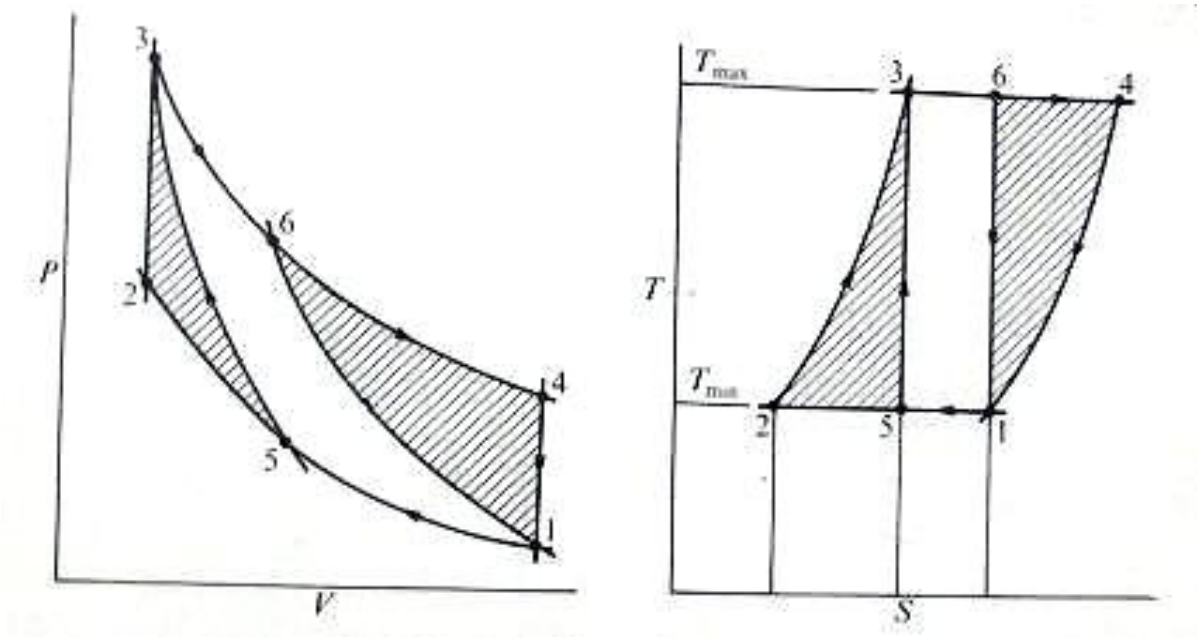

Figure 3.8 Stirling (cross-hatched) and Carnot (1, 5, 3, 6) cycle comparison with similar values for max/min temperatures, pressures, and volumes (Walker, 1980)

3.3.2 Isothermal Ideal Engine Assumptions (Urieli and Berchowitz, 1984)

1. The engine has five components including the compression space, cooler, regenerator, heater, and expansion space as shown in Figure 3.9;
2. Each component has a uniform instantaneous temperature, pressure, and mass;
3. No pressure drop occurs;
4. No working fluid leakage losses occur;
5. Ideal gas applies;

6. Engine speed is constant;
7. Steady-state of the cycle occurs; and
8. Kinetic and potential energy for the working fluid is neglected.

3.3.3 Ideal Analysis Set of Equations (Urieli and Berchowitz, 1984)

For an ideal analysis of the Stirling engine, the mass is uniformly distributed throughout the engine and the ideal gas law is valid. Applying the ideal gas law, the total pressure in the engine is given by Equation (3.4) where m is the mass of the working fluid in the engine, R is the ideal gas constant, Vc is the compression space volume, V_k is the cooler space volume, V_r is the regenerator space volume, V_h is the heater space volume, V_e is the expansion space volume, T_k is the cooler temperature, and T_h is the heater temperature.

$$P = m * R * \left(\frac{V_c}{T_k} + \frac{V_k}{T_k} + \frac{V_r * In\left(T_h / T_k\right)}{(T_h - T_k)} + \frac{V_h}{T_h} + \frac{V_e}{T_k} \right)^{-1} \quad \text{..... (3.4)}$$

The heat transferred from the compression space and the heats transferred to the expansion space are functions of the engine pressure and the crank angle:

$$Q_c = W_c = \int P \frac{dV_c}{d\theta} d\theta \quad \text{..... (3.5)}$$

$$Q_e = W_e = \int P \frac{dV_e}{d\theta} d\theta \quad \text{..... (3.6)}$$

The total work (W) produced by the engine is the sum of the negative work (W_C) from the compression space and the positive work (W_e) from the expansion space:

$$W = W_c + W_e \quad \text{..... (3.7)}$$

The total Stirling engine efficiency will then be the total work divided by the heat transferred to the expansion space which is equivalent to the Carnot efficiency:

$$\eta_{Carnot} = W/Q_e \quad \text{..... (3.8)}$$

The five components of the Stirling engine are depicted in Figure 3.9 and the corresponding temperature distribution in those components is shown.

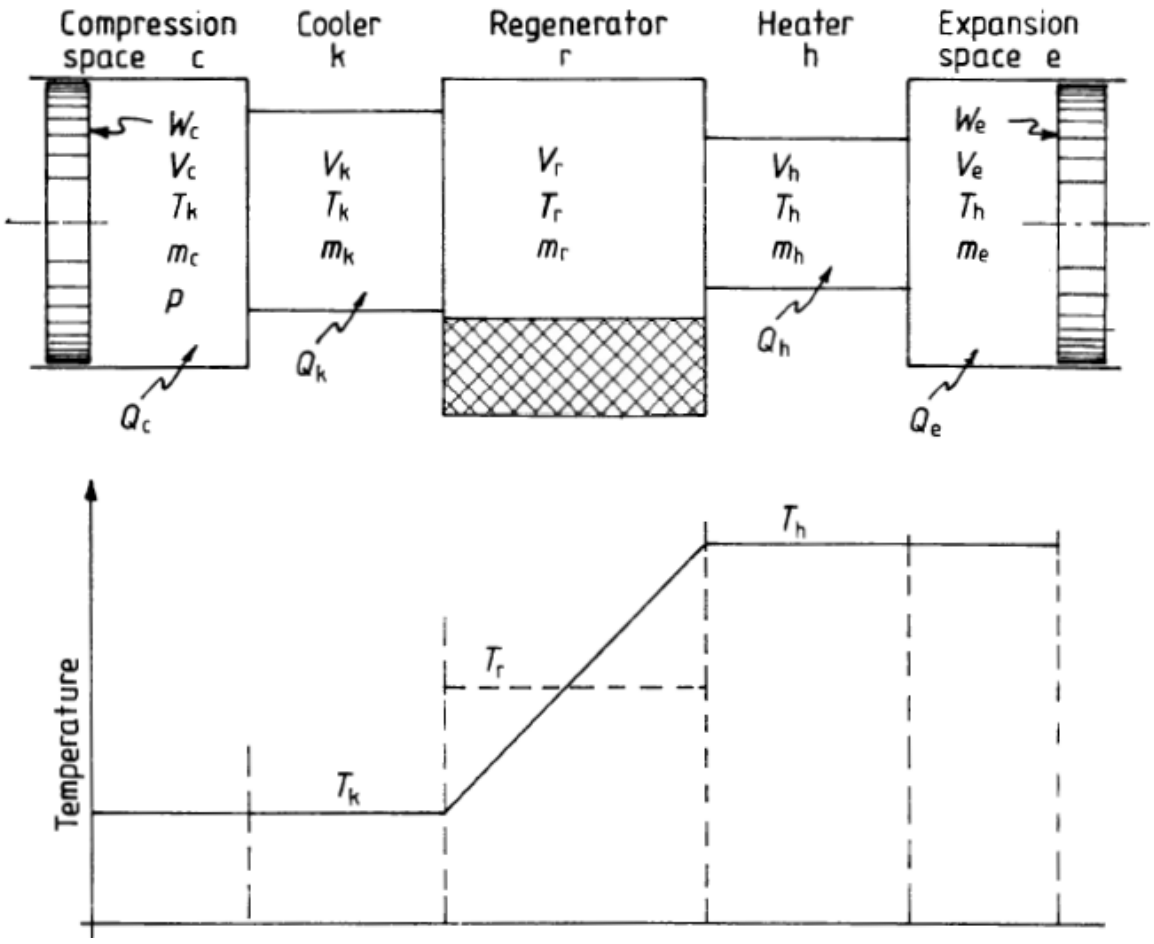

Figure 3.9 Ideal Isothermal Model (Urieli and Berchowitz, 1984)

3.3.4 Quasi Steady Flow Analysis

The "Quasi Steady Flow" model was developed since the flow patterns in Stirling engines are not steady and vary significantly over the cycle, and non-ideal heat exchangers are considered

(Urieli and Berchowitz, 1984). The difference between the Quasi Steady Flow and Adiabatic models is the temperature drop between the compression space and cooler, the temperature drop between the heater and the expansion space, the working fluid temperatures are no longer constant over the cycle, and there are pressure losses across the cooler, regenerator, and heater as shown in Figure 3.10 (Urieli and Berchowitz, 1984). It was found in spherical bed regenerators that the friction factors and heat transfer coefficients were 20 percent higher for periodic flow conditions compared to steady flow conditions (Urieli and Berchowitz, 1984).

The Quasi Steady Flow method including pressure drops is more realistic than an Ideal or Adiabatic analysis, but it still does not take several losses into effect. There may be a substantial conduction loss through the walls surrounding the regenerator, shuttle loss from the displacer (for beta/gamma engines), and adiabatic compression loss (Urieli and Berchowitz, 1984). The adiabatic compression loss results from the temperature difference between the cylinder wall sand the working spaces causing a transfer of heat at ineffective times during the cycle (Urieli and Berchowitz, 1984). A significant fraction of losses is also predicted to come from pressure losses in the heat exchangers, which are greater than the estimates from steady flow correlations (Urieli and Berchowitz, 1984). The NASA Lewis Research Center reported that the friction factor in the regenerator had to be multiplied by a factor of four to obtain similar values for the measured and predicted output power of Stirling engines (Urieli and Berchowitz, 1984).

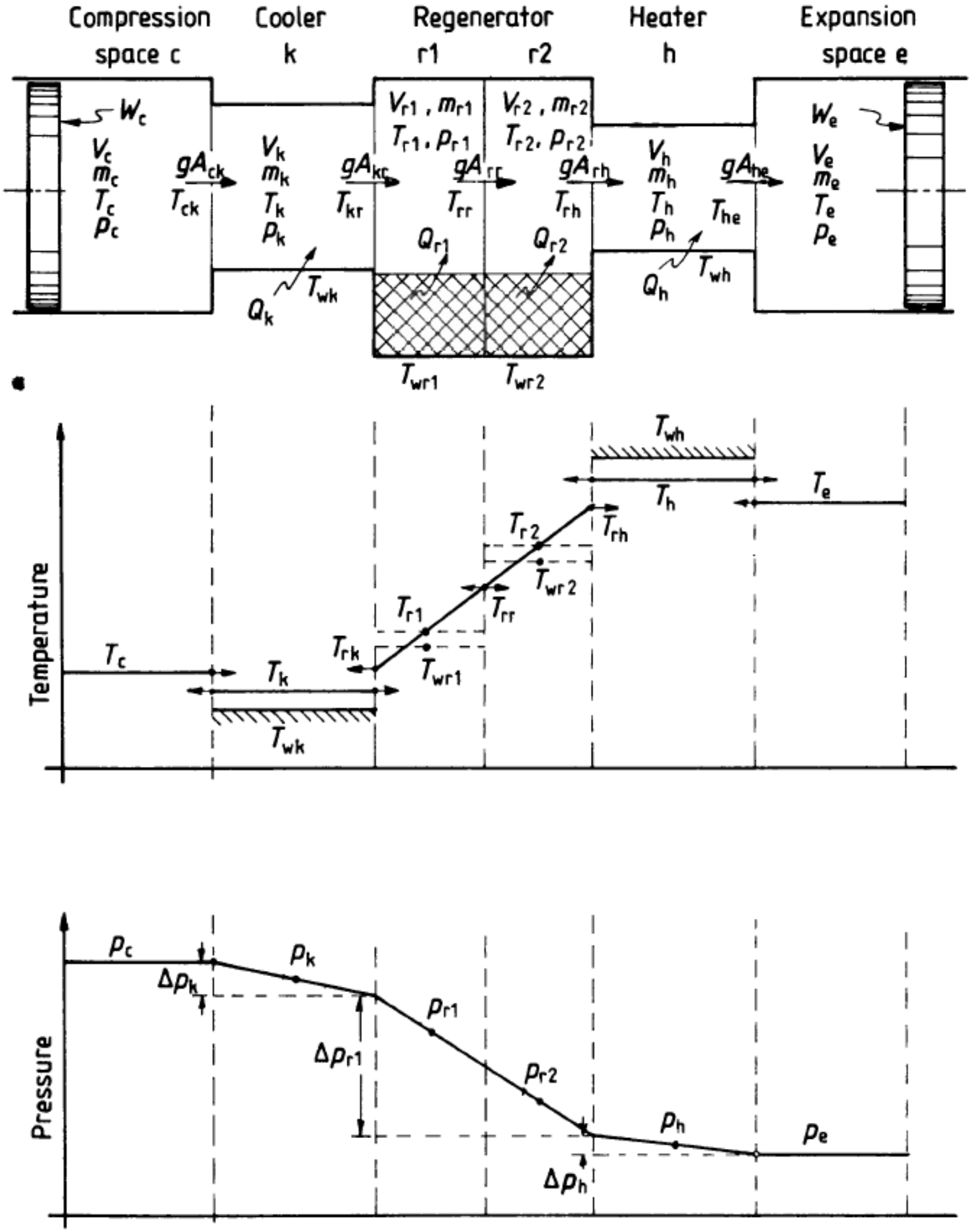

Figure 3.10 The Quasi Steady Flow Model (Urieli and Berchowitz, 1984)

3.3.5 Summary of Stirling Engine Theoretical Analyses

The Quasi steady flow model gives better predictions of Stirling engine performance than the ideal and adiabatic analysis, but still does not accurately account for all losses in the Stirling engine. A breakdown of the engine efficiency based on various losses is given in Figure 3.6. The Schmidt analysis operates at the ideal Carnot efficiency and each additional loss including adiabatic working spaces, adiabatic residual loss, flow loss, and thermal conductivity loss degrades the engine efficiency further (Walker, 1980). The adiabatic residual loss is a result of a phase difference between pressure and volume within the working space. The phase angle α in Figure 3.11 is defined as the angle of the expansion space volume variation leading those in the compression space.

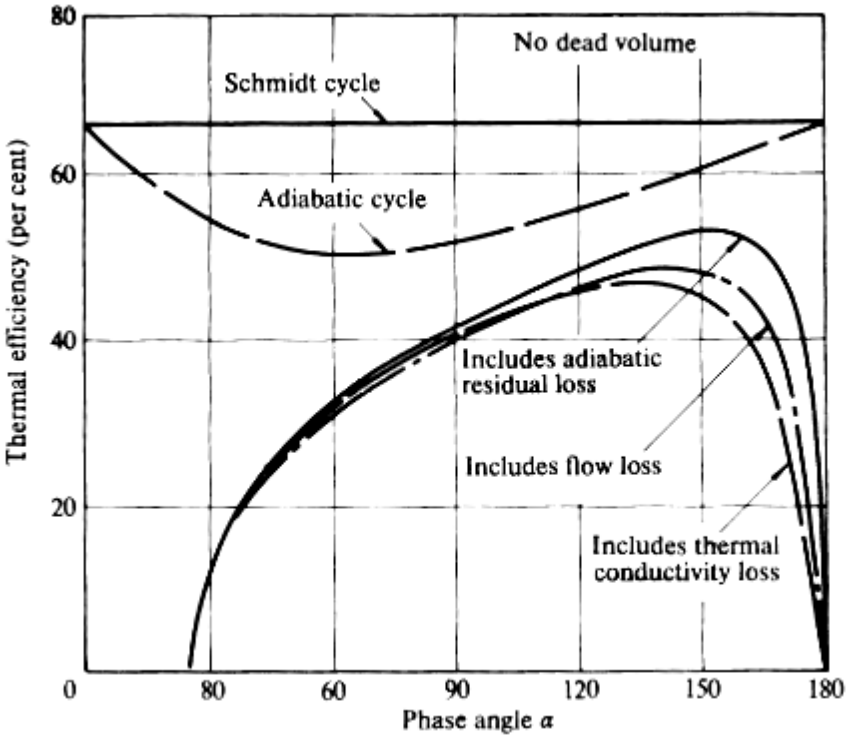

Figure 3.11 Engine efficiencies as a function of phase angle for various losses (Walker, 1980)

3.3.6 Practical Stirling Engine Performance Analyses

The practical Stirling cycle includes many details that the ideal processes neglect. The actual cycle is not reversible, compression and expansion processes are not isothermal, the entire mass of the working fluid is not always in the compression space or expansion space, and there are voids in the regenerator, cylinder clearance space, and connecting piping (Walker, 1980). The practical Stirling cycle also includes pistons that are continuously moving and contributing to friction between the piston and cylinder, and the regenerator is not assumed to have a perfect effectiveness. Flow loss occurs in the regenerator and heat exchangers which can be observed in

Figure 3.12 by the variation in pressure between the expansion and compression spaces. The work lost in the regenerator and heat exchangers is represented by the hatched area in Figure 3.13. After including all of these losses, a well-designed Stirling engine will have efficiencies between 40 and 70 percent of the theoretical Carnot value (Walker, 1980). The practical analyses cannot account for all of the previous loss mechanisms because of compounding errors, so practical analyses often involve performance correlations that have shown to be accurate or making performance curve fits from data.

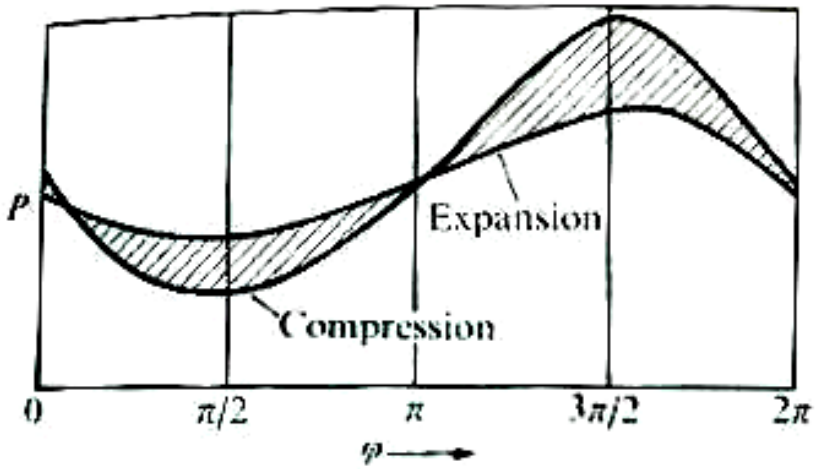

Figure 3.12 Pressure Variation between the Expansion and Compression Spaces (Walker, 1980)

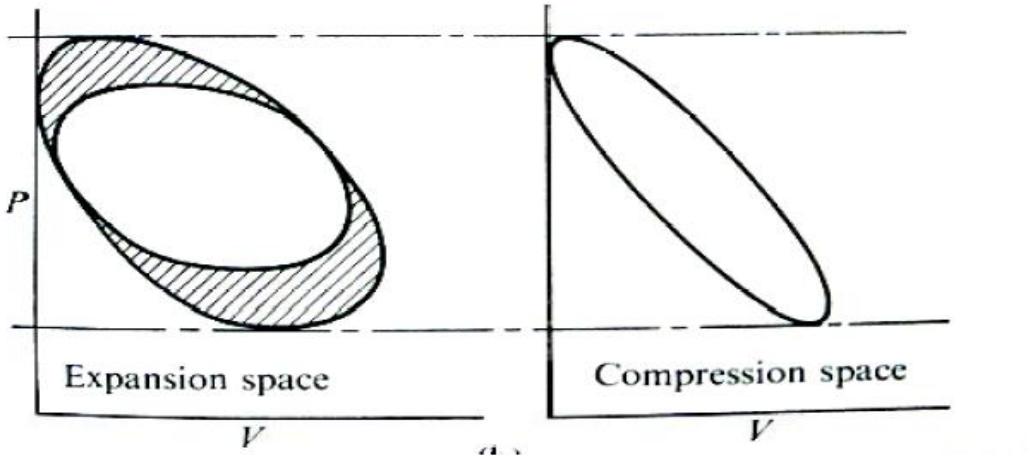

Figure 3.13 P-V Diagram for Expansion and Compression Space for a Stirling Cycle. The hatched area represents work lost from the regenerator and heat exchangers (Walker, 1980)

3.3.6.1 Beale Number Power Correlation

William Beale observed that most engines have similar performance based on the Schmidt optimizations involving the dead volume ratio, temperature ratio, swept volume ratio, and phase angle advance (Urieli, 1984). He observed that most Stirling engines operate with similar internal efficiency losses, so a simple performance prediction could be made. By observing experimental data, determined the power output of the Stirling engine to be based on the (dimensionless) Beale number:

$$P_{SE} = Beale * P_{mean} * P_{mean} * V_{sw} * f \quad \text{..... (3.9)}$$

Where P_{SE} is the Stirling engine output power, Beale is the Beale number, P_{mean} is the mean engine pressure, V_{sw} is the swept volume of the engine, and f is the engine frequency (Urieli, 1984). A typical value for the Beale number is 0.15. The Beale number power correlation is more practical than the theoretical analyses and more accurately predicts the performance of a Stirling engine.

3.3.6.2 West Number Power Correlation

The Beale number Stirling engine performance correlation does not include terms for the hot or cold sink temperatures in the engine. The performance of a Stirling engine depends on these temperatures, so the West number correlation was devised to include these temperature terms.

The predicted power output of the Stirling engine based on the (dimensionless) West number is given by:

$$P_{SE} = West * P_{mean} * V_{sw} * f\left(\frac{T_E - T_c}{T_E + T_c}\right) \quad \ldots\ldots\ldots\ldots\ldots\ldots\ldots\ldots\ldots\ldots\ldots\ldots\ldots\ldots\ldots\ldots\ldots\ldots \quad (3.10)$$

Where West is the West number, T_E is the expansion space temperature, T_C is the compression space temperature (Hirata, 2002). The power estimated using the West number includes consideration of the expansion and compression space temperatures, and should provide more accurate estimates of the engine power if these parameters were varied. A typical value for the

West number is between 0.25 and 0.35 (Hirata, 2002).

3.4 Stirling Engine Efficiency with Regenerative and Pressure Losses

A Stirling engine efficiency correlation was developed by Petrescu et al. (2002) by combining two theoretical thermodynamic techniques The efficiency correlation takes into account the Carnot efficiency, pressure losses, and regenerator losses involving both internal and external irreversibility. Two adjusting coefficients were determined based on experimental data to obtain accurate analytical results for the efficiency correlation. The Stirling engine efficiency is given by Equation (3.11) (Petrescu et al, 2000)

$$\eta_{SE} = \eta_{Carnot} * \eta_{II,irrev} = \eta_{Carnot} * \eta_{II,\Delta T} * \eta_{II,X} * \eta_{II,\Delta p} \quad \ldots\ldots\ldots\ldots\ldots\ldots\ldots\ldots\ldots\ldots\ldots\ldots\ldots\ldots\ldots\ldots\ldots\ldots \quad (3.11)$$

where the Carnot cycle efficiency (η_{Carnot}) is a function of the cooler (T_C) and heater (T_E)temperatures in Equation (3.12)

$$\eta_{Carnot} = \left(1 - \frac{T_C}{T_E}\right) \quad \ldots\ldots\ldots\ldots\ldots\ldots\ldots\ldots\ldots\ldots\ldots\ldots\ldots\ldots\ldots\ldots\ldots\ldots\ldots\ldots\ldots\ldots \quad (3.12)$$

The irreversibility factor due to a temperature difference between the heat source and heat sink is given by Equation (3.13)

$$\eta_{II,\Delta T} = 1 \Big/ \left(1 + \sqrt{\frac{T_C}{T_E}}\right) \quad \text{..... (3.13)}$$

Incomplete regeneration can contribute to significant losses in Stirling engines. These heat transfer losses are a function of piston speed, cylinder and regenerator dimensions, regenerator and working fluid properties, and operating conditions (Petrescu et al, 2002). The factor for losses due to incomplete regeneration is given by Equation (3.14) where η_{II}, X denotes the efficiency factor for the regenerator, C_v is the gas specific heat at constant volume, R is the gas constant, ε_v is the compression ratio (V_1/V_2), X represents all the losses from incomplete heat transfer in the regenerator.

$$\eta_{II,X} = \frac{1}{1 + \frac{X * C_v}{R * In(\varepsilon_v)} * \left(1 - \sqrt{\frac{T_C}{T_E}}\right)} \quad \text{..... (3.14)}$$

The value for X was determined using the first law and heat transfer principles for the regenerator and working fluid and is defined in Equation (3.15) (Petrescu et al, 2000):

$$X = X_1 * y + X_2 * (1 - y) \quad \text{..... (3.15)}$$

Differential equations from this analysis were integrated using a lumped analysis, which gave pessimistic results using X_1 (Petrescu et al, 2000):

$$X_1 = \frac{1 + 2 * M + e^{-B}}{2 * (1 + M)} \quad \text{..... (3.16)}$$

Using a linear distribution of the temperature for the regenerator and working fluid gave optimistic results for X_2 (Petrescu et al, 2000):

$$X_2 = \frac{M + e^{-B}}{(1 + M)} \quad \text{..... (3.17)}$$

Experimental data were used to obtain the adjusting parameter y which was found by Petrescuet al (2000) to be 0.72 or 0.27 in the Reno paper by Petrescu et al (2002). The term M given in

Equation (3.18) is the ratio of the mass multiplied by capacitance of the working fluid to that of the regenerator.

$$M = \frac{m_g * C_v}{m_r * C_r} \quad \text{..... (3.18)}$$

The term B in Equation (3.19) is a function of the regenerator heat transfer coefficient hr, the area of the regenerator A_r involved with heat transfer, the stroke of the piston S, and the speed of the piston w (Petrescu, 2000).

$$B = (+M) * \frac{h_r * A_r}{m_g * C_v} * \frac{S}{w} \quad \text{..... (3.19)}$$

The speed of the piston is dependent on the stroke and engine speed (n_r) given by:

$$W = 2 * S * n_r / 60 \quad \text{..... (3.20)}$$

The regenerator heat transfer coefficient due to convection is:

$$h_r = \frac{0.395 * (4 * P_m / R * T_C) * w^{0.424} * C_p * (T_m) * v * (T_m)^{0.576}}{(+\tau) * \left[1 - \frac{\pi}{4 * (b/d) + 1}\right] * D_r^{0.576} * P_r^{2/3}} \quad \text{..... (3.21)}$$

where P_m is the mean pressure in the engine, υ and C_p are the viscosity and thermal capacitance of the working fluid evaluated at the mean temperature T_m, D_r is the diameter of the regenerator, d is the diameter of the regenerator wire, b is the distance between wires in the regenerator, and Pr is the Prandtl number.

The equation for the pressure losses factor results from determining the losses of the pistons operating at a finite speed, the working fluid moving through the regenerator, and mechanical friction, and is given by:

$$\eta_{\text{II},\Delta P} = 1 - \frac{\frac{w}{w_{S,L}} * \gamma * (+\sqrt{\tau}) * In(\varepsilon_v) + 5 * \left(\frac{w}{w_{S,L}}\right)^2 * N_S}{\tau * \eta' * In(\varepsilon_v)} - \frac{\frac{3 * (0.94 + 0.045 * w) * 10^5}{4 * P_1}}{\tau * \eta' * In(\varepsilon_v)} \quad (3.22)$$

where Ns is the number of screens in the regenerator, τ is temperature ratio, P_1 defined in

Equation (3.25) is a function of the mean pressure (P_m), volumetric ratio (ε_v), and temperature ratio (τ), w is the piston speed, $w_{S,L}$ is the speed of sound at the sink temperature (T_C), and η' is the Carnot efficiency multiplied by the regenerator losses factor given in Equation (3.23).

$$\eta' = \eta_{CC} * \eta_{I\,I,X} \quad \text{.....} \quad (3.23)$$

The sound speed at the cooler temperature is defined in Equation (3.24) where γ is the specific heat ratio.

$$W_{S,L} = \sqrt{\gamma * R * T_C} \quad \text{.....} \quad (3.24)$$

The term P_1 is defined:

$$P_1 = \frac{4 * P_m}{(\varepsilon_v + 1)(\tau + 1)} \quad \text{.....} \quad (3.25)$$

The temperature ratio τ is defined:

$$\tau = \frac{T_E}{T_c} \quad \text{.....} \quad (3.26)$$

A model was developed (See Appendix B) in Engineering Equation Solver (EES) using the correlation given by Equation (3.11) to duplicate the results of the 4-95 MKII engine in Table 3.3. The results of the Petrescu model did not accurately predict the efficiency of the 4-95 engine as indicated in Figure 3.13. The maximum efficiency of the 4-95 engine is rated to be around 41 % and not 29.4 % as published in Table 3.3 (Stine and Diver, 1994). The peak net SES Stirling dish system efficiency using the 4-95 engines (accounting for collector, receiver, engine, and parasitic losses) is 29.4 % (Mancini et al, 2003). The predicted model results of the 4-95 MKII engine in Table 3.4 indicates that the calculated efficiency (28.9 %) for this model is not close to the operating efficiency of 41 % for unexplained reasons. There was no response from the authors to the email requests for clarification about their method.

Table 3.2 Output of EES for Stirling Engine

Output of EES for Stirling Engine		
A_dish=91 [m^2]	h=35.77	tau=3.203
A_R=4.083	Insolation=180 [W/m^2]	TC=310 [k]
B=21.41	intercept factor=0.97 [-]	TC_max=310 [k]
b2=1.000E-07 [m]	k_spec=1.383	TE=993 [k]
Cp=14.89	M=37.08	TE_max=995 [k]
Cv=10.77	MM_H2=2.016	Th=1083 [k]
Cv_g=10.77	m_g=0.402	Tk=293 [k]
C_R=0.5838	m_R=0.2 [kg]	TR=586.7
d=0.00004 [m]	nu=3.739E-08	T_H2_ave=651.5
DNI=180	N_cylinders=4	T_m=651.5
D_R=0.057 [m]	N_S=1600	T_S_L=293
epsilon_v=3.375	P1=435040	V1=0.00054
eta_2_DELTA_T=0.6578	Patm=101325 [Pa]	V2=0.00016
eta_CC=0.7295	Power_in_SE=11983	Vmax=0.00054
eta_generator=0.95 [-]	Pr=0.7286	Vmin=0.00016
eta_II_DELTA_P=-312.4	Pressure_mean=2.000E+06	Volume_displacement=0.00038 [m^3]
eta_II_irrev=-102.1	P_atm=101325	w=9.6
eta_II_X=0.4968	R=4.124	wS_L=40.88
eta_Petruscu=0	reflectivity=0.91 [-]	X=0.9832
eta_prime=0.3624	RPM=1800 [rpm]	X1=0.9869
eta_receiver=0.86 [-]	S=0.16	X2=0.9737
gamma=1.383	stroke_cyl=0.04 [m]	y=0.72

Table 3.3 Comparison of the Petrescu et al. results and the actual engine performance (Petrescu et al, 2000)

Stirling Engine	Actual power [kW]	Calculated Power [kW]	Actual Efficiency	Calculated Efficiency
NS-03M, regime 1(economy)	2.03	2.182	0.359	0.3392
NS-03M, regime 2 (max. power)	3.81	4.196	0.310	0.3297
NS-03T, regime 1(economy)	3.08	3.145	0.326	0.3189
NS-03T, regime 2(max. power)	4.14	4.450	0.303	0.3096
NS-30A, regime 1(economy)	23.2	29.450	0.375	0.3570
NS-30A, regime 2(max. power)	30.4	33.820	0.330	0.3366
NS-30S, regime 1(economy)	30.9	33.780	0.372	0.3660
NS-30S, regime2(max. power)	45.600	45.620	0.352	0.3526
STM4-120	25.000	26.360	0.400	0.4014
V-160	9.000	8.825	0.300	0.3080
4-95MKII	25.000	28.400	0.294	0.2890
4-275	50.000	48.610	0.420	0.4119
GPU-3	3.960	4.160	0.127	0.1263
MP1002 CA	0.200	0.194	0.156	0.1536
Free Piston Stirling Engine	9.000	9.165	0.330	0.3310
RE-1000	0.939	1.005	0.258	0.2285

CHAPTER FOUR

TRNSYS Modeling and Simulation of the Stirling Dish System

4.1 An Introduction to TRNSYS

TRNSYS is a transient system simulation program with a modular structure. The program is well suited to simulate the performance of systems, the behavior of which is a function of the passage of time. This is the case if outside conditions that influence the system behavior change, such as weather conditions, or if the system components themselves go through conditions that vary with time.

There can be several components of the same type specified in one simulation. The way this identification is accomplished is that each component is assigned an identifying type number that is component specific. A second number, the unit number is unique; one can only be used once in a simulation. Different unit numbers can be associated with the same type number, although there are limitations on how many types of one kind can be used in one simulation.

A system is set up in TRNSYS by means of an input file, called a TRNSYS deck. This deck contains all the information that specifies the components and how the components interact. The system is set up by connecting all inputs and outputs in an appropriate way to simulate the real system

This deck contains all the information that specifies the components and how the components interact. The system is set up by connecting all inputs and outputs in an appropriate way to simulate the real system. Once a system is set up in a TRNSYS deck, the program can be run over a user defined time interval. The time interval is divided into equal number of time steps.

At each time step the program calls each component and solves all the mathematical equations that specify the component performance. The program iteratively calls the system component until a stationary state is reached. The stationary state is reached when all the calculated inputs to the components remain constant between two iterations. Naturally, in a numerical solution such as calculated by TRNSYS, there will always be a difference in results between two iterations. Therefore the user has to specify tolerances that define a stationary state.

Aside from the components that simulate actual physical parts of the system, there are predefined utility components that can be used in the simulation. One of them is the data reader. The data reader is able to read data from a user supplied data file that has to be assigned in the TRNSYS deck. At every time step of the simulation the data file then reads the desired values from the file and makes them accessible to the components.

Another kind of utility component is a printer that stores output data in a file. Several printers can be defined in one deck. These output files can be imported into a spreadsheet program and the results further examined. The online plotter can be used to make the progress of the simulation visible on the screen, so that the user can immediately decide whether a run was useful or not. Additionally, a quantity integrator is available to integrate values over time.

A special feature of the TRNSYS program package is the possibility to create a user-friendly input file called a TRNSED file. When the TRNSED program is started, the user only has to supply the important parameters and can change these easily for different simulations. In this way the program is accessible to users who are not experienced in using TRNSYS but are only interested in examining a particular system. Modular simulation of a system requires the identification of components whose collective performance describes the performance of the system. Each component is formulated by mathematical equations that describe its physical behavior.

The mathematical models for each component are formulated in FORTRAN code, so that they can be used within the TRNSYS program. Formulation of the components has to be in accordance with the required TRNSYS format. A basic principle in this format is the specification of parameters, inputs and outputs for each component. Parameters are constant values that are used to model a component

Inputs are time-dependent variables that can come from a user supplied data source such as weather data or from outputs of other components. (Source TRNSYS manual).

4.2 Creating a New Component

This section will briefly illustrate how to generate new components using the Simulation Studio.

Create the component proforma

- Launch the Simulation Studio and go to File/New

- Select "component" (see Figure 4.1)
- In the component "General" tab, type in the component's object and its Type number. It is important to assign a Type number different from zero. The selected number should also be in the [201; 300] range in order to avoid conflicts with existing libraries.

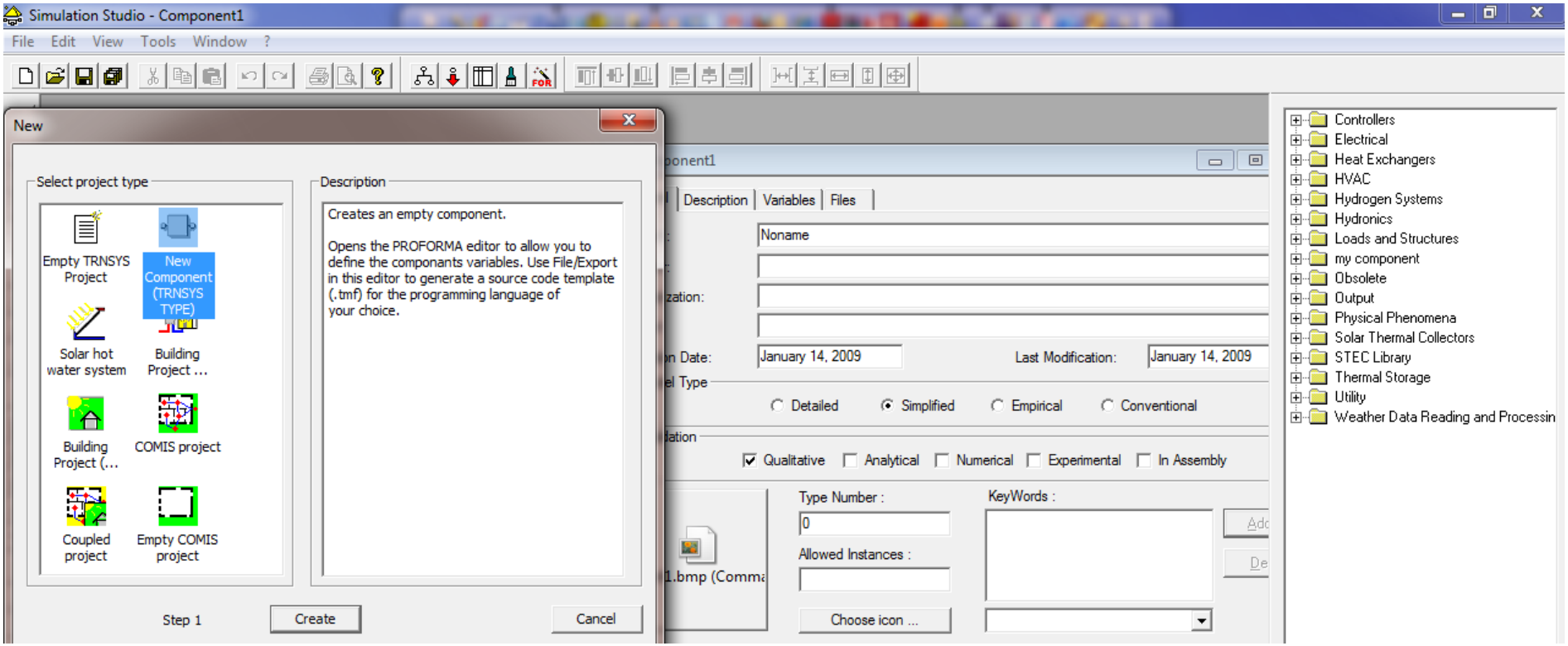

Figure 4.1 Creating a New Component Proforma

- Variables can be then added to the proforma in the "Variables" tab. Click on "variables", select the "Parameters" tab and click on "Add". Parameter information can be entered in the row that has been created or click on "Modify" to have a more detailed view (see Figure 4.2).

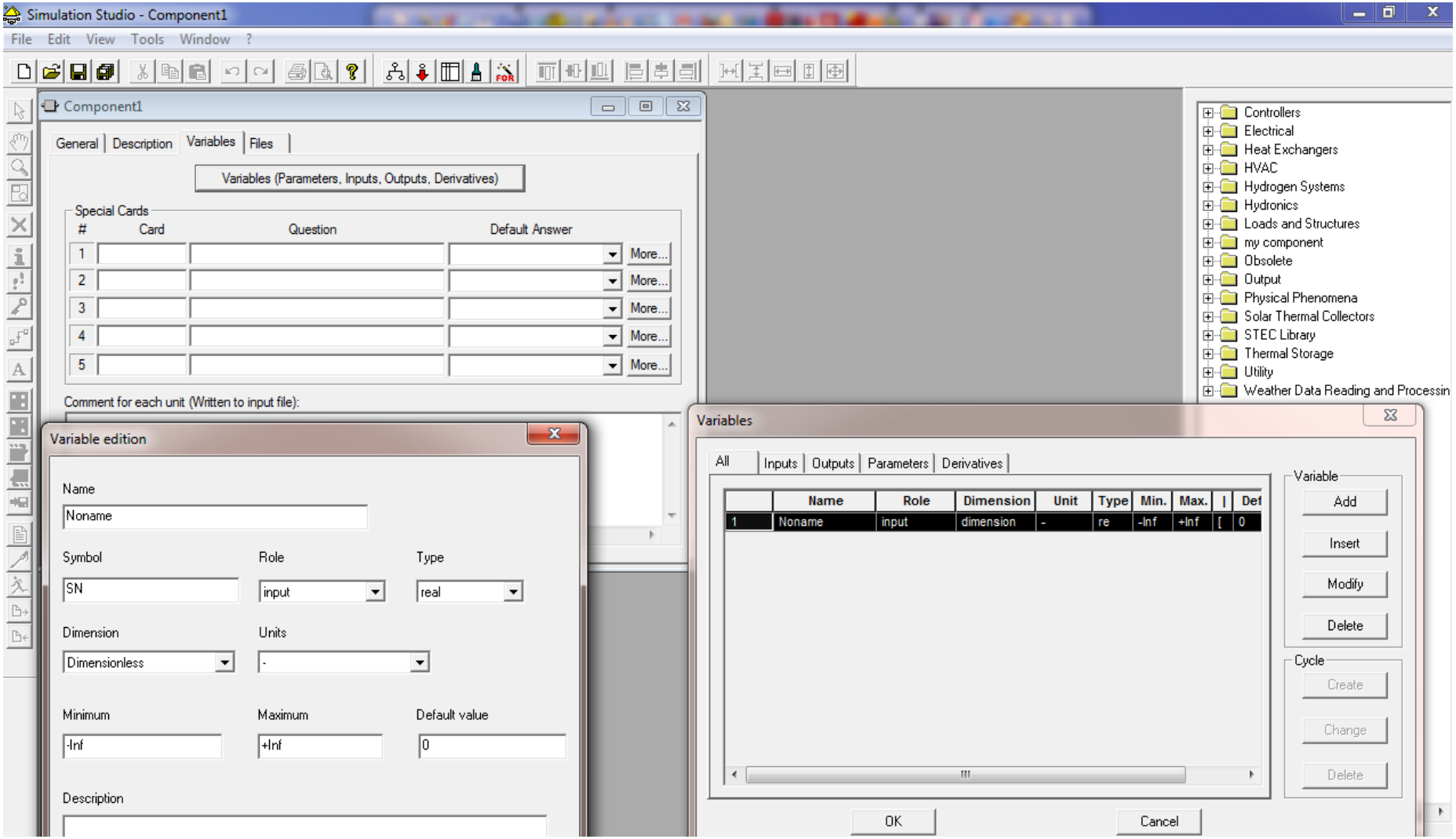

Figure 4.2 Creating a New Component Proforma

- Save the Performa. To be accessible in the Studio, the Performa needs to be in"%TRNSYS16%\Studio\Proformas". A folder, for example, called "My Components" is created and saved as "Type200.tmf".

- Open "File/Export as/Fortran" and create a "Type200" folder anywhere on the disk, (e.g. in "My Projects"). Save the component as Type200.for there (see Figure 4.3).

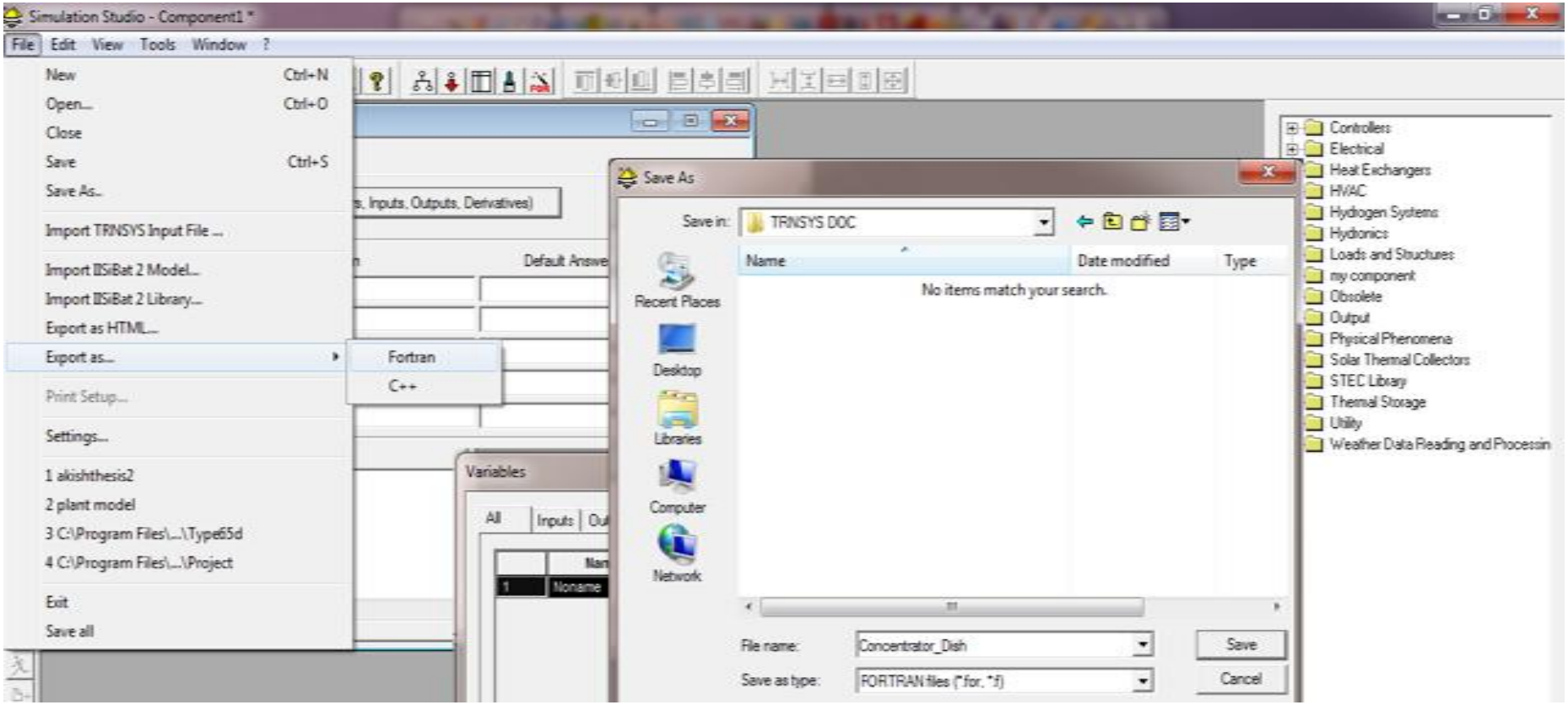

Figure 4.3 Exporting as Fortran

The Studio will then do several things for the user (see the dialog box in Figure 4-4):

- Create a FORTRAN skeleton for the created Type (Type200.for)
- Generate a project that you can open in the Compaq Visual FORTRAN 6.6 compiler or in the Intel Visual Fortran compiler. That project includes all the settings you need in order to generate an external DLL that will be placed in the \UserLib\Release DLLs or\UserLib\Debug DLLs folder, where TRNSYS will be able to load the created Type.
- Open the project in the compiler that is setup in File/Settings/Directories/Fortran environment (by default the settings are correct for CVF 6.6, if it has been installed, in the default location.

The following will assume that Compaq Visual FORTRAN 6.6 is installed on the machine.

- The skeleton includes all basic TRNSYS manipulations. At the minimum, you need to replace question marks in the lines that calculate outputs from inputs (see Figure 4.4)

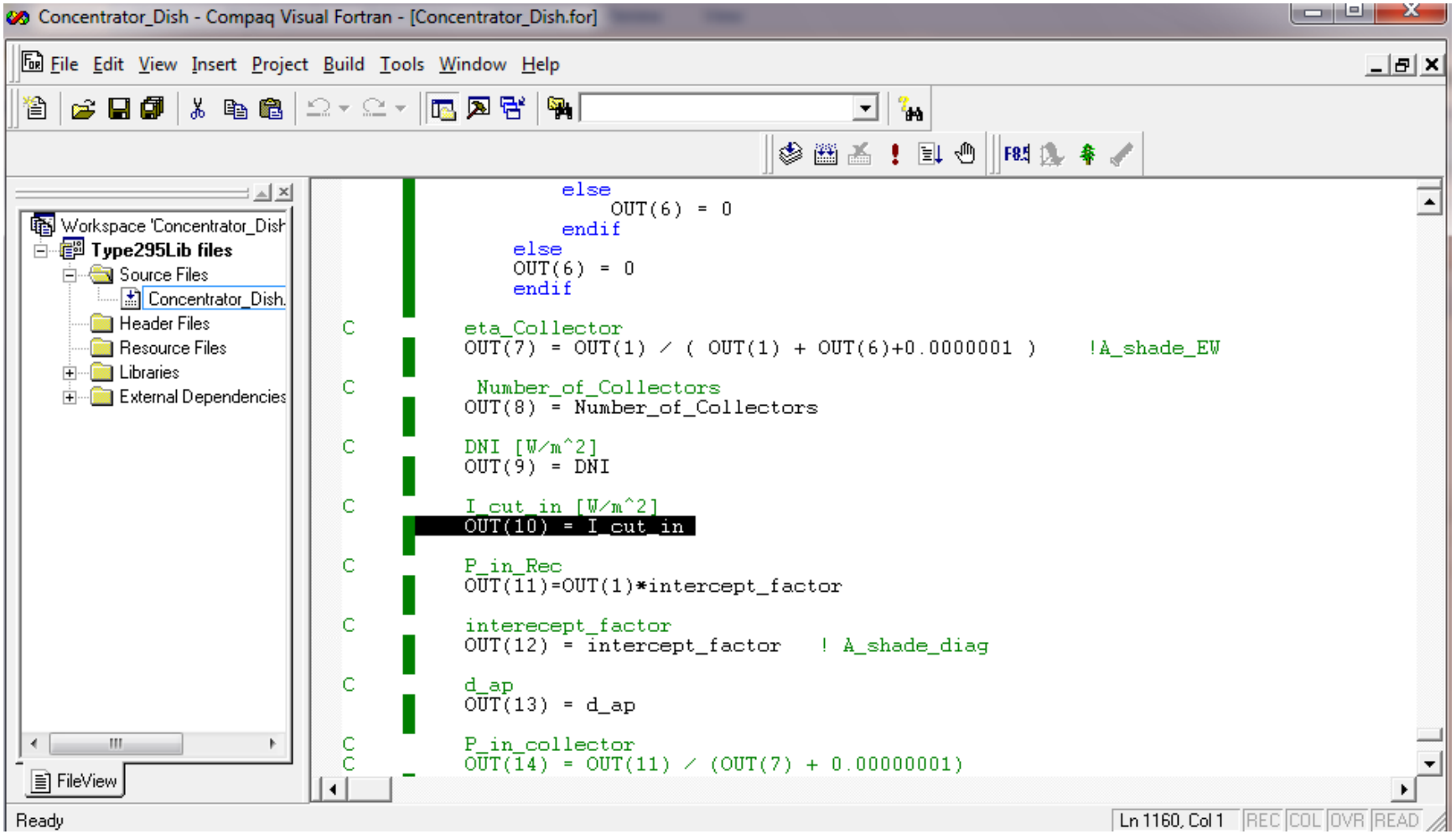

Figure 4.4 Setting the Component Outputs

- Equations (s) of the output are written in the line in place of the question mark (?).After writing the equation(s) F7 is pressed to build the .DLL file. This will generate"Type200.dll"inthe‘UserLib\Debug DLLs directory if there is no error (see Figure 4.5).

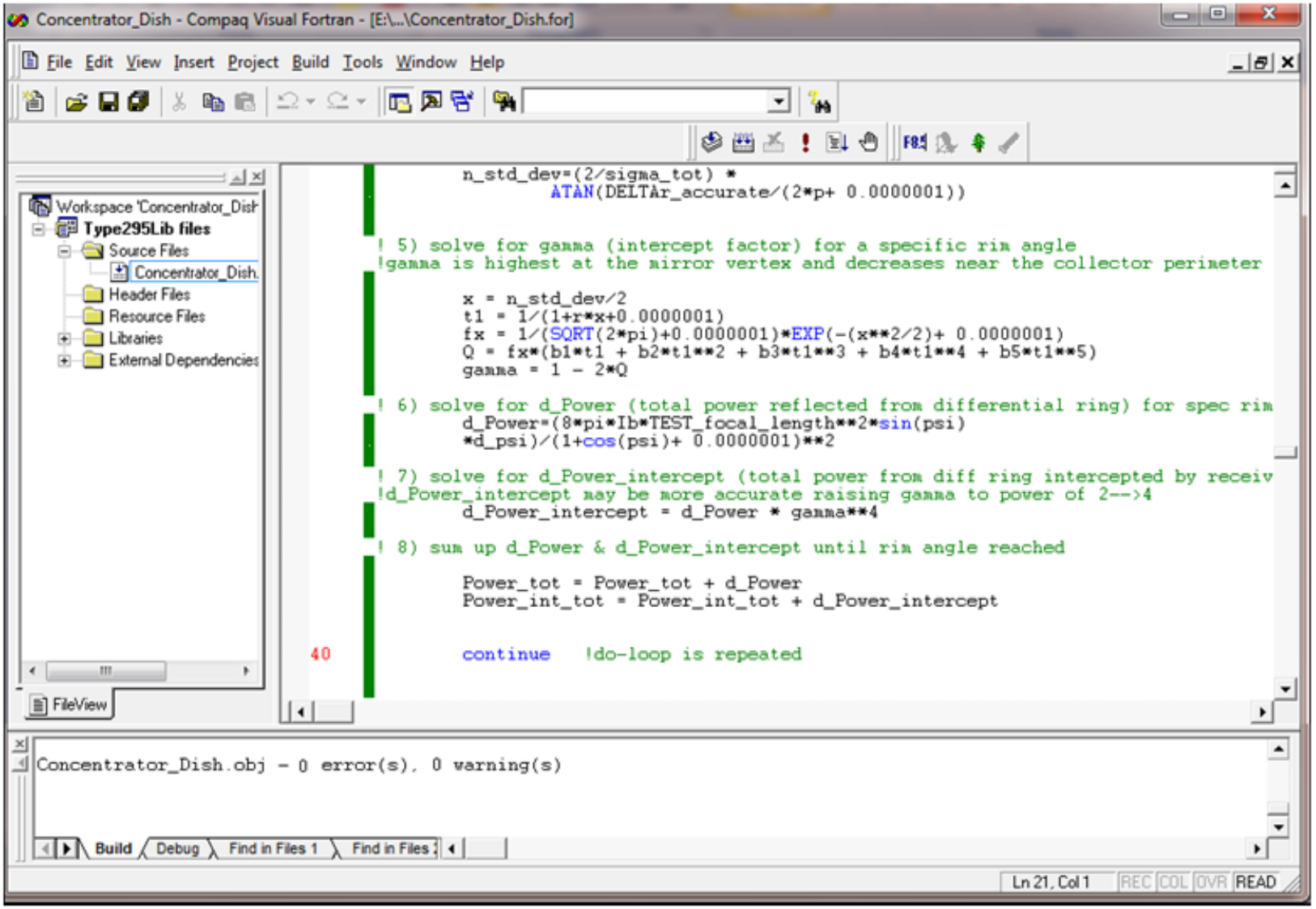

Figure 4.5 Compiling the Component and Building the DLL

- Open ‘Build/Set Active Configuration’, and select the ‘Release’ project configuration and select “Ok”. Press F7 to build the DLL. This will generate "Type200.dll" in the ‘UserLib\Release DLLs ’directory. TRNSYS loads external libraries depending on the mode in which the main DLL was compiled: ‘UserLib\ReleaseDLLs’ and ‘User Lib\Debug DLLs’. In this case, it will use the Release director
- Activate the Simulation Studio and create a project to use the new component. Go to” File/New/EmptyProjects".InorderforthenewlycreatedPerformatoappearinthe direct access tool (component list on the right of the screen), it is refreshed using “Direct Access/Refresh tree" (see Figure 4.6).

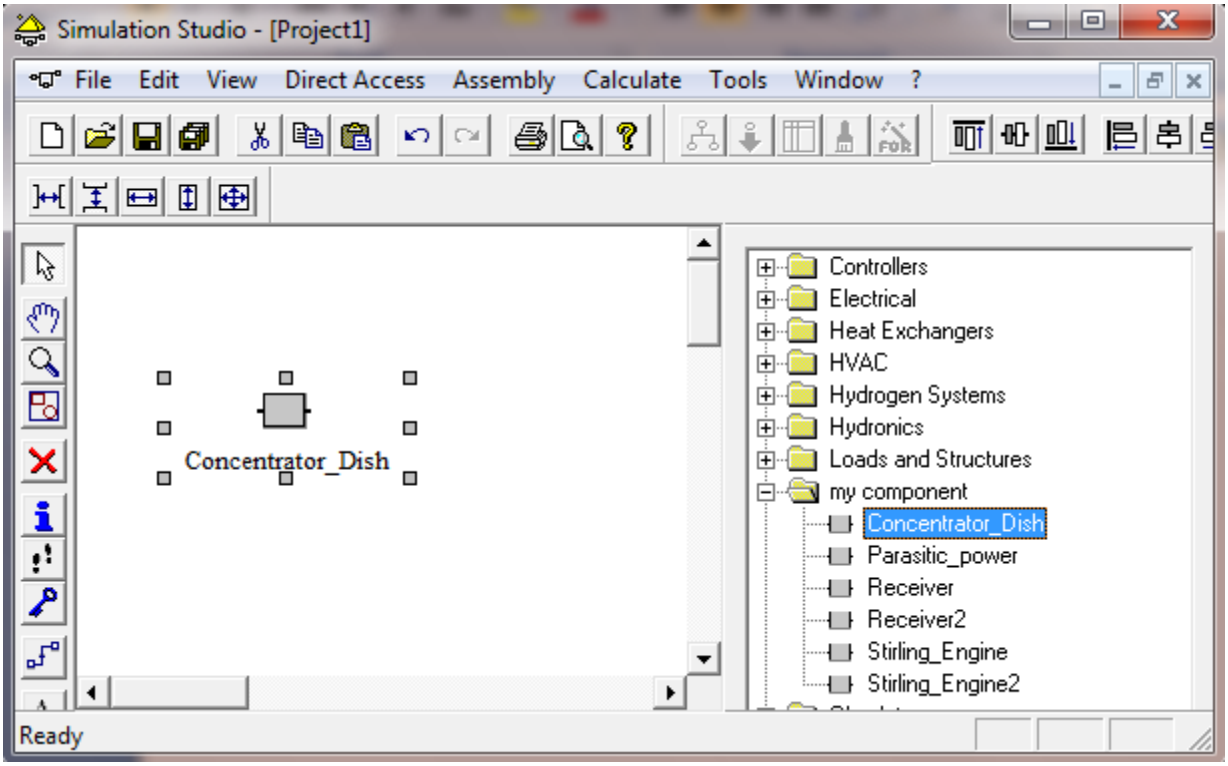

Figure 4.6 Using the New Component in a Project

In this thesis, four of the components added are Concentrator_Dish, Receiver, Stirling engine, Parasitic power. Below is given an illustration of the inclusion of the dryer into the TRNSYS component Types.

- From the simulation studio, click on File-New and then click on New Component-and finally on create(see Figure 4.7)

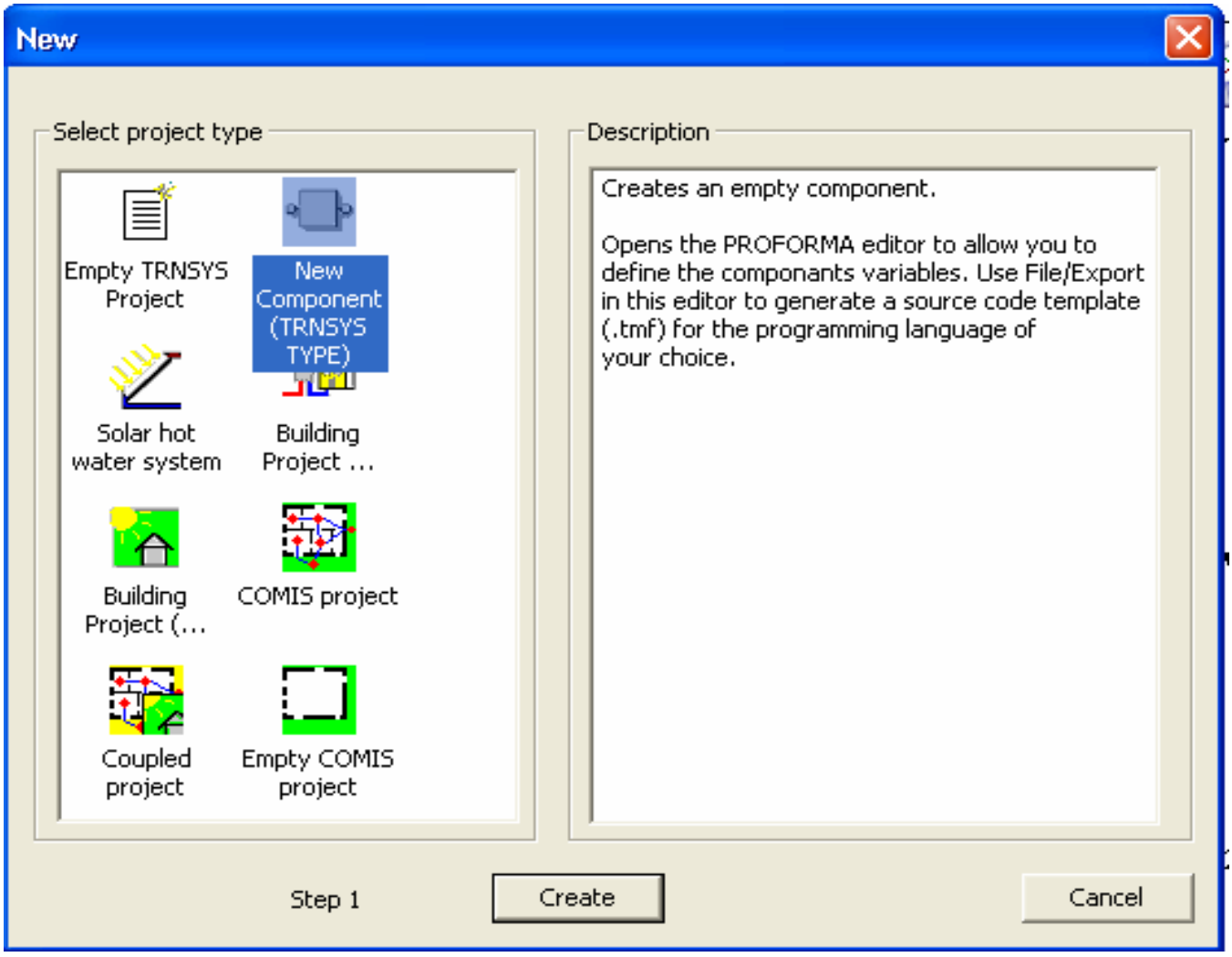

Figure 4.7 Creating a New Component Proforma (1a)

- On the Component1 window select General and enter the Object name and Type Number, (see Figure 4.8).

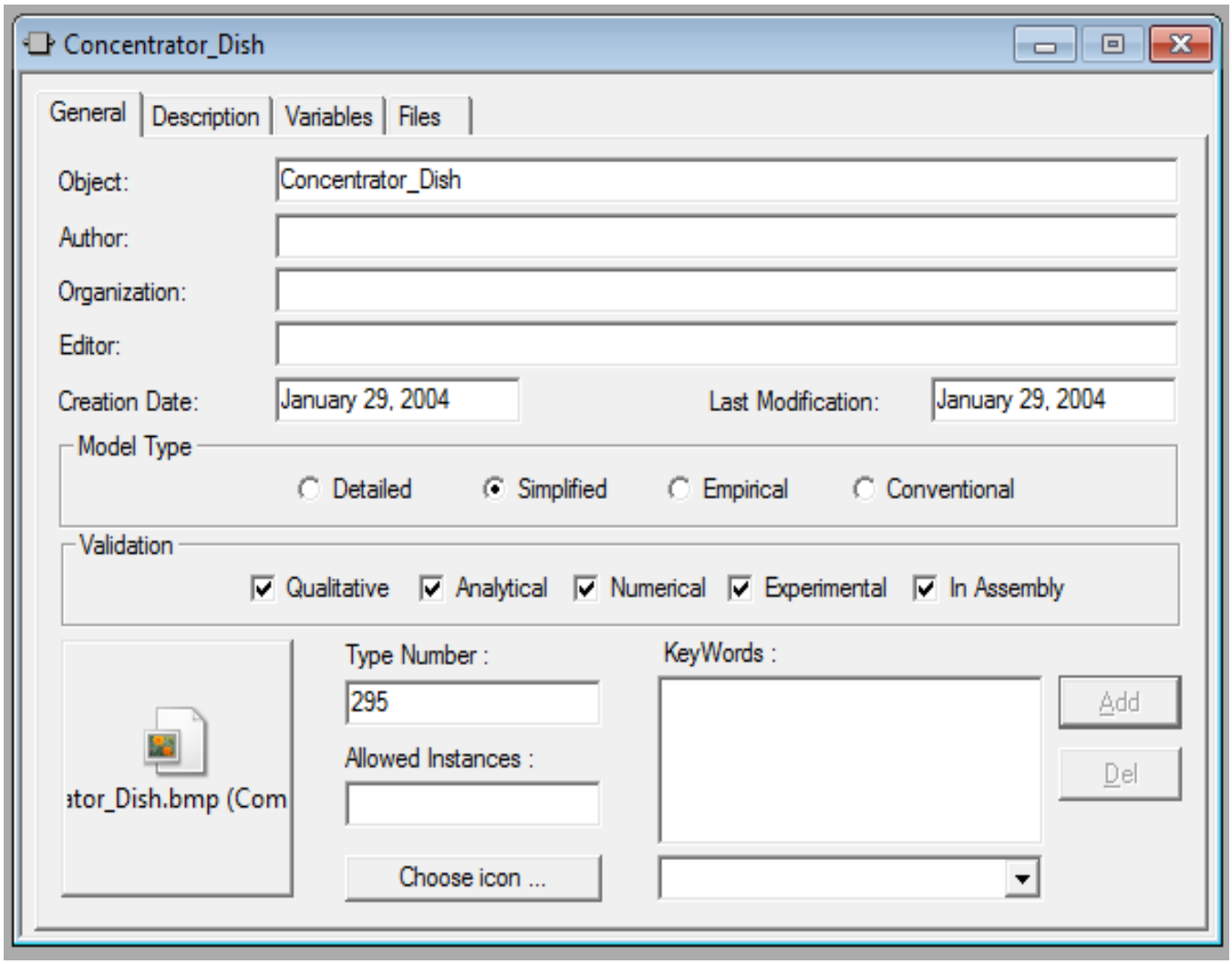

Figure 4.8 Entering Object Name and Type Number for the New Component

- Pick on the Variables menu and then click on Variables (Parameters, Inputs, Outputs, and Derivatives) button. The row sunder Name, Role, Dimension, Unit, et care filled appropriately for the Inputs, the Outputs, the Parameters and Derivatives by clicking on the Add button. After all the required Inputs, Outputs, Parameters, etc. are entered click on OK, see Figure 4.9.

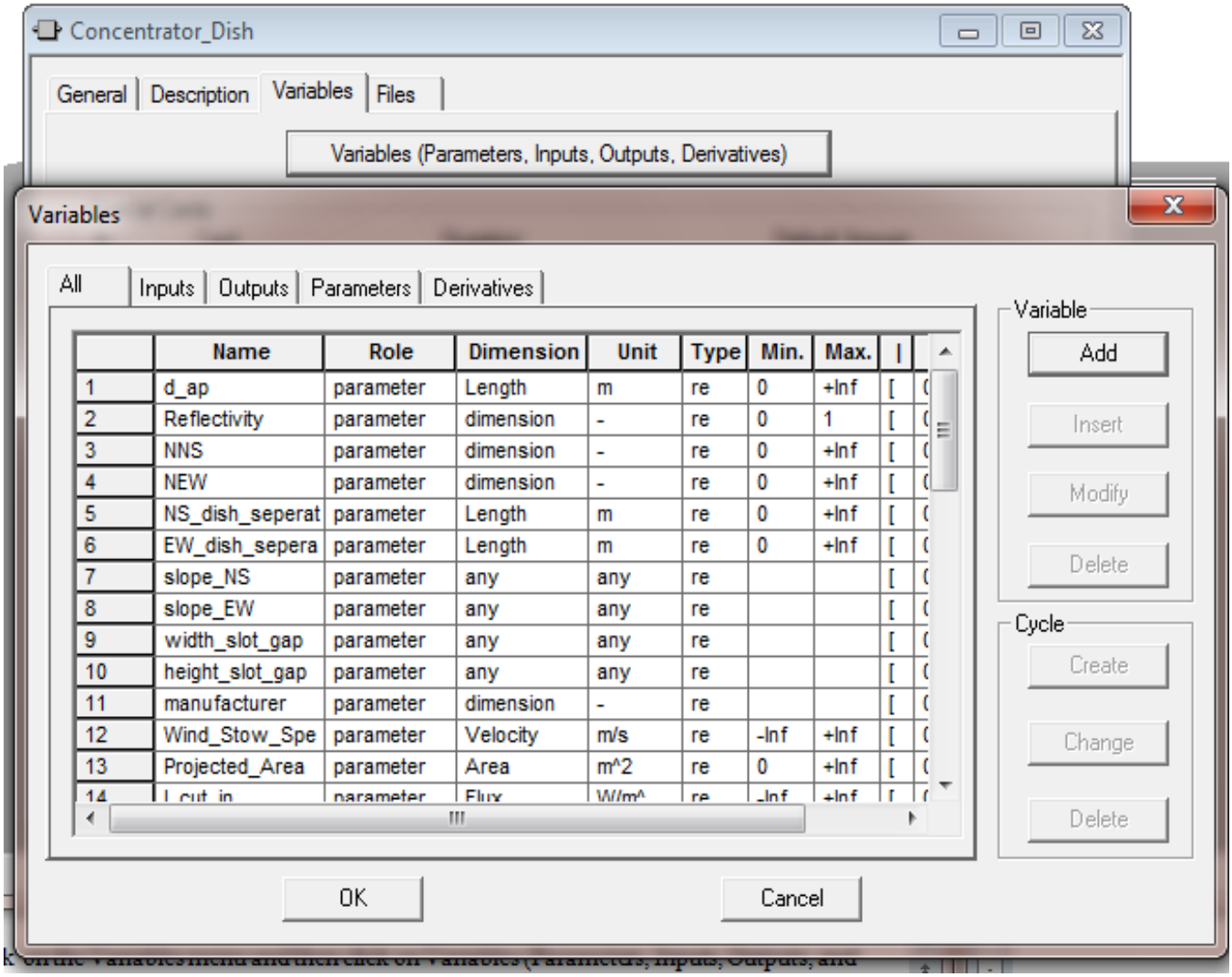

Figure 4.9 Entering Variables for the New Component

- Then click on File-Save and save the new component in the directory of Trnsys 16-Studio-Performa-in the folder "My Components" then click on the Save button, see Figure 4.10.

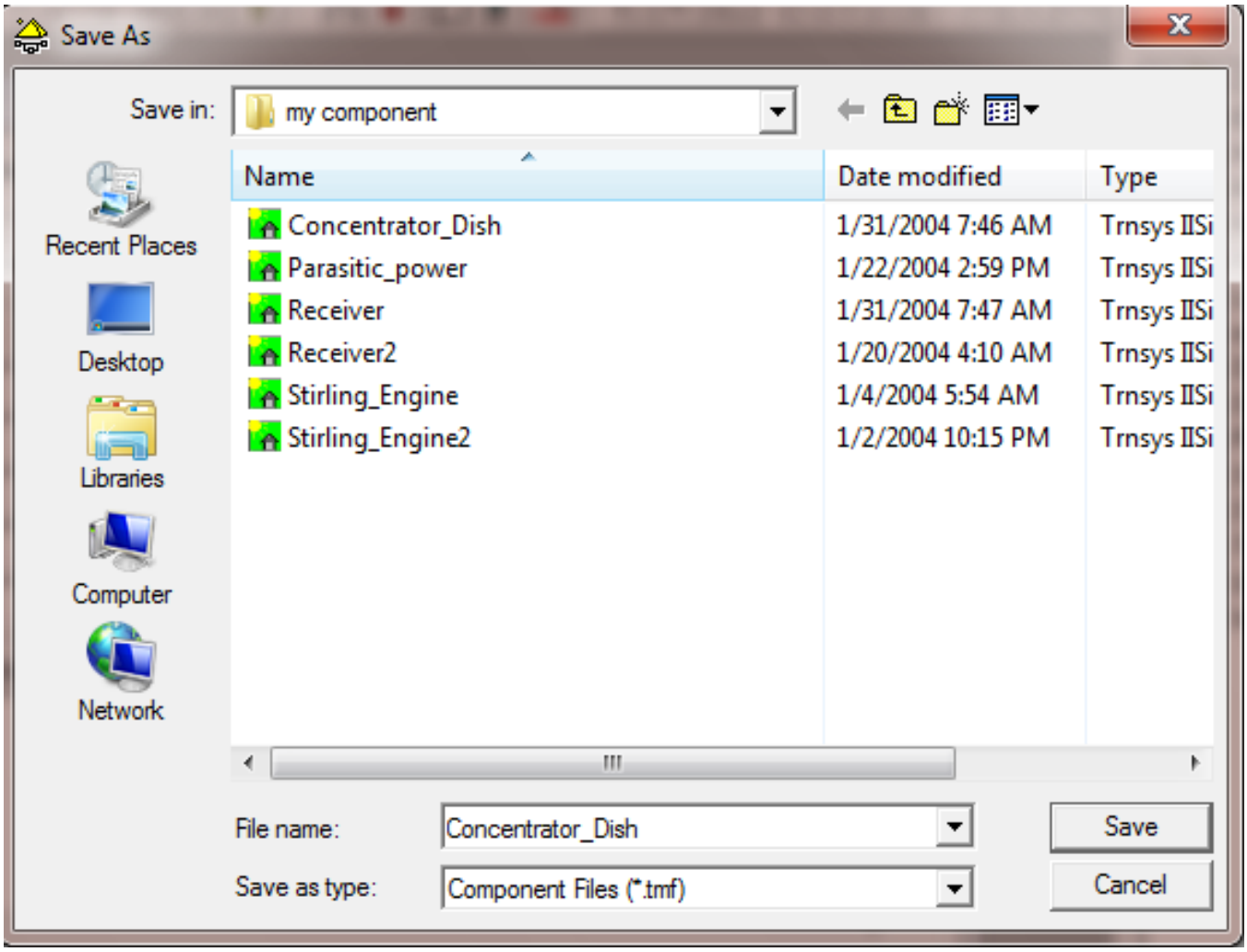

Figure 4.10 Saving the New Component

- Then click on File-Export as… and pick on FORTRAN and save the component type "Type N" in a new folder that has been created.

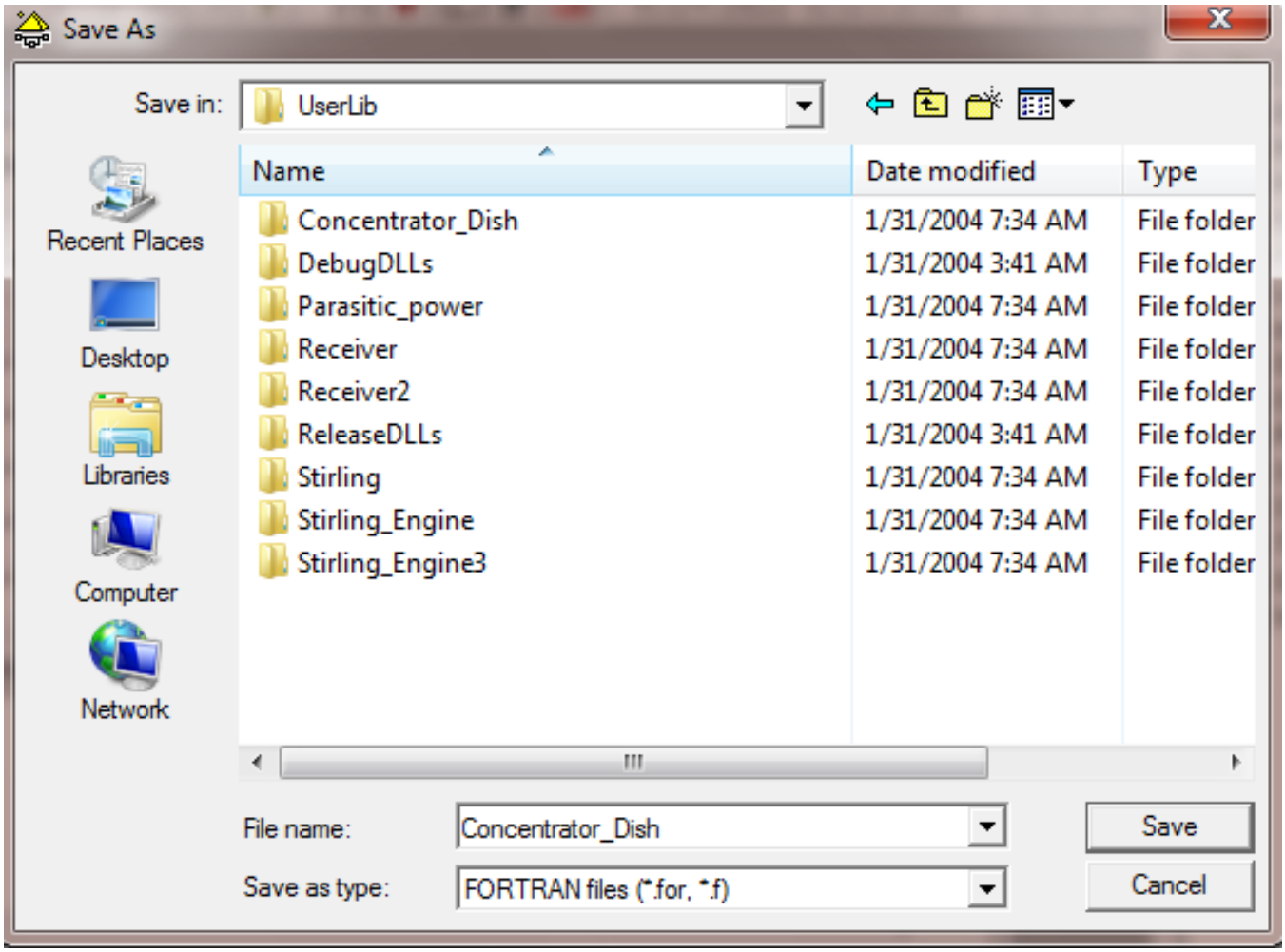

Figure 4.11 Saving the Generated FORTRAN Subroutine of the New Component

- Finally, the equations (s) for the component are entered in place of the question mark (?), out (1) **=?** as shown in Figure 4.12**.**

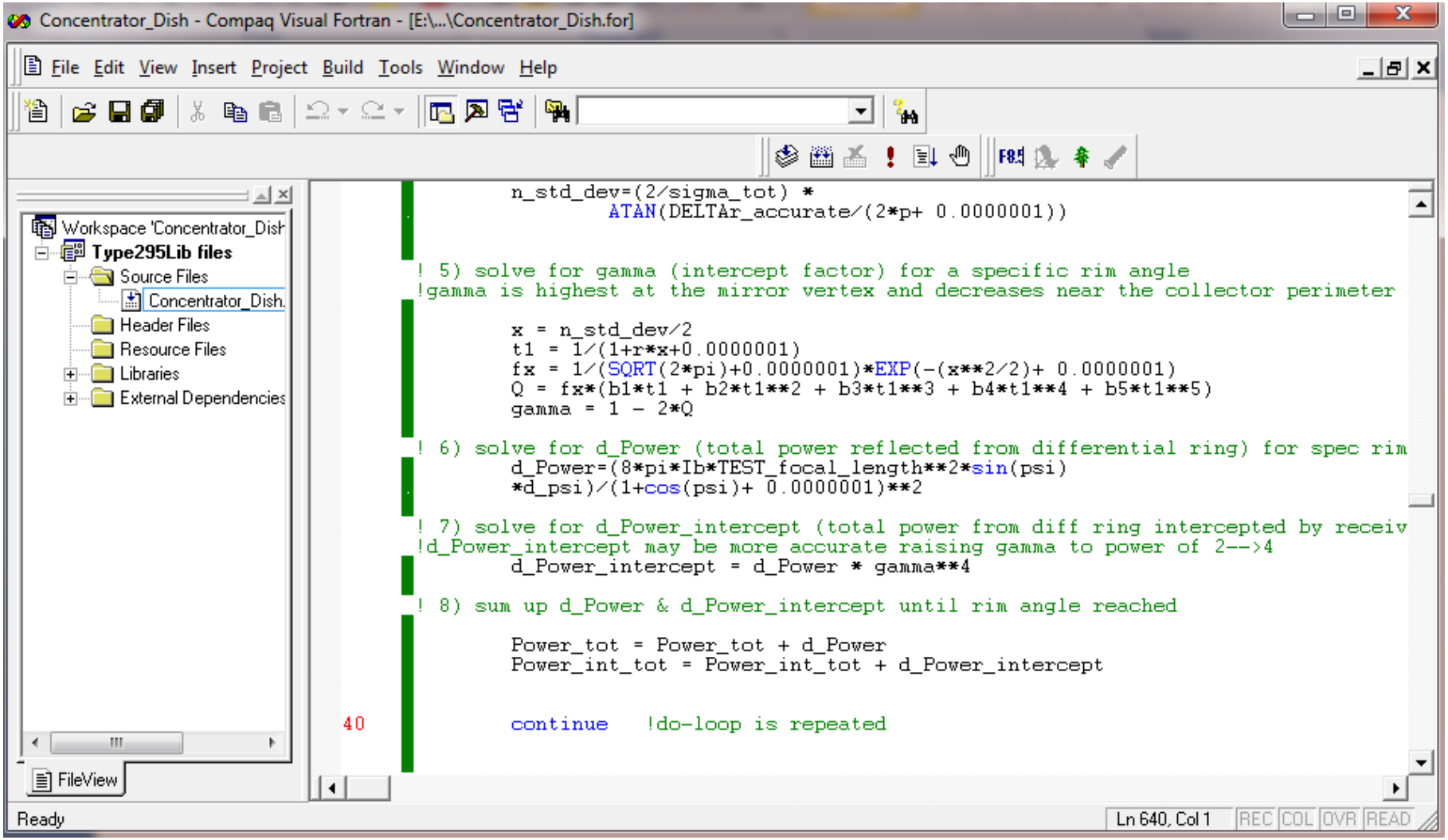

Figure 4.12 Entering Equation (s) in to the Subroutine of the New Component

- Then the component's inputs are connected to the component's output its output is connected to an on line plotter (see Figure 4.13).

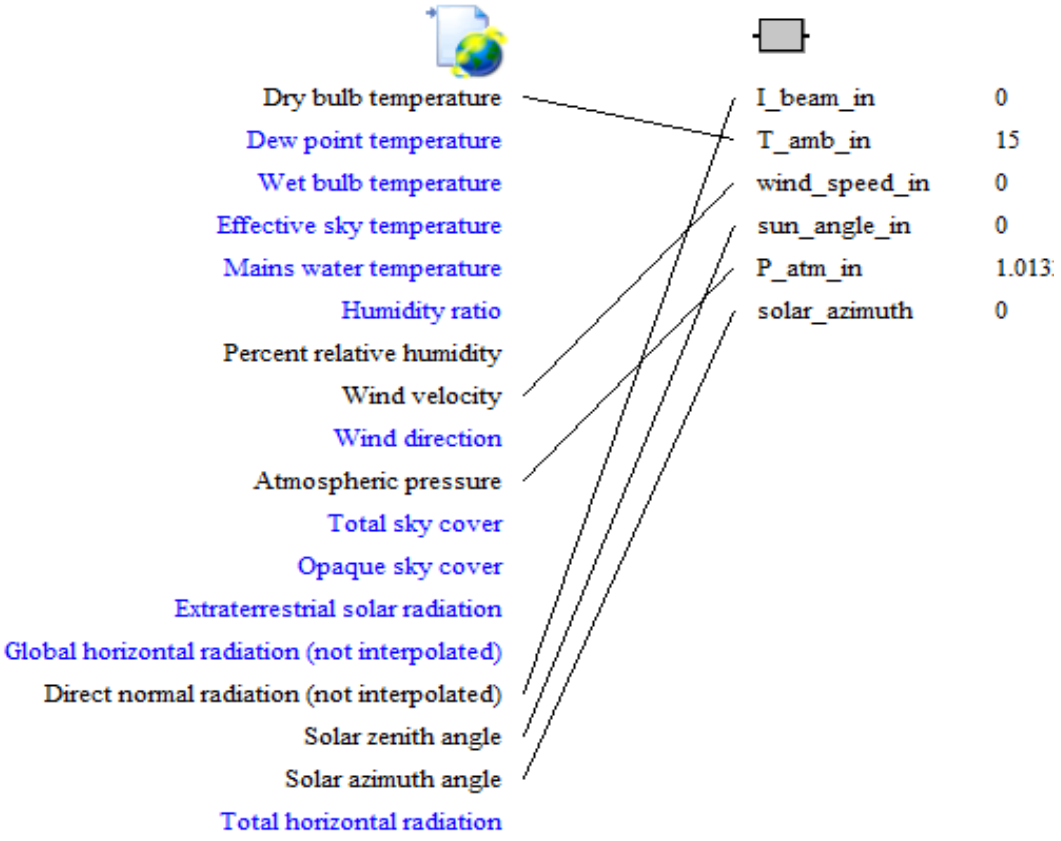

Figure 4.13 Shows the TRNSYS Input File with the Components Placed in Position.

4.3 System Simulation Using TRNSYS

The goal was to create a detailed model that accurately predicts Stirling dish power plant behavior on short time scales (i.e. hours) and through transients. Consequently, the TRNSYS model predictions are plotted on a monthly basis. Results are shown for sunny and cloudy month in 2001 with solar-only operation. Figure 4.14 shows the weather conditions at Kombolcha for the year 2001.

The simulation is done for year 2001 G.C under Kombolcha weather condition. The weather data for the Kombolcha considered is found from SEWERA website in a text and TMY formats.

The results for other months of the year are shown in Appendix D

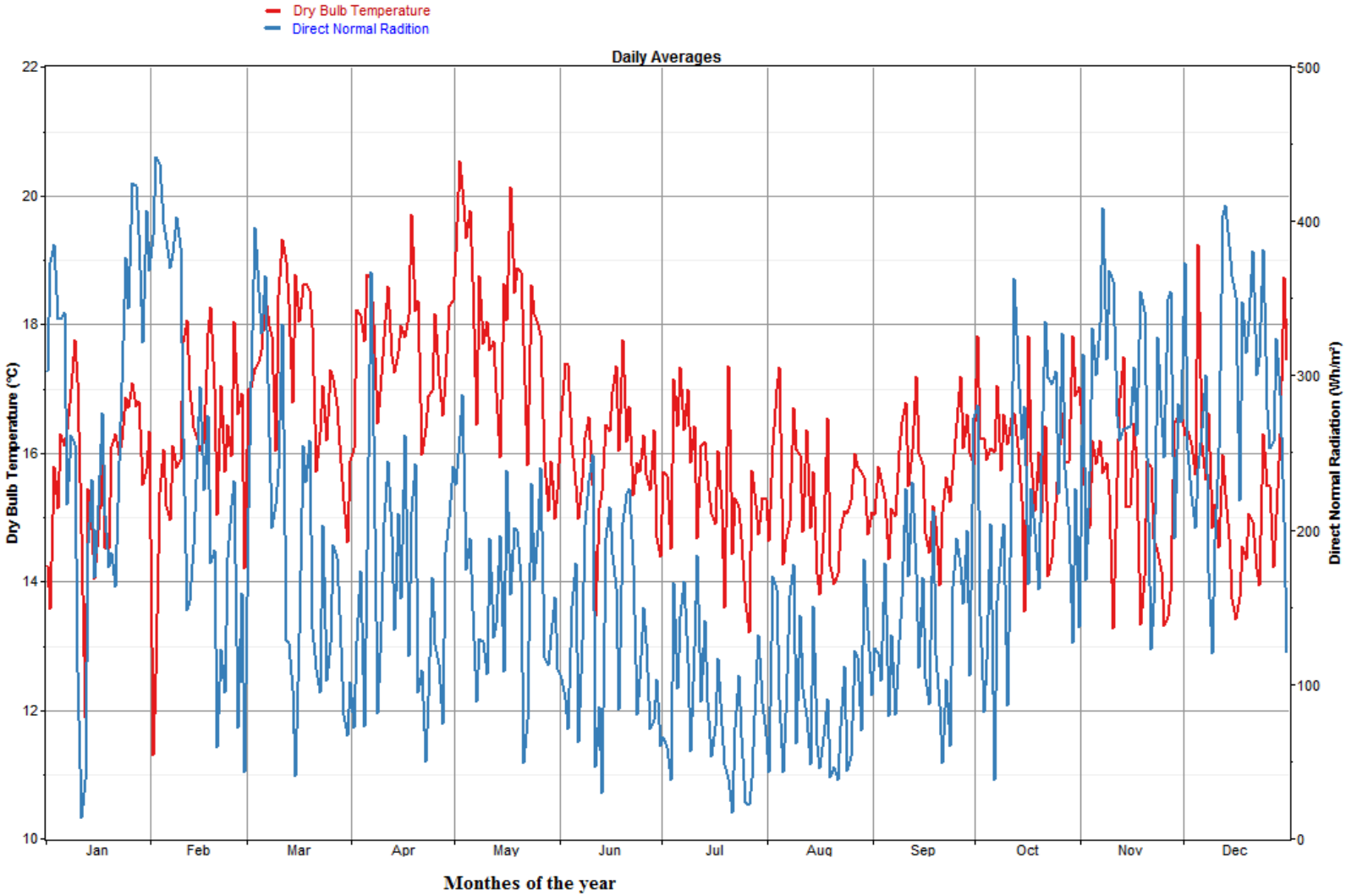

Figure 4.14 Daily Average Weather Conditions at Kombolcha.

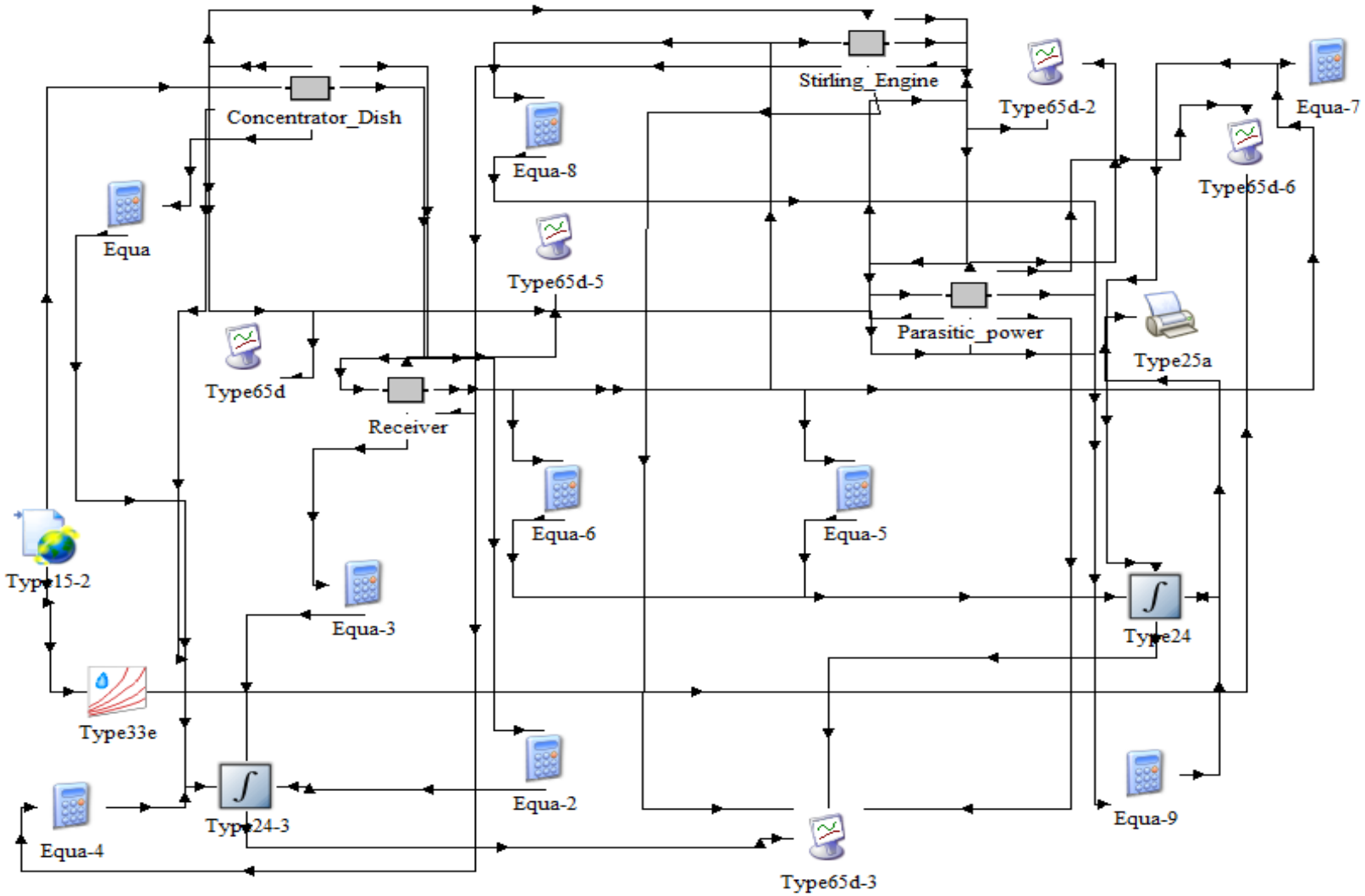

Figure 4.15 TRNSYS Representation the Power Plant Model

4.3.1 Simulation Result for Clear Month February, 2001

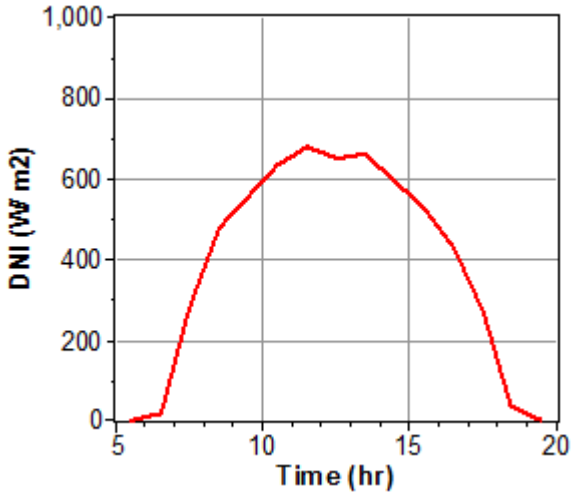

Figure 4.16 Direct Normal Radiation

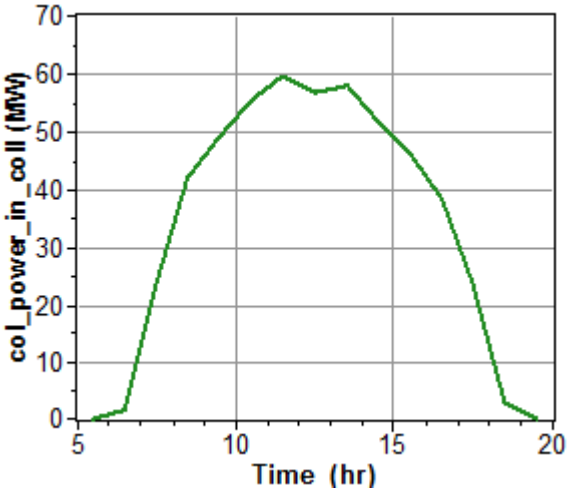

Figure 4.17 Power Input at the Collector

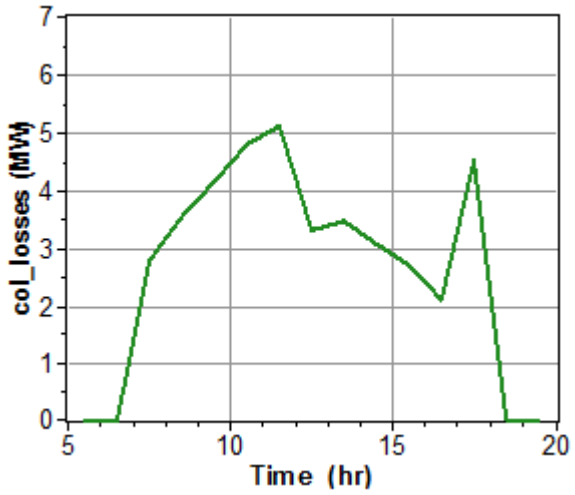

Figure 4.18 Collector Losses

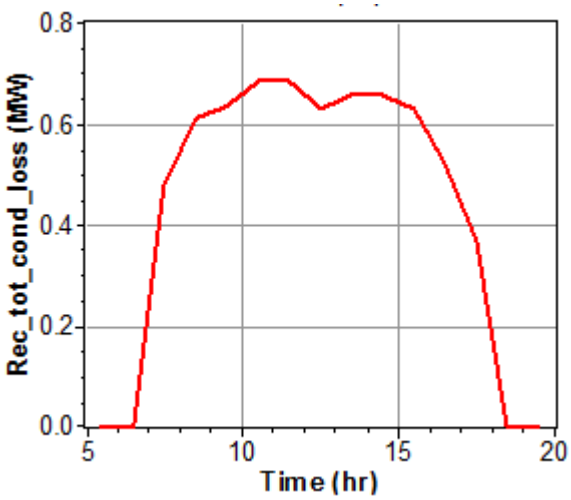

Figure 4.19 Radiation Total Conduction Loss

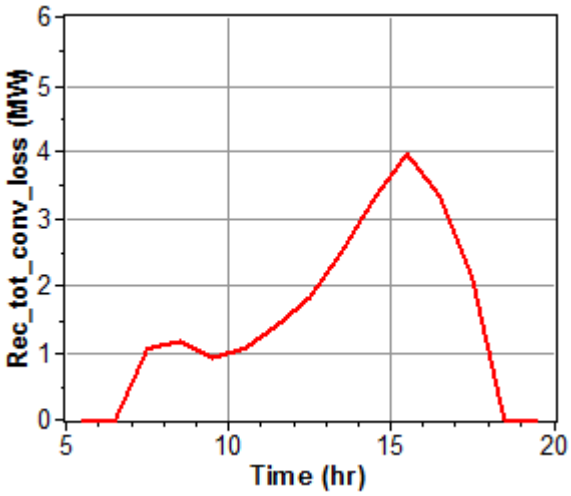

Figure 4.20 Receiver Total Convection Loss

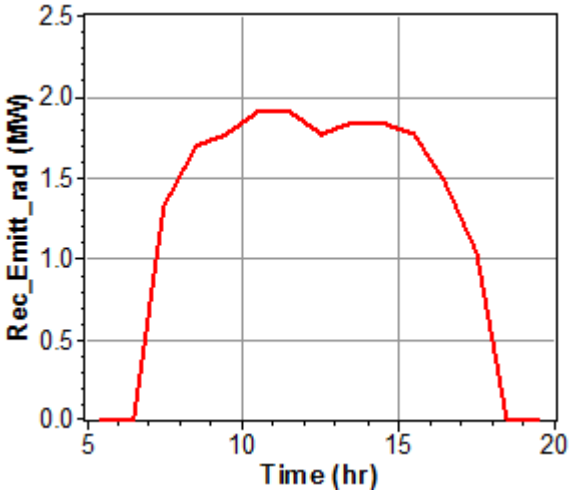

Figure 4.21 Receiver Radiation Loss

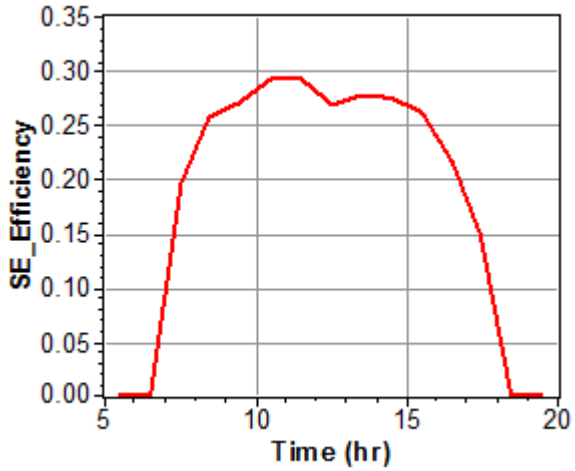

Figure 4.22 Stirling Engine Efficiency

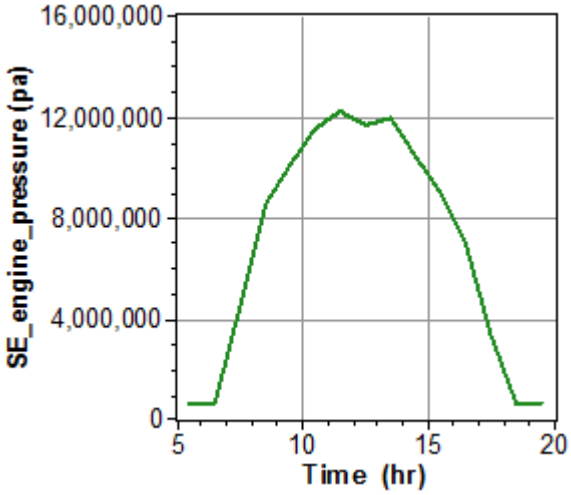

Figure 4.23 Stirling Engine Pressure

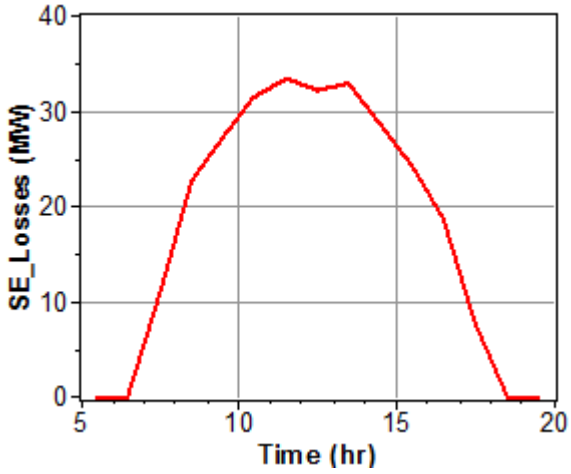

Figure 4.24 Stirling Engine Losses

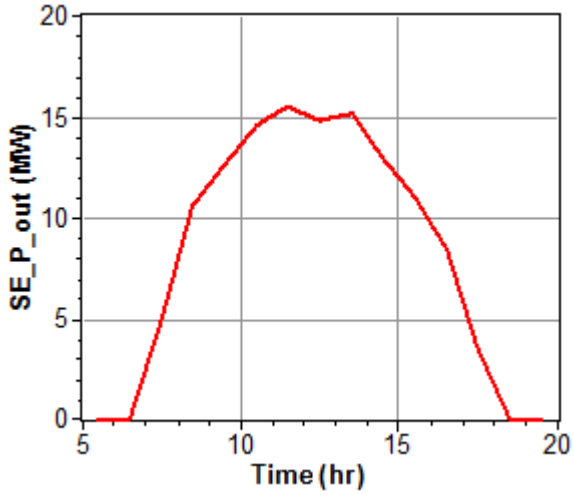

Figure 4.25 Stirling Engine Gross Power Out

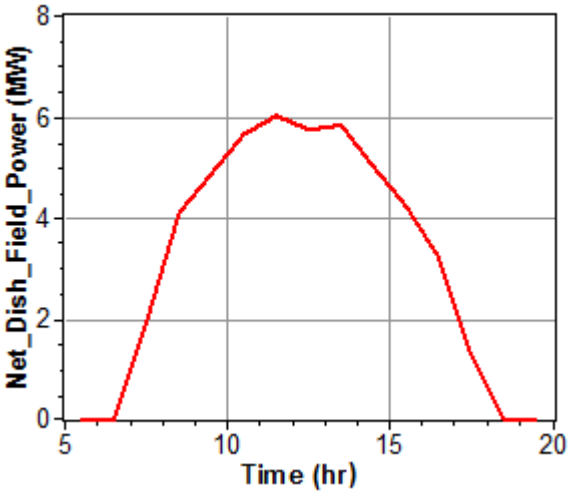

Figure 4.26 Net Dish Field Power Output

4.3.2 Simulation Result for cloudy Month August, 2001

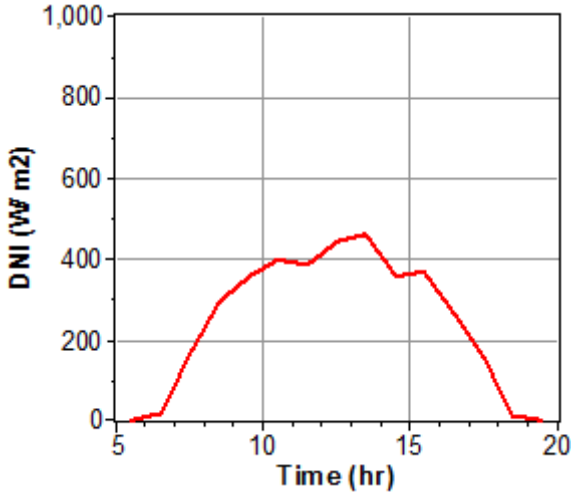

Figure 4.27 Direct Normal Radiation

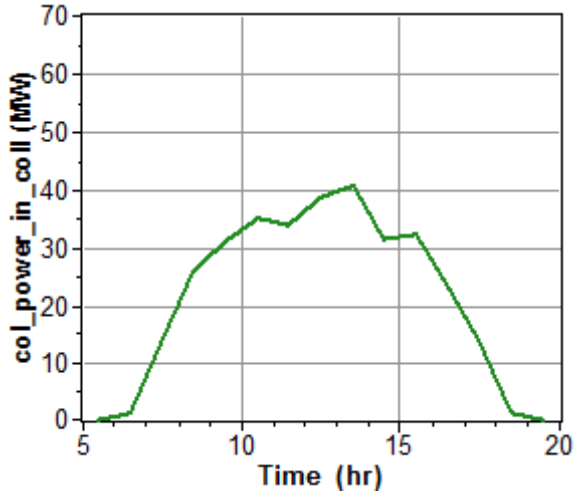

Figure 4.28 Power Input at the Collector

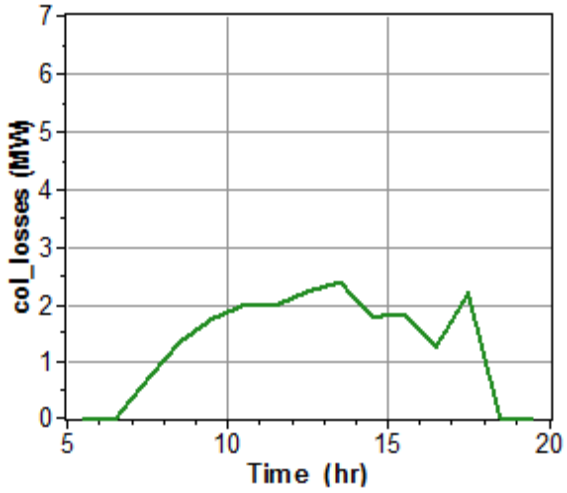

Figure 4.29 Collector Losses

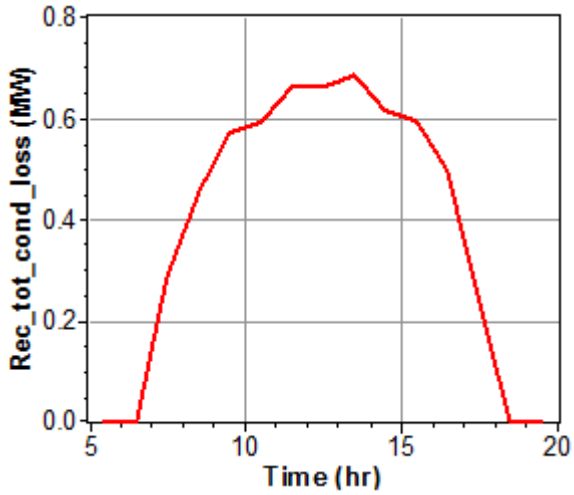

Figure 4.30 Total Conduction Loss

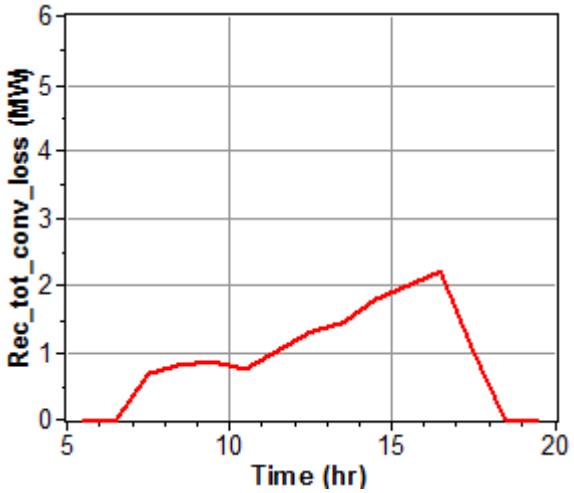

Figure 4.31 Receiver Total Convection

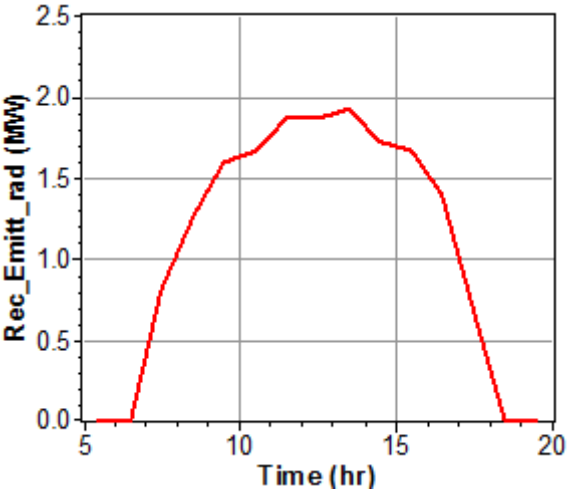

Figure 4.32 Receiver Radiation Loss

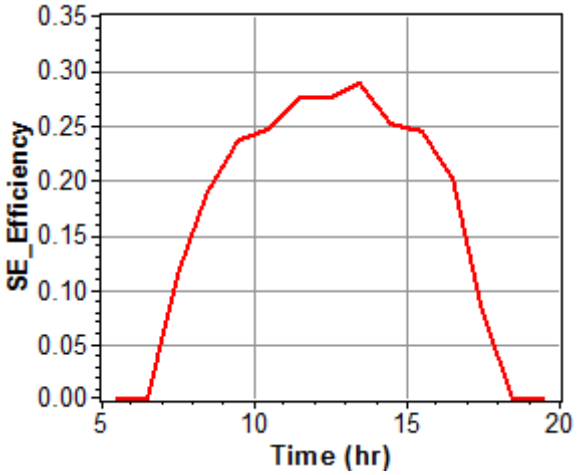

Figure 4.33 Stirling Engine Efficiency

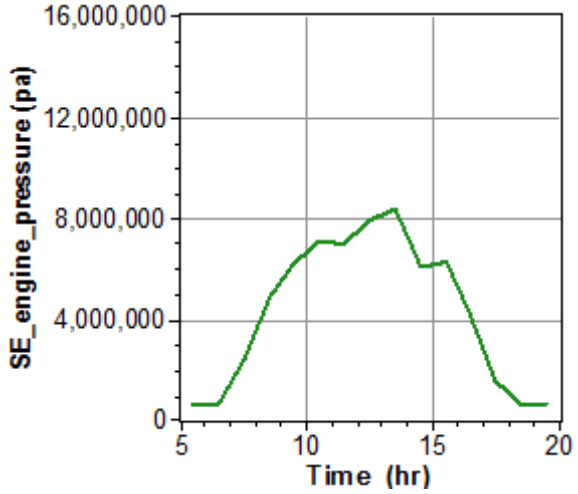

Figure 4.34 Stirling Engine Pressure

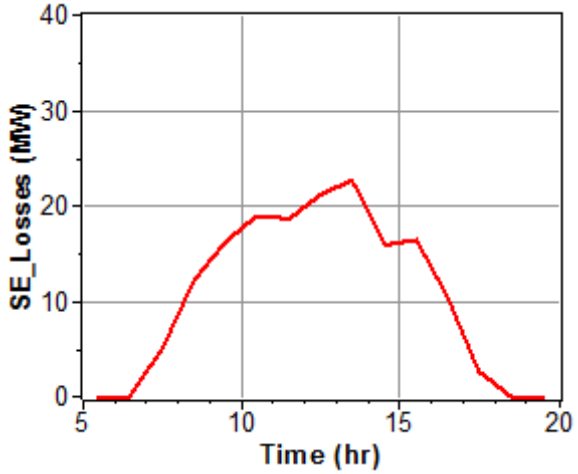

Figure 4.35 Stirling Engine Losses

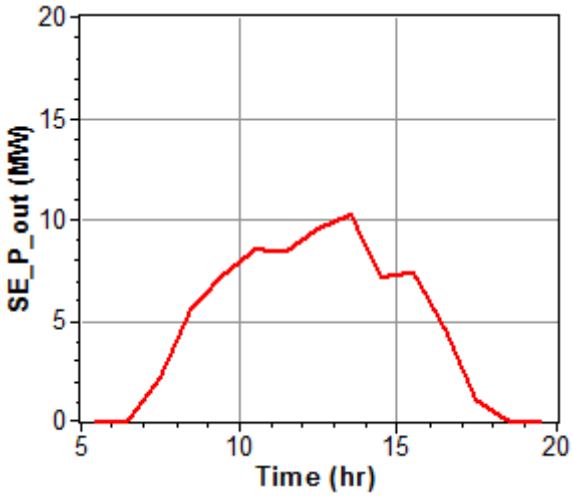

Figure 4.36 Stirling Engine Gross Power Out

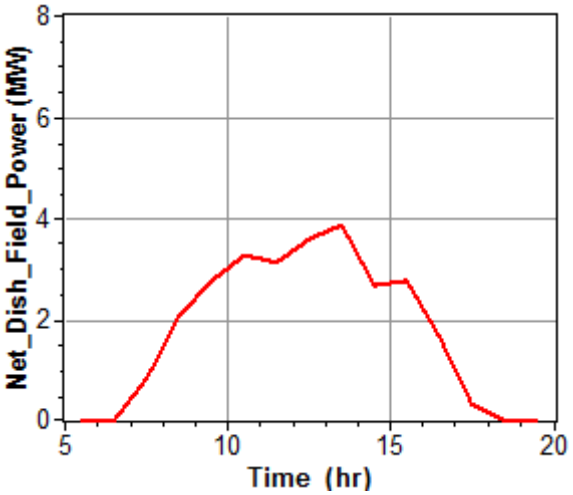

Figure 4.37 Net Dish Field Power Output

CHAPTER FIVE

Cost and Financial Analysis of the Stirling Dish System

5.1 Introduction

Solar Advisor makes performance predictions and economic estimates for grid-connected solar power projects in the distributed and central generation markets. The solar technologies currently represented in SAM include concentrating solar power (CSP) parabolic trough, dish-Stirling, and power tower systems, as well as flat plate and concentrating photovoltaic technologies.

Solar Advisor is based on an hourly simulation engine that interacts with performance, cost, and finance models to calculate energy output, energy costs, and cash flows. SAM incorporates the best available models to allow analysis of the impact of changes to the physical system on the overall economics.

User Interface Overview

The main window consists of a navigation menu and data page. Navigation buttons in the navigation menu select the data page to display. Data pages display results and input data. Tabs along the top of the window provide access to each case in the file. The menu bar provides access to command menus.

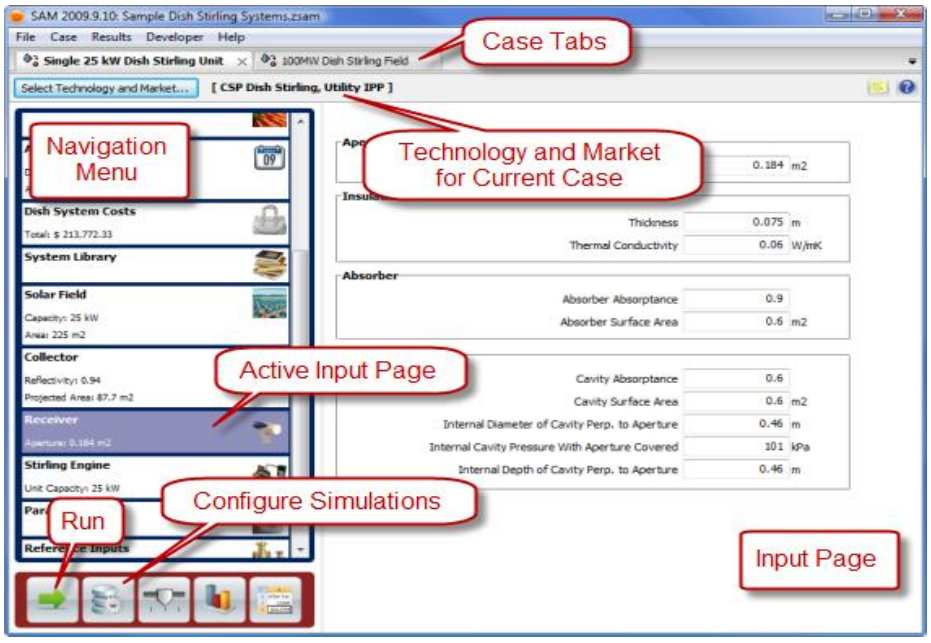

Figure 5.1 SAM user Interface for Dish System (TRNSYS Manual)

The main window gives you access to the input pages for each of the cases in the project:

5.2 Financial and Incentive Models

Solar Advisor's economic model calculates a project's cash flow over a specified analysis period. The cash flow captures installation and operating costs, taxes, incentives, and the cost of debt. Solar Advisor uses the system's hourly output for a single year generated by the performance model, and then calculates a series of annual cash flows for revenues from electricity sales and incentive payments, tax liabilities (accounting for any tax credits for which the project is eligible), and loan principal and interest payments.

Solar Advisor reports a set of economic metrics such as the levelized cost of energy that it calculates from the cash flow. Solar Advisor also generates a detailed cash flow table that one can use to evaluate a project's value. The economic model can represent projects in the residential, commercial, and utility markets, and account for a wide range of incentive payments and tax credits, which can be based on investment amounts, capacity ratings, and annual electricity production. Residential and commercial projects are assumed to be financed through either a loan or cash payment, and to recover investment costs by selling electricity through either a net metering or time-of-use pricing agreement. For these projects, SAM reports a payback period and net present value in addition to the detailed cash flow table. Utility and commercial third-party projects are assumed to sell electricity through a power purchase agreement at a fixed price with optional annual escalation, and to be required to meet a set of financing constraints. For utility projects, SAM calculates an electricity sales price, internal rate of return, and minimum debt service coverage ratio. Projects with commercial and utility financing can be modeled with or without depreciation using MACRS depreciation schedules or customized schedules.

5.2.1 Project Cash Flow

Solar Advisor reports annual data in the cash flow table, including the system's annual electric output in kWh, electricity price in $/kWh, net-metering receipts or sales revenue, project expenses, taxes, and cost streams used to calculate the project payback. The cash flow table only displays data from on the analysis base case, which is the set of results calculated from the input variable values that are visible on the input pages. Solar Advisor calculates the values for the cash flow and other economic metrics after completing the performance simulation calculations. The model uses the first year annual energy output value from the simulation results in the cash flow calculations. It also uses input variable values from the input pages.

5.2.1.1 Energy (kWh)

The energy quantity reported for year one is equal to the Annual Energy value displayed in the Metrics table. The quantities in year two and subsequent years is based on the year one value adjusted for the degradation rate.

5.2.1.2 Energy Price ($/kWh)

For commercial and residential projects, the energy price is the annual average utility rate where as for utility and commercial third party projects, the energy price is the 1st Year PPA price displayed in the Metrics table. For year two and later, the energy price is the first year price adjusted by the PPA escalation rate also displayed on the Metrics table.

5.2.1.3 Energy Value ($)

Residential and commercial projects may receive net-metering offset payments for electricity generated by the project. Commercial projects pay federal and state income tax on these payments. For utility projects, annual revenues are determined in each year by the annual energy output and the electricity sales price for that year.

Energy Value = Energy (kWh) x Energy Price ($/kWh)

5.2.1.4 Operating Expenses

The operating expenses include operation and maintenance costs, and insurance and property tax payments. The value in the Operating Costs row of the cash flow table is calculated as follows:

Operating Costs = Fixed O&M Annual + O&M + Variable O&M + Fuel O&M + Insurance + Property Taxes

The operation and maintenance (O&M) costs are defined on the system costs page and escalated in each year after year one using both the escalation rate for each O&M category and the inflation rate value. The insurance and property tax rates apply to the total installed cost value. CSP trough, CSP tower, and generic fossil systems also include an annual cost of fuel in the total operating expense. When the fossil fill fraction variable on the Thermal Storage page for troughs or towers is greater than zero, the systems consume fuel for backup energy. But For photovoltaic and CSP dish systems, the fuel cost is always zero.

5.2.1.5 Operating Income and Deductible Expenses

For residential and commercial projects, the deductible expenses are project costs that can be deducted from federal and state income taxes.

For residential projects, the deductible expense amount equals the property tax amount:

Deductible Expenses = - Property Taxes

For commercial projects, all operating costs are deductible:

Deductible Expenses = - Operating Costs

For utility projects, the operating income is the difference between revenues and operating costs:

Operating Income = Revenues - Operating Costs

5.2.1.6 Income, Taxes and Incentives

All projects pay state and federal taxes on the total taxable income for each year when the state and federal annual tax rates are non-zero. Federal and state tax cash flows are displayed in two separate sections of the cash flow spreadsheet, under the rows labeled Tax Effect on Equity (State) and Tax Effect on Equity (Federal). The tax amount for each year appears in the Tax Savings row under each section.

5.2.1.7 Depreciation

For utility and commercial third party ownership projects with a depreciation option defined on the Financials page, Solar Advisor displays the depreciation amount in the State Depreciation and Federal Depreciation rows of the cash flow table. The depreciation amounts and applicable years are determined by the options on the Financials page.

5.3 SAM Input Pages for Dish System

The model calculates the cost of generating electricity based on information you provide about a project's location, installation and operating costs, type of financing, applicable tax credits and incentives, and system specifications. The model provides options for parametric studies, sensitivity analysis, optimization, and statistical analyses to investigate impacts of variations and uncertainty in performance, cost, and financial parameters on model results.

The economic model can represent projects in the residential, commercial, and utility markets, and account for a wide range of incentive payments and tax credits, which can be based on investment amounts, capacity ratings, and annual electricity production.

Residential and commercial projects are assumed to be financed through either a loan or cash payment, and to recover investment costs by selling electricity through either a net metering or time-of-use pricing agreement. Utility and commercial third-party projects are assumed to sell electricity through a power purchase agreement at a fixed price with optional annual escalation, and to be required to meet a set of financing constraints.

For utility projects, SAM calculates an electricity sales price, internal rate of return, and minimum debt service coverage ratio. Projects with commercial and utility financing can be modeled with or without depreciation using MACRS depreciation schedules or customized schedules.

Here there are input pages. The navigation menu provides access to the input pages.

5.3.1 Climate page

Table 5.1 Input Page for Climate from Navigation Menu

Input Page	Purpose
	Specify a weather file for the system's location

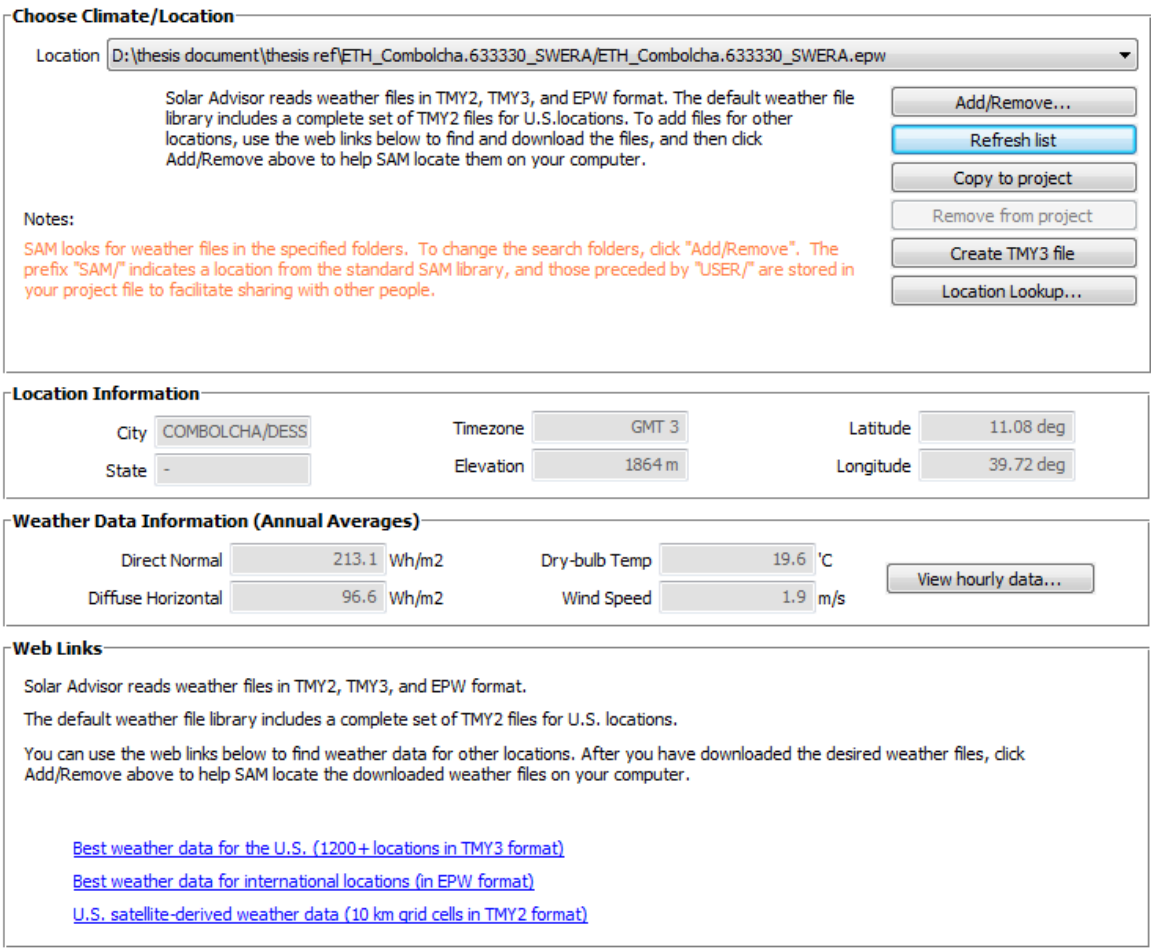

Figure 5.2 Climate Page

Choose Climate/Location

Location

A filename preceded by "SAM/" is a standard weather data file included with Solar Advisor and stored in the \exelib\climate files folder. A filename preceded by "USER/" is a file in a folder that you have added to the weather file search path list.

Add/Remove

Add or remove a folder on your computer from the list of folders Solar Advisor searches for files with the TMY2, TMY3, or EPW file extension. Solar Advisor will list all weather files in folders that you add to the search list in the location list. See Adding and Removing Weather File Search Paths for details.

Refresh List

Refreshes the list of files in the location list, Solar Advisor automatically refreshes the list each time you visit the Climate page. If you add a weather file to one of the folders in the search list, you may need to refresh the list for the file to be visible in the location list.

5.3.2 Financing page

The Financing page displays the variables that Solar Advisor uses to calculate the project cash flow and other related financial metrics. The variables that appear on the Financing page depend on the financing option specified.

In this case CSP Power dish technology for Utility IPP market is analyzed. In the financials page the analysis period, inflation period, loan amount, taxes and insurance, power purchase agreements and other inputs are found.

Table 5.2 The Financial Input Page

Input Page	Purpose
	Define the project's debt structure and rate of return constraints as appropriate for the type of project

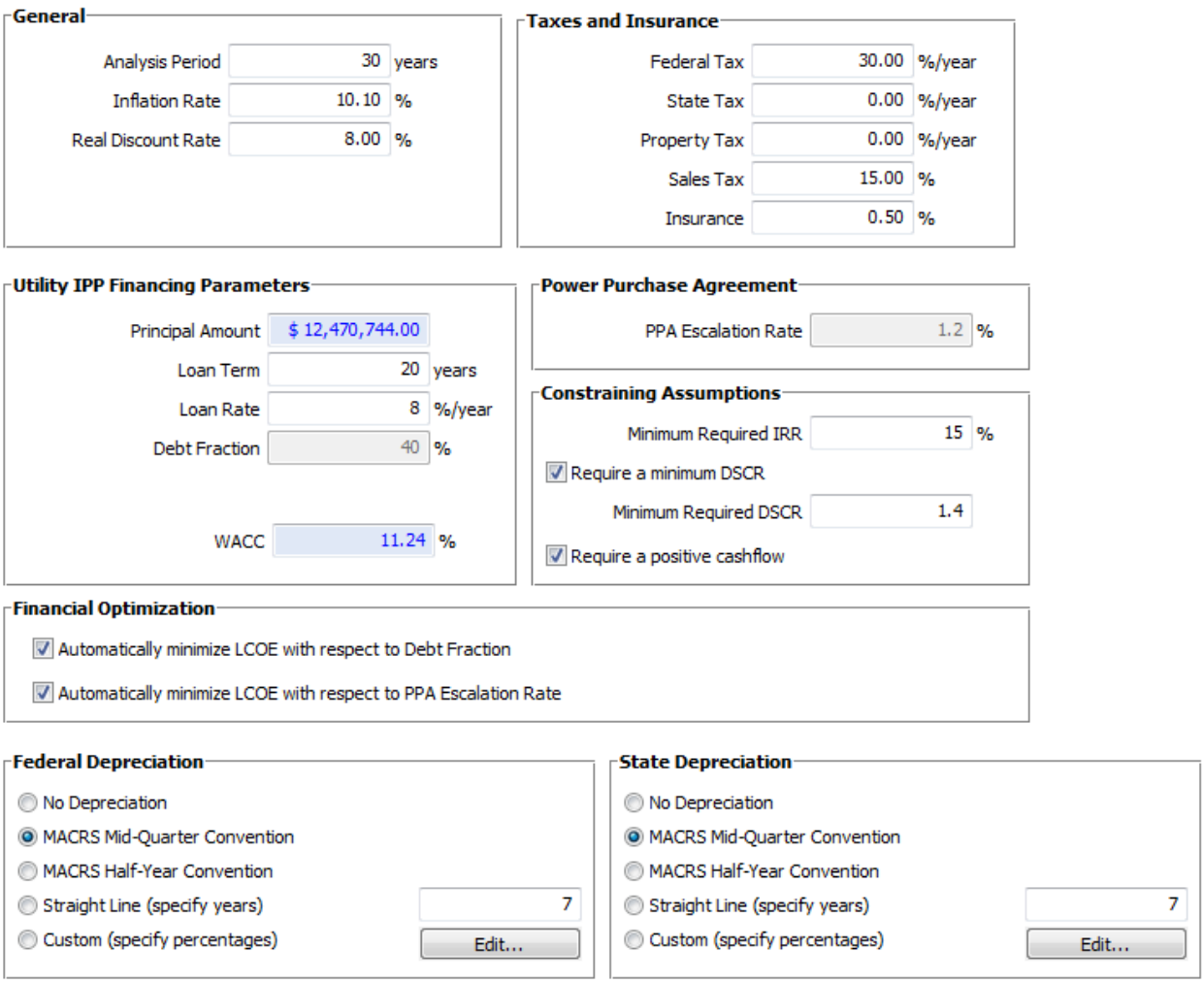

Figure 5.3 Financial Page

Annual System Performance

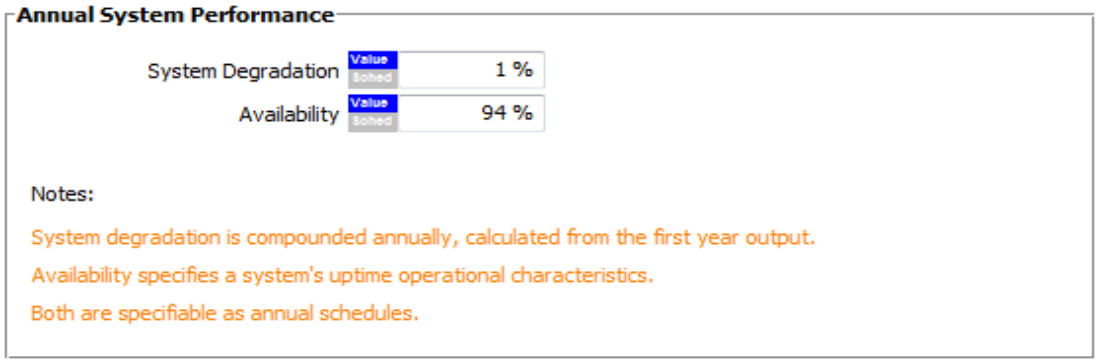

Figure 5.4 Annual System Performance Page

5.3.3 Dish System Costs

In the costs page, SAM calculates the different estimates for direct, indirect, and operation and maintenance cost components for the project. This page is used to determine the total installed cost that can be used as input for the financial page.

The direct capital costs include site improvements, Collector Cost, Receiver Cost, Stirling Engine Cost, and contingency costs for the project. According to this analysis a total direct capital cost is $23,982,200.00.

An indirect cost is typically one that cannot be identified with a specific piece of equipment or installation service, and may include all other costs that are built into the price of the system, such as profit, overhead, and shipping costs.

Engineering procurement, sales tax, land and project management costs are considered as indirect capital costs which in this case estimated to be $7,194,660.00.

The total installed capital cost is the sum of direct and indirect capital costs which is $31,176,860.00 as shown in Figure 5.5

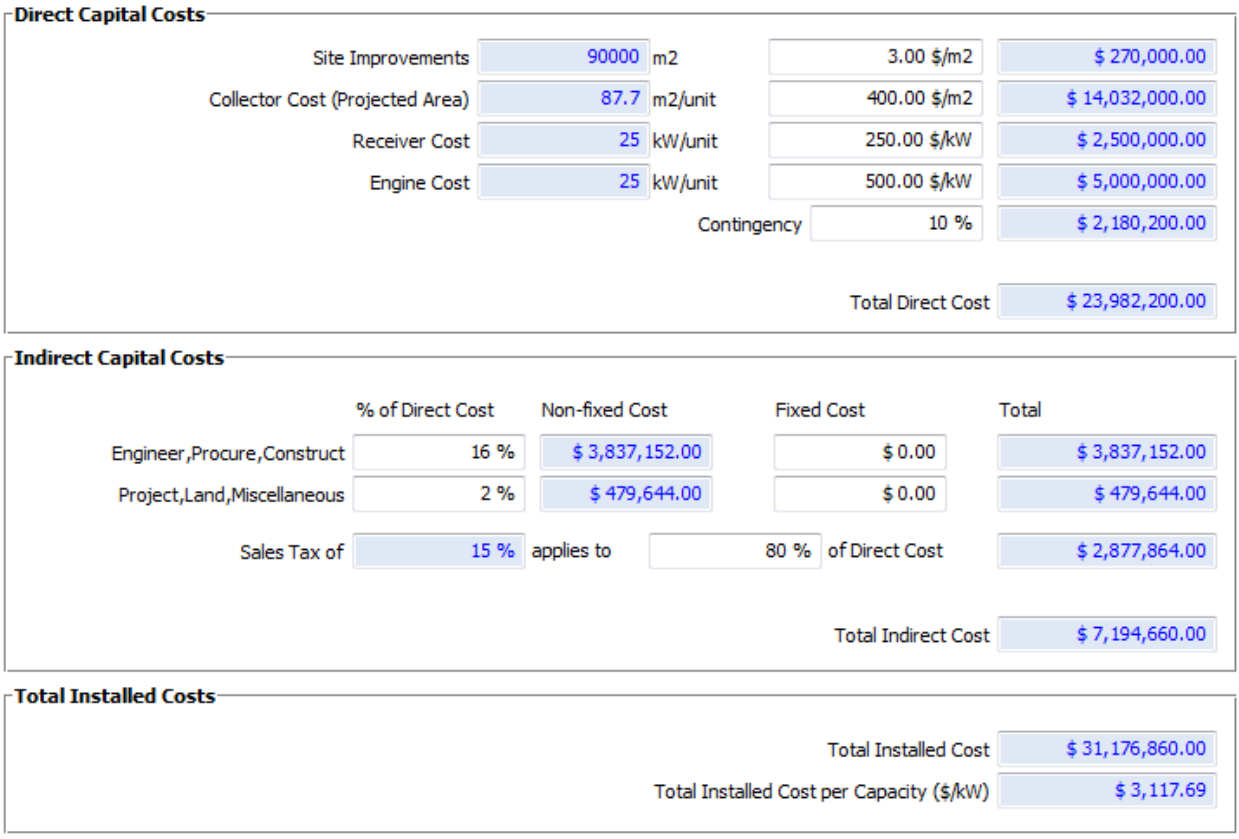

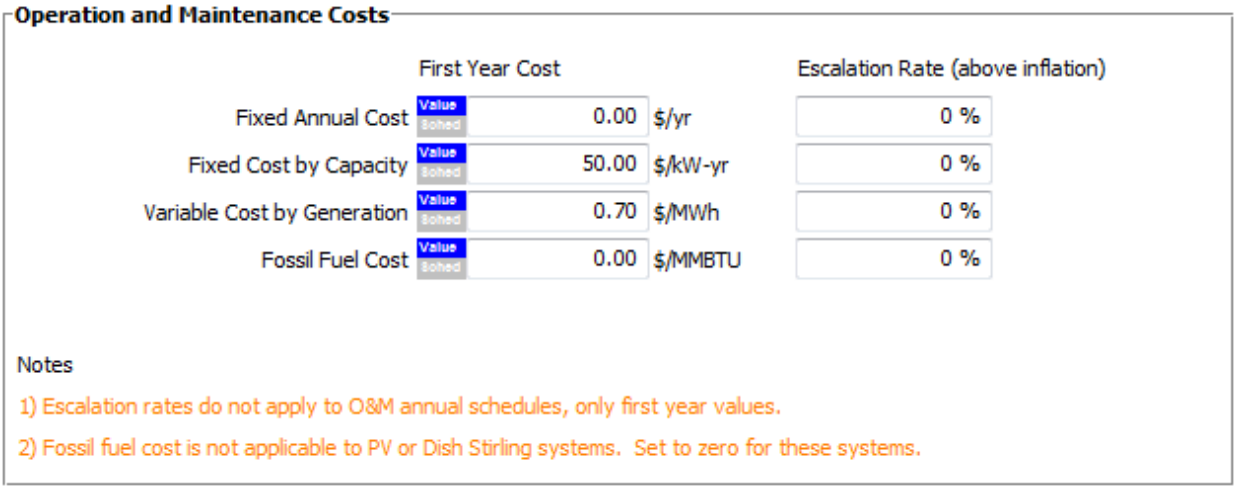

Figure 5.5 Dish System cost Page

5.3.4 Dish solar Field Page

The parameters on the Solar Field page define the size of the solar field and the layout of the dish network. To explore the impact of these parameters on the system's costs and performance, change the value of the parameter. The solar field is assumed to be a rectangular field with collectors oriented north-south and east-west.

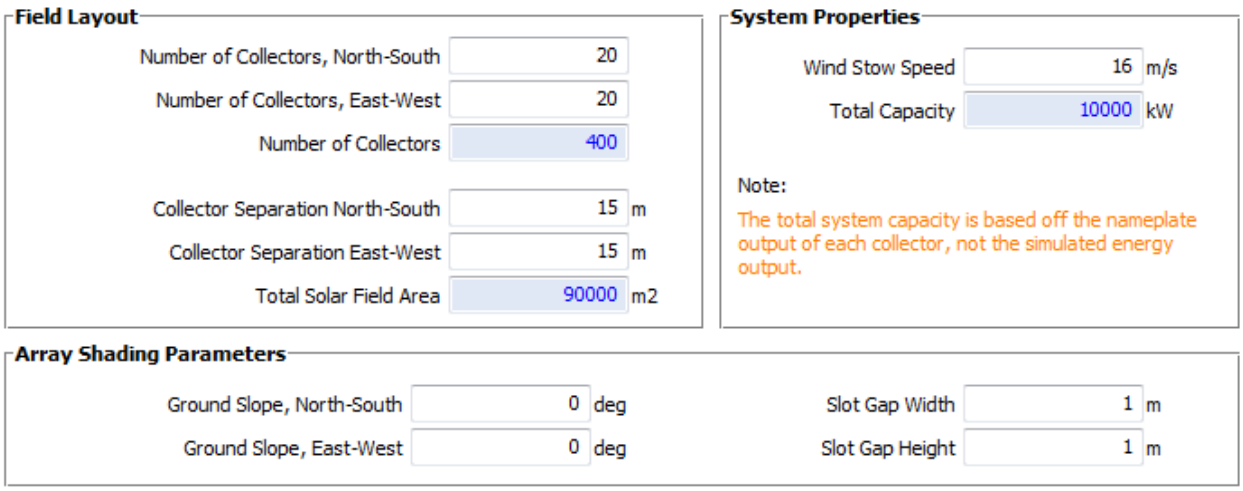

Figure 5.6 Solar Field Page

5.3.5 Solar dish collector page

The collector consists of parabolic mirrors, a support structure, and two-axis tracking system. The mirrors focus direct normal solar radiation on the aperture of the receiver. The receiver

aperture size is typically optimized to maximize the quantity of reflected solar radiation that enters the receiver and minimize convection and radiation losses out of the aperture.

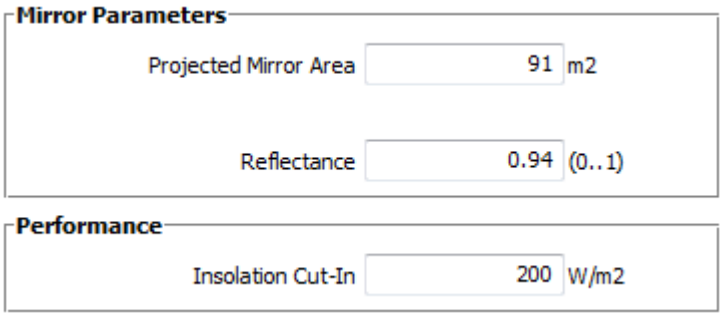

Figure 5.7 Collector Page

5.3.6 Receiver page

The receiver absorbs thermal energy from the parabolic concentrator and transfers the energy to the working fluid of the Stirling engine. The receiver consists of an aperture and absorber. The receiver aperture is located at the parabolic concentrator's focal point. The current version of Solar Advisor models one receiver type, direct illumination receivers, in which solar radiation is directly absorbed by absorber tubes containing the working fluid. Direct illumination receivers are the receiver type most commonly used for dish-Stirling systems.

Solar Advisor uses the receiver parameters to calculate thermal losses from the receiver, which typically account for over 50% of the system's total losses. Other system losses include collector losses due to mirror reflectivity, receiver intercept losses, and Stirling engine losses. Receiver thermal losses are due to conduction, convection, and radiation:

- Conductive losses through the receiver housing
- Conductive losses through the receiver housing.
- Natural convection from the cavity in the absence of wind
- Emission losses due to thermal radiation emitted from the receiver aperture
- Forced convection in the presence of wind
- Radiation losses reflected off of the receiver cavity surfaces and out of the receiver through the aperture.

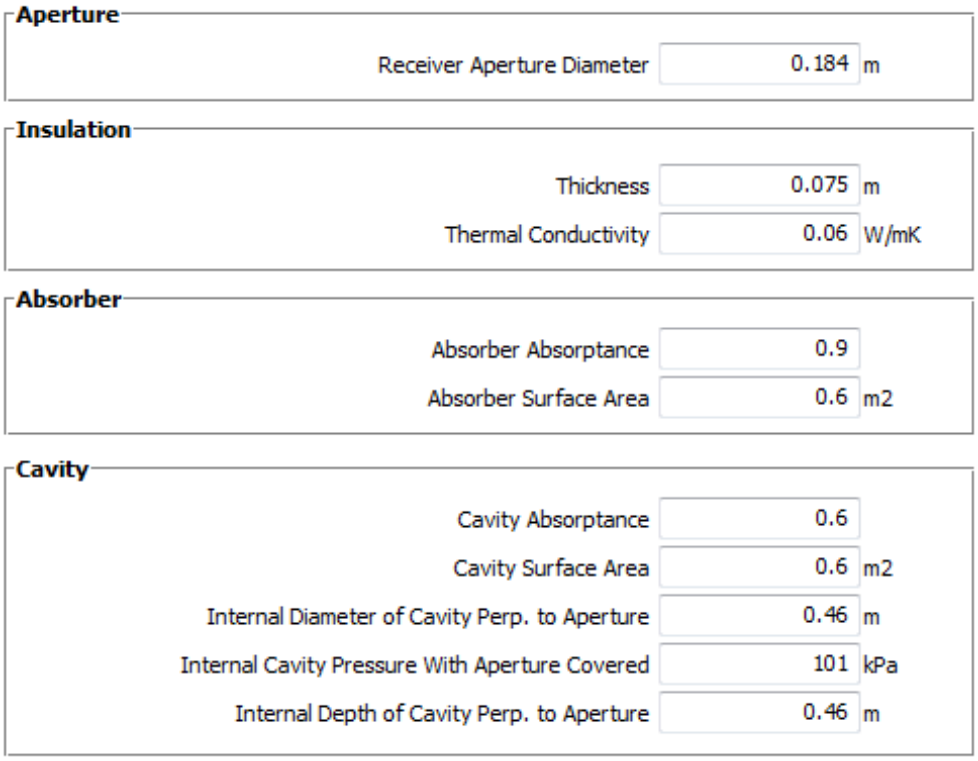

Figure 5.8 Receiver Page

5.3.7 Stirling Engine page

The Stirling engine converts heat from the receiver's absorber to mechanical power that drives an electric generator.

The Stirling engine model is based on the Beale curve-fit equation with temperature correction described in Fraser (2008). The model calculates the average hourly engine power output in Watts as a function of the Beale curve-fit equation, pressure curve-fit equation, the engine displacement and operating speed, and expansion space (heater head) temperatures. The Beale curve-fit equation calculates the engine's gross output power as a function of the input power calculated by the collector and receiver models. Solar Advisor determines the compression space temperature from the ambient temperatures in the weather data file.

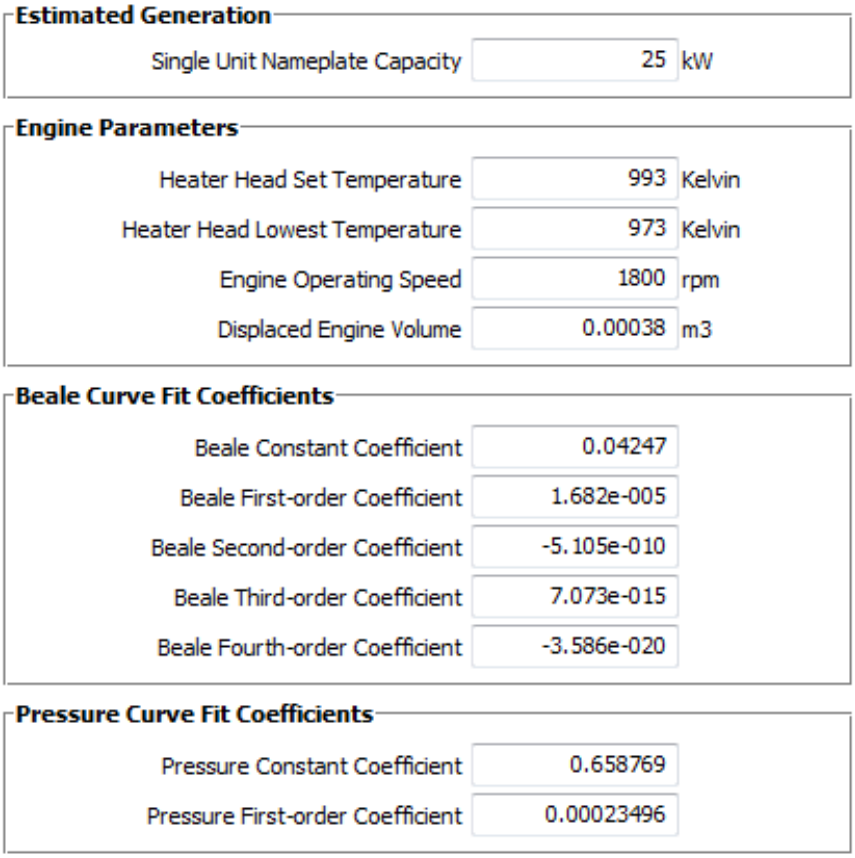

Figure 5.9 Stirling Engine Page

5.3.8 Parasitic page

The input variables on the Parasitics page are used to calculate the compression space temperature and the electrical power consumption of pumps, cooling fans, and tracking controls.

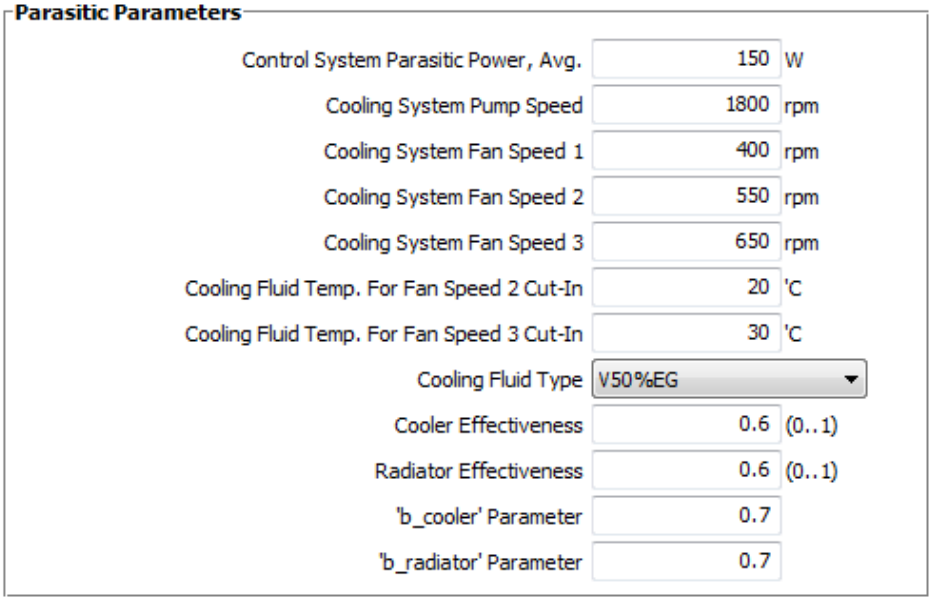

Figure 5.10 Parasitic Page

5.3.9 Reference inputs page

Solar Advisor uses the reference condition parameters in an iterative process to calculate the total collector error for a given set of values for the aperture diameter, focal length, and collector diameter. Once the collector error is calculated, that value can be used to calculate a new intercept factor for different aperture diameters

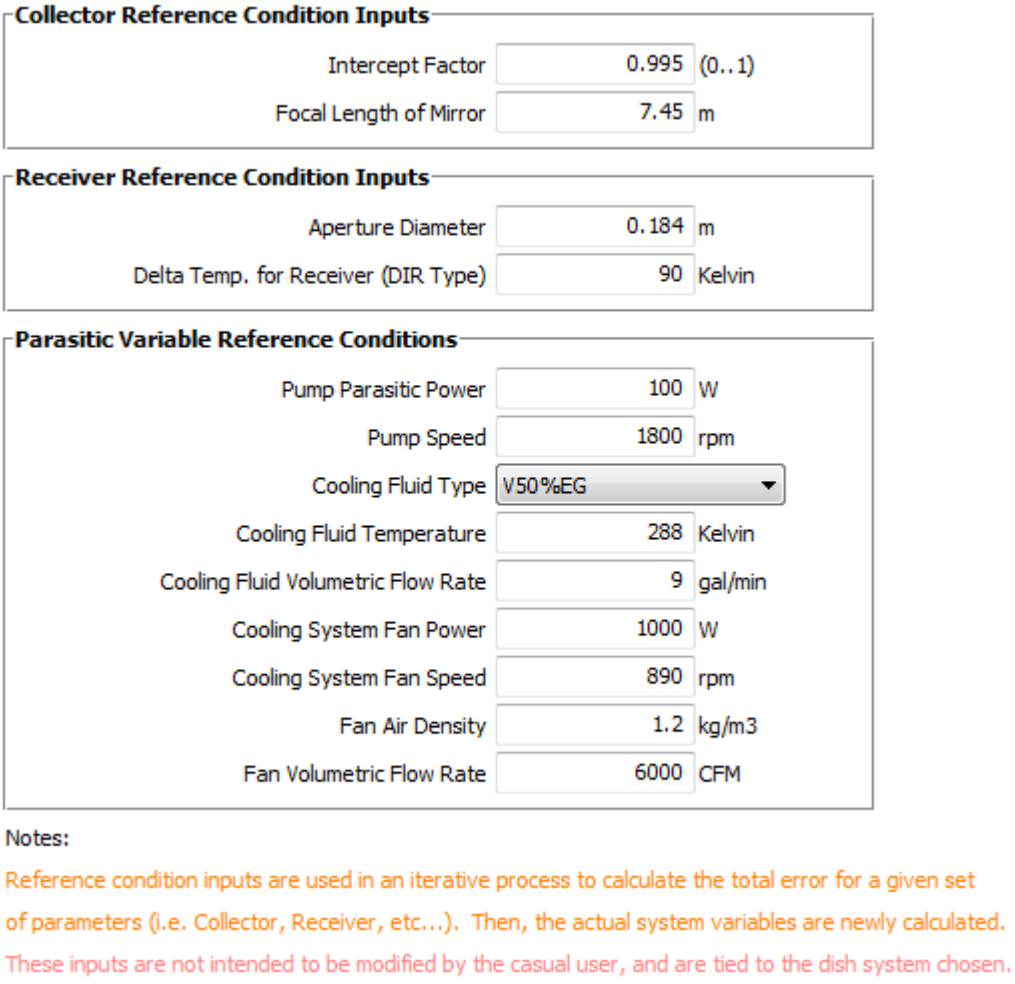

Figure 5.11 Reference inputs Page

5.3.10 System summary

Table 5.3 Input pages for system summary

Input Page	Purpose
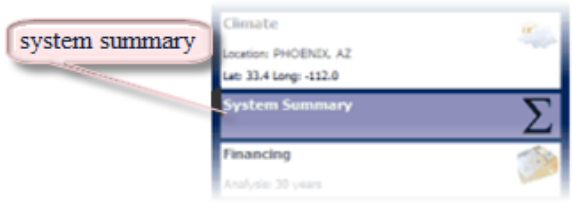	Displays key characteristics of the system based on input variables on other pages

System Nameplate Capacity (kW)

For concentrating solar power systems, the value is equivalent to the power block's rated capacity, which is an input on the Stirling Engine page dish systems.

The nameplate capacity is the value that Solar Advisor uses to calculate cost per kilowatt values displayed on the cost pages and used for economic modeling.

Total Direct Cost ($)

The total cost of installation equipment and services, calculated on the system cost page.

Total Installed Cost ($)

The project's total capital cost, including direct and indirect costs, calculated on the system cost page.

Total Installed Cost per Capacity ($/kW)

The total installed cost divided by the system nameplate capacity, also displayed on the system cost page.

Analysis Period (years)

Number of years covered by the analysis. Typically equivalent to the project or investment life, also displayed on the Financing page.

Inflation Rate (%/year)

Annual rate of change of prices, typically based on a price index. Solar Advisor uses the inflation rate to calculate costs in the cash flows for years after year one, also displayed on the Financing page.

Real Discount Rate (%/year)

A measure of the time value of money expressed as an annual rate. Solar Advisor uses the real discount rate to calculate the present value (value in year one) of cash flows over the analysis period and to calculate annualized costs, also displayed on the Financing page.

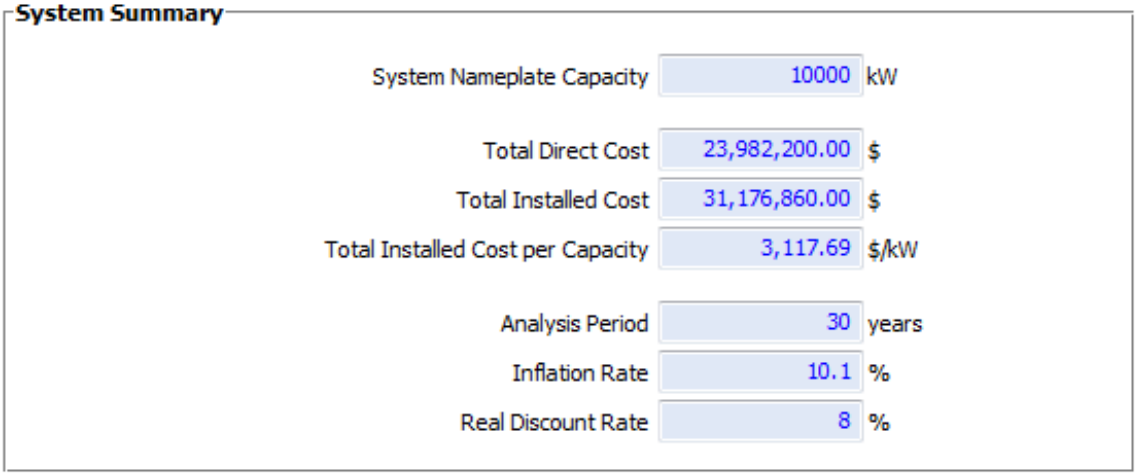

Figure 5.12 System Summary Page

5.4 SAM Output Variables Description

The Solar Advisor Model is a performance and economic model based on an hourly simulation engine that interacts with performance, cost, and finance models to calculate energy output, energy costs, and cash flows. The results of SAM analysis were presented in this section.

5.4.1 Levelized Cost of Energy (LCOE)

The levelized cost of energy (LCOE) in cents per kilowatt-hour accounts for a project's installation, financing, tax, and operating costs and the quantity of electricity it produces over its life. The LCOE makes it possible to compare alternatives with different project lifetimes and performance characteristics. Analysts can use the LCOE to compare the option of installing a residential or commercial project to purchasing electricity from an electric service provider, or to compare utility and third-party ownership projects with investments in energy efficiency, other renewable energy projects, or conventional fossil fuel projects. The LCOE captures the trade-off between typically higher-capital-cost, lower-operating-cost renewable energy

projects, and lower-capital-cost, higher-operating-cost fossil fuel-based projects. Solar Advisor calculates the LCOE for residential and commercial projects differently than it does for utility and commercial third-party ownership projects as described below. One can specify the project's financing type (residential, commercial, commercial third-party, and utility) in the Technology and Market window. For all projects, Solar Advisor calculates both a real and nominal LCOE value. The real LCOE accounts for the effect of inflation over the life of the project. The nominal LCOE excludes inflation from the calculation.

5.4.2 LCOE for Residential and Commercial Projects

For a project using one of the Residential Market or Commercial Market (except Third-Party Ownership) financing options, the LCOE is the cost of installing and operating a system per unit of electricity it produces over the project's life. Solar Advisor assumes that projects with residential or commercial financing are distributed energy projects installed on a residential or commercial property, and that power generation equipment operates on the retail customer side of the electric meter. For these projects, it is possible to compare a project's LCOE to the electricity rate that the residence or commercial entity would pay to an electric service provider if the project were not installed.

Solar Advisor uses the inflation rate to calculate Year 2 and later costs in the cash flow based on the cost input values specified. The inflation rate accounts for expected price increases over the project life for future operating costs. For the real LCOE, the real discount rate appears in the denominator's total energy output term as:

$$\text{real LCOE} = \frac{\sum_{n=0}^{N} \frac{C_n}{(1+d_{nominal})^n}}{\sum_{n=1}^{N} \frac{Q_n}{(1+d_{real})^n}} \qquad \ldots\ldots\ldots\ldots\ldots\ldots\ldots\ldots\ldots\ldots\ldots\ldots\ldots\ldots\ldots\ldots.... (5.1)$$

Similarly, for the nominal LCOE, the nominal discount rate appears in the denominator's total energy output term:

$$\text{nominal LCOE} = \sum_{n=0}^{N} \frac{C_n}{(1+d_{nominal})^n} \sum_{n=1}^{N} \frac{Q_n}{(1+d_{nominal})^n} \ldots\ldots\ldots\ldots\ldots\ldots\ldots\ldots\ldots (5.2)$$

The summation in the numerator term starts at n = 0 to include project's capital costs incurred in year zero of the cash flow and shown as the Total Installed Cost on the system costs pages. The summation in the denominator term begins at n = 1, which is the first year that the project produces energy.

5.4.3 LCOE for Utility IPP and Commercial Third Party Projects

For a project using either the Utility and IPP or Commercial Market - Third-Party Ownership financing option, the LCOE is the amount that the project must receive for each unit of electricity it sells to meet financial returns targets. This makes the LCOE for these projects very sensitive to the values specified for the minimum IRR, minimum DSCR, and positive cash flow.

Solar Advisor assumes that utility IPP (independent power producer) and commercial third-party ownership projects are power generation projects installed on the utility side of consumer power meters. These projects recover capital, operating, and financing costs through electricity sales to a utility customer or other off-taker through a power purchase agreement with a fixed annual electricity sales price and optional annual escalation rate.

For these projects, the LCOE is effectively a levelized price of electricity because it is based on the present worth of the project's revenue stream. The electricity sales price reported in the cash flow for year one is equivalent to the first year power purchase price, which Solar Advisor reports as 1st Year PPA Price in the metrics table. Solar Advisor uses the real discount rate and inflation rate to calculate the present worth of future costs. The discount rate accounts for the time value of money and the relative degree of risk for alternative investments.

Solar Advisor uses the inflation rate to calculate Year 2 and later costs in the cash flow based on the cost input values specified on the system costs page. The inflation rate accounts for expected price increases over the project life for future operating costs. For the real LCOE, the real discount rate appears in the denominator's total energy output term:

$$\text{real LCOE} = \sum_{n=0}^{N} \frac{R_n}{(1+d_{\text{nominal}})^n} \sum_{n=1}^{N} \frac{Q_n}{(1+d_{\text{real}})^n} \quad (5.3)$$

Similarly, for the nominal LCOE, the nominal discount rate appears in the total energy output term:

$$\text{nominal LCOE} = \sum_{n=0}^{N} \frac{R_n}{(1+d_{\text{nominal}})^n} \sum_{n=1}^{N} \frac{Q_n}{(1+d_{\text{nominal}})^n} \quad (5.4)$$

5.4.4 Real and Nominal LCOE

Solar Advisor reports both a real LCOE and a nominal LCOE value. The form of the discount rate used in the denominator's total energy output term of the equations described above determines the form of the LCOE.

The real LCOE is a constant dollar value that is adjusted for inflation. Because the nominal discount rate used to compute the nominal LCOE includes inflation, inflation is effectively factored out of the nominal LCOE. The nominal LCOE is a current dollar value. If the inflation rate is set to zero, the real and nominal LCOE will be equal. The choice of real or nominal LCOE depends on the analysis. Most long-term analyses are conducted in real (constant) dollars to account for many years of inflation over the project life, whereas most short term analyses use nominal (current) dollars. The nominal discount rate can be calculated based on the values of the real discount rate and the inflation rate:

$$\mathrm{dnominald}_{\mathrm{nominal}} = (1 + \mathrm{d}_{\mathrm{real}})(1 + \mathrm{e}) - 1 \quad (5.5)$$

5.4.5 1st Year Power Purchase Agreement (PPA) Price

The first year PPA price is the electricity sales price for projects with Utility and IPP or Commercial - Third- Party Ownership financing. Solar Advisor assumes that such projects sell electricity through a power purchase agreement (PPA) at a fixed price over the life of the project with an optional annual escalation rate. The first year PPA Price and annual escalation rate (PPA Escalation rate on the Financing page) determine the project's annual revenues. Solar Advisor calculates the annual revenues to meet the minimum requirements of the internal rate of return (IRR), debt service coverage ratio (DSCR), and positive cash flow, which are defined as constraining assumptions. Because of the way the first year PPA price, IRR, and minimum DSCR interact, Solar Advisor uses an iterative algorithm to determine the values of these variables. For projects with Utility and IPP financing, the constraining assumptions defined are the Minimum Required IRR and the Minimum Required DSCR, and a positive cash flow requirement. But for projects with Third-Party Ownership financing, there is a single constraining assumption defined on the Financing page which is the Minimum Required IRR.

The following equations show the calculations used in the iterative algorithm to determine the IRR and minimum DSCR, which are both reported as results. The internal rate of return is the discount rate, IRR in the equation below, that corresponds to a project net present value, NPV, of zero whereas the minimum DSCR is the minimum debt-service coverage ratio that Solar Advisor calculates for projects with Utility and IPP or Commercial - Third-Party Ownership financing. The debt-service coverage ratio in each year n is the ratio of operating income to expenses in that year. Solar Advisor calculates the minimum debt-service coverage ratio to be greater than or equal to the minimum required DSCR target defined.

$$NPV = \sum_{n=1}^{N} \frac{R_n - C_{AfterTax,n}}{(1+IRR)^n} + C_{AfterTax,0} = 0 \quad (5.6)$$

$$DSCR_n = \frac{R_n - C_{Operating,n}}{C_{Intererest,n} + C_{Principal,n}} \quad (5.7)$$

5.4.6 Annual Energy

The annual energy quantity reported in the Metric table is the total electric generation in kWh for the first year that the project operates, equivalent to Year one in the project cash flow. The output in subsequent years may be lower than in the first year depending on the value of the degradation rate

Capacity Factor

The capacity factor is the ratio of the system's predicted electrical output in the first year of operation to the output had the system operated at its nameplate capacity:

$$CF = \frac{E_{OutputYear1}}{P_{SystemCapacity.8760}} \quad (5.8)$$

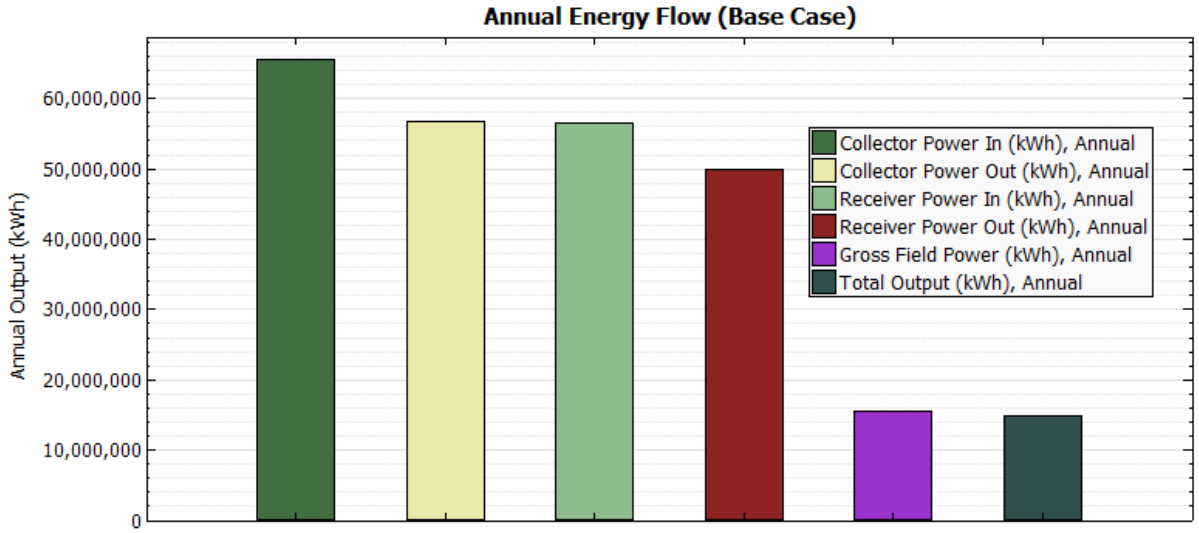

Figure 5.13 Annual Energy Flow

Table 5.4 Annual Energy Flow

Collector Power In (kWh), Annual	Collector Power Out (kWh), Annual	Receiver Power In (kWh), Annual	Receiver Power Out (kWh), Annual	Gross Field Power (kWh), Annual	Total Output (kWh), Annual	Annual Energy (kWh)
65475300	56842700	56558500	49799900	15576100	14894800	14001100

5.4.7 Debt Fraction and PPA Escalation

The debt fraction is the percentage of the project total installed cost that is financed through a loan and the PPA escalation rate is an annual escalation rate that Solar Advisor uses to calculate future electricity sales prices based on the first year PPA price, The values are reported as a results only for projects with Utility and IPP or Commercial - Third-Party Ownership financing. For these types of projects, depending on the financial optimization option, the debt fraction and PPA are either a user defined input on the Financing page, or a value that Solar Advisor calculates. When the Automatically minimize LCOE with respect to Debt Fraction and PPA Escalation Rate option are checked, Solar Advisor finds the debt fraction and PPA Escalation Rate that results in the lowest levelized cost of energy. Solar Advisor uses the debt fraction to calculate the principal and interest payments, and used in the iterative search algorithm described in 1st Year PPA Price.

Net Present Value

The net present value is the present value of the after-tax cash flow discounted to year one using the nominal discount rate, plus the after-tax cash flow in year zero:

$$\mathrm{NPV} = \sum_{n=1}^{N} \frac{R_n - C_{\mathrm{AfterTax},n}}{(1+d_{\mathrm{nominal}})^n} + C_{\mathrm{AfterTax},0} \quad \text{..... (5.9)}$$

5.4.8 After Tax Cash Flow

Year zero of the cash flow represents project capital cost. The capital cost is equal to the total installed cost displayed on the system costs page minus the loan principal amount. Year one is the first year that the project generates electricity. The cash flow for year one and subsequent years account for project expenses, income from electricity sales, taxes, and incentive payments. For Utility power producer, the after tax cash flow for year one and subsequent year is given by:

After Tax Cash flow = After Tax Cost + Revenues

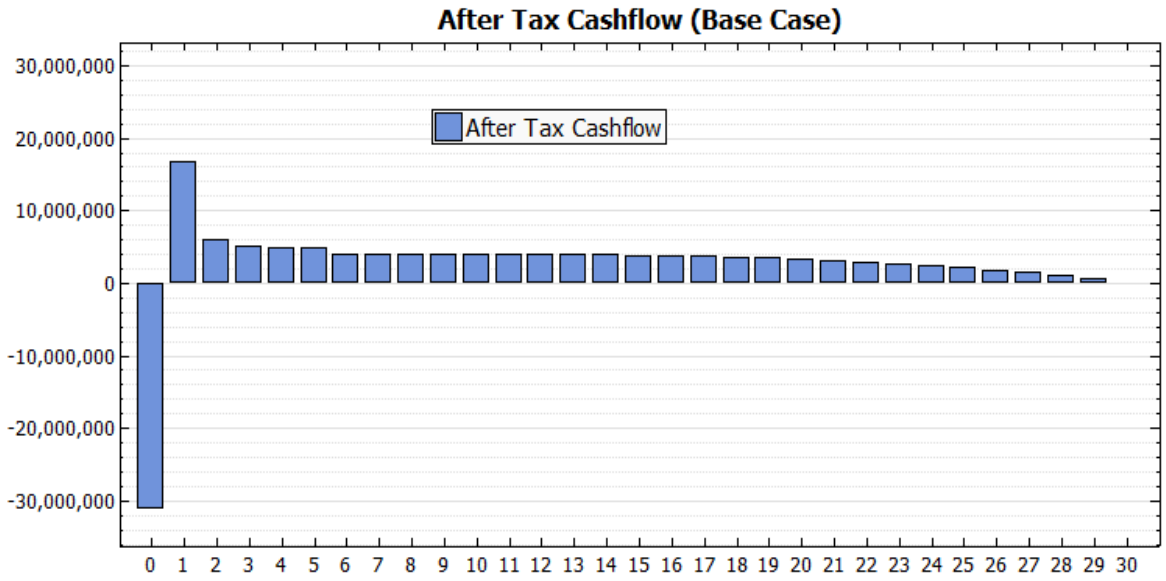

Figure 5.14 After Tax Cash Flow

Table 5.5 Project Cash Flow

Year	After Tax Cash Flow	Year	After Tax Cash Flow	Year	After Tax Cash Flow
0	-31176900	11	4001270	21	3159700
1	16827200	12	3981260	22	2963530
2	5932840	13	3950880	23	2737420
3	5140570	14	3908920	24	2478150
4	4806680	15	3854060	25	2182180
5	4833680	16	3784810	26	1845590
6	4090540	17	3699550	27	1464080
7	3998120	18	3596500	28	1032900
8	4009590	19	3473660	29	546802
9	4014490	20	3328860	30	36
10	4012020				

5.4.9 Payback period

The payback period (PBP) for the investment is the number of years for which the net present value (NPV) is zero, or it can be defined as the time needed for the cumulative savings to equal the initial investment.

Based on the above cash flow, the payback period is calculated as:

Table 5.6 The Payback Period

Year	After Tax Cash Flow	Commutative Cash Flow
0	-31176900	
1	16827200	-14349700
2	5932840	-8416860
3	5140570	-3276290
4	4806680	1530390

Payback period= 3years + 3276290/ 4806680 year = 3.682 years

Hence the money invested on the system, dish-engine; can be returned in approximately four years period which is much less than its life time. Thus the system is economically feasible.

5.4.10 Cost Stacked Bar

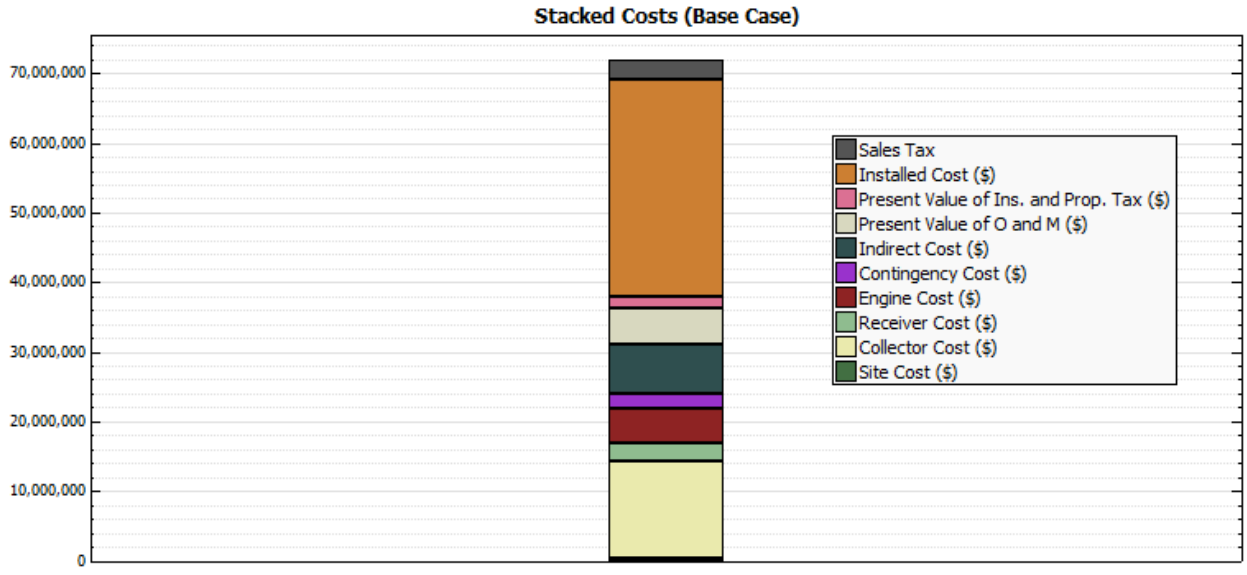

Figure 5. 15 Cost Stacked Bar

Table 5.7 Cost Stacked Bar

Site Cost ($)	Collector Cost ($)	Receiver Cost ($)	Engine Cost ($)	Contingency Cost ($)	Indirect Cost ($)	Present Value of O and M ($)	Present Value of Ins. and Prop. Tax ($)	Installed Cost ($)	Sales Tax
270000	14032000	2500000	5000000	2180200	7194660	5204160	1593930	31176900	2877860

5.4.11 Monthly Energy Flow

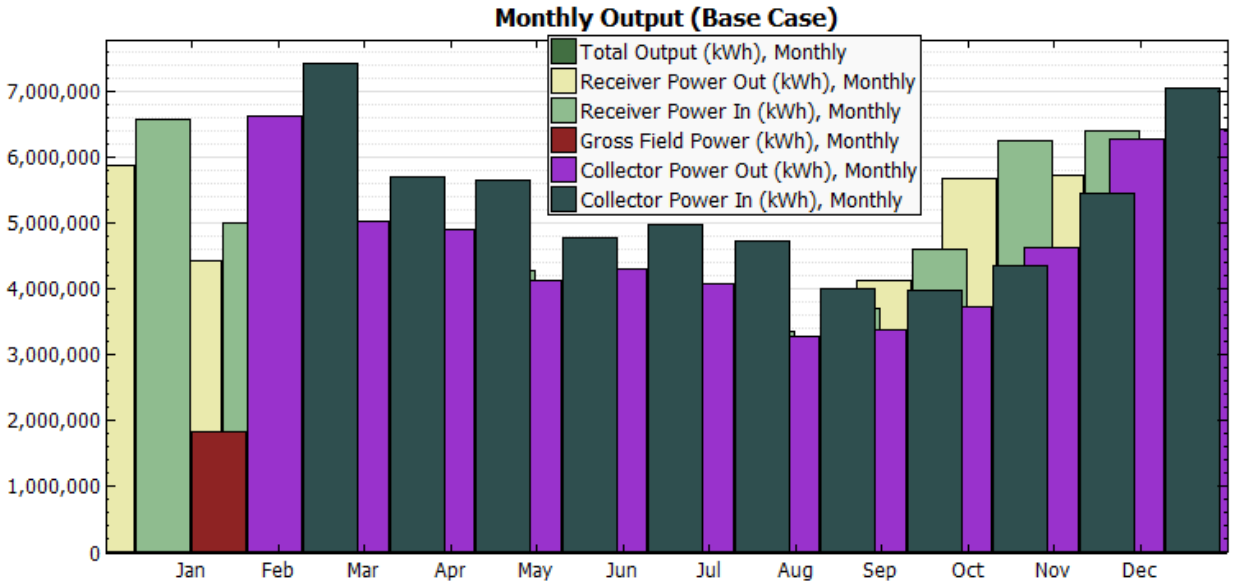

Figure 5.16 Monthly Energy Flow

Table 5.8 Monthly Energy Flow

Month	Total Output (kWh), Monthly	Receiver Power Out (kWh), Monthly	Receiver Power In (kWh), Monthly	Gross Field Power (kWh), Monthly	Collector Power Out (kWh), Monthly	Collector Power In (kWh), Monthly
1	1782700	5877720	6595180	1847000	6628320	7425630
2	1340610	4430350	5000630	1394150	5025760	5705310
3	1288930	4297320	4888270	1347790	4912830	5653980
4	1086440	3650410	4107710	1139790	4128360	4794840
5	1053790	3592160	4290840	1112140	4312400	4988940
6	1021150	3490610	4068470	1077660	4088910	4724860
7	813647	2794290	3277950	861992	3294420	4018240
8	836198	2885580	3359560	889083	3376440	3988910
9	960303	3256060	3708930	1012010	3727560	4350550
10	1234880	4126960	4612540	1293220	4635720	5468380
11	1729870	5674190	6250640	1791970	6282050	7055750
12	1746320	5724240	6397810	1809260	6429960	7299940

CHAPTER SIX

6.1 Conclusion

In conclusions, the need for the construction of a parabolic dish solar steam generator arose as an alternative to solve the thermal energy needs of the populace. This will also reduce the total dependency on fossil fuels and other non-renewable and exhaustible energy source which have be known to be depleted with ages to come as they are being used up.

A computational model was created and used to investigate the effects of system design parameters for a Stirling dish system. The model, implemented in TRNSYS, can be used to predict how a system design change influences the net energy production in a specific location using input weather data files.

In TRNSYS model the heater head temperature that results in the maximum net efficiency is a function of the receiver losses and the engine efficiency. The current heater head operating temperature is 993 K and increasing this temperature has been prevented due to material limitations.

The engine pressure is controlled to maintain a constant heater head temperature, so it will fluctuate constantly throughout the day.

The engine efficiency was greater at higher engine input powers for colder ambient temperatures. This behavior results from the engine operating more efficiently at colder ambient temperatures as explained by the second law of thermodynamics.

According to the cost and financial analysis of the project the total direct capital cost is $23,982,200.00.and the total indirect capital costs is estimated to be $7,194,660.00. The total installed capital cost is the sum of direct and indirect capital costs which is $31,176,860.00. The project payback is in about 4 years for its life time of 30 years.

6.2 Recommendation

Future work should to be done to research Brayton cycle engines and determine how a performance curve could be made for the gas turbine for a TRNSYS component.

The lower cost will be achieved through: improvements in mirrors and support structures, improvements in hybrid heat-pipe and volumetric receivers coupled to Stirling and Brayton engines, and development of control systems for fully automatic operation; and improvements in system integration by reduction of parasitic loads, optimization of startup procedures, better control strategies, and hybrid operation of the Stirling and Brayton engines.

A performance and economic analysis using gas turbines instead of Stirling engines in a closed cycle using hydrogen or helium as the working fluid would be of value. Analyzing a combined cycle using gas turbines in place of the Stirling engines and a centrally located steam turbine in the bottoming cycle may also be a valuable design study. Gas turbines can be purchased off-the-shelf so they likely would be less expensive than Stirling engines on a large scale.

Tracking Error produces unexpected less power output. A good solar tracker can typically lead to an increase in power generation capacity of 30-50%.So detail performance analysis must be done at this area.

Mirror soiling can contribute to a significant reduction in the performance of Stirling dish systems. So the mirrors must washed on a regular two week schedule

Although many researchers have analyzed Stirling engines, there still remains room for further development.

References

1. Çengel, Yunus A., and Boles, Michel A., *Thermodynamics an Engineering Approach*. 5th Edition, 2005.

2. Department of Energy Concentrating Solar Website.
   Available at: http://www.energylan.sandia.gov/sunlab/overview.htm

3. D. Howard and R.G. Harley, *Modeling of Dish-Stirling Solar Thermal Power Generation*, in Proc. 2010 IEEE Power Engineering Society General Meeting, Jul. 25-29, 2010, Minn., MN. [Accepted].

4. Duffie, John A., and Beckman, William A., *Solar Engineering of Thermal Processes*. 2nd edition, New York: John Wiley and Sons, Inc., 1991.

5. *Engineering Equation Solver (EES)*. Middleton, WI: F-Chart Software, 2005.
   Available at: http://www.fchart.com.

6. Hirata, Koichi. *Koichi Hirata Stirling Engine Homepage*.
   Available at: <http://www.bekkoame.ne.jp/~khirata/>

7. Incropera, Frank P., and DeWitt, David P., *Fundamentals of Heat and Mass Transfer*. 5th edition, New York: John Wiley and Sons, Inc., 2002.

8. Keveney, Matt., *Animated Engines*, 2001.
   Available at: http://www.keveney.com/Engines.html

9. Moran, Michael J, and Shapiro, Howard N., *Fundamentals of Engineering Thermodynamics*. 4th Edition, John Wiley and Sons, 2002.

10. National Renewable Energy Laboratory. (2010 Mar.). Concentrating Solar Power Projects.
    Available at: http://www.nrel.gov/csp/solarpaces/

11. National Renewable Energy Laboratory, Report No. NREL/TP-620-39726: Power Technologies Energy Data Book, Fourth Edition.
    Available at:http://www.nrel.gov/analysis/power_databook/docs/pdf/39728_complete.pdf

12. Osborn, D.B., 1980, *Generalized Shading Analysis for Paraboloidal Collector Fields*, Paper Number 80-Pet-33.

13. PAUL R. FRASER, *Stirling Dish System Performance Prediction Model*, Master of Science (Mechanical Engineering) at the University of Wisconsin-Madison, 2008.

14. Petrescu, Stoian, et al. *Analysis and Optimization of Solar-Dish/Stirling Engines*. Solar 2002. Reno, Nevada, June 15-20.

15. SAM User Guide, SAM Software,

Available at: https://www.nrel.gov/analysis/sam.

16. Schwarzbözl, Peter and Zentrum, Deutsches. *A TRNSYS Model Library for Solar Thermal Electric Components (STEC)*. A Reference Manual, Release 3.0,2006.

17. Sharke, Paul. *Sun Rises On Big Solar*.
Available at:
http://www.designnews.com/article/CA6294752.html?ref=nbra&text=sun+rises+on

18. Stine, W. B., and Frank Kreith, eds., *Mechanical Engineering Handbook*. Boca Raton: CRC Press LLC, 1999.

19. *Stirling Energy Systems*. (2010, Jun.). SES-Tessera Solar Corporate Video.

Available at: http://www.Stirling energy.com/

20. Stirling Energy Systems. (2008, Feb.). Sandia, *Stirling Energy Systems Set New World Record for Solar-to-Grid Conversion Efficiency*.
Available at: http://www.Stirling energy.com/pdf/2008-02-12.pdf

21. *TRNSYS – A Transient System Simulation Program*. Madison, WI: University of Wisconsin-Madison Solar Energy Laboratory.

Available at: http://sel.me.wisc.edu/trnsys/

22. Urieli. (2010, Jan. 1). *Stirling Cycle Machine Analysis*.

Available at: http://www.ent.ohiou.edu/~urieli/Stirling /me422.html.

23. U.S. Department of Energy, **Solar Energy Technologies Program**: Multi Year Program Plan 2008-2012.
Available at: http://www1.eere.energy.gov/solar/pdfs/solar_program_mypp_2008-2012.pdf

24. U.S. Energy Information Administration, Report No. DOE/EIA-0383: Annual Energy Outlook 2010 with Projections to 2035.
Available at: www.eia.doe.gov/oiaf/aeo/

25. Weather Data.

Available at http://swera.unep.net.

26. WGAssociates. Introduction to WGAssociates and Solar Dish/Stirling Power Systems.

Available at: http://www.energylan.sandia.gov/sunlab/PDFs/WGA.pdf

27. Yilma Tadesse, *Simulation of Solar Powered Stirling Engine for Small Scale Irrigation Application*, Master of Science (Mechanical Engineering) at Addis Ababa, 2009.

Appendix A

TRNSYS Model Descriptions

A Stirling dish system model was created in TRNSYS to determine the location dependent performance of the systems. Separate components were created for the parabolic collector, receiver, Stirling engine, and the parasitic power. The TRNSYS model predict show the system performance changes based on location dependent variables consisting of the wind velocity, direct normal insolation, ambient temperature, ambient pressure (altitude), and the sun elevation angle.

TRNSYS Parabolic Collector Model

The parabolic concentrator model predicts the radiative power intercepted by the receiver ($P_{in,rec}$) based on the direct normal insolation (I_{DNI}), projected area of the mirror(A_{proj}),wind cut-out velocity, intercept factor ($\varphi_{\text{int,fac}}$), mirror reflectivity (ρ_{ref}), and the shading factor (φ_{shade}) as given by Equation (A.1)

$$P_{in,rec} = I_{DNI} * A_{proj} * \rho_{ref} * \varphi_{\text{int, fac}} * \varphi_{shade} \quad \text{..... (A.1)}$$

The wind cut-out velocity is value indicating the wind speed at which the parabolic concentrator will be sent into as to w position to prevent wind damage. The shading factor ($\varphi shade$) is determined using theory from Osborn (1980). The shading factor is a function of the number of parabolic concentrators, the collector diameter, and the North-South and East-West collector separation distance.

The intercept factor ($\varphi_{\text{int,fac}}$) in Equation(A.1) is the fraction of energy reflected from the parabolic concentrator that enters the receiver aperture. The TRNSYS model uses theory from Stine and Harrigan (1985) and requires as an input the intercept factor for a specific receiver aperture diameter, focal length, and collector diameter. The model then determines the total collector error (σ_{tot}) in mille-radians by iterating Eq. (A.2) with a guess value for the total collector error until the appropriate value for the input of the intercept factor is found. Once the total concentrator error is determined, it can be used to obtain a new intercept factor for a different receiver aperture diameter using the same theory.

The terms $P_{intercept,\ tot}$ is the total power intercepted by the receiver, $P_{reflect,\ tot}$ is the total power reflected by the collector, Γ is the intercept factor for a specific differential ring evaluated at the ring-specific rim angle(ψ). The total rim angle at the collector perimeter is given by ψ_{rim},

I_{DNI} is the direct normal insolation, f is the focal length of the mirror, and A_{proj} is the projected area of the mirror. The ring specific intercept factor (Γ) is a function of the total error (σ_{tot}) as shown in Equations (A.3) and (A.4). The terms $Q(n)$ is a function of the number of standard deviations (n) described in Stine and Harrigan (1985), d_{ap} is the receiver aperture diameter, and p is the length between the foci and the specific differential ring on the collector. The concentrator model, combined with the receiver model described below, allows an optimal receiver aperture diameter to provide the greatest solar net energy transfer to the Stirling engine to be found.

The TRNSYS model automatically proceeds through the following steps to find the intercept factor based on the diameter of the receiver aperture for specific collector systems:

$$\varphi_{\text{int},\,fac} = \left(\Phi_{\text{int}\,ercept,tot}\right)\left(\Phi_{reflect,tot}\right) = \left(\sum_{\psi=0^0}^{\psi_{rim}} \frac{\Gamma * 8\pi * I_{DNI} * f^2 * \sin\left(\psi\right) * \Delta\psi}{\left(1+\cos\left(\psi\right)\right)^2}\right) \Big/ \left(I_{DNI} * A_{proj}\right) \quad \text{(A.2)}$$

$$\Gamma = 1 - 2 * Q\left(n\right) \quad \text{(A.3)}$$

$$n = 2 \Big/ \sigma_{tot} * \tan^{-1}\left(d_{ap} * \cos\left(\psi\right) \Big/ 2 * p\right) \quad \text{(A.4)}$$

1. Solve for the collector rim angle based on the collector focal length and diameter
2. Guess a small value for the total collector error
3. Solve for the number of standard deviations for a specific rim angle (differential ring) based on the guess value for the total collector error
4. Solve for the intercept factor for a specific rim angle in the collector based on the number of standard deviations for the rim angle
5. Solve for the total power reflected from the differential ring
6. Determine the total power intercepted by the receiver for the specific rim angle
7. Sum up the total power reflected over the entire collector(summation of #5)
8. Sum up the total power intercepted by the receiver for the entire collector (sum#6)
9. Divide #8 by #7
10. If #9 is less than the appropriate intercept factor, then guess a larger value for the total collector error in #2 and repeat steps #3 through #10
11. The total collector error is solved to give the correct intercept factor for the one data point measured at a specific aperture diameter
12. Once the total collect or error is determined, the previous steps are modified slightly and

the total collector error is used to determine what the new intercept factor is for a different aperture diameter

Table A.1 The Parameters, Inputs, and Outputs for the TRNSYS Parabolic Collector Model

Parameters	**Inputs**	**Outputs**
Receiver (not collector) aperture diameter	Direct normal insolation	Collector output power
Mirror reflectivity	Ambient temperature	Ambient temperature
Number of collectors North-South	Wind speed	Atmospheric pressure
Number of collectors East-West	Sun zenith angle	Wind speed
Dish separation distance North-South	Atmospheric pressure	Sun elevation angle
Dish separation distance East-West	Solar azimuth angle	Collector losses
Manufacturer		Efficiency of the collector
Wind stow speed		Number of collectors
Projected area of the mirror		Direct normal insolation
Insolation cut in		Insolation cut in
Test receiver aperture diameter for the test intercept factor		Input power to the receiver
Test intercept factor		Receiver intercept factor
Test focal length of the mirror		Receiver aperture diameter
Total area of the mirror		Input power to the collector
		Dish separation distance North-South
		Dish separation distance East-West
		Shading factor

TRNSYS Receiver Model

The TRNSYS receiver model computes the thermal input power to the Stirling engine by subtracting the receiver thermal losses due to conduction, convection, and radiation from the total power intercepted by the receiver as shown in Equation (A.5). The conduction losses (q_{cond}) through the receiver housing are minimal. The natural convection coefficient used for the receiver cavity is location and time-of-day dependent and is determined from the Nusselt number correlation by Stine and McDonald (1989) in Equations (A.6) and (A.7) with the interior cavity diameter parallel to the aperture as the characteristic length. The forced convection heat transfer coefficient for receiver cavity is based on Ma (1993) as shown in Equation (A.8). The total convection heat transfer coefficient according to Ma is given by Equation (A.9) with the natural convection coefficient derived from Equation (A.6). The total receiver heat loss rate due to convection is given by Equation (A.10) where A_{cav} is the total surface area of the cavity interior.

$$P_{in,SE} = P_{in,rec} - q_{rad,reflect} - \left(q_{cond} + q_{conv,tot} + q_{rad,emit} \right)_{losses} \quad \text{(A.5)}$$

$$Nu_{nut,conv} = 0.088 * Gr^{1/3} * \left(T_{cav}/T_{amb}\right)^{0.18} * \left(\cos\theta\right)^{2.47} * \left(d_{ap}/d_{cav}\right)^{s} \quad \text{(A.6)}$$

$$S = -0.982 * \left(d_{ap}/d_{cav}\right) + 1.12 \quad \text{(A.7)}$$

$$h_{forced} = 0.1967 * v^{1.849} \quad \text{(A.8)}$$

$$h_{total,convection} = h_{natural} + h_{forced} \quad \text{(A.9)}$$

$$q_{conv,tot} = h_{tot,convection} * A_{cav} * \left(T_{cav} - T_{amb}\right) \quad \text{(A.10)}$$

The term $P_{in,SE}$ in Equation (A.5) represents the thermal input power to the Stirling engine while $q_{conv,tot}$, $q_{rad,emit}$, and $q_{rad,reflect}$ represent the rate of heat loss from the receiver by convection (natural and forced), emitted radiation out of the receiver aperture, and the reflected radiation out of the aperture, respectively. The quantity, $Nu_{nat,conv}$, in Equation (A.6) represents the free convection Nusselt number with the interior cavity diameter as the characteristic length. Gr is the Grashof number using the interior cavity diameter as the characteristic length, T_{cav} is the average temperature of the interior cavity walls, T_{amb} is the ambient temperature, θ is the sun elevation angle, d_{ap} is the aperture diameter, d_{cav} is the cavity diameter parallel to the receiver aperture and v is the wind speed. The emitted radiation from the receiver cavity ($q_{rad,emit}$) is

estimated as the thermal emission given by the Stefan-Boltzmann law in Equation(A.11) where, ε is the emissivity of the cavity, A_{ap} is the surface area of the receiver aperture opening, and σ is the Stefan-Boltzmann constant. The reflected radiation ($q_{rad,reflect}$) from the receiver is given by Duffie and Beckman (2006) shown in Equations (A.12) and (A.13) where α_{eff} is the effective absorptance of the cavity, α_{cav} is the absorptance of the cavity interior surface, and A_{cav} is the interior cavity surface area.

$$\dot{q}_{rad,emmit} = \varepsilon * A_{ap} * \sigma * \left(T_{cav}^4 - T_{amb}^4\right) \quad \text{(A.11)}$$

$$\alpha_{eff} = \frac{\alpha_{cav}}{\alpha_{cav} + \left(1 - \alpha_{cav}\right) * \left(A_{ap} / A_{cav}\right)} \quad \text{(A.12)}$$

$$\dot{q}_{rad,reflect} = \left(1 - \alpha_{eff}\right) * \dot{q}_{in,receiver} \quad \text{(A.13)}$$

An aperture cover can be used for hybrid systems to supplement solar energy with natural gas or for systems that replace the Stirling engine with a gas turbine. A receiver aperture cover can be simulated in the TRNSYS model providing a value for the cover transmittance for radiation at normal incidence (τ_c). An aperture cover will reduce the transmitted energy through the cover to the receiver cavity due to reflection as shown in Equations (A.14) and (A.15) but it will also reduce radiation and convection losses from the receiver cavity. The terms τ_c and τ_d are the transmittance of the cover for incident solar radiation and isotropic diffuse radiation respectively.

$$\tau_e * \alpha_{eff} = \tau_e * \left[\frac{\alpha_{cav}}{\alpha_{cav} + \left(1 - \alpha_{cav}\right) * \tau_d \left(A_{ap} / A_{cav}\right)}\right] \quad \text{(A.14)}$$

$$\dot{q}_{rad,reflect} = \left(1 - \tau_c * \alpha_{cav}\right) * \dot{q}_{in,receiver} \quad \text{(A.15)}$$

Convection from the cavity to the aperture cover is determined using internal volume convection correlations given by Eqs. (A.16) and (A.17) (Incropera and DeWitt, 2002). Convection from the exterior plate surface to the environment is found by combining free convection with forced convection using Equation (A.21) with the value for *n* in Eq. (A.21) chosen to be three (Incropera and DeWitt, 2002).Free convection from a flat plate at the appropriate sun elevation angle is given by Equation (A.18) and (A.19) with forced convection

given by Equation (A.20). The characteristic length used for these equations is the receiver aperture diameter. The terms *Pr*, *Re*, and *Ra* are the Prandtl, Reynolds, and Rayleigh numbers respectively.

$$\bar{Nu}_{internal} = 1 + \left[\bar{Nu}_{ix=90^0} - 1 \right] * \sin(90^0 + \theta) \quad \text{(A.16)}$$

$$\bar{Nu}_{\tau=90^0} = 0.18 * \left(\frac{\Pr}{0.2 + \Pr} * Ra \right)^{0.29} \quad \text{(A.17)}$$

$$\bar{Nu}_{exterior,free} = 0.68 + \frac{0.67 * Ra^{1/4}}{\left[1 + (0.492/\Pr)^{9/16} \right]^{4/9}} \quad (Ra \le 10^9; 0^0 \le \theta \le 60^0) \quad \text{(A.18)}$$

$$\bar{Nu}_{exterior,free} = 0.27 * Ra^{1/4} \quad (10^5 \le Ra \le 10^{10}; 60^0 \le \theta \le 90^0) \quad \text{(A.19)}$$

$$\bar{Nu}_{exterior,forced,lam} = 0.664 * \mathrm{Re}^{1/2} * \Pr^{1/3} \quad \text{(A.20)}$$

$$h_{combined,convection} = \left[h_{free}^n + h_{forced}^n \right]^{1/n} \quad \text{(A.21)}$$

Most systems use a DIR receiver even though there flux receiver improves the system performance. Integration issues for a reflux receiver can be challenging for four-cylinder engines such as the SES Stirling engine, so SES is not planning on using reflux receivers at this point.

Table A.2 The Parameters, Inputs, and Outputs for the TRNSYS Receiver Model

Parameters	**Inputs**	**Outputs**
Receiver type	Input power to the receiver	Receiver output power
Transmittance of the aperture cover	Ambient temperature	Ambient temperature
Manufacturer	Atmospheric pressure	Receiver losses
Absorptance of the absorber	Wind speed	Efficiency of the receiver
Surface area of the absorber	Sun elevation angle	Engine heater head operating temp
Absorptance of the cavity	Number of collectors	Number of Collectors

wall		
Surface area of the cavity wall	Heater head temperature (set point	Density of ambient air
Receiver insulation thickness	Heater head temperature (lowest)	DNI
Insulation thermal conductivity	DNI	Insolation cut in
Internal diameter of the cavity perpendicular to the receiver aperture	Insolation cut in	Reflected radiation losses
Internal cavity pressure when a cover is over the aperture	Receiver aperture diameter	Radiation losses from long-wave emission
Internal depth of the cavity perpendicular to the aperture		Receiver convection losses
		Receiver conduction losses

TRNSYS Stirling Engine& Generator Model

Data for the gross output power (P_{Gross}) was based on a Beale number (*Beale*) curve at part-to full-load using a temperature correction term ($T_{correct}$) from finite-time theory (McMahan et al, 2007) as given by Equation(A.23). The temperature correction term includes values for the expansion (T_E) and compression space (T_C) temperatures. The expansion space temperature is the heater head operating temperature. One individual day of data is used to determine the temperature corrected Beale number ($Beale_{\#corrected}$) in Equation (A.23) with the input power to the Stirling engine determined by the collector and receiver models using Equation (A.5). The terms P_{mean}, V_{SW}, and f refer to them e an engine pressure, swept volume, and engine frequency.

$$Beale\#_{corrected} = P_{Gross} / \left(P_{mean} * V_{sw} * f * T_{correct} \right) \quad \text{(A.22)}$$

$$T_{correct} = \left(1 - T_E / T_C \right)^{0.5} \quad \text{(A.23)}$$

Once a curve fit is generated using data for a specific engine, the gross output power of the engine is predicted using Equation (A.24) where the Beale number ($Beale_{curve}$) is determined fromthecurvefitinFigureA-1andtheinputpowertotheengine. The other terms in Equation (A.24) are determined either using TRNSYS TMY-2data, or another data set. The temperature-corrected performance of the Stirling engine component allows for system optimization by altering the heater head (expansion space) temperature, fan or pump operating speeds, or replacing the fan and radiator with a central cooling tower.

$$P_{Gross} = Beale_{curve} * P_{mean} * V_{sw} * f * T_{correct} \quad \text{(A.24)}$$

The expansion space temperature can also be modified to determine the effect on system performance. A term can be input for the lowest temperature of the heater head, which would occur in a 4-cylinder engine (SES&SAIC) with varying heater head temperatures. Similar to improving the receiver efficiency by reducing the temperature drop between the receiver and engine heater head, the engine performance will improve by reducing the temperature drop from the highest and lowest heater head in a multiple cylinder engine. This change in performance is simulated in the TRNSYS model by using the lowest heater head temperature in the engine.

Table A.3 The Parameters, Inputs, and Outputs for the TRNSYS Stirling Engine Model

Parameters	**Inputs**	**Outputs**
Manufacturer	Input power to the Stirling engine	Gross output power of the Stirling dish system
Heater head set temperature	Ambient temperature	Ambient temperature
Heater head lowest temperature	Number of Collectors	Stirling engine losses
Beale constant coefficient from curve fit	Compression space temperature (Stirling engine cold sink temperature)	Stirling engine efficiency
Beale first-order coefficient from curve fit	Density of air	Density of ambient air

Beale second-order coefficient from curve fit	DNI	DNI
Beale third-order coefficient from curve fit	Engine hot-end operating temperature	Engine lowest operating heater head temp
Beale fourth-order coefficient from curve fit	Insolation cut in	Heater head highest temperature (set point)
Pressure constant coefficient from curve fit	Input power to the collector	Displaced volume of engine
Pressure first-order coefficient from curve fit		Engine frequency
Engine operating speed		Engine pressure
Displaced volume of the engine		Number of parabolic collectors
		Insolation cut in
		Gross system operating efficiency

TRNSYS Parasitic Power Model

A cooling system model was generated to predict the compression space temperature of the Stirling engine and the parasitic power consumption of the Stirling dish system. The compression space temperature affects the Stirling engine performance and the predicted parasitic power is used to obtain the net power from the system. The compression space temperature is determined with inputs of the ambient temperature, pump speed, fan speed, and the effectiveness of the radiator and cooler at test conditions. The appropriate effectiveness-NTU correlations (Incropera and DeWitt, 2002) are used in the TRNSYS model to predict how the radiator or cooler effectiveness will change at different operating speeds. The fan and pump parasitic powers are determined using the "fan laws "and the dimensionless pump performance equations. The net system power (P_{Net}) is found by subtracting the parasitic power of the tracking and controls ($P_{controls}$), pump (P_{pump}), and fan (Pf_{an}) from the gross output power

($P_{Gross,op}$) of the engine as shown in Equation (A.25). The pump and controls parasitic power are initiated in the TRNSYS model when the direct normal insolation is positive, where as the parasitic power from the fan is not included until the DNI is higher than the insolation cut-in value, which corresponds to when the fan is connected to the grid.

$$P_{Net} = P_{Gross,op} - (P_{controls} + P_{fan} + P_{pump}) \quad \text{(A.25)}$$

Table A.4 The Parameters, Inputs, and Outputs for the TRNSYS Parasitic Power Model

Parameters	**Inputs**	**Outputs**
Cooling tower on [0-radiator and fan , 1-cooling tower]	Gross output power of the Stirling dish system	Net output power of the Stirling dish system(for one collector including system availability
Cooling tower mode [1-natural draft (no fans), 2-forced draft]	Ambient temperature	Total parasitic power of the radiator fan, radiator pump, and tracking controls
Cooling tower water distribution pipe diameter	Number of Collectors	Compression space temperature
Mass flow rate of the cooling tower water	Density of air	Stirling dish system fan parasitic power
Mass flow rate of the cooling tower water during tower test conditions	DNI	Stirling dish system pump parasitic power
Material of the cooling tower water distribution piping[1-plastic, 2-cast iron, 3-riveted steel]	Engine lowest heater-head operating temp	Inlet cooling water temperature to the cooling tower
Efficiency of the cooling tower water distribution pump	Displaced volume	Mass flow rate of the cooling tower water

Fan control signal [-] 0-off, 1-on, values between 0 and 1 are the fraction of the rated volumetric flow rate of the fan	Engine frequency	Ambient temperature
Effectiveness of the counter flow heat exchanger between the cooling tower fluid loop and the Stirling dish cooling fluid loop	Engine pressure	Fan control signal
Dish system availability	Insolation cut in	Compression space temperature
Stirling dish cooling system pump operating speed	Engine rejected thermal load	Parasitic power of the cooling tower
Stirling dish cooling system fan operating speed 1	Cooling tower water outlet temperature	Temperature of the Stirling dish system cooling fluid into the radiator
Stirling dish cooling system fan operating speed 2	Atmospheric pressure	Temperature of the Stirling dish system cooling fluid out of the radiator
Stirling dish cooling system fan operating speed 3	Dish separation distance north to south	Net Stirling dish system efficiency
Stirling dish cooling system cooling fluid temperature for fan speed 2 cut-in	Dish separation distance east to west	
Stirling dish cooling systemcooling fluid temperature for fan speed 3 cut-in	Parasitic power of the cooling tower fan	
Cooler effectiveness at test	Input power to the	

conditions	collector	
Radiator effectiveness at test conditions		
Cooling fluid		
Manufacturer		
Average control system parasitic power		
Stirling dish cooling system pump test parasitic power		
Stirling dish cooling system pump test speed		
Pump test cooling fluid		
Cooling fluid test temperature		
Cooling fluid test volumetric flow rate		
Stirling dish cooling system fan test power		
Stirling dish cooling system fan test speed		
Stirling dish cooling system fan test air density		
Stirling dish cooling system fan test volumetric flow rate		

Appendix B

EES Model for the Stirling Engine

"parameters"

"values in parametric table"

RPM = 1800[rpm] "engine speed (1/s) "

Volume_displacement = 0.00038[m^3] "displaced volume of engine"

TC = 310[K] "compression space temp of engine"

TE = 993[K] "expansion space temp of engine"

Insolation = 180[W/m^2] "varied in parametric table between 180 and 1000W/m^2"

Pressure_mean = 2[Pa]*10^6 "mean engine pressure varied in parametric table between 2E6 and 2E7Pa"

Patm = 101325 [Pa]

P_atm = Patm

TE_max = 995[K] "expansion space operating temperature"

Th = 1083 [K] "heater operating temperature (absorber temperature)"

TC_max = 310[k] "compression space temperature"

Tk = 293[k] "cooler temperature....should be just above ambient"

DNI = Insolation

A_dish = 91 [m^2]

intercept_factor = 0.97 [-]

eta_receiver = 0.86 [-]

reflectivity = 0.91 [-]

eta_generator = 0.95[-]

Power_in_SE = Insolation * A_dish * reflectivity *intercept_factor*eta_receiver

"_____engine parameters_____"

k_spec = Cp / Cv

V1 = 540 [cm^3] * convert(cm^3,m^3) "max volume at state 1"

V2 = V1 - 380 [cm^3] * convert(cm^3,m^3) "minimum volume at state 2"

T_S_L = Tk"sink (cooler) temperature"

w_S_L = sqrt(gamma*R*T_S_L) "speed of piston for the sound speed at sink temperature"

Vmax = V1 "max volume for P-V diagram"

Vmin = V2 "min volume for P-V diagram"

epsilon_v = (V1 / V2) "volumetric compression ratio"

gamma = Cp / Cv"specific heat ratio"

Cv = Cv(H2 , T =AVERAGE(TC,TE)) "spec heat constant volume"

Cv_g = Cv

Cp = Cp(H2 , T =AVERAGE(TC,TE)) "spec heat constant pressure"

MM_H2 = MolarMass(H2)

R = R# / MM_H2 "working gas constant"

T_H2_ave = (TE + TC) / 2

m_g = Pressure_mean*V1 / (R*T_H2_ave) "estimate Urieli p39 & ideal gas law""mass of working gas"

N_cylinders = 4 "number of cylinders"

stroke_cyl = 0.04[m] "stroke for each cylinder"

S = (N_cylinders*stroke_cyl) "total stroke of the piston [m]"

T_m = AVERAGE(TC,TE) "mean temperature of gas"

Pr = Prandtl(H2,T=T_m) "Prandtl number"

nu=Viscosity(H2,T=T_m)*Volume(H2,T=T_m,P=Pressure_mean) "viscosity of working gas [m^2 / s]"

P1 = (4*Pressure_mean) / ((epsilon_v + 1) * (tau + 1)) "initial state inlet pressure"

tau = (TE / TC) "ratio of working gas extreme temperatures"

w = 2*S*RPM/(60 [s/min]) "speed of piston [m/s]"

"_____regenerator parameters_____"

m_R = 0.2 [kg] "mass of regenerator"

TR = (TE - TC) / (ln(TE / TC)) "mean effective regenerator temp...NASA ref"

c_R = c_('Stainless_AISI316', TR) "specific heat of regenerator"

A_R = pi*(D_R /2)^2 * N_S "! total surface area guessed""heat transfer surface area of regenerator"

D_R = .057[m] "diameter of regenerator"

b2 = 1e-7[m] "!guess""distance between wires in the regenerator"

d = 4e-5[m] "!guess....not sensitive""regenerator wire diameter"

N_S = 1600 "! 2 x 200 in each of 4 cylinders""number of screens in the regenerator""_____"

"Regeneration losses"

y = 0.72 "y is an adjusting coefficient"

eta_II_X = 1 / (1 + X *(1-sqrt(Tk / Th))/ ((gamma-1)*ln(epsilon_v))) "Regeneration losses"

X = X1 * y + X2*(1 - y) " X is coefficient of regenerative losses"

X1 = (1 + 2*M + EXP(-B)) / (2 * (1 + M))

X2 = (M + EXP(-B)) / (1 + M)

M = (m_g * Cv_g) / (m_R * c_R)

B = (1 + M) * (h*A_R) / (m_g*Cv_g)*(S / w)

h = (0.395*(4*Pressure_mean / (R*TC)) * w^(0.424) * Cp * nu^0.576) / ((1+tau) * (1 - (PI / (4*((b2/d)+1))))*D_R^0.576 * Pr^(2/3)) "convection heat x-fercoef to regenerator""_____"

"!Pressure losses"

eta_II_DELTA_P = 1 - (((w / w_S_L) * gamma*(1 + sqrt(tau))* ln(epsilon_v) + 5 * (w/w_S_L)^2 * N_S) /(tau * eta_prime * ln(epsilon_v)) + ((3*(0.94[m/s]+0.045*w)*(10^5)[Pa-s/m]) / (4*P1)) /(tau*eta_prime*ln(epsilon_v)))

eta_prime = eta_CC * eta_II_X"_____"

"! Stirling cycle efficiency"

eta_CC = 1 - (Tk / Th) "Carnot efficiency"

eta_2_DELTA_T = 1 / (1+sqrt(Tk/Th))

eta_II_irrev = eta_II_X * eta_II_DELTA_P*eta_2_DELTA_T "second law efficiency including irreversibilities"

eta_Petruscu = MAX(0,eta_CC * eta_II_irrev) "Stirling engine total efficiency""_____"

Appendix C

Stirling Engine Types

There are two common types of Stirling engines that have been used for power production: the kinematic and the free-piston engine.

Kinematic engines have the power piston connected to the crankshaft by a connecting rod, which is attached to a cross-head to eliminate lateral forces against the cylinder walls. A linear seal is used between the cross-head and piston to seal the region between high and lower pressures to allow the bearing surfaces to remain lubricated in the low-pressure area while preventing fouling of the heat exchanger surface in the high-pressure region. Kinematic Stirling engines are currently being used in the Stirling dish systems by all of the major manufacturers.

An alternative design to the crankshaft with the cross-head is to use a swash plate or wobble plate drive. A slanted drive surface is connected to the drive shaft at an angle and moves the fixed piston push rods up or down while the drive surface rotates. The stroke length can be controlled by varying the drive surface angle with respect to the axis of rotation.

Free piston Stirling engines do not have the power piston connected to a crankshaft, but rather cycle back and forth between the working fluid and another gas. Free-piston Stirling engines have a lower cost, longer life, and minimal maintenance with respect to kinematic Stirling engines but no free-piston Stirling dish systems are currently planned for direct solar dish applications.

Stirling engine configurations

There are three basic engine design configurations that have been used for Stirling engines or Engineers classify Stirling engines into three distinct types. These include alpha, beta, and gamma configurations.

The alpha configuration uses a separate cylinder for the expansion and compression space to move the working gas, with the cylinders held at different temperatures while the beta and gamma configurations use a displacer piston to move the working fluid between the expansion and compression spaces.

Alpha Stirling

An alpha Stirling contains two separate power pistons in separate cylinders, one "hot" piston and one "cold" piston. The hot piston cylinder is situated inside the higher temperature heat exchanger and the cold piston cylinder is situated inside the low temperature heat exchanger. This type of engine has a very high power-to-volume ratio but has technical problems due to the usually high temperature of the "hot" piston and the durability of its seals.

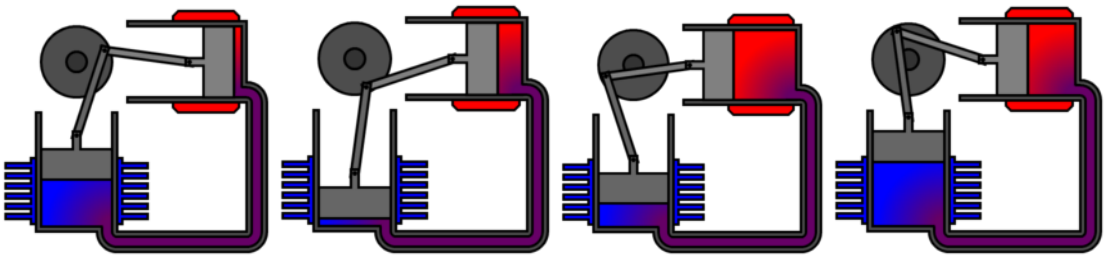

Figure C.1 Alpha Type Stirling Engine (http:// wikipedia.org)

Figure C.2 Actual Alpha Type Stirling Engine (http://www.sbp.de)

Beta Stirling

A beta Stirling has a single power piston arranged within the same cylinder on the same shaft as a displacer piston. The displacer piston is a loose fit and does not extract any power from the expanding gas but only serves to shuttle the working gas from the hot heat exchanger to the cold heat exchanger. When the working gas is pushed to the hot end of the cylinder it expands and pushes the power piston. When it is pushed to the cold end of the cylinder it contracts and the

momentum of the machine, usually enhanced by a flywheel, pushes the power piston the other way to compress the gas.

Unlike the alpha type, the beta type avoids the technical problems of hot moving seals.

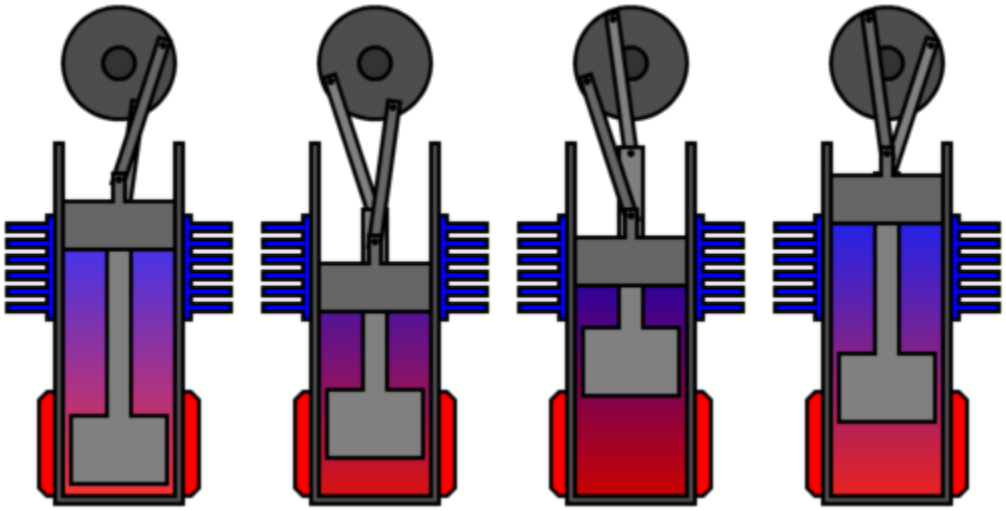

Figure C.3 Beta Type Stirling Engine (www.physics.sfasu.edu)

A beta Stirling has two pistons within the same cylinder both connected to the same crankshaft. One of these is the tightly fitted power piston and the other a loosely fitted displacement piston.

Gamma Stirling

A gamma Stirling is simply a beta Stirling in which the power piston is mounted in a separate cylinder alongside the displacer piston cylinder, but is still connected to the same flywheel. The gas in the two cylinders can flow freely between them and remains a single body. This configuration produces a lower compression ratio but is mechanically simpler and often used in multi-cylinder Stirling engines. Stirling engines with regenerators have a cycle that matches the Carnot cycle. The Carnot cycle determines the maximum theoretical efficiency of a heat engine. The temperatures must be measured in absolute degrees (Kelvin or Rankine) for this formula to work.

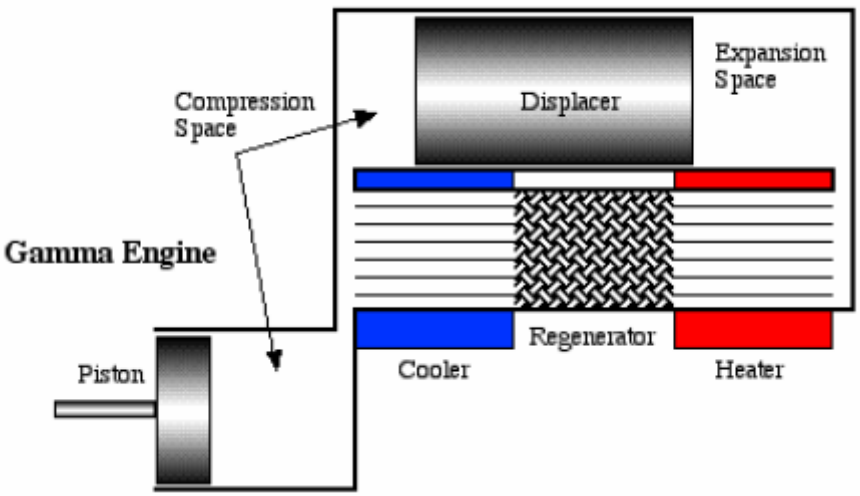

Figure C.4 Gamma Configuration Stirling Engine (Urieli, 2007)

Appendix D

Simulation result for the remaining months

January:

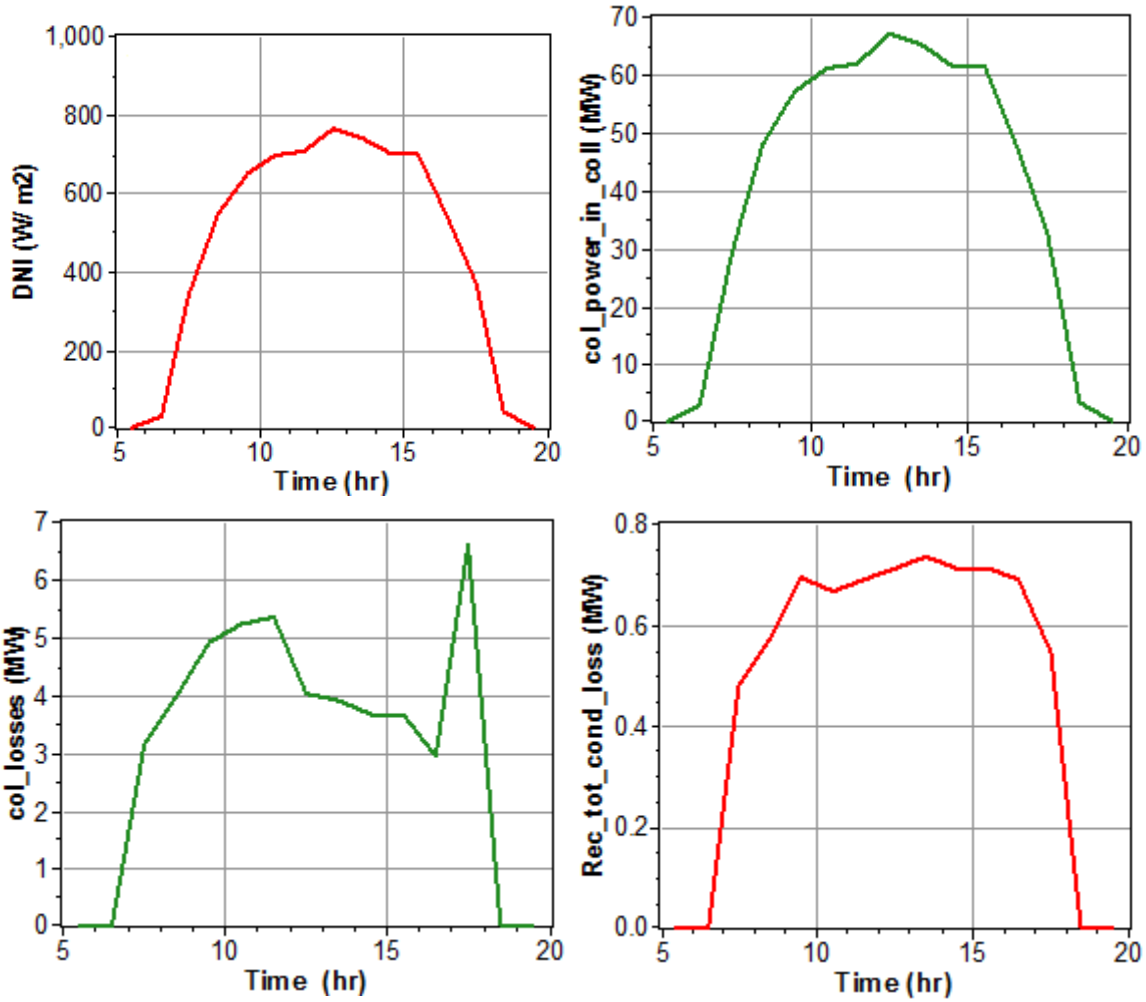

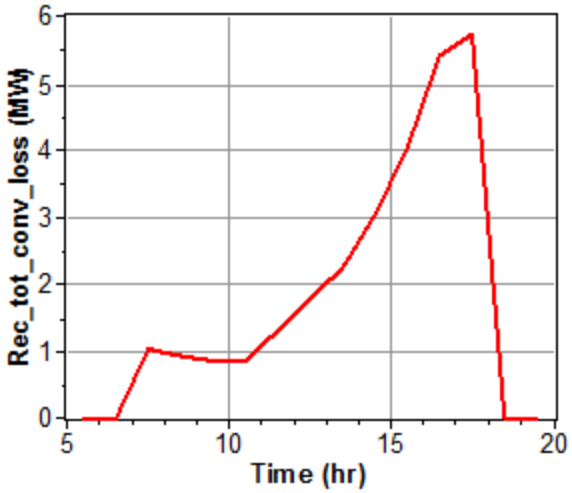
Rec_tot_conv_loss (MW)
Time (hr)

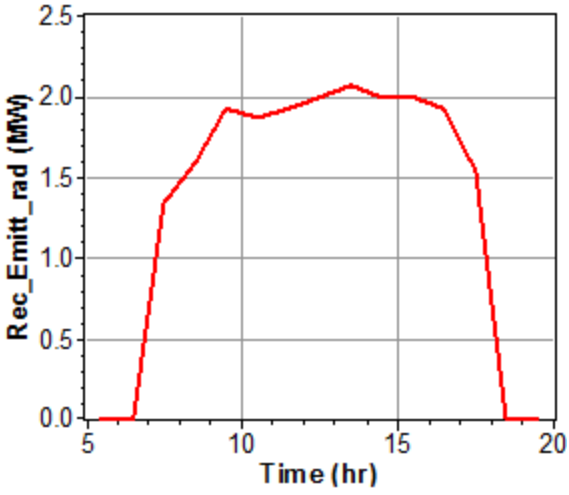
Rec_Emitt_rad (MW)
Time (hr)

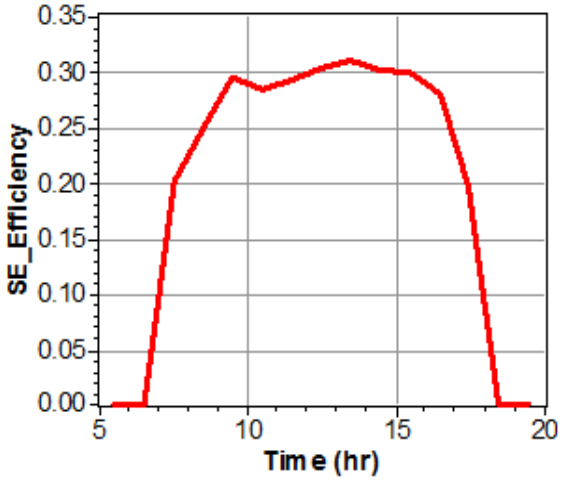
SE_Efficiency
Time (hr)

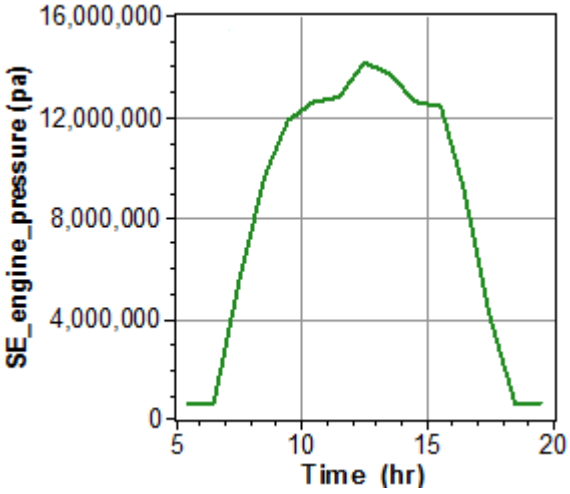
SE_engine_pressure (pa)
Time (hr)

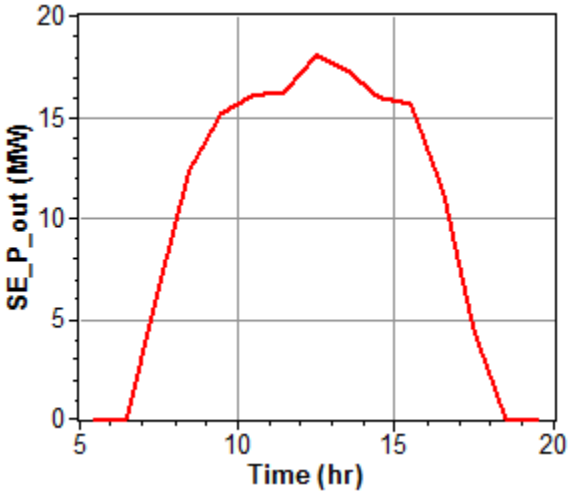
SE_P_out (MW)
Time (hr)

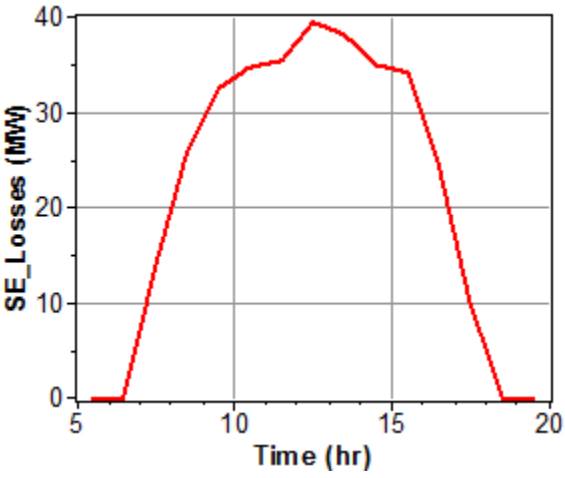
SE_Losses (MW)
Time (hr)

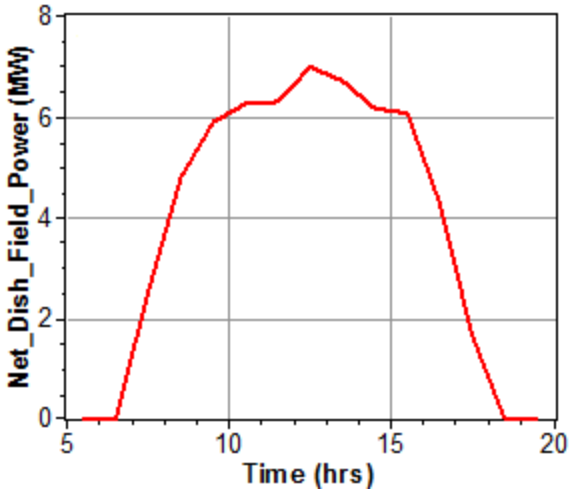
Net_Dish_Field_Power (MW)
0
2
4
6
8
5
10
15
20
Time (hrs)

March:

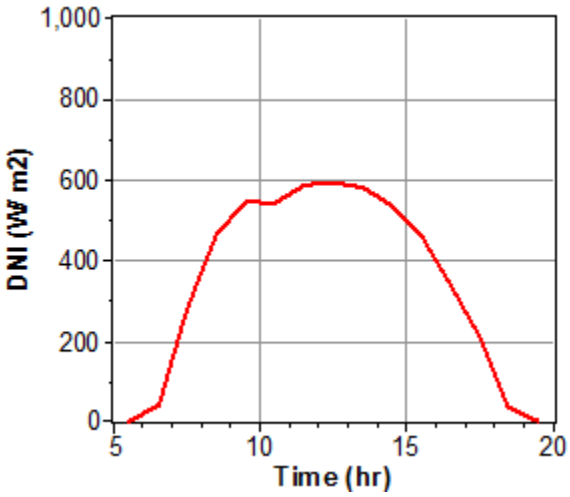
DNI (W/m2)
1,000
800
600
400
200
0
5
10
15
20
Time (hr)

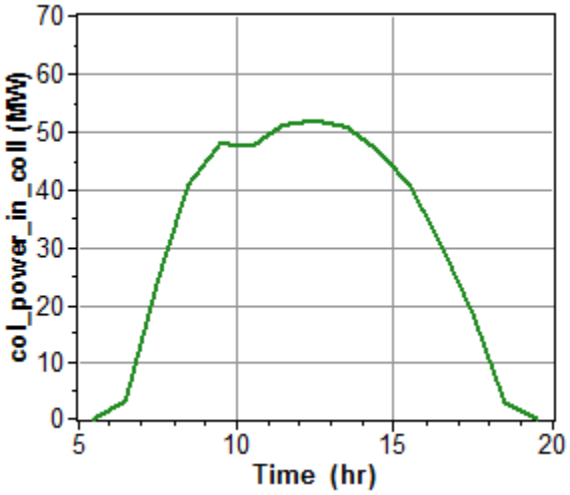
col_power_in_coll (MW)
70
60
50
40
30
20
10
0
5
10
15
20
Time (hr)

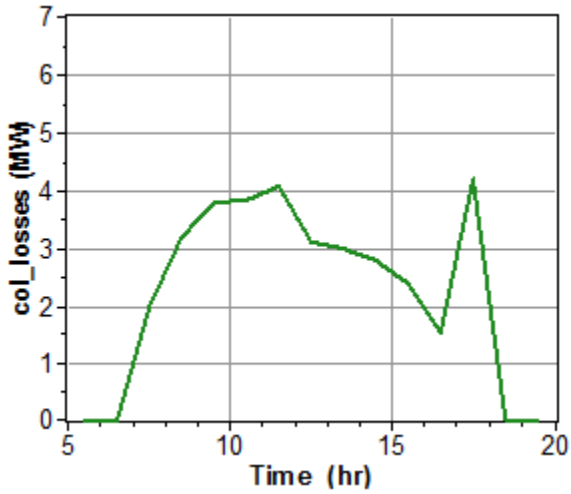
col_losses (MW)
7
6
5
4
3
2
1
0
5
10
15
20
Time (hr)

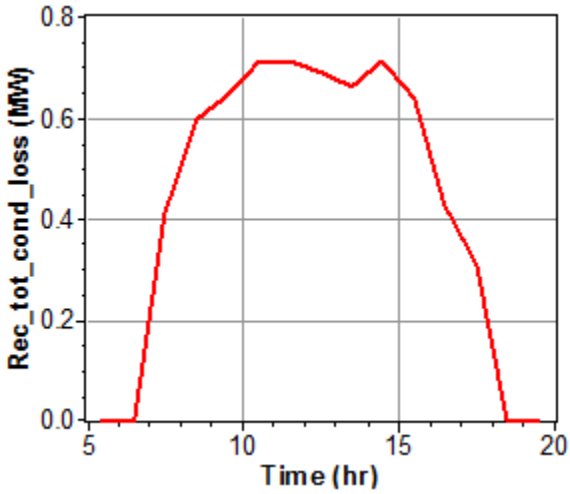
Rec_tot_cond_loss (MW)
0.8
0.6
0.4
0.2
0.0
5
10
15
20
Time (hr)

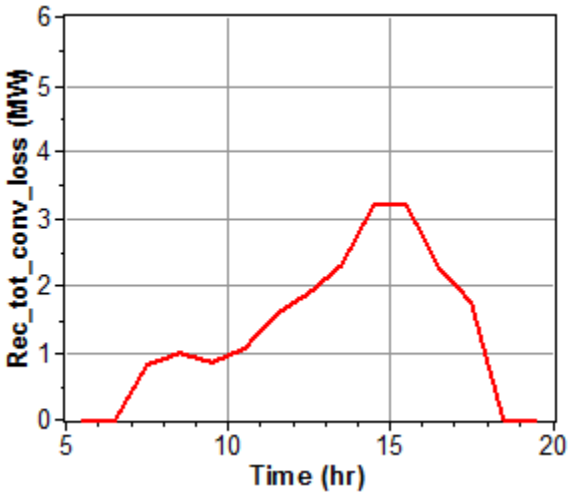
Rec_tot_conv_loss (MW)
6
5
4
3
2
1
0
5
10
15
20
Time (hr)

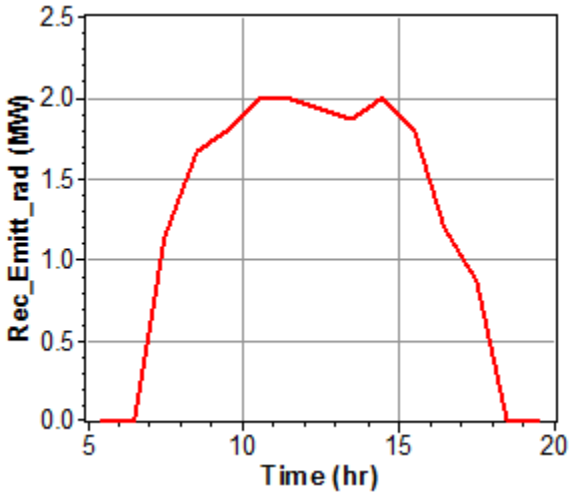
Rec_Emitt_rad (MW)
2.5
2.0
1.5
1.0
0.5
0.0
5
10
15
20
Time (hr)

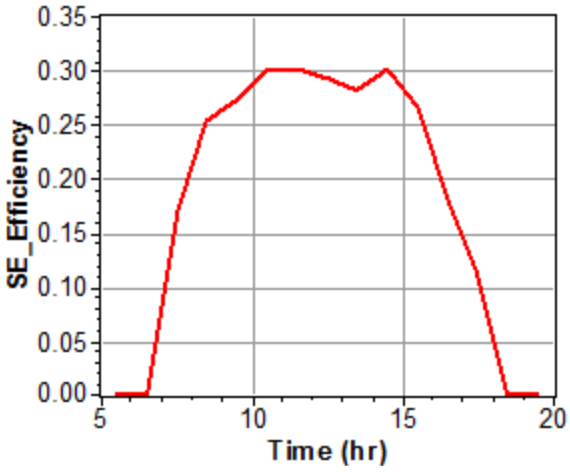
SE_Efficiency
0.35
0.30
0.25
0.20
0.15
0.10
0.05
0.00
5
10
15
20
Time (hr)

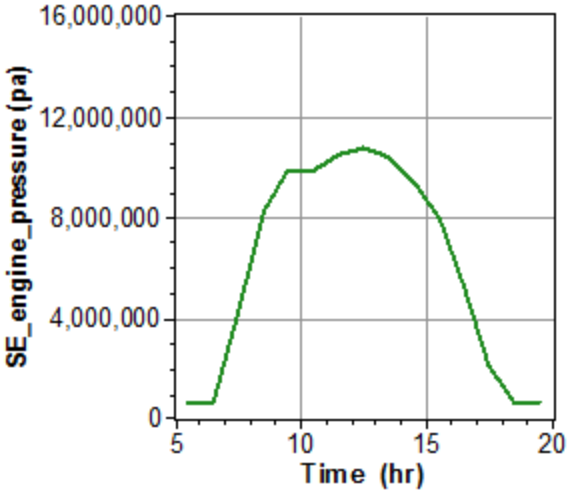
SE_engine_pressure (pa)
16,000,000
12,000,000
8,000,000
4,000,000
0
5
10
15
20
Time (hr)

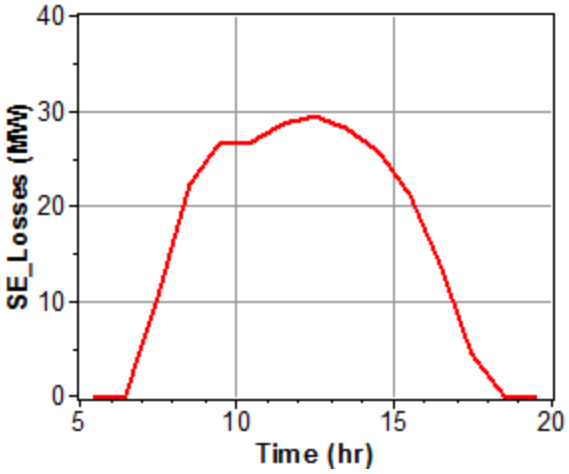
SE_Losses (MW)
40
30
20
10
0
5
10
15
20
Time (hr)

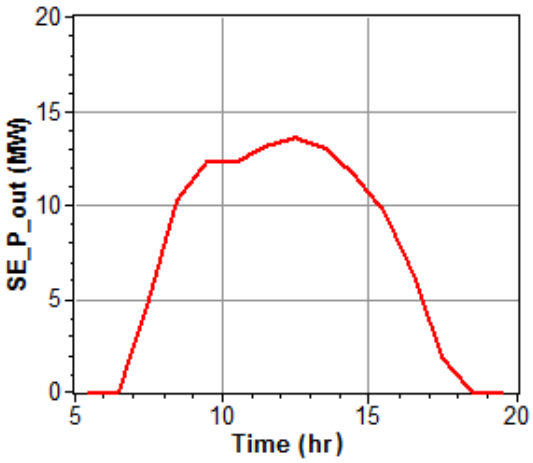
SE_P_out (MW)
20
15
10
5
0
5
10
15
20
Time (hr)

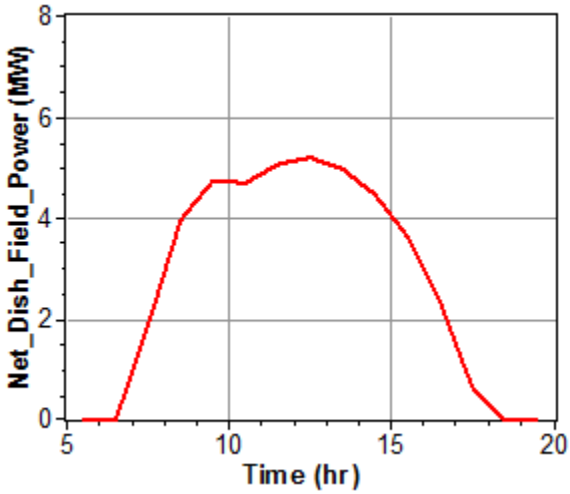
Net_Dish_Field_Power (MW)
8
6
4
2
0
5
10
15
20
Time (hr)

April:

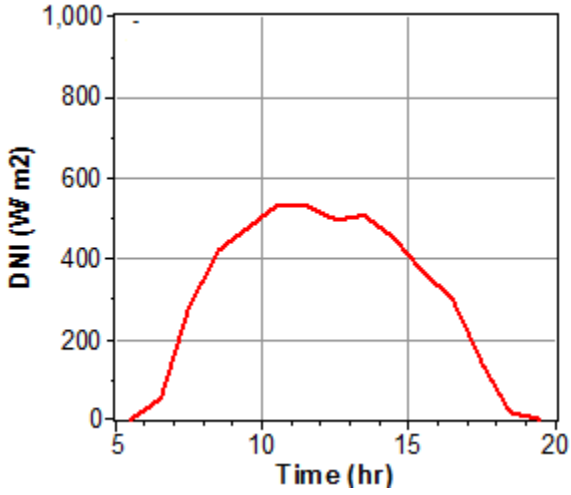
DNI (W/m2)
1,000
800
600
400
200
0
5
10
15
20
Time (hr)

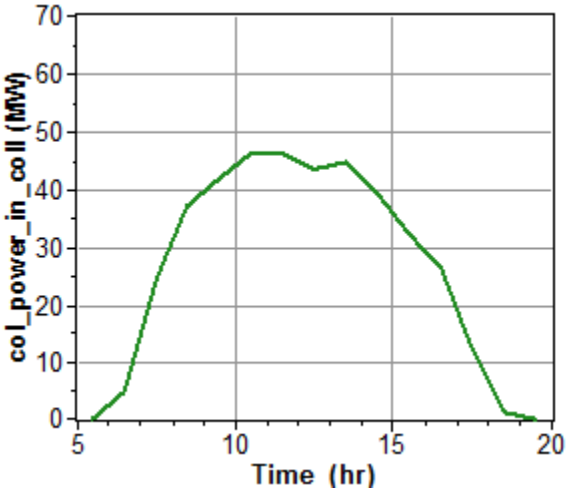
col_power_in_coll (MW)
70
60
50
40
30
20
10
0
5
10
15
20
Time (hr)

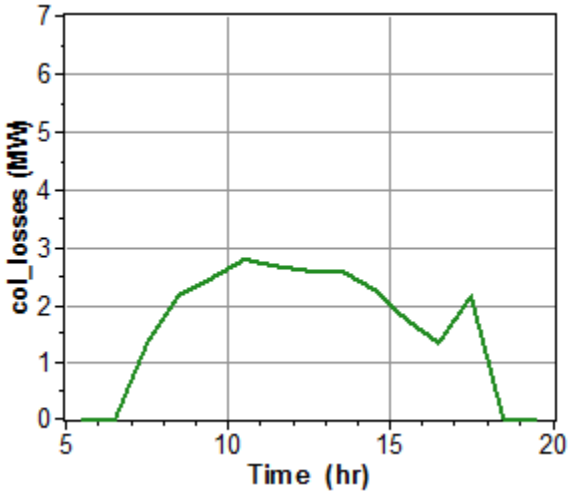
col_losses (MW)
7
6
5
4
3
2
1
0
5
10
15
20
Time (hr)

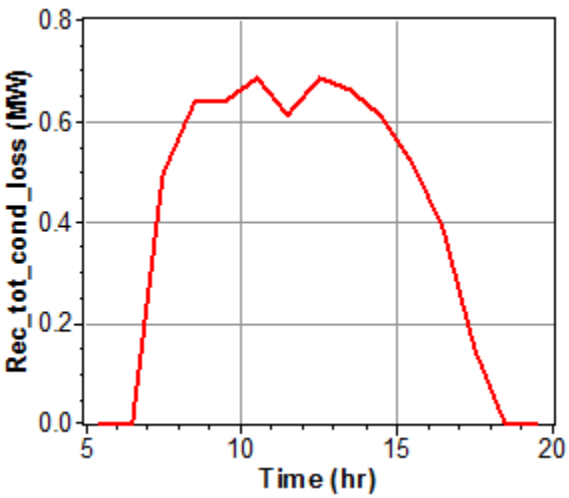
Rec_tot_cond_loss (MW)
0.8
0.6
0.4
0.2
0.0
5
10
15
20
Time (hr)

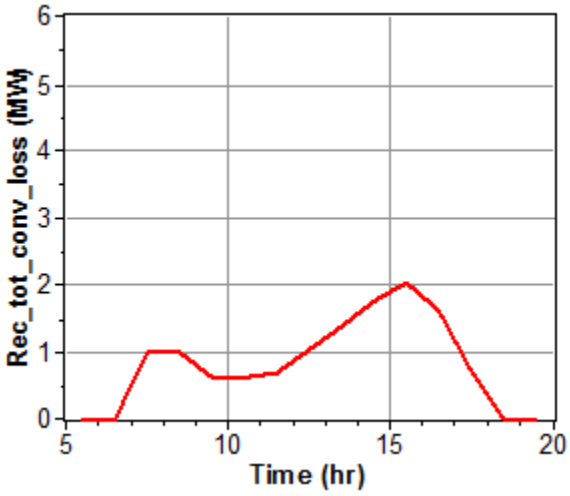
Rec_tot_conv_loss (MW)
6
5
4
3
2
1
0
5
10
15
20
Time (hr)

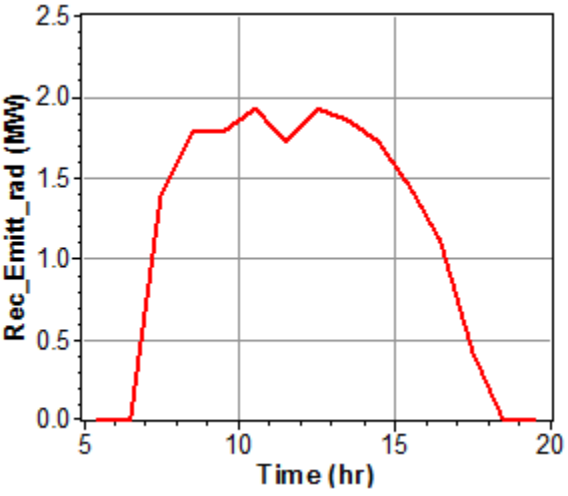
Rec_Emitt_rad (MW)
2.5
2.0
1.5
1.0
0.5
0.0
5
10
15
20
Time (hr)

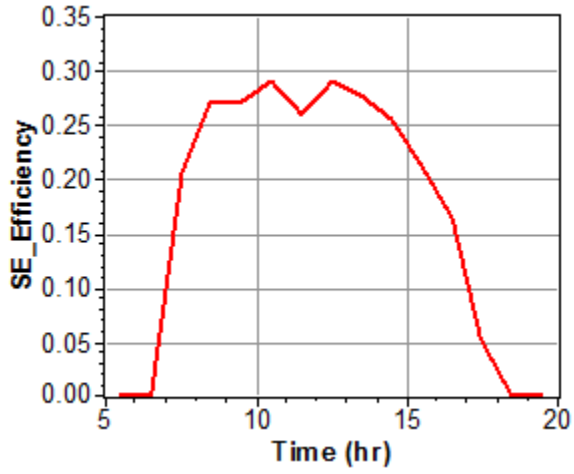
SE_Efficiency
0.35
0.30
0.25
0.20
0.15
0.10
0.05
0.00
5
10
15
20
Time (hr)

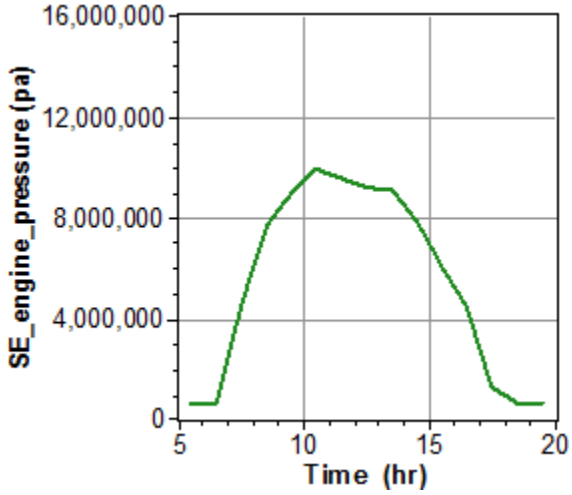
SE_engine_pressure (pa)
16,000,000
12,000,000
8,000,000
4,000,000
0
5
10
15
20
Time (hr)

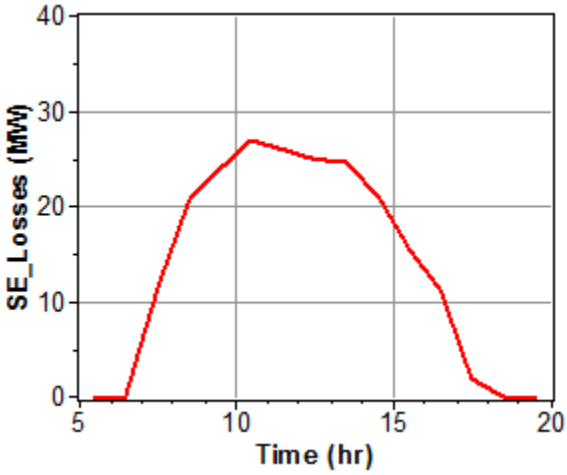
SE_Losses (MW)
40
30
20
10
0
5
10
15
20
Time (hr)

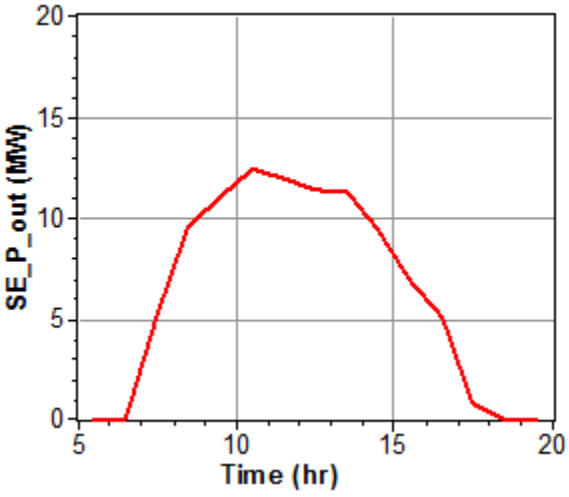
SE_P_out (MW)
20
15
10
5
0
5
10
15
20
Time (hr)

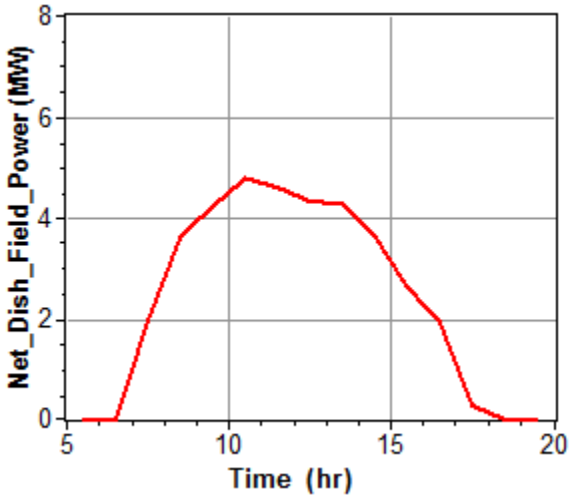
Net_Dish_Field_Power (MW)
8
6
4
2
0
5
10
15
20
Time (hr)

May:

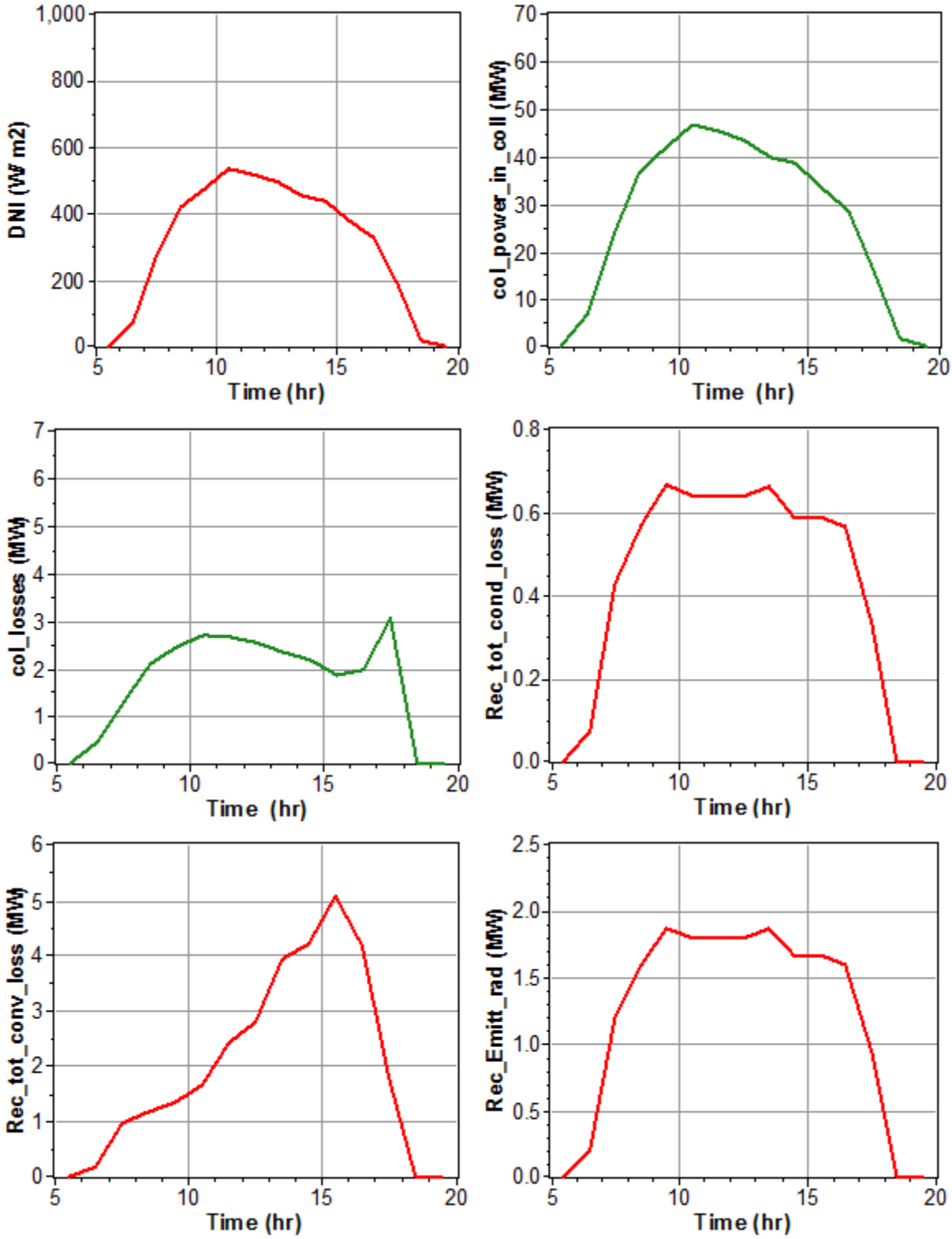
DNI (W/m2)
Time (hr)
col_power_in_coll (MW)
Time (hr)
col_losses (MW)
Time (hr)
Rec_tot_cond_loss (MW)
Time (hr)
Rec_tot_conv_loss (MW)
Time (hr)
Rec_Emitt_rad (MW)
Time (hr)

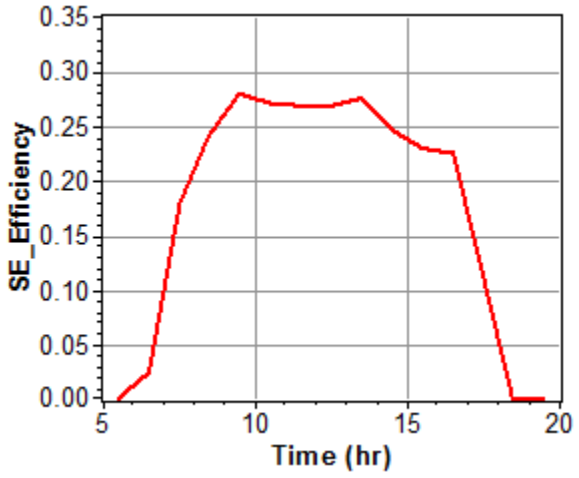
SE_Efficiency
0.35
0.30
0.25
0.20
0.15
0.10
0.05
0.00
5
10
15
20
Time (hr)

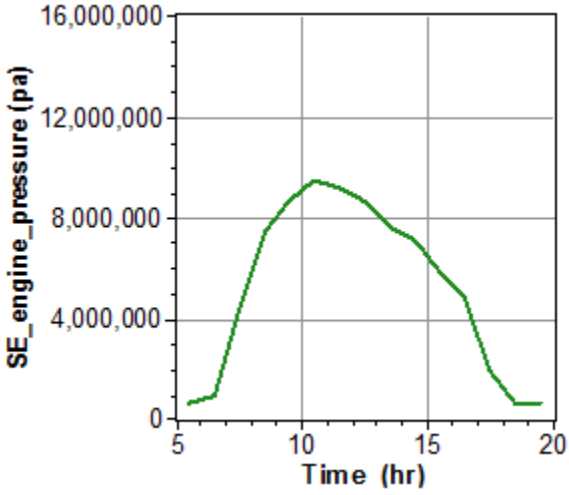
SE_engine_pressure (pa)
16,000,000
12,000,000
8,000,000
4,000,000
0
5
10
15
20
Time (hr)

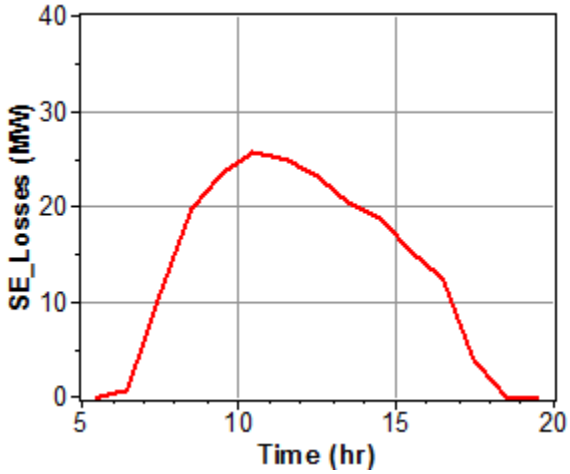
SE_Losses (MW)
40
30
20
10
0
5
10
15
20
Time (hr)

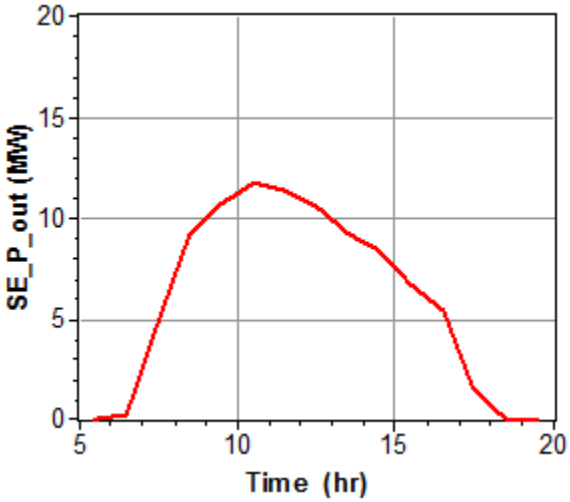
SE_P_out (MW)
20
15
10
5
0
5
10
15
20
Time (hr)

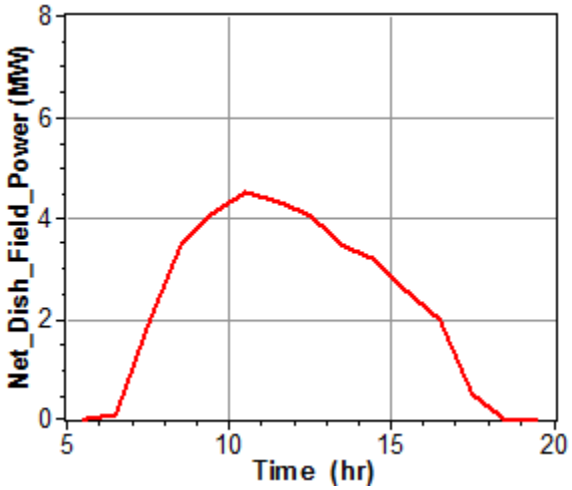
Net_Dish_Field_Power (MW)
8
6
4
2
0
5
10
15
20
Time (hr)

June:

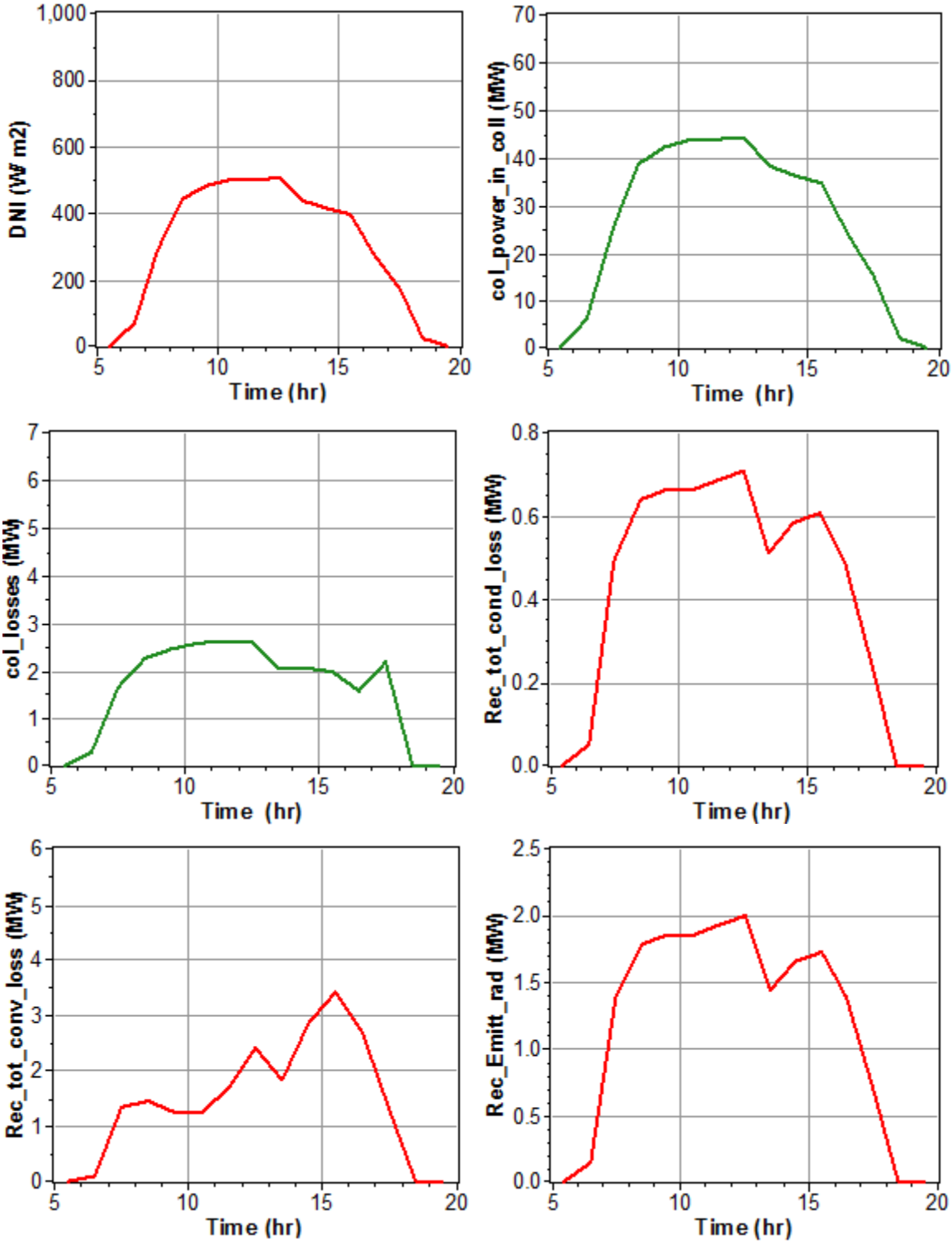
DNI (W/ m2)
1,000
800
600
400
200
0
5
10
15
20
Time (hr)
col_power_in_coll (MW)
70
60
50
40
30
20
10
0
5
10
15
20
Time (hr)
col_losses (MW)
7
6
5
4
3
2
1
0
5
10
15
20
Time (hr)
Rec_tot_cond_loss (MW)
0.8
0.6
0.4
0.2
0.0
5
10
15
20
Time (hr)
Rec_tot_conv_loss (MW)
6
5
4
3
2
1
0
5
10
15
20
Time (hr)
Rec_Emitt_rad (MW)
2.5
2.0
1.5
1.0
0.5
0.0
5
10
15
20
Time (hr)

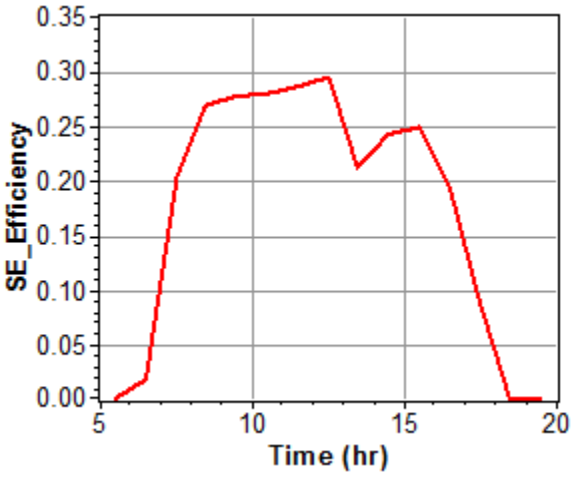
SE_Efficiency
0.35
0.30
0.25
0.20
0.15
0.10
0.05
0.00
5
10
15
20
Time (hr)

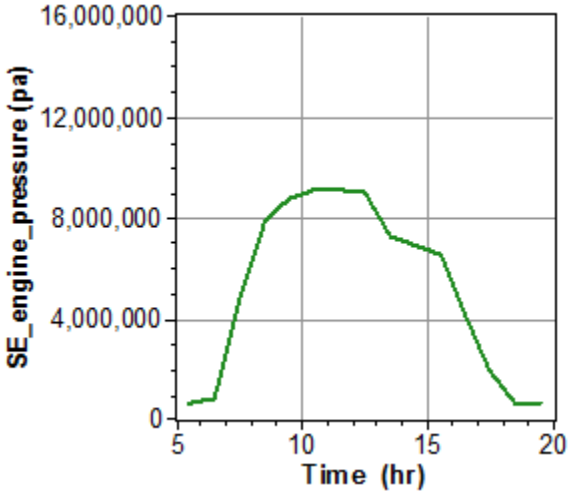
SE_engine_pressure (pa)
16,000,000
12,000,000
8,000,000
4,000,000
0
5
10
15
20
Time (hr)

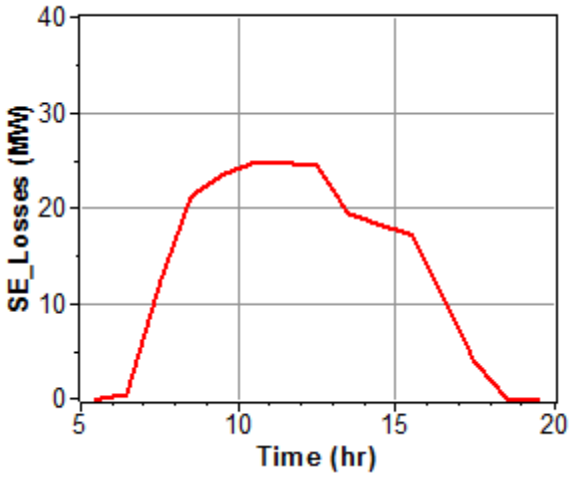
SE_Losses (MW)
40
30
20
10
0
5
10
15
20
Time (hr)

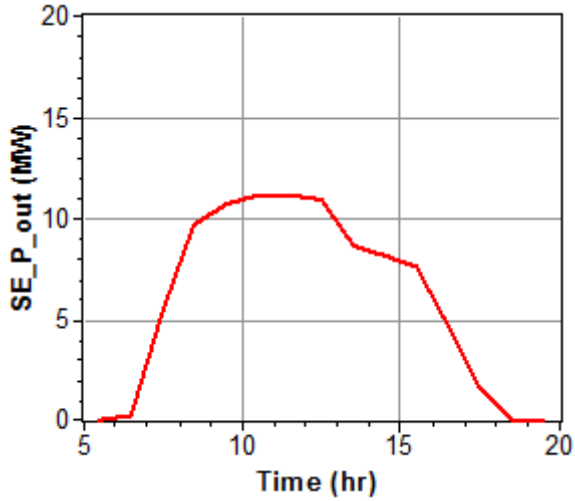
SE_P_out (MW)
20
15
10
5
0
5
10
15
20
Time (hr)

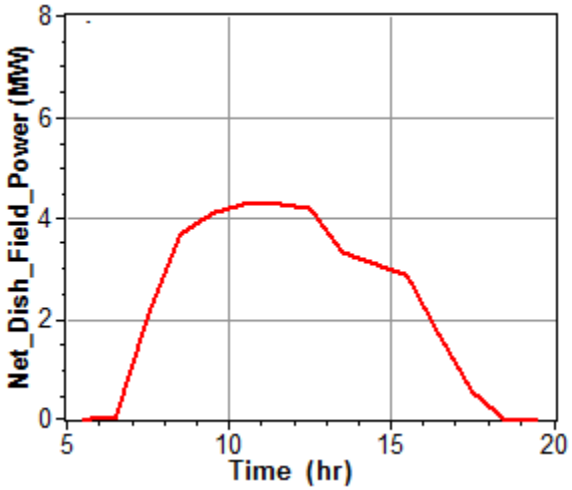
Net_Dish_Field_Power (MW)
8
6
4
2
0
5
10
15
20
Time (hr)

July:

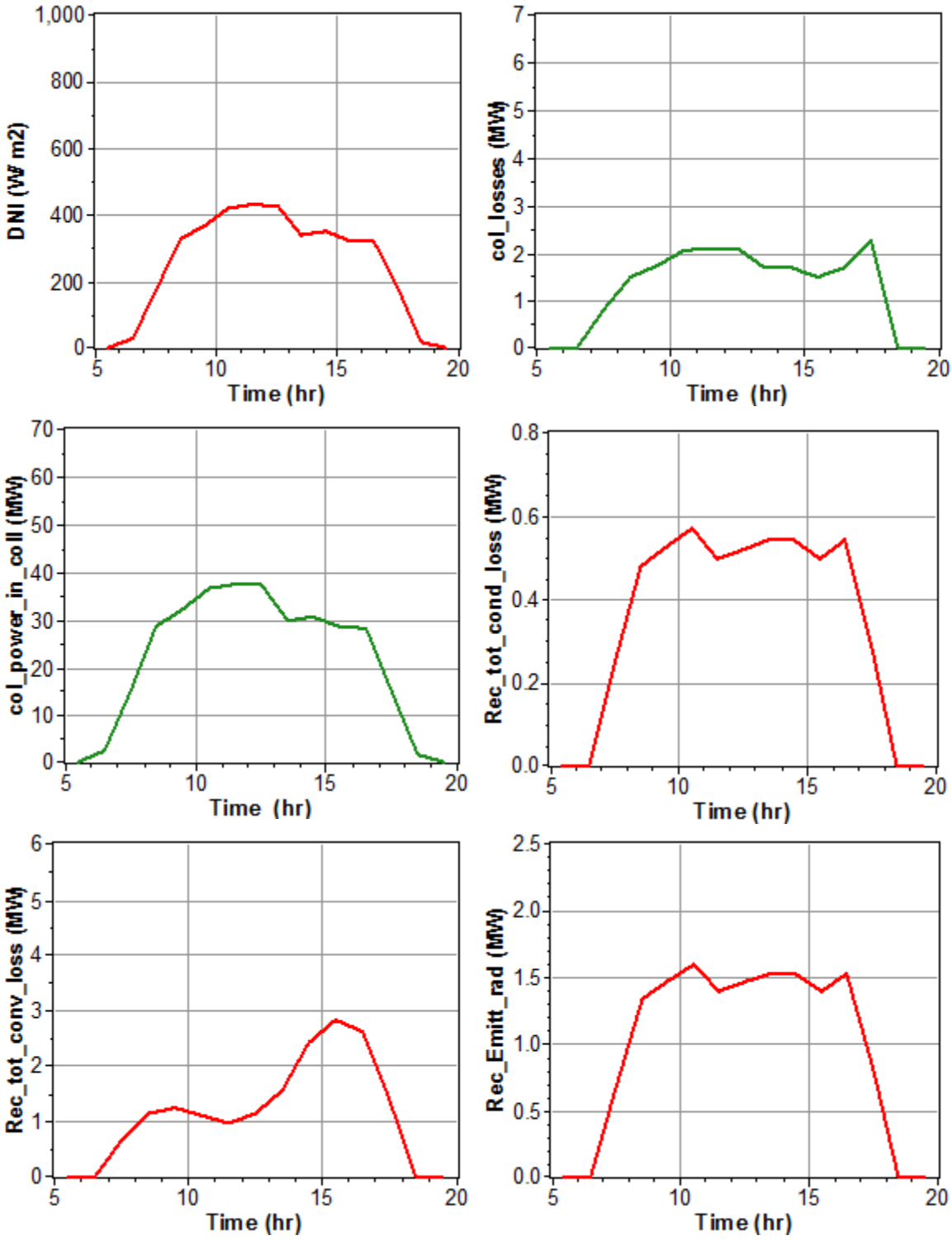
DNI (W m2)
1,000
800
600
400
200
0
5
10
15
20
Time (hr)
col_losses (MW)
7
6
5
4
3
2
1
0
5
10
15
20
Time (hr)
col_power_in_coll (MW)
70
60
50
40
30
20
10
0
5
10
15
20
Time (hr)
Rec_tot_cond_loss (MW)
0.8
0.6
0.4
0.2
0.0
5
10
15
20
Time (hr)
Rec_tot_conv_loss (MW)
6
5
4
3
2
1
0
5
10
15
20
Time (hr)
Rec_Emitt_rad (MW)
2.5
2.0
1.5
1.0
0.5
0.0
5
10
15
20
Time (hr)

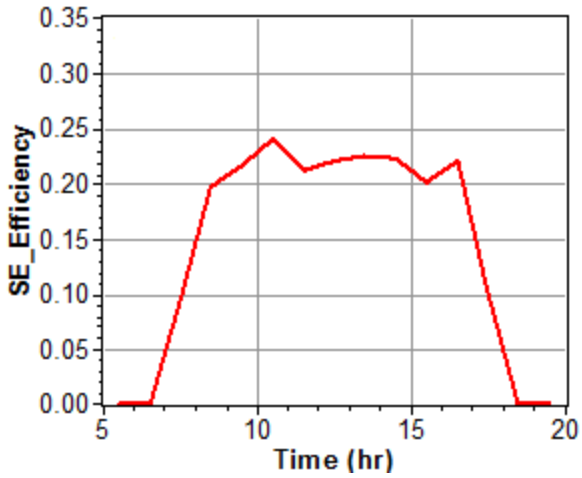
SE_Efficiency
0.35
0.30
0.25
0.20
0.15
0.10
0.05
0.00
5
10
15
20
Time (hr)

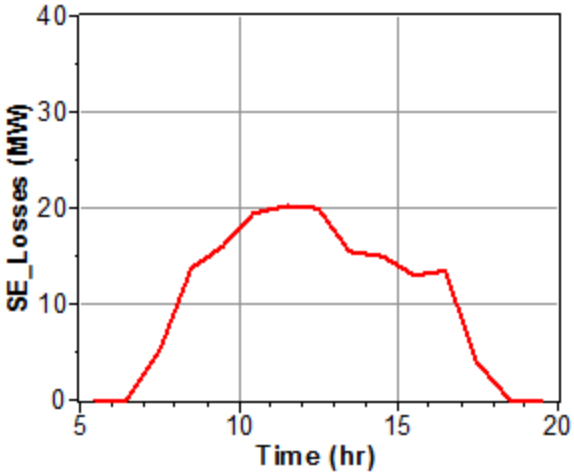
SE_Losses (MW)
40
30
20
10
0
5
10
15
20
Time (hr)

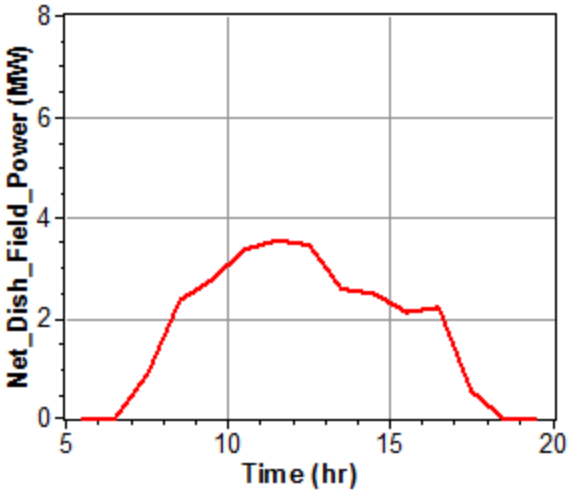
Net_Dish_Field_Power (MW)
8
6
4
2
0
5
10
15
20
Time (hr)

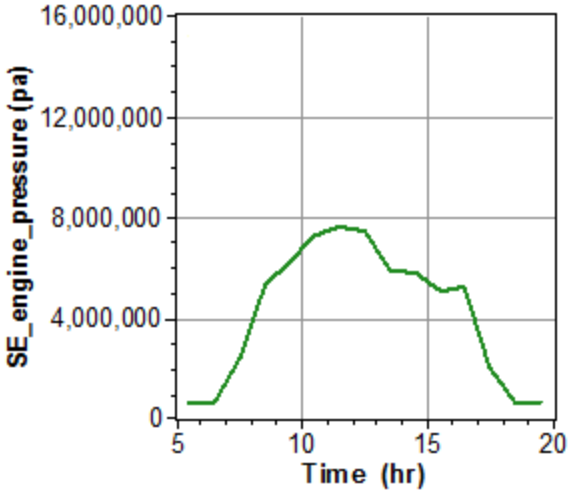
SE_engine_pressure (pa)
16,000,000
12,000,000
8,000,000
4,000,000
0
5
10
15
20
Time (hr)

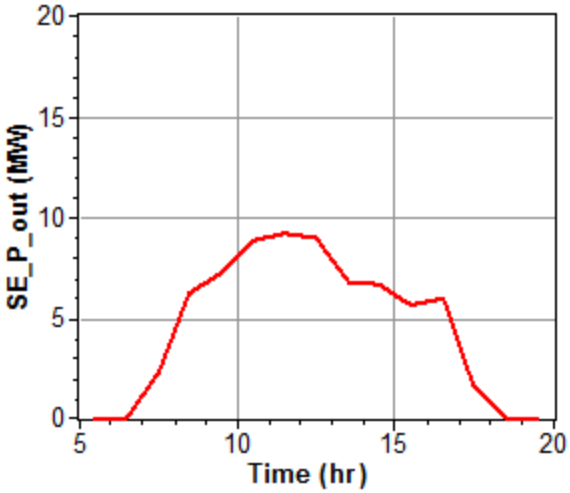
SE_P_out (MW)
20
15
10
5
0
5
10
15
20
Time (hr)

September:

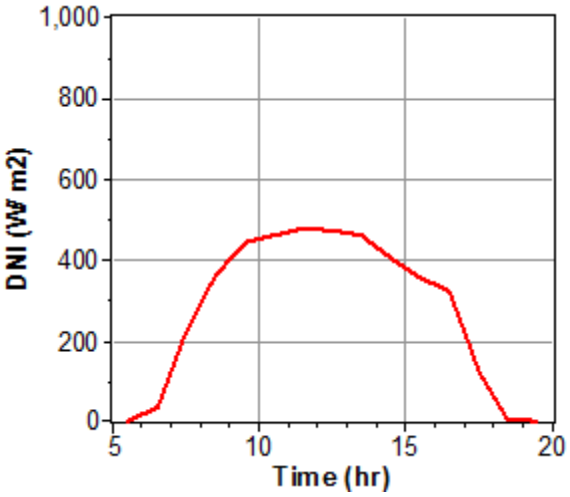
DNI (W/ m2)
1,000
800
600
400
200
0
5
10
15
20
Time (hr)

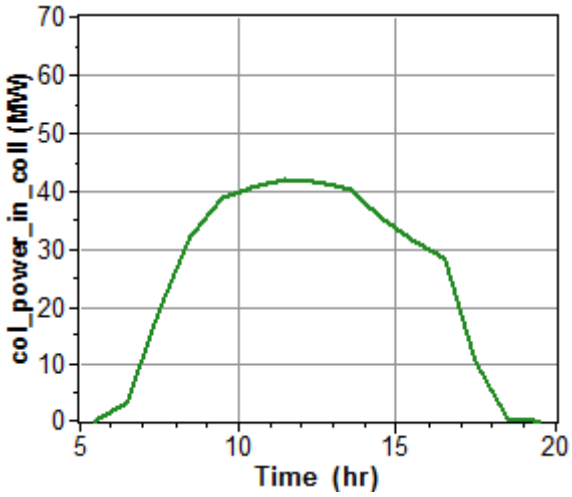
col_power_in_coll (MW)
70
60
50
40
30
20
10
0
5
10
15
20
Time (hr)

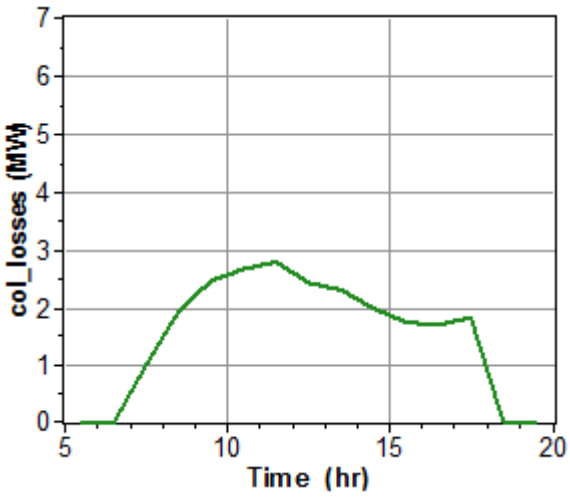
col_losses (MW)
7
6
5
4
3
2
1
0
5
10
15
20
Time (hr)

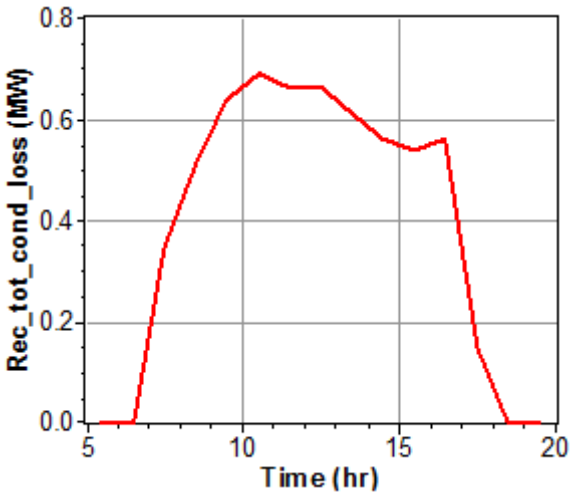
Rec_tot_cond_loss (MW)
0.8
0.6
0.4
0.2
0.0
5
10
15
20
Time (hr)

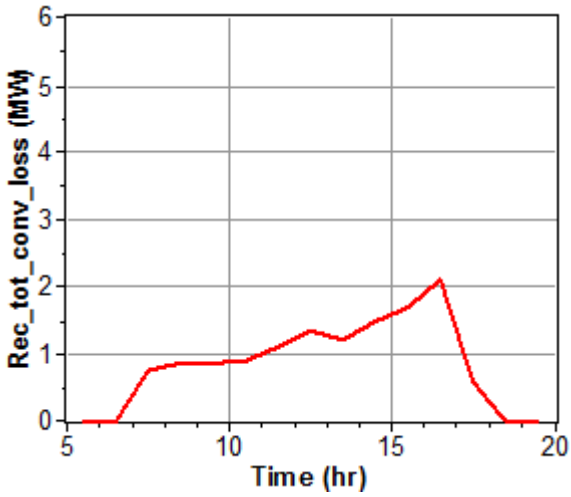
Rec_tot_conv_loss (MW)
6
5
4
3
2
1
0
5
10
15
20
Time (hr)

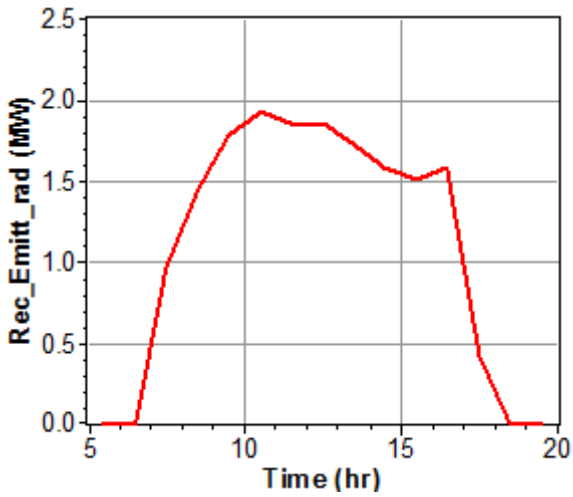
Rec_Emitt_rad (MW)
2.5
2.0
1.5
1.0
0.5
0.0
5
10
15
20
Time (hr)

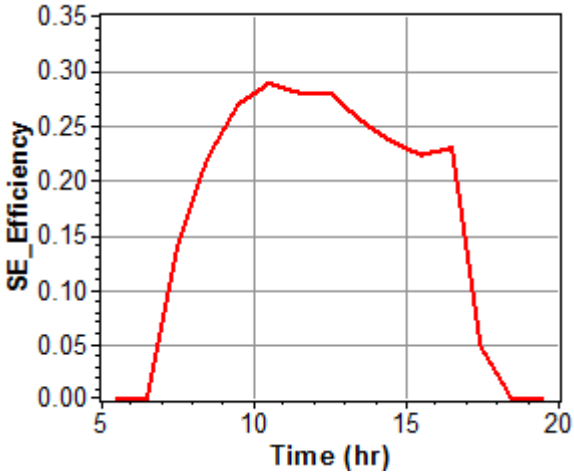
SE_Efficiency
0.35
0.30
0.25
0.20
0.15
0.10
0.05
0.00
5
10
15
20
Time (hr)

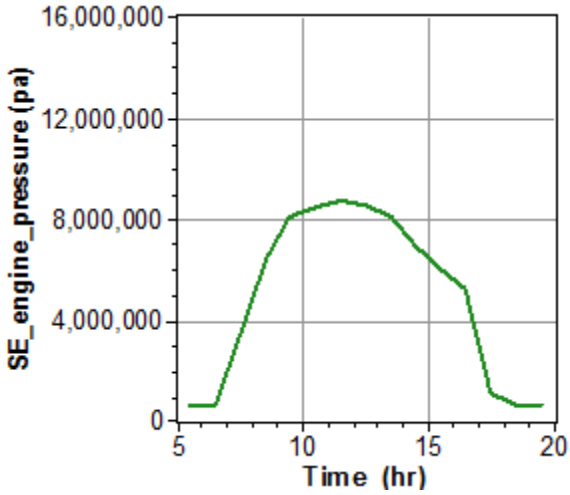
SE_engine_pressure (pa)
16,000,000
12,000,000
8,000,000
4,000,000
0
5
10
15
20
Time (hr)

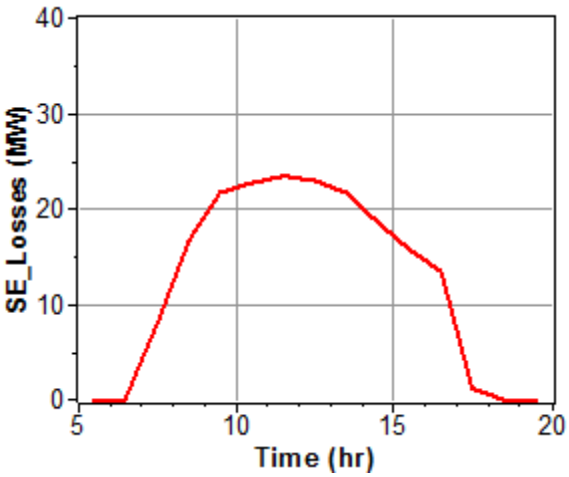
SE_Losses (MW)
40
30
20
10
0
5
10
15
20
Time (hr)

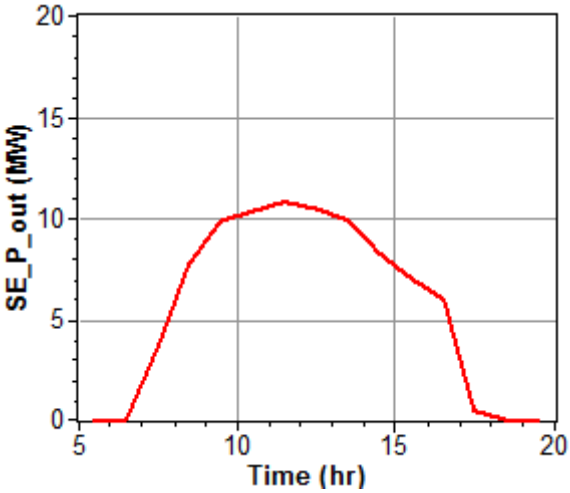
SE_P_out (MW)
20
15
10
5
0
5
10
15
20
Time (hr)

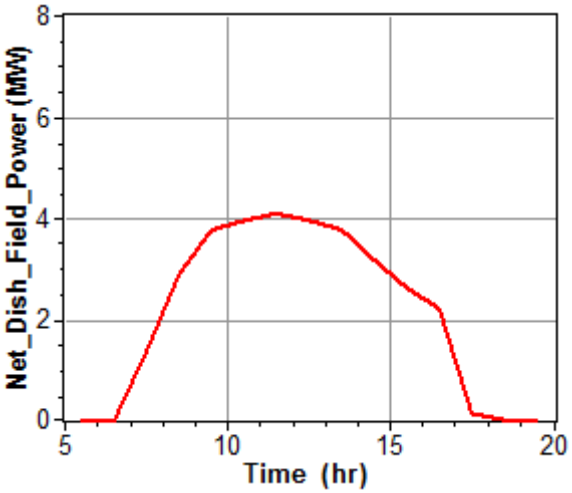
Net_Dish_Field_Power (MW)
8
6
4
2
0
5
10
15
20
Time (hr)

October:

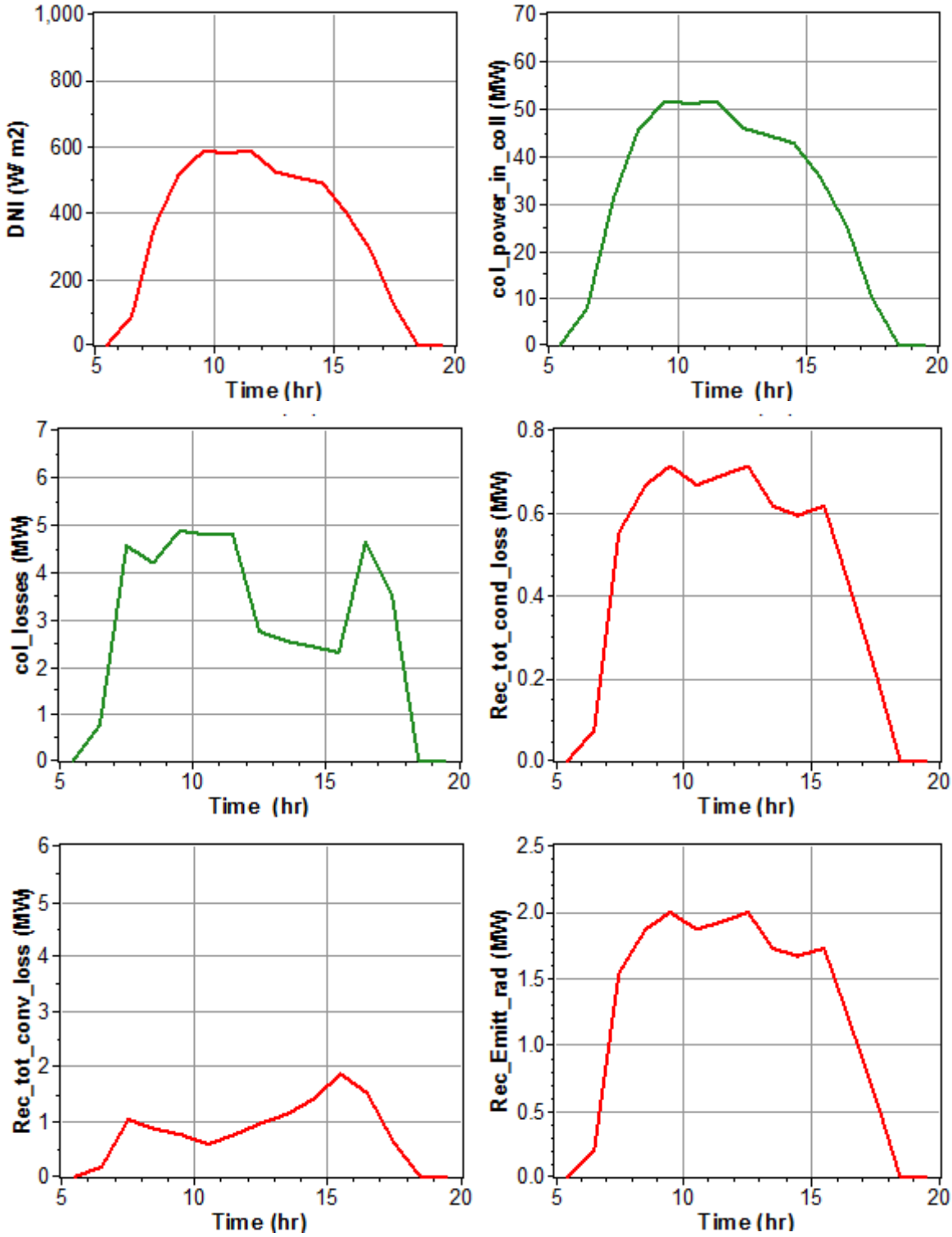
DNI (W/m2)
Time (hr)
col_power_in_coll (MW)
Time (hr)
col_losses (MW)
Time (hr)
Rec_tot_cond_loss (MW)
Time (hr)
Rec_tot_conv_loss (MW)
Time (hr)
Rec_Emitt_rad (MW)
Time (hr)

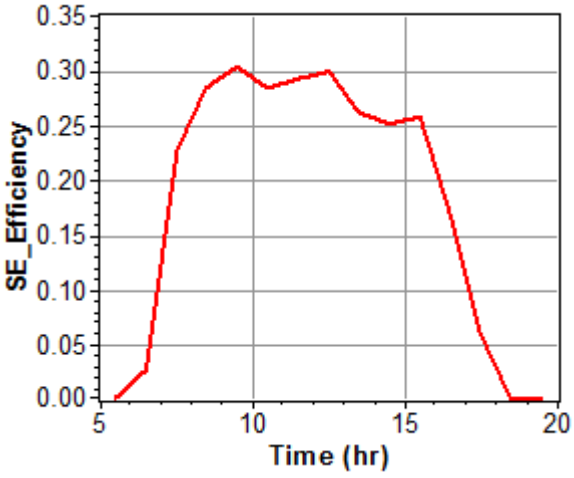
SE_Efficiency
0.35
0.30
0.25
0.20
0.15
0.10
0.05
0.00
5
10
15
20
Time (hr)

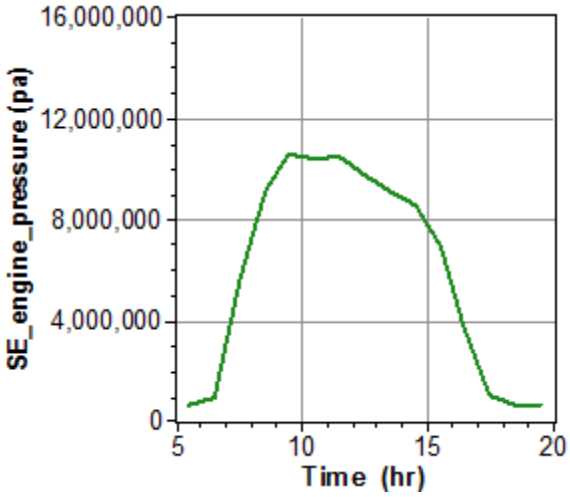
SE_engine_pressure (pa)
16,000,000
12,000,000
8,000,000
4,000,000
0
5
10
15
20
Time (hr)

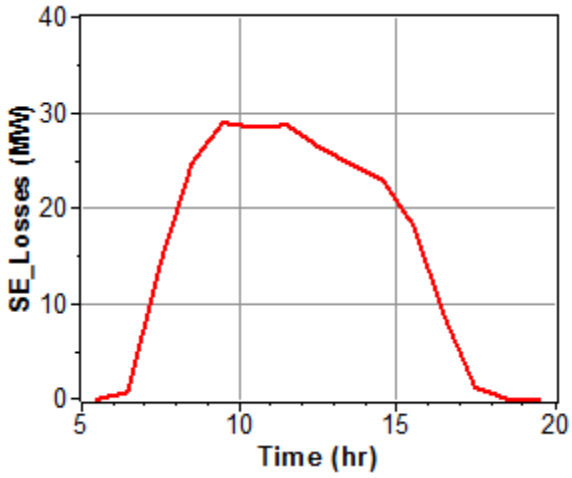
SE_Losses (MW)
40
30
20
10
0
5
10
15
20
Time (hr)

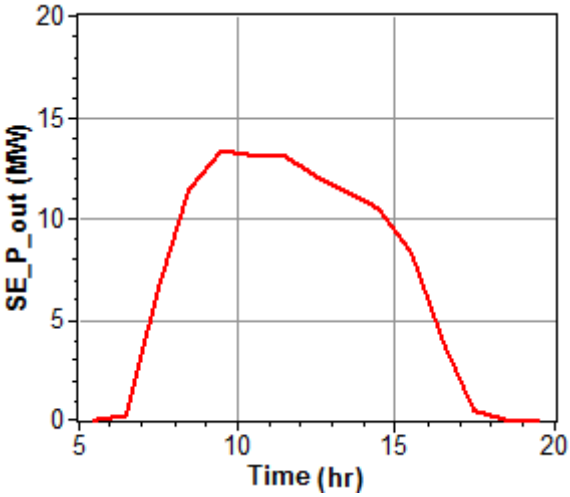
SE_P_out (MW)
20
15
10
5
0
5
10
15
20
Time (hr)

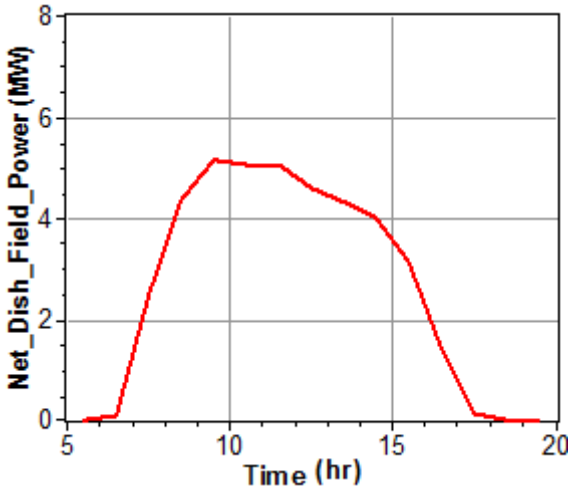
Net_Dish_Field_Power (MW)
8
6
4
2
0
5
10
15
20
Time (hr)

November:

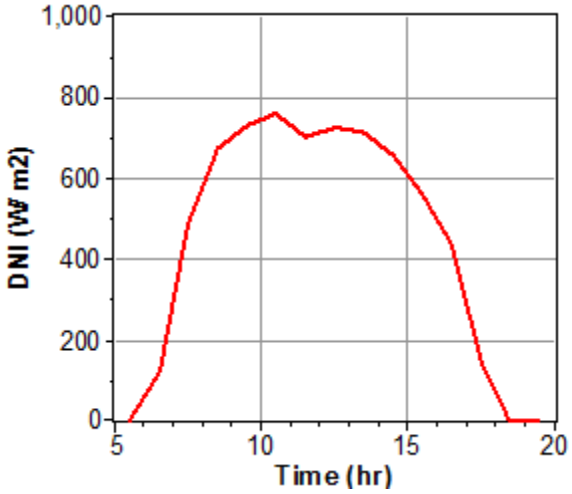
DNI (W/ m2)
1,000
800
600
400
200
0
5
10
15
20
Time (hr)

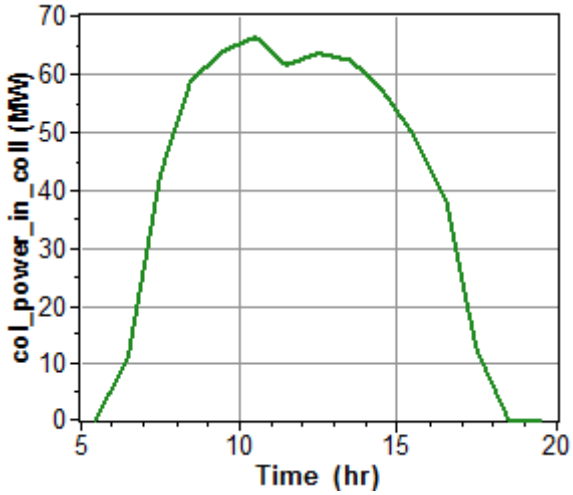
col_power_in_coll (MW)
70
60
50
40
30
20
10
0
5
10
15
20
Time (hr)

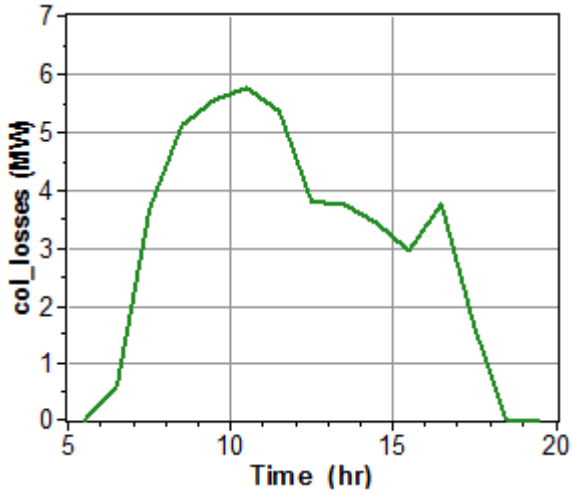
col_losses (MW)
7
6
5
4
3
2
1
0
5
10
15
20
Time (hr)

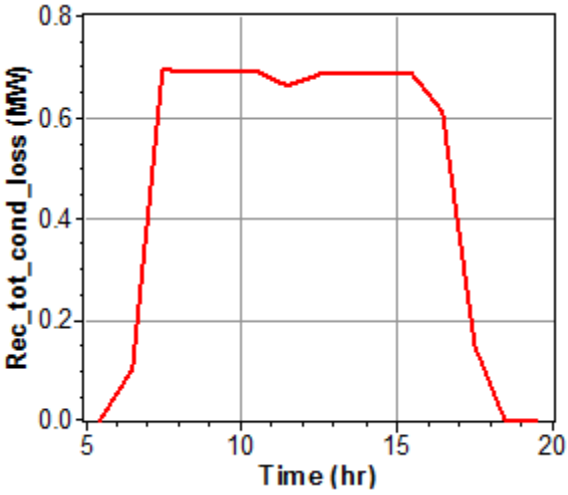
Rec_tot_cond_loss (MW)
0.8
0.6
0.4
0.2
0.0
5
10
15
20
Time (hr)

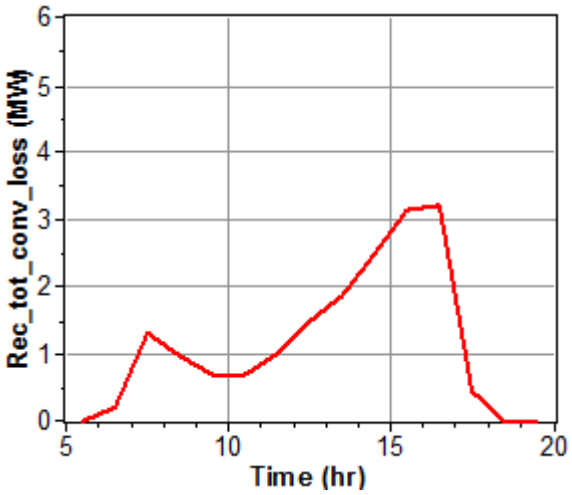
Rec_tot_conv_loss (MW)
6
5
4
3
2
1
0
5
10
15
20
Time (hr)

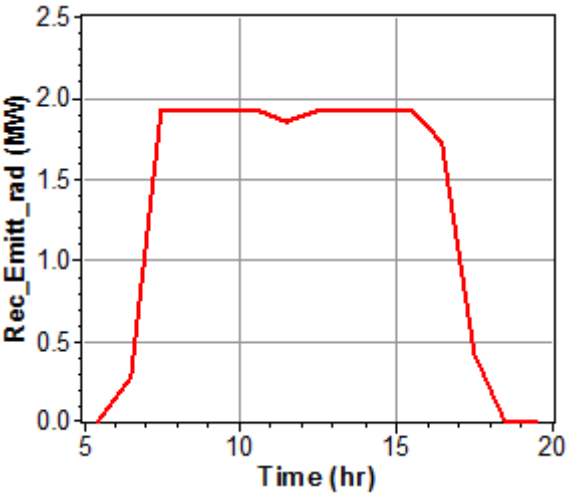
Rec_Emitt_rad (MW)
2.5
2.0
1.5
1.0
0.5
0.0
5
10
15
20
Time (hr)

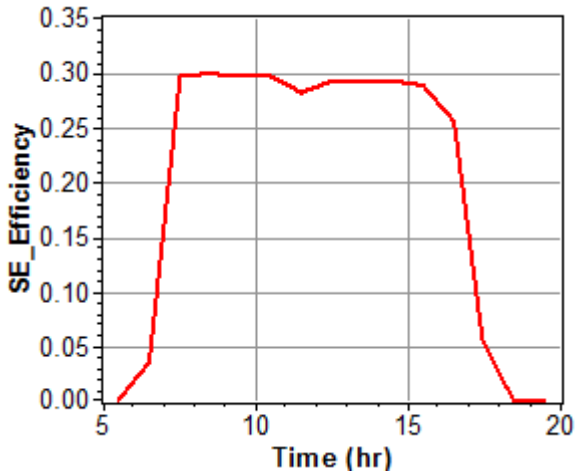
SE_Efficiency
0.35
0.30
0.25
0.20
0.15
0.10
0.05
0.00
5
10
15
20
Time (hr)

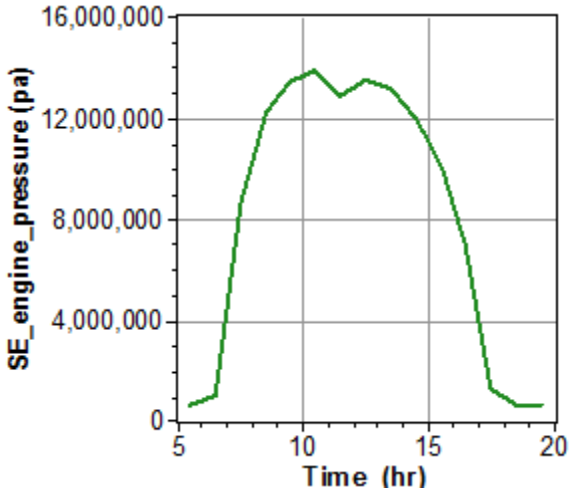
SE_engine_pressure (pa)
16,000,000
12,000,000
8,000,000
4,000,000
0
5
10
15
20
Time (hr)

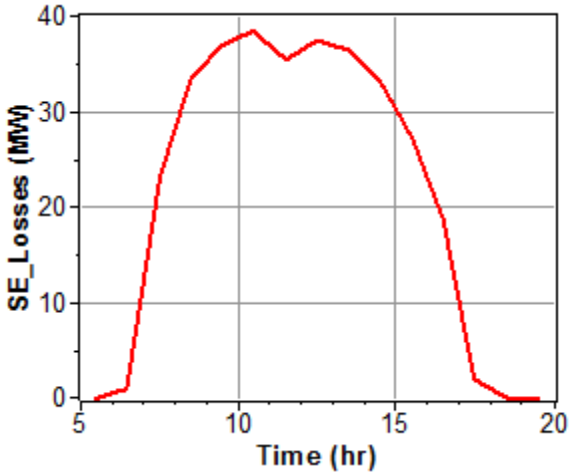
SE_Losses (MW)
40
30
20
10
0
5
10
15
20
Time (hr)

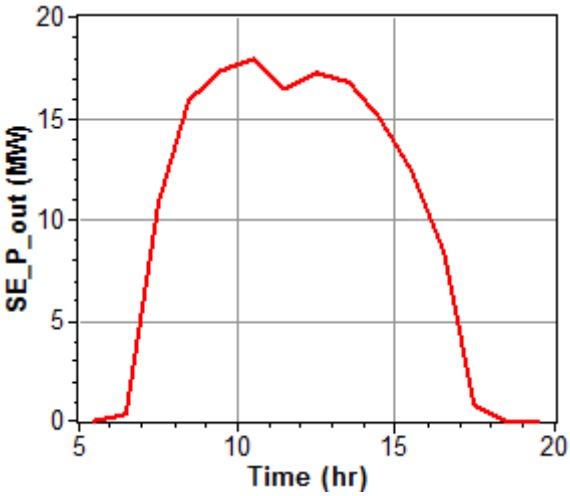
SE_P_out (MW)
20
15
10
5
0
5
10
15
20
Time (hr)

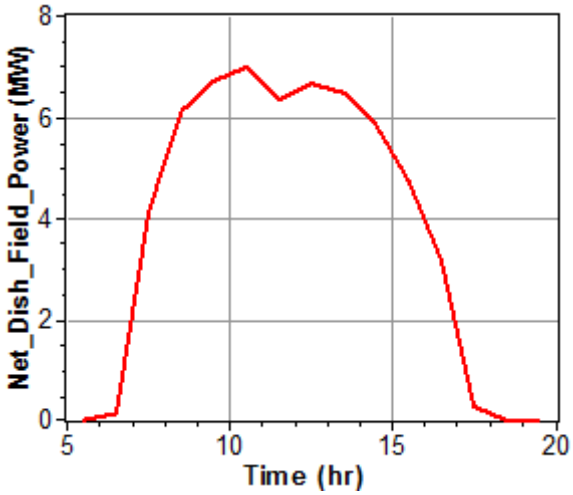
Net_Dish_Field_Power (MW)
8
6
4
2
0
5
10
15
20
Time (hr)

December:

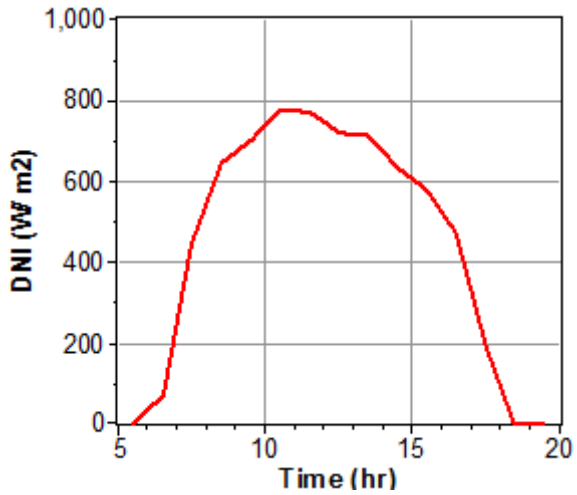
DNI (W/m2)
1,000
800
600
400
200
0
5
10
15
20
Time (hr)

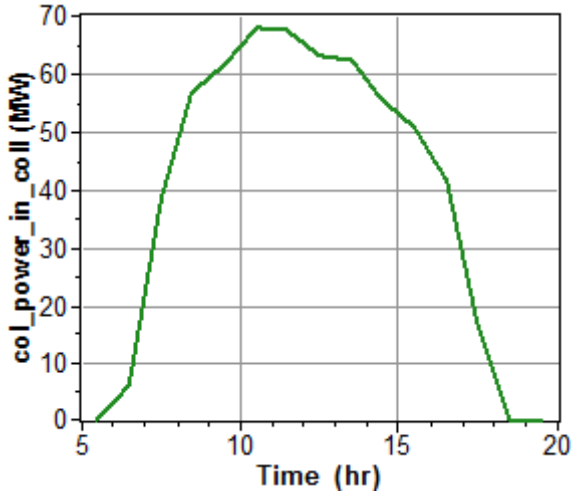
col_power_in_coll (MW)
70
60
50
40
30
20
10
0
5
10
15
20
Time (hr)

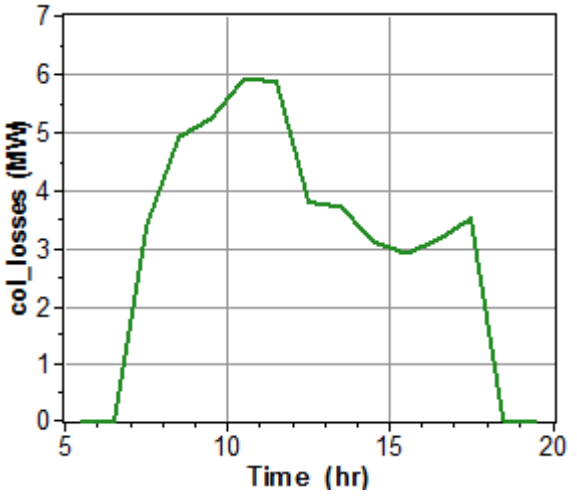
col_losses (MW)
7
6
5
4
3
2
1
0
5
10
15
20
Time (hr)

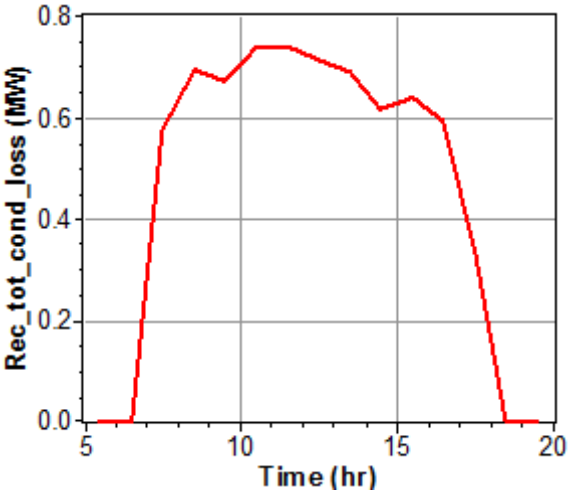
Rec_tot_cond_loss (MW)
0.8
0.6
0.4
0.2
0.0
5
10
15
20
Time (hr)

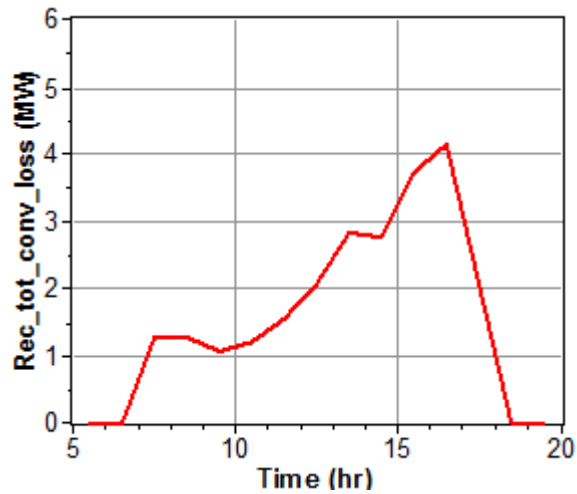
Rec_tot_conv_loss (MW)
6
5
4
3
2
1
0
5
10
15
20
Time (hr)

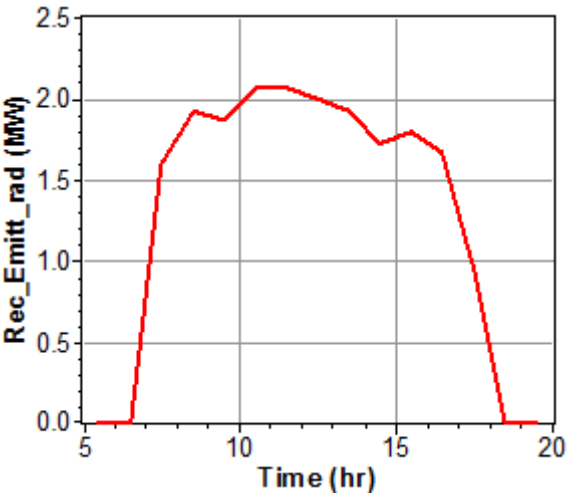
Rec_Emitt_rad (MW)
2.5
2.0
1.5
1.0
0.5
0.0
5
10
15
20
Time (hr)

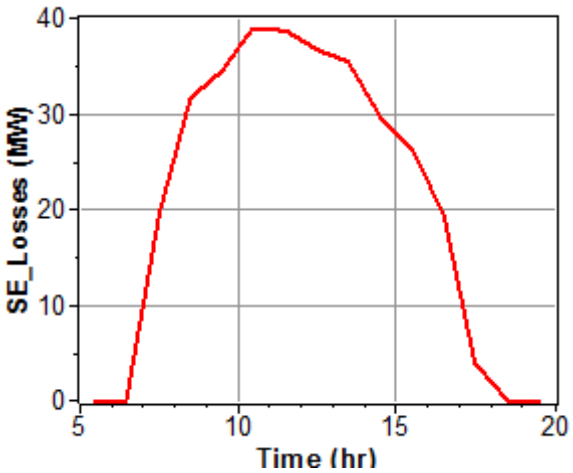
SE_Losses (MW)
40
30
20
10
0
5
10
15
20
Time (hr)

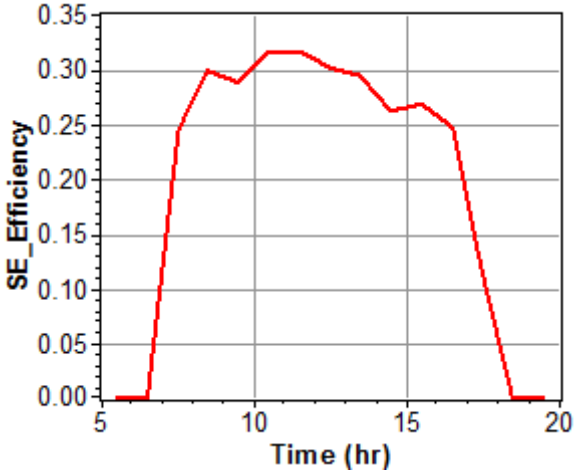
SE_Efficiency
0.35
0.30
0.25
0.20
0.15
0.10
0.05
0.00
5
10
15
20
Time (hr)

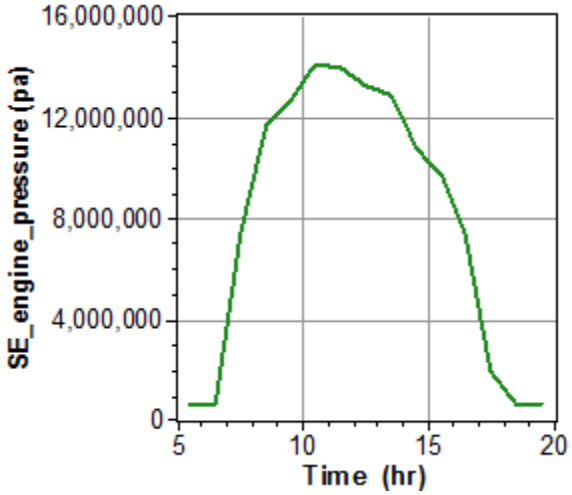
SE_engine_pressure (pa)
16,000,000
12,000,000
8,000,000
4,000,000
0
5
10
15
20
Time (hr)

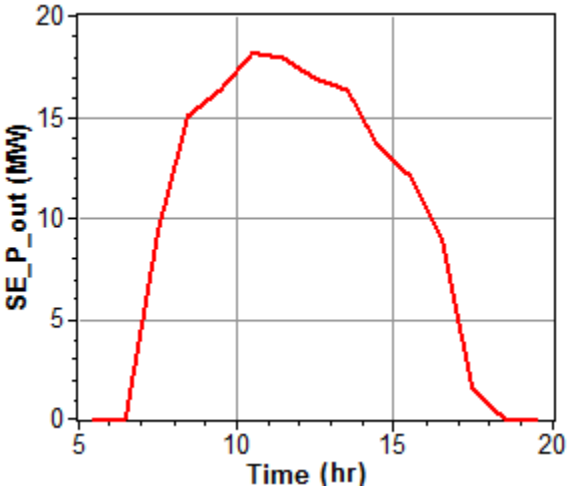
SE_P_out (MW)
20
15
10
5
0
5
10
15
20
Time (hr)

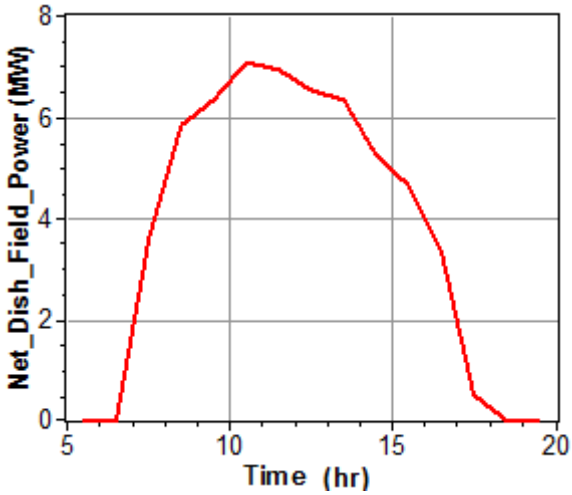
Net_Dish_Field_Power (MW)
8
6
4
2
0
5
10
15
20
Time (hr)